

2-1  
411X

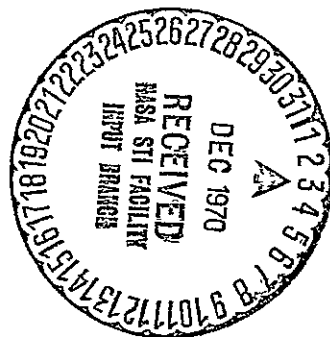
445-MS-I  
(2 cys)

JUNE 22, 1970  
70SD632

# EVALUATION OF OMNIWEAVE (GE) METHOD OF COMPOSITE FABRICATION - GRAPHITE FILAMENT

FINAL REPORT  
CONTRACT NO. NAS8-24777  
JUNE 31, 1969 TO MAY 31, 1970

FACILITY FORM 602	N71-11441	
	(ACCESSION NUMBER)	(THRU)
	227 (PAGES)	G3
	CR-102916 (NASA CR OR TMX OR AD NUMBER)	18 (CATEGORY)



Prepared for

National Aeronautics & Space Administration  
Marshall Space Flight Center, Alabama 35812

**GENERAL ELECTRIC**  
**Re-entry & Environmental**  
**Systems Division**  
PHILADELPHIA, PENNSYLVANIA

Reproduced by  
**NATIONAL TECHNICAL**  
**INFORMATION SERVICE**  
Springfield, Va. 22151

JUNE 22,1970

70SD632

# EVALUATION OF OMNIWEAVE (GE) METHOD OF COMPOSITE FABRICATION - GRAPHITE FILAMENT

FINAL REPORT  
CONTRACT NO.NAS8-24777  
JUNE 31,1969 TO MAY 31,1970

BY

M. WEXLER  
R. FENTON  
D. LOWE  
H. EDIGHOFFER  
R. BELMAN

Prepared for

National Aeronautics & Space Administration  
Marshall Space Flight Center, Alabama 35812

Submitted by

Materials Laboratory  
General Electric Company  
Re-Entry and Environmental Systems Division  
PO Box 8555  
Philadelphia, Pennsylvania 19101

Furnished under U.S. Government Contract Number NAS8-24777 and only those portions hereof which are marked and indicated as being subject to this restriction should not be released outside the Government or be disclosed, used, or duplicated for procurement or manufacturing purposes except as otherwise authorized by contract without the permission of General Electric Company. This legend should be marked in any portion hereof, in whole or in part. This restriction does not limit the Government's right to use or disclose and data obtained from another source without restriction.

## FOREWORD

The work described in this report was performed at General Electric Re-Entry and Environmental Systems Division, Materials Laboratory, located at the General Electric Valley Forge Space Technology Center, King of Prussia, Pennsylvania. Technical supervision was provided from the NASA-Marshall Space Flight Center, Huntsville, Alabama, by Mr. H. M. Walker. The principal technical investigator for GE/RESO was Melvin Wexler.

The principal contributors to the technical effort and preparation of this report are listed below:

Fabrication of Omniweave Composites	Melvin Wexler Richard Fenton
Mechanical Testing of Omniweave	David Lowe
Omniweave Structural Analyses	Harold Edighoffer Richard Belman

The authors wish to acknowledge the aid of the following personnel who provided expert consultation to the program.

Omniweave Equipment Development	George Groschke Jack Callendar
Mechanical Characterization	Wilfred Connell
Omniweave Manufacture	Charles Foster

The authors want to thank the following personnel for their fine efforts in performing key functions which ensured the success of the program:

Omniweave Fabrication	Vincent Arcidiacono Frank Manning
Mechanical Property Measurement	Jordan Konnell
Mechanical Property Data Reduction	Marie Bamberg

## ABSTRACT

Twenty-two (22) Omniweave fabrics were woven of S-glass, Morganite Type II, Thornel 50S, Boron and mixed fiber combinations of these materials using epoxy prepregged weaving elements to demonstrate the manufacturing feasibility of this weaving approach. Selected composites produced from these multidirectional fabrics were evaluated for flexure, tensile, compression and interlaminar shear properties to note the effect of weave geometry and fiber type on mechanical properties. Analyses were performed using the "OMNI" computer code to estimate composite properties. Off-axis tensile data obtained on unidirectional S-glass/epoxy composites were used to determine the effective translation of resin/fiber properties to the Omniweave construction. Structural analyses indicated that Omniweave composites of Morganite and/or Boron can be utilized for structural skin applications at significant weight savings over state-of-the-art materials.



# TABLE OF CONTENTS

Section		Page
	FOREWORD .....	
	ABSTRACT .....	
1	SUMMARY .....	1-1
	1.1 Manufacturing Feasibility .....	1-1
	1.2 Mechanical Properties .....	1-1
	1.3 Structural Analysis .....	1-2
2	INTRODUCTION .....	2-1
3	EXPERIMENTAL PROGRAM PLAN .....	3-1
4	FABRICATION OF OMNIWEAVE COMPOSITES .....	4-1
	4.1 Introduction to Omniweave Concept .....	4-1
	4.1.1 Omniweave Processing .....	4-4
	4.1.2 Selected Omniweave Geometries .....	4-7
	4.2 Materials Selection .....	4-15
	4.2.1 Fiber Selection .....	4-15
	4.2.2 Resin Selection .....	4-15
	4.3 Fabrication of Unidirectional Test Coupons .....	4-19
	4.4 Preliminary Processing Studies .....	4-21
	4.4.1 S-Glass/USP23 .....	4-21
	4.4.2 Morganite Type II/USP23 .....	4-21
	4.4.3 Thornel 50S/USP23 .....	4-21
	4.4.4 Boron (W) Core/HT424 Resin .....	4-22
	4.5 Omniweave Fabric Production .....	4-23
	4.5.1 S-Glass/USP23 Omniweave Fabrics .....	4-23
	4.5.2 Morganite Type II/USP23 Omniweave Fabrics .....	4-28
	4.5.3 Thornel 50S/USP23 Omniweave Fabric .....	4-28
	4.5.4 Boron/HT424 Prepreg Omniweave Fabrics .....	4-30
	4.5.5 Mixed Fiber Omniweave Fabrics .....	4-30
	4.6 Omniweave Composite Fabrication .....	4-34
	4.6.1 Glass/USP23 Omniweave Composites .....	4-34
	4.6.2 Morganite/USP23 Omniweave Composites .....	4-34
	4.6.3 Boron, Thornel and Mixed Fiber Onniweave Composites .....	4-34
	4.7 Fabrication of Omniweave/Honeycomb Demonstration Items .....	4-40
	4.8 Summary and Conclusions .....	4-43

## TABLE OF CONTENTS (Continued)

Section		Page
5	MECHANICAL EVALUATION OF OMNIWEAVE COMPOSITES . . . . .	5-1
5.1	Testing of Unidirectional Test Coupons . . . . .	5-1
5.2	Flexural Test Data . . . . .	5-8
5.2.1	S-Glass/Epoxy Omniweave Flexural Data . . . . .	5-8
5.2.2	Morganite Type II/Epoxy Flexural Properties . . . . .	5-11
5.3	Tensile Test Data . . . . .	
5.3.1	S-Glass Epoxy Omniweave Tensile Properties . . . . .	5-11
5.3.2	Morganite Type II/Epoxy Omniweave Tensile Properties . . . . .	5-11
5.3.3	Boron, Thornel 50S, and Mixed Fiber Omniweave Tensile Specimens . . . . .	5-24
5.4	Compression Test Data . . . . .	5-28
5.4.1	S-Glass/Epoxy Omniweave Compression Tests . . . . .	5-28
5.4.2	Morganite Type II/Epoxy Omniweave Compression Tests . . . . .	5-29
5.5	Short Beam Shear Test Data . . . . .	5-31
5.6	Conclusions . . . . .	5-34
6	OMNIWEAVE STRUCTURAL ANALYSES . . . . .	6-1
6.1	Introduction to the OMNI Computer Program . . . . .	6-1
6.2	Prediction of Omniweave Properties and Comparison with Test Data . . . . .	6-6
6.2.1	Properties of S-Glass Omniweave Composites from Uniaxial Tests . . . . .	6-6
6.2.2	Final Design Curves . . . . .	6-15
6.2.3	Preliminary Design Curves . . . . .	6-15
6.3	Application of Omniweave to Launch Vehicle Booster Systems . . . . .	6-15
6.4	Conclusions . . . . .	6-28
7	DISCUSSION AND CONCLUSIONS . . . . .	7-1
7.1	Omniweave Weaving Process . . . . .	7-2
7.2	Omniweave Molding Process . . . . .	7-2
7.3	Omniweave Test Data and Structural Analysis . . . . .	7-3
8	RECOMMENDATIONS . . . . .	8-1
8.1	Weaving Process Optimization . . . . .	8-1
8.2	Molding Process Optimization . . . . .	8-1
8.3	Evaluation of Test Speciment Configurations . . . . .	8-2
8.4	Other Applications for Omniweave Composites . . . . .	8-2

## TABLE OF CONTENTS (Continued)

Section	Page
9	BIBLIOGRAPHY ..... 9-1
10	APPENDIX ..... 10-1
10.1	Formulae Used in Characterizing S-Glass, Morganite II, Boron, and Thornel 50S Composites ..... 10-1
10.2	Formulae Used in Characterizing Mixed Fiber Omniweave Composites ..... 10-2
10.3	Tensile Specimen Preparation ..... 10-3
10.4	Analyses of Off Axis Tensile Testing of Unidirectional Composites ..... 10-4
10.5	Omniweave Tensile Stress-Strain Curves ..... 10-10
10.6	Preliminary Omniweave Prediction Curves ..... 10-10
10.6.1	S-Glass Omniweave Composites ..... 10-10
10.6.2	Morganite II Omniweave Composites ..... 10-39
10.6.3	Thornel 50S Omniweave Composites ..... 10-39
10.6.4	Boron Omniweave Composites ..... 10-42
10.6.5	Margin-of-Safety and Thermal Expansion Predictions ..... 10-42

## LIST OF ILLUSTRATIONS

Figure		Page
3-1	Program Logic Diagram . . . . .	3-2
4-1	Standard Omniweave (45° Fiber Pitch Angle) Yarn Move- ment Mechanism . . . . .	4-2
4-2	Fiber Pitch Angle Omniweave: Multidimensional Reinforce- ment in Which the Fibers Follow Paths Parallel to the Diagonals of Intersecting Planes . . . . .	4-3
4-3	Yarn Preparation for use with Omniweave Equipment . . . . .	4-5
4-4	Yarn Attachment Techniques . . . . .	4-6
4-5	Combing of Stitch Crossovers . . . . .	4-7
4-6	Omniweave Combing Devices . . . . .	4-8
4-7	Selected Omniweave Geometries . . . . .	4-9
4-8	Yarn Movement Mechanism for 45-degree FPA Omniweave Geometry . . . . .	4-10
4-9	Yarn Movement Mechanism for 45-degree LID Omniweave Geometry . . . . .	4-12
4-10	Yarn Movement Mechanism for 18-degree LID Omniweave Geometry . . . . .	4-13
4-11	Yarn Movement Mechanism for Triaxial Omniweave Geometry . . . . .	4-14
4-12	S21D-85 Omniweave Fabric . . . . .	4-25
4-13	S21A-91 Omniweave Fabric . . . . .	4-25
4-14	S21A-92 Omniweave Fabric . . . . .	4-25
4-15	S21F-93 Omniweave Fabric . . . . .	4-27
4-16	S21F-94 Omniweave Fabric . . . . .	4-27
4-17	S21D-103 Omniweave Fabric . . . . .	4-27
4-18	S21D-104 Omniweave Fabric . . . . .	4-27
4-19	S21A/L-204 Omniweave Fabric Weaving Conditions . . . . .	4-29
4-20	S21A/L Omniweave Fabric . . . . .	4-29
4-21	G51A-86 Omniweave Fabric . . . . .	4-29
4-22	G51A/L-207 Omniweave Fabric . . . . .	4-29
4-23	Nest Fiber Arrays for Mixed Fiber 45-degree FPA Geometries . . . . .	4-32
4-24	I11A-101-10 25/75 Boron/S-Glass Omniweave Fabric . . . . .	4-33
4-25	S21A-91/Plastic Honeycomb Core/S21A-92 Structural Sandwich Assembly . . . . .	4-41
4-26	S21D85/Aluminum Honeycomb Core/S21D-104 Structural Sandwich Assembly . . . . .	4-42

# LIST OF ILLUSTRATIONS (Continued)

Figure		Page
5-1	Unidirectional Tensile Specimen Geometry . . . . .	5-2
5-2	Strain Gage Location and Identification . . . . .	5-4
5-3	Post-Test Photographs of Off-Axis Unidirectional Test Specimens . . . . .	5-6
5-4	The Effect of Fiber Orientation on Flexural Strength of S-Glass/USP23 Omniweave Composites . . . . .	5-13
5-5	The Effect of Fiber Orientation on Flexural Modulus of S-Glass/USP23 Omniweave Composites . . . . .	5-14
5-6	Effect of Omniweave Construction and Weave Thickness on Flexural Strength of S-Glass/USP-23 Composite . . . . .	5-15
5-7	Flexural Strength of S-Glass/USP23 Omniweave Composites Tested along Fiber Axis . . . . .	5-16
5-8	Flexural Modulus of S-Glass/USP23 Omniweave Composites Tested along Fiber Axis . . . . .	5-16
5-9	The Effect of Cure Cycle on Flexural Strength of S21A-94 S-Glass/USP23 Omniweave Composites . . . . .	5-17
5-10	The Effect of Cure Cycle on Flexural Strength of S21D-104 S-Glass/USP23 Omniweave Composites . . . . .	5-18
5-11	Typical S-Glass/Epoxy Flexure Specimens after Testing . . . . .	5-19
5-12	The Effect of Fiber Orientation on Flexural Strength of Morganite II/USP23 Omniweave Composites . . . . .	5-20
5-13	The Effect of Fiber Orientation on Flexural Modulus of Morganite II/USP23 Omniweave Composites . . . . .	5-21
5-14	Typical Morganite Omniweave Flexure Specimen Failure Modes . . . . .	5-22
5-15	Failure Modes of S-Glass Omniweave Tensile Specimens . . . . .	5-23
5-16	Morganite Omniweave Tensile Specimens After Test . . . . .	5-25
5-17	Tensile Failure Modes of Boron Omniweave Composites . . . . .	5-27
5-18	Post-Test Photograph of Mixed Fiber Omniweave Tensile Specimens . . . . .	5-27
5-19	Compressive Failure of S-Glass Omniweave Composites . . . . .	5-30
5-20	Typical Short Beam Shear Failure Modes for S-Glass Omniweave Composites . . . . .	5-23
6-1	Description of Omniweave Fiber System . . . . .	6-2
6-2	Omniweave Method of Analysis . . . . .	6-3
6-3	S-Glass Off-Axis Modulus Test Data . . . . .	6-8
6-4	S-Glass Off-Axis Strength Test Data . . . . .	6-9
6-5	S-Glass Off-Axis Tensile Strength . . . . .	6-10
6-6	S-Glass Omniweave Tensile Strength . . . . .	6-12

# LIST OF ILLUSTRATIONS (Continued)

Figure		Page
6-7	S-Glass Omniweave Compressive Strength . . . . .	6-13
6-8	S-Glass Omniweave Modulus of Elasticity . . . . .	6-14
6-9	Axial Tensile Strength of Morganite II Omniweave . . . . .	6-16
6-10	Morganite II Omniweave Compressive Strength . . . . .	6-17
6-11	Longitudinal Elastic Modulus-Morganite II Omniweave . . . . .	6-18
6-12'	Thornel-50 Omniweave Tensile Strength Prediction . . . . .	6-19
6-13	Thornel-50 Omniweave Compressive Strength Prediction . . . . .	6-20
6-14	Thornel-50 Omniweave Tensile Modulus Prediction . . . . .	6-21
6-15	Boron Omniweave Tensile Strength . . . . .	6-22
6-16	Boron Omniweave Compressive Strength . . . . .	6-23
6-17	Boron Omniweave Tensile Modulus . . . . .	6-24
6-18	Axial Strength Using Hill's Modified Failure Criteria- Omniweave Quartz Phenolic . . . . .	6-25
10-1	Shear Strain/Axial Stress Coupling . . . . .	10-7
10-2	Shear Coupling Parameters . . . . .	10-9
10-3	Tensile Stress-Strain Curves - S21A-84 Axial Direction . . . . .	10-11
10-4	Tensile Stress-Strain Curves - S21A-84, Transverse Direction . . . . .	10-12
10-5	Tensile Stress-Strain Curves - S21D-104, Axial Direction . . . . .	10-13
10-6	Tensile Stress-Strain Curves - S21D-104, Transverse Direction . . . . .	10-14
10-7	Tensile Stress-Strain Curves - S21A/L-204, Axial Direction . . . . .	10-15
10-8	Tensile Stress-Strain Curves - S21A/L-204, Transverse Direction . . . . .	10-16
10-9	Tensile Stress-Strain Curves - G51D-96, Axial Orientation . . . . .	10-17
10-10	Tensile Stress-Strain Curves - G51D-96, Transverse Direction . . . . .	10-18
10-11	Tensile Stress-Strain Curves - G51A/L-207, Axial Direction . . . . .	10-19
10-12	Tensile Stress-Strain Curves - G51A/L-207, Transverse Direction . . . . .	10-20
10-13	Tensile Stress-Strain Curves - I11A-101-1, Axial Direction . . . . .	10-21
10-14	Tensile Stress-Strain Curves - I11A-101-2 . . . . .	10-22
10-15	Tensile Stress-Strain Curves - I11A-101-3 . . . . .	10-23

# LIST OF ILLUSTRATIONS (Continued)

Figure		Page
10-16	Tensile Stress-Strain Curves - I11A-101-4, Axial Direction . . . . .	10-24
10-17	Tensile Stress-Strain Curves - I11A-101-6, Axial Direction . . . . .	10-25
10-18	Tensile Stress-Strain Curves - G71A-98, Axial Direction . . . . .	10-26
10-19	Tensile Stress-Strain Curves - I11A-101-A, Axial Direction . . . . .	10-27
10-20	Tensile Stress-Strain Curves - I11A-101-9, Axial Direction . . . . .	10-28
10-21	Tensile Stress-Strain Curves - I11A-101-10, Axial Direction . . . . .	10-29
10-22	Tensile Stress-Strain Curves - I11A-101-11, Axial Direction . . . . .	10-30
10-23	Axial Strength Predictions Using Max. Stress Criteria - S-Glass Omniweave Composites . . . . .	10-31
10-24	Elastic Moduli Prediction - S-Glass Omniweave Composites . . .	10-32
10-25	Margins of Safety (Thermal Loading Only) - S-Glass Omniweave Composites . . . . .	10-33
10-26	Margins of Safety (Thermal plus Mechanical Loading) - S-Glass Omniweave Composites . . . . .	10-34
10-27	Shear Moduli - S-Glass Omniweave Composites . . . . .	10-35
10-28	Poisson's Ratio for S-Glass Omniweave Composites . . . . .	10-36
10-29	Poisson's Ratio for S-Glass Omniweave Composites . . . . .	10-37
10-30	Coefficient of Thermal Expansion for S-Glass Omniweave Composites . . . . .	10-38
10-31	Axial Strength for Morganite II Omniweave Composites Using Max. Stress Criteria . . . . .	10-44
10-32	Axial Strength of Morganite II Omniweave Composites . . . . .	10-45
10-33	Elastic Moduli of Morganite II Omniweave Composites . . . . .	10-46
10-34	Poisson's Ratio of Morganite II Omniweave Composites . . . . .	10-47
10-35	Axial Strength of Morganite II Omniweave Composites using Hill's Modified Failure Criteria . . . . .	10-48
10-36	Longitudinal Elastic Modulus of Morganite II Omniweave Composites . . . . .	10-49
10-37	Poisson's Ratio of Morganite II Omniweave Composites . . . . .	10-50

# LIST OF ILLUSTRATIONS (Continued)

Figure		Page
10-38	Strength Prediction Curves for Morganite II Omniweave Composites using Hills Failure Criteria . . . . .	10-51
10-39	Elastic Moduli Prediction Curves for Morganite II Omniweave Composites . . . . .	10-52
10-40	Margins of Safety (Thermal Loading Only) for Morganite II Omniweave Composites . . . . .	10-53
10-41	Margins of Safety (Thermal Plus Mechanical Loading for Morganite II Omniweave Composites . . . . .	10-54
10-42	Shear Moduli of Morganite II Omniweave Composites . . . . .	10-55
10-43	Poisson's Ratio for Morganite II Omniweave Composites . . . . .	10-56
10-44	Coefficients of Thermal Expansion for Morganite II Omniweave Composites . . . . .	10-57
10-45	Radial Strength of Morganite II Omniweave Composites . . . . .	10-58
10-46	Axial Strength Predictions for Morganite II Omniweave Composites . . . . .	10-59
10-47	Hill's Margins of Safety for Morganite II Omniweave Composites . . . . .	10-60
10-48	Coefficients of Thermal Expansion for Morganite II Omniweave Composites . . . . .	10-61
10-49	Poisson's Ratio of Morganite II Omniweave Composites . . . . .	10-62
10-50	Poisson's Ratio of Morganite II Omniweave Composites . . . . .	10-63
10-51	Shear Moduli Curves for Morganite II Omniweave Composites . . . . .	10-64
10-52	Elastic Moduli Curves for Morganite II Omniweave Composites . . . . .	10-65
10-53	Margins of Safety (Thermal Plus Mechanical Loading) for Morganite II Omniweave Composites . . . . .	10-66
10-54	Margins of Safety (Thermal Load Only) for Morganite II Omniweave Composites . . . . .	10-67
10-55	Axial Strength Curves for Thornel 50 Omniweave Composites using Max Stress Criteria . . . . .	10-68
10-56	Elastic Moduli of Omniweave Composites . . . . .	10-69
10-57	Margins of Safety (Thermal Loading Only) for Thornel 50 Omniweave Composites . . . . .	10-70
10-58	Margins of Safety (Thermal Plus Mechanical Loading) for Thornel 50 Omniweave Composites . . . . .	10-71
10-59	Shear Moduli Curves for Thornel 50 Omniweave Composites . . .	10-72



# LIST OF ILLUSTRATIONS (Continued)

Figure		Page
10-60	Poisson's Ratios for Thornel 50 Omniweave Composites . . . . .	10-73
10-61	Poisson's Ratios for Thornel 50 Omniweave Composites . . . . .	10-74
10-62	Thermal Expansion Curves for Thornel 50 Omniweave Composites . . . . .	10-75
10-63	Axial Strength of Boron Omniweave Composites . . . . .	10-76
10-64	Elastic Moduli of Boron Omniweave Composites . . . . .	10-77
10-65	Margins of Safety (Thermal Loading Only) for Boron Omniweave Composites . . . . .	10-78
10-66	Margins of Safety (Thermal Plus Mechanical Loading) for Boron Omniweave Composites . . . . .	10-79
10-67	Shear Moduli Curves for Boron Omniweave Composites . . . . .	10-80
10-68	Poisson's Ratios of Boron Omniweave Composites . . . . .	10-81
10-69	Poisson's Ratio Curves for Boron Omniweave Composites . . .	10-82
10-70	Coefficients of Thermal Expansion for Boron Omniweave Composites . . . . .	10-83

## LIST OF TABLES

Table		Page
2-1	Typical Properties of Filamentary Materials . . . . .	2-1
3-1	Omniweave Materials Matrix . . . . .	3-3
4-1	Fiber Characteristics . . . . .	4-16
4-2	Resin Characteristics . . . . .	4-16
4-3	Prepreg Fiber Characteristics . . . . .	4-18
4-4	Omniweave Cure Cycles for USP23 Epoxy Composites . . . . .	4-19
4-5	S-Glass/USP23 Unidirectional Composite Characterization . . . . .	4-20
4-6	Processing Summary of Omniweave Fabrics . . . . .	4-24
4-7	Cure Cycles Utilized in Fabricating Omniweave Composites . . . . .	4-35
4-8	Molding and Characterization of S-Glass/USP23 Omniweave Composites . . . . .	4-36
4-9	Molding and Characterization of Morganite/USP23 Omniweave Composites . . . . .	4-37
4-10	Molding and Characterization of Boron, Thornel and Mixed Fiber Omniweave Composites . . . . .	4-38
5-1	Physical Characteristics of Unidirectional S-Glass/USP23 Epoxy Test Panels . . . . .	5-3
5-2	S-Glass/USP23 Unidirectional Tensile Data . . . . .	5-5
5-3	Tensile Strength of S-Glass/USP23 Epoxy Composite 90- Degrees to Fibers . . . . .	5-6
5-4	Comparison of Unidirectional S-Glass/Epoxy Data with Literature Reported Values . . . . .	5-7
5-5	Unidirectional Tensile Properties of Morganite Type II/Epoxy Composites (Literature Data) . . . . .	5-7
5-6	Flexure Test Results: S-Glass/USP23 Omniweave Composites . . . . .	5-9
5-7	Flexure Test Results: Morganite II/USP23 Omniweave Composites . . . . .	5-12
5-8	Tension Test Results: S-Glass / USP23 Omniweave Composites . . . . .	5-22
5-9	Tension Test Results: Morganite II/USP23 Omniweave Composites . . . . .	5-24
5-10	Tension Test Results: Boron, Thornel 50S and Mixed Fiber Omniweave Systems . . . . .	5-26
5-11	Compression Test Results: S-Glass/USP23 Omniweave Composites . . . . .	5-28
5-12	Compression Test Results: Morganite II/USP23 Omniweave Composites . . . . .	5-29

# LIST OF TABLES (Continued)

Table		Page
5-13	Comparison of Morganite Type II/Epoxy Omniweave Transverse Compression Data with Literature Reported Values for Unidirectional Material . . . . .	5-30
5-14	Short Beam Shear Test Results: S-Glass/USP23 Omniweave Composites . . . . .	5-31
5-15	Short Beam Shear Test Results: Morganite II/USP23 Omniweave Composites . . . . .	5-32
6-1	Inputs and Outputs of Omni . . . . .	6-4
6-2	Basic Material Property Inputs used in Initial Analysis . . . . .	6-5
6-3	S-Glass Unidirectional Moduli from Test Data . . . . .	6-7
6-4	S-Glass Unidirectional Strength From Test Data . . . . .	6-11
6-5	Predicted Omniweave Strength . . . . .	6-26
6-6	Predicted Specific Strength Comparisons of Honeycomb Facing Materials . . . . .	6-27
7-1	Omniweave Development Status . . . . .	7-1
7-2	Effect of Prepreg Conditions on Flexural Properties of Uni-directional S-Glass/Epoxy Composites <sup>(16)</sup> . . . . .	7-3
7-3	Effect of Cure Cycle on Flexural Properties of S-Glass/USP23 Omniweave Composites . . . . .	7-4
7-4	The Effect of Epoxy Resin Matrix Material on Mechanical Properties of Unidirectional S-Glass/Epoxy Composites . . . . .	7-5
7-5	Unidirectional Tensile Properties of Morganite Type II/Epoxy Composites . . . . .	7-6
7-6	Boron/HT424 Omniweave Tensile Strengths . . . . .	7-7
7-7	Comparison of Morganite Type II/Epoxy Omniweave Transverse Compression Data with Literature Reported Values for Unidirectional Material . . . . .	7-8
10-1	Estimated Unidirectional Moduli of Morganite II and S-Glass Composition . . . . .	10-10
10-2	Basic Fiber and Binder Properties Used in Preliminary Predictions . . . . .	10-40
10-3	Property Values for Omniweave Composites with a 18° Layered in Depth Fiber Configuration . . . . .	10-41
10-4	Catalog of Critical Factors for Morganite II Omniweave with a Lid Fiber Configuration . . . . .	10-42

**SECTION 1**  
**SUMMARY**

## SECTION 1

### SUMMARY

This report summarizes the results of an initial survey on the manufacturing feasibility, mechanical properties and utility of Omniweave structural composites:

#### 1.1 MANUFACTURING FEASIBILITY

1. The ability of the Omniweave weaving process to produce multidirectional fabric reinforcement using S-glass, Morganite Type II, Thornel 50S, Boron and combinations of the above has been demonstrated. A total of 22 Omniweave fabrics were produced. Weaving difficulties were experienced with Thornel 50S and Boron (in large width specimens).
2. Four different Omniweave geometries were employed. All fabrics were produced using prepregged yarns or filament tapes.
3. Molded composites were prepared from all fabrics produced. In most cases, level of porosity was less than five percent.
4. Several demonstration Omniweave structural skin assemblies were prepared and delivered to NASA-MSFC to demonstrate feasibility.

#### 1.2 MECHANICAL PROPERTIES

1. Flexural, tensile, compressive, shear, and interlaminar properties were determined for selected Omniweave composites.
2. Boron/HT424 Omniweave composites exhibited maximum tensile properties which was comparable to those of a unidirectional composite of similar fiber volume fraction.
3. Omniweave composites of S-glass and Morganite had mechanical properties slightly lower than those predicted by structural analysis indicating that improvements in processing techniques should be sought.
4. Data trends indicate that a) the layered-in-depth Omniweave construction yields higher in-plane strength characteristics than the fiber pitch angle construction, and b) strength and moduli data varied with fiber orientation as predicted.
5. The transverse compressive properties of several S-glass and Morganite composites were significantly higher than expected.
6. Interlaminar shear failure values using the short beam shear approach could not be obtained; primary mode of failure was predominantly flexural stress.

### 1.3 STRUCTURAL ANALYSIS

1. Mechanical property prediction curves for S-glass, Morganite II, Thornel 50S and Boron Omniweave composites were generated as a function of Omniweave geometry and fiber volume fraction using the "OMNI" computer program. In general, the mechanical data follows closely these prediction curves.
2. Off-axis tensile tests were performed on S-glass/epoxy unidirectional composite to furnish realistic inputs into the "OMNI" computer code.
3. The utilization of Omniweave for launch vehicle structural skin application was analyzed with the general conclusions that significant weight savings can be realized in both the unpressurized (60 percent weight savings) and pressurized (30 percent weight savings) booster regions through the use of Boron or Morganite Omniweave structural composites.

**SECTION 2**  
**INTRODUCTION**

## SECTION 2

### INTRODUCTION

Within the last decade, many new filamentary materials have been developed having significant promise as structural composite reinforcements because of their high specific strength and modulus characteristics (Table 2-1). These fiber materials are generally processed into unidirectional prepregged sheets which are then laid up at angles relevant to the application requirements and cured. Similarly, filament winding techniques have been devised to produce weight-efficient structural shell composites whose properties are tailored to the application. These filamentary composites have excellent in-plane properties but exhibit low interlaminar shear strengths thus limiting their utility. Moreover, it has been postulated that fatigue properties are limited by this delamination tendency upon flexural cycling.

Within the last year, GE-RESO has initiated the development of a novel weaving approach called Omniweave. The Omniweave process can produce multidirectionally reinforced, thick fabrics using advanced fiber materials. These fabrics are composed of interlocking fiber elements which travel in depth so that discrete fiber layers are not formed. This absence of resin bonded layers should enhance the composite shear strength and improve fatigue characteristics. The penalty for the improvement in these properties is a slight drop in in-plane strength and modulus corresponding to the radial fiber path angle. The Omniweave interlocking fiber geometry can be tailored to meet complex load requirements. Moreover, the weaving of complex shapes such as integrally ribbed structural shells, I beams, struts, and trusses are potentially feasible.

TABLE 2-1. TYPICAL PROPERTIES OF FILAMENTARY MATERIALS <sup>(2, 3)</sup>

Material	Density (lbs/in <sup>3</sup> )	Young's Modulus (psi x 10 <sup>-6</sup> )	Ultimate Tensile Strength, (psi x 10 <sup>-3</sup> )	Specific Modulus (in x 10 <sup>-6</sup> )	Specific Tensile Strength (in x 10 <sup>-6</sup> )
E-Glass	0.092	10	250	104	2.7
S-Glass	0.092	10	500	104	5.5
Morganite Type II	0.063	35-45	350-450	560-710	5.6-7.1
Thornel 50	0.061	50	220	814	3.6
Boron	0.096	50	500	530	5.3
Aluminum*	0.097	10	70	102	0.72
Steel (Drawn Wire)	0.280	30	400-600	104	1.4-2.1
Beryllium*	0.066	45	150	470	2.3

\*Values listed are for bulk materials



The potential of Omniweave as a superior method of structural composite fabrication resulted in the funding by NASA-MSFC for an exploratory effort to investigate this fabrication concept.

The objective of this development program was to generate information for NASA-MSFC consideration relative to the manufacture and application of GE Omniweave fiber reinforced composites for possible use in launch vehicle structures.

The goals for this initial study were four-fold:

- a. Explore the manufacturing capabilities of the GE Omniweave process.
- b. Assess and modify the analytical methods used to predict Omniweave mechanical properties.
- c. Generate preliminary mechanical property data on Omniweave composites.
- d. Assess the capability of the Omniweave process to produce useful structural composites, particularly in relation to launch vehicle structural skin/honeycomb core sandwich constructions.

Section 3 describes in detail the experimental program plan used as a guideline towards achieving these program objectives.

Twenty-two Omniweave fabrics composites using S-glass, Morganite Type II, Thornel 50S, Boron and mixed fiber epoxy prepreg systems were produced to study the manufacturing potential of the Omniweave process. Four different Omniweave geometries were utilized. A description of the Omniweave concept and a summation of Omniweave fabrication is presented in Section 4.

A wide spectrum of mechanical data was generated on selected Omniweave composites including data on flexural, tensile, compressive and shear characteristics. These data are summarized in Section 5.

Analytical predictions of Omniweave property data and comparisons with test data are presented as a function of fiber type, fiber volume fraction and weave geometry in Section 6. In addition, a preliminary assessment of Omniweave structural capabilities as a launch vehicle structural honeycomb skin is presented in Section 6.

Section 7 summarizes the results of the study contract in detail and compares Omniweave property data to that of other filamentary composite materials reported in the literature.

Section 8 offers recommendations for further work leading to the improvement and utilization of Omniweave composites as efficient structural materials.

The contracted work was performed between June 31, 1969 and May 31, 1970.

**SECTION 3**  
**EXPERIMENTAL PROGRAM PLAN**

## SECTION 3

### EXPERIMENTAL PROGRAM PLAN

#### EXPERIMENTAL PROGRAM PLAN

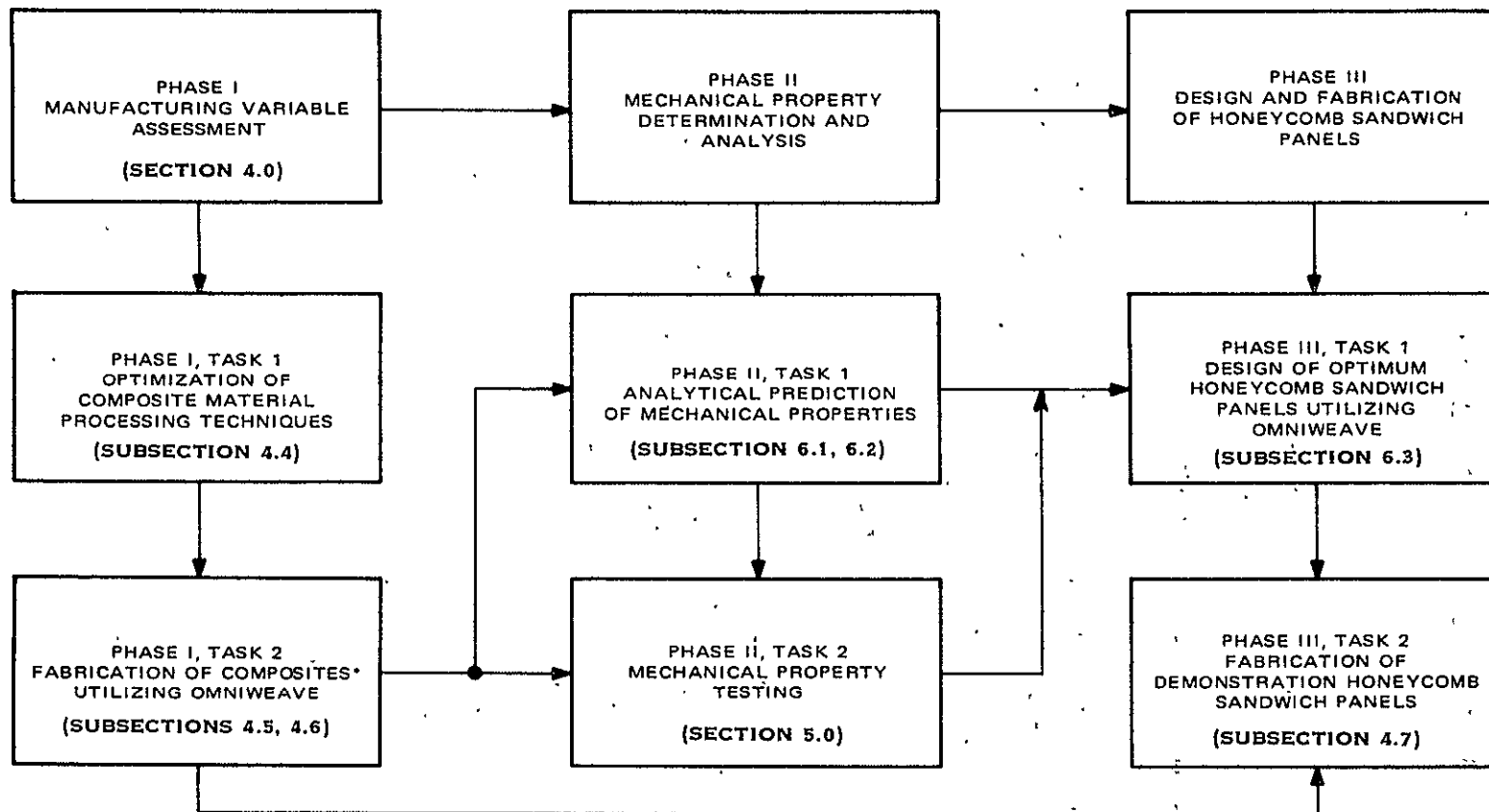
The primary goal of this study program is to note the effect of manufacturing process variables on physical and mechanical properties of Omniweave composites in relation to possible application to launch vehicle structures. The logic diagram shown in Figure 3-1 describes the program plan adhered to in order to meet these overall objectives.

Table 3-1 presents the Omniweave composite matrix. Twenty-two (22) epoxy resin composites of S-glass, Morganite Type II, Thornel 50S, boron (tungsten core) and mixed fiber systems were produced in Phase I. In addition, unidirectional S-glass/epoxy composites were fabricated for off-axis tensile evaluation to provide basic inputs needed for mechanical property predictions.

A significant portion of Phase I was devoted to improvement of manufacturing techniques such as weaving parameters and molding methods.

In Phase II, the "OMNI" computer program was employed to predict mechanical test performance of the fabricated composites. Flexural properties of most of the Omniweave composites were obtained during the preliminary screening phase and selected systems were further evaluated for tensile, compressive and shear properties.

In Phase III, the use of Omniweave composites for launch vehicle structural skins was analyzed. Several honeycomb core/Omniweave skin assemblies were produced and delivered to NASA-MSFC to illustrate the utility of Omniweave structural composites as launch vehicle components.



\*MATERIALS MATRIX IS GIVEN IN TABLE 3-1

Figure 3-1. Program Logic Diagram

TABLE 3-1. OMNIWEAVE MATERIALS MATRIX

Material	Weave Geometry	Thickness, Layers	Fabric Designation
S-Glass/USP23 Epoxy prepreg (9)	45 FPA	6	S21A-84
	45 FPA	12	S21A-91
	45 FPA	18	S21A-92
	45 LID	6	S21D-85
	45 LID	12	S21D-103
	45 LID	18	S21D-104
	18 LID	6	S21F-93
	18 LID	12	S21F-94
	45 FPA plus Longitudinals	12	S21A/L-204
Morganite-Type II/ USP23 epoxy prepreg (3)	45 FPA	12	G51A-86
	45 LID	12	G51D-96
	45 FPA plus Longitudinals	5	G51A/L-207
Thornel 50S/USP23 epoxy prepreg (1)	45 FPA	6	G71A-98
Boron (W Core)/ HT424 epoxy- phenolic resin (5)	45 FPA	6	I11A-101-1
		6	I11A-101-2
		6	I11A-101-3
		6	I11A-101-4
		6	I11A-101-6
Mixed Fiber Systems (4)			
50/50 Boron/HT424/ Morganite Type II/ USP 23	45 FPA	6	I11A-101-A
50/50 Boron/HT424/ S-Glass/USP23	45 FPA	6	I11A-101-9
25/75 Boron/HT424/ S-Glass/USP23	45 FPA	6	I11A-101-10
50/50 Morganite Type II/USP23/S-Glass/ USP23	45 FPA	6	I11A-101-11

**SECTION 4**  
**FABRICATION OF OMNIWEAVE COMPOSITES**

## SECTION 4

### FABRICATION OF OMNIWEAVE COMPOSITES

#### 4.1 INTRODUCTION TO OMNIWEAVE CONCEPT

Omniweave is the generic name for a weaving process which can produce a wide spectrum of multidirectionally reinforced fabrics by the controlled movement of warp yarns. All fiber ends are located in a weaving nest in which the fibers can be cycled into any direction by the combination of sequential X-directional and Y-directional nest shifts. Yarns move past each other at an angle  $\theta$  defined by  $\theta = \tan^{-1}$  Y-directional movement/X-directional movement. This angle  $\theta$  is termed the fiber pitch angle (FPA). To arrive at a better understanding of the Omniweave process, an examination of the yarn movements in a 45° FPA Omniweave cycle may prove helpful. These movements, and the relative simplicity of the process, are described for a 24-yarn construction in Figure 4-1. Each of the numbered squares in Figure 4-1 represents a warp end. The spacers lettered "E" are push rods which invade the weaving nest to direct traffic in a predesigned fashion. The corner squares are permanent "Stops"---no vertical or horizontal movement occurs in these rows. The 45° FPA weaving cycle may be broken down into four distinct operations (refer to Figure 4-1).

<u>Type of Motion</u>	<u>Cycle Step No.</u>	<u>Yarn Movement</u>
1. Horizontal Shifting	①→②	Rows A, C move 1 unit left Rows B, D move 1 unit right
2. Vertical Shifting	①→②	Rows E, G move 1 unit up Rows F, H move 1 unit down
3. Horizontal Shifting	②→③	Rows A, C move 1 unit right Rows B, D move 1 unit left
4. Vertical Shifting	③→④	Rows E, G move 1 unit down Rows F, H move 1 unit up
5. Horizontal Shifting	④→①	Repeat of ①→②

During this cycling procedure, yarns are transferred from row to row (travelling in depth). Upon close examination of Figure 4-1 it can be seen that all yarns move 1-unit in the hoop or fabric width direction followed by 1-unit movement in the fabric thickness or radial direction. The path followed by the yarn is described by the hypotenuse of the triangle formed by the X-Y coordinate travel; if the X-Y motions are of equal length (as in the case described above) a 45-degree FPA Omniweave is produced. Also, it may be noted that there are four paths followed by all the weaving fibers which are parallel to the diagonals of intersecting planes (Figure 4-2). Since these intersecting

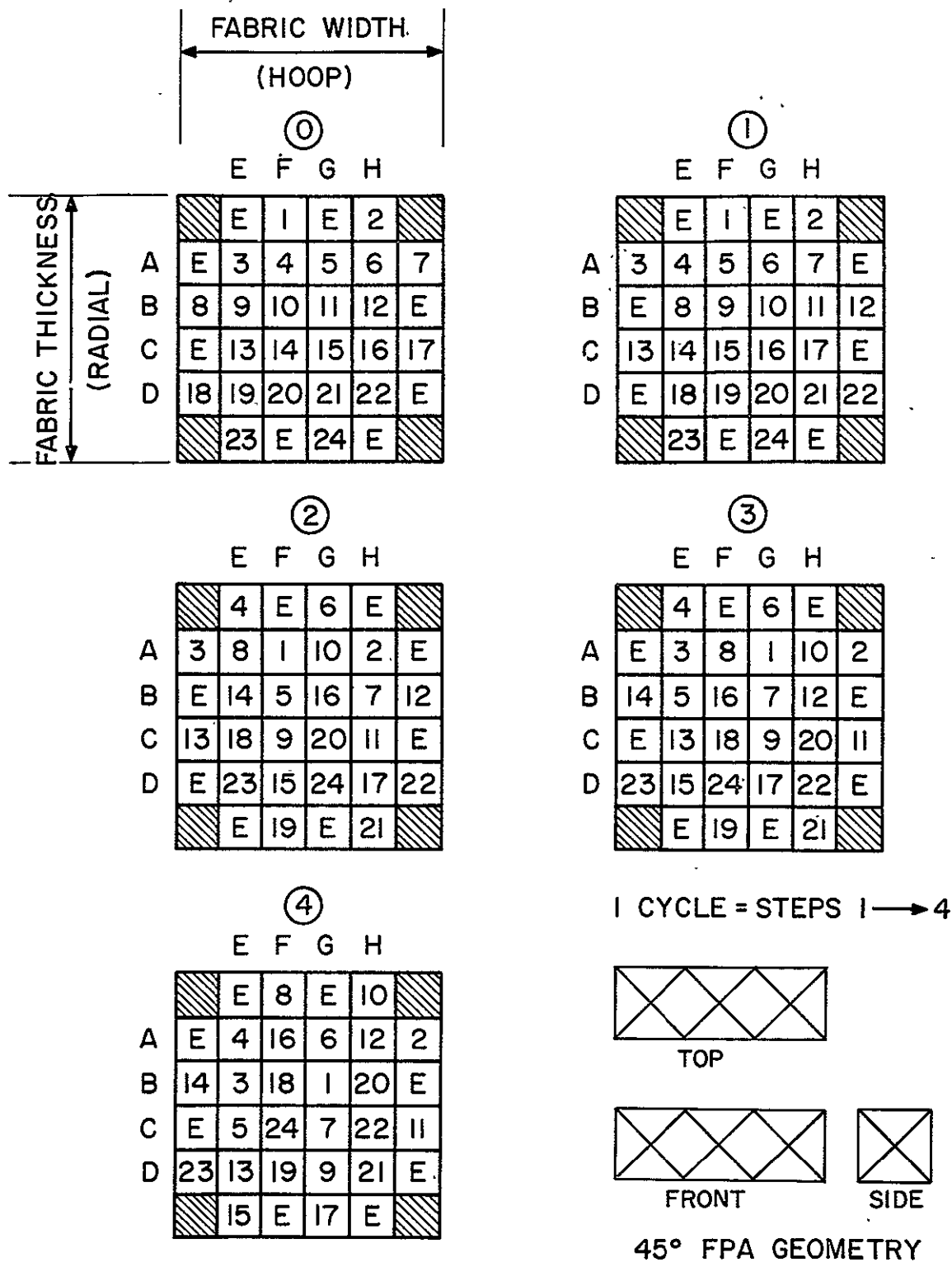


Figure 4-1. Standard Omniweave (45° Fiber Pitch Angle)  
Yarn Movement Mechanism



#### [4 - DIRECTIONAL FIBROUS REINFORCEMENT]

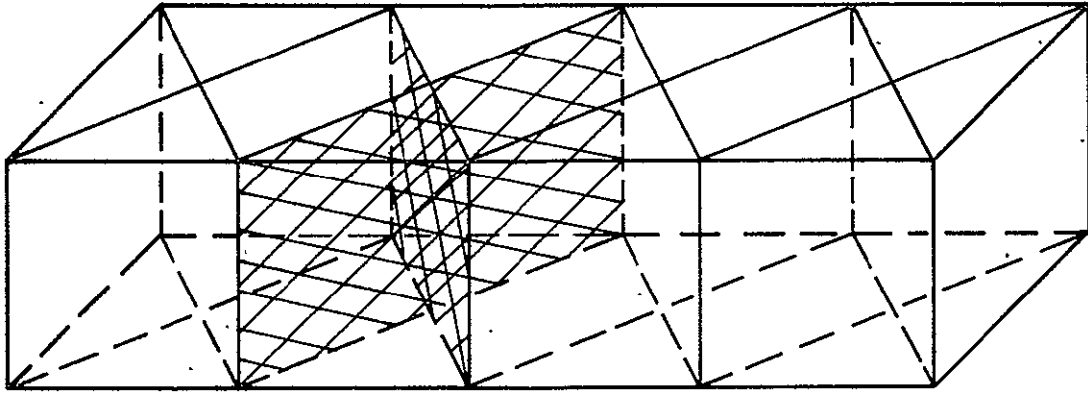


Figure 4-2. Fiber Pitch Angle Omniweave: Multidimensional Reinforcement in Which the Fibers Follow Paths Parallel to the Diagonals of Intersecting Planes

planes are perpendicular, a "caltrop" or "Body Centered Cubic" fiber array is produced, resulting in a geometry in which all fibers are theoretically 45-degrees to all orthogonal planes.\*

It may be shown from Figure 4-1 that a multitude of fiber geometries can be affected by manipulating the travel length of the row shifts. An odd unit vertical travel (moving 1, 3, 5, etc., units) will result in the fibers travelling through-the-thickness until they surface; an even unit vertical travel (2, 4, 6, etc., units) will cause the yarn to reverse direction and intraweave so that an interlocked, bias oriented knit fabric is produced. Manipulation of the row shifting directions, while keeping the unit travel constant, can result in other unique weave constructions such as the 45-degree layered-in-depth (LID) geometry (Figure 4-9). By holding alternate vertical rows constant, moving the horizontal rows two units and by changing the vertical row shift directions, a balanced fiber pitch angle weave containing longitudinals can be fabricated (Figure 4-11). Therefore, it can be seen from the foregoing discussion that Omniweave is a versatile weaving pattern which can produce many geometries of interest for a wide range of aerospace and commercial applications.

---

\*For this particular study, a 5 to 10-degree angle through-the-thickness was purposely sought to enhance in-plane properties.

#### 4.1.1 OMNIWEAVE PROCESSING

The GE Omniweave process currently uses finite filament lengths, the ends of which are connected to the nest array. Continuous fibers such as quartz, carbon or other unimpregnated or prepregged yarns are prepared into equal length units by spaced wrapping of the yarns onto a spoked mandrel (Figure 4-3). Each skein produced in this manner can contain up to 16 yarn bundles, each with a maximum length of six feet. These yarns are connected to the nest array and stressed so that equal lengths result. Attachment may proceed through an intermediate nylon monofilament coupling loop which is internally connected to a nest insert (Figure 4-4a). Discontinuous fibers such as Morganite Type II (meter length) and yarns which cannot be looped are attached by several techniques, one of which is heat-shrinkable tubing to splice the fiber to the filament/insert assembly, (Figure 4-4b). After loading, the weave fibers are combed thoroughly by inserting rods between parallel rows of yarn to prevent premature yarn crossovers and to remove slack prior to nest cycling. An Omniweave is produced by cycling the yarns in the weaving nest, followed by combing the crossovers to the prewoven length. Figure 4-5 illustrates the combing procedure.

Depending upon the particular Omniweave geometry, fiber handling characteristics, and intended application, the following combing options may be employed:

Weaving Fiber Conditions	Combing Tools	Weaving Packing Options
Lax (supported)	Full pin tooth comb	High packing pressure
Stressed (unsupported)	Full blade comb	Low packing pressure
	Partial blade comb	Fiber spreading
	Single blade comb	Fiber tensioning

When the weaving fibers are stressed (weighted) during the weaving process, the fiber crossovers assume an axial orientation with a shallow fiber angle in the radial direction. By weaving with the yarn ends supported (lax), the fiber crossovers assume an angle closer to the theoretical angle but with a lower fabric density.

A full pin tooth or full blade combing tool will simultaneously carry all stitches to the prewoven fabric length. Due to multiple fiber interferences, minimal fiber separation and low stitch density results. Weaving speed is significantly enhanced. A partial blade comb does allow for greater individual fiber separation and packing. The best combing implement is the single tooth comb since it can cause greater weave compaction by forcing individual crossovers closer to the prewoven length. This technique is the most time-consuming but results in significant enhancement of fabric density. Figure 4-6 presents photographs of specific combing devices.

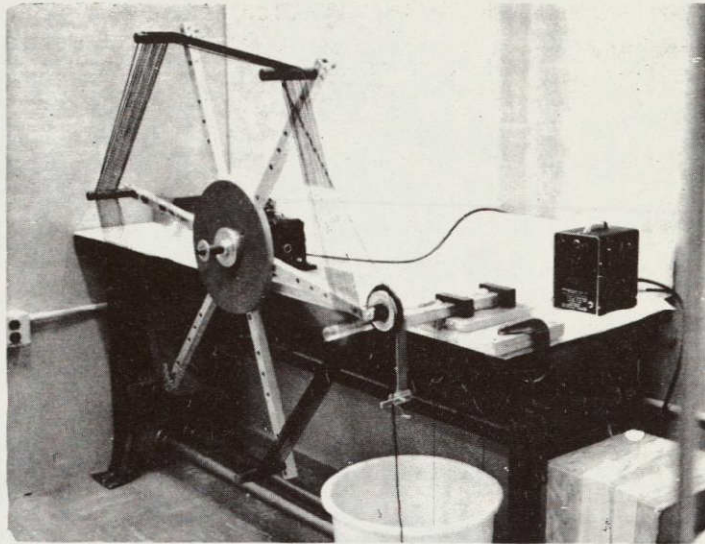


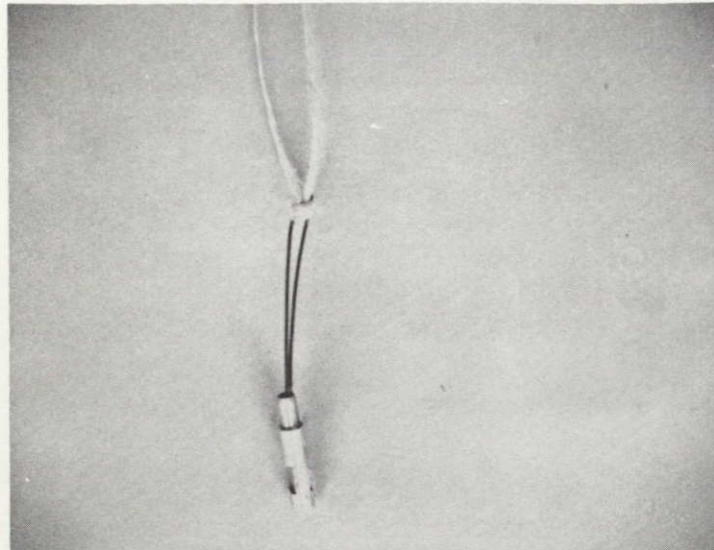
Figure 4-3. Yarn Preparation for use with Omniweave Equipment

Stitch packing by high comb pressure is a rapid weaving technique but increases the amount of fiber crimp. Low comb pressure packing results in a low density weave with a shallow radial angle but with minimal fiber damage. The fiber spreading technique will allow weave crossovers to nest fairly well and aids in weave densification. In the fiber tensioning approach, all weaving yarns are pulled away from the prewoven length, minimizing crimp and producing a weave approaching the theoretical limit in density. However, it is a time-consuming process which is not practical for the production of most weaves.

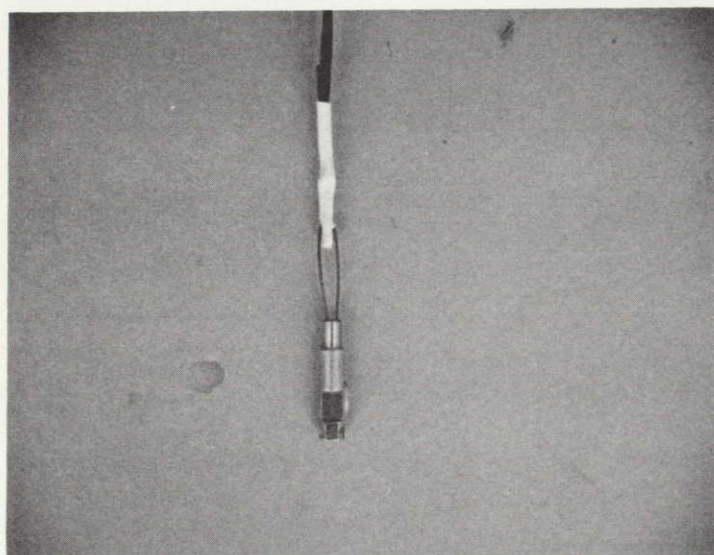
The Omniweave process has been operational for approximately one year during which time it has been learned what can and cannot be done with the equipment which was built primarily to demonstrate the potential of Omniweave. During this time period, improvements in yarn handling and combing techniques have been made which have resulted in higher woven fabric densities and weave uniformity.

The development of more sophisticated finite length equipment and continuous equipment (which may require no combing) will result in higher weave densities with greater uniformity produced at a lower cost. Continuous equipment will eliminate limitations due to finite yarn lengths and more complex Omniweave geometries and shapes will be fabricable.





a. Monofilament Coupling Attachment



b. Heat-Shrinkable Tubing Splice Technique

Figure 4-4. Yarn Attachment Techniques

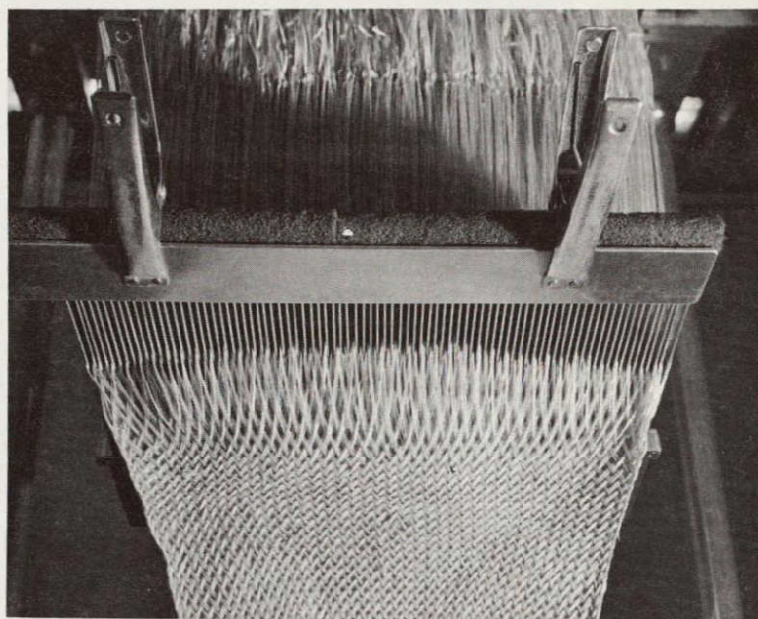


Figure 4-5. Combing of Stitch Crossovers

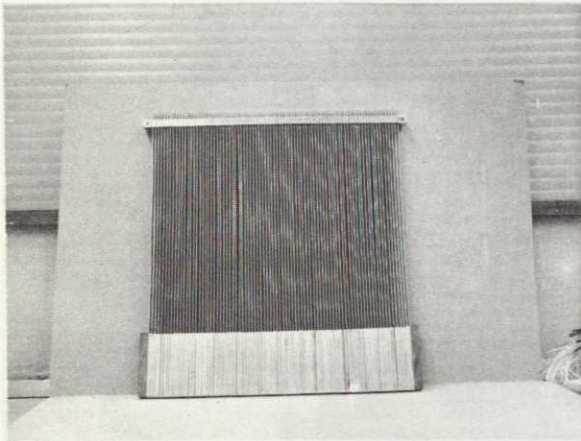
#### 4.1.2 SELECTED OMNIWEAVE GEOMETRIES

Four Omniweave configurations were selected for evaluation in this study program. These geometries furnish an insight into the effect of geometry on structural properties. These geometries were:

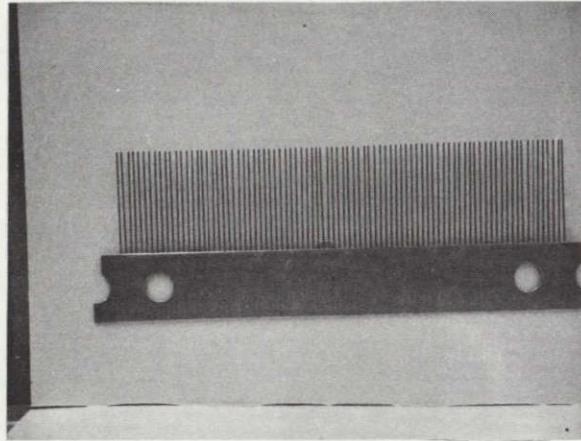
1. 45-degree Fiber Pitch Angle Construction (Figure 4-7a)
2. 45-degree Layered-In-Depth Construction (Figure 4-7b)
3. 18-degree Layered-In-Depth Construction (Figure 4-7c)
4. 45-degree Fiber Pitch Angle Construction with Longitudinals--(triaxial) construction (Figure 4-7d)

The 45-degree FPA geometry produces an Omniweave fabric very similar in construction to braid (Figure 4-2). Fibers travel from surface to surface passing each other at a constant radial angle of 5 to 45-degrees. As the radial angle is decreased, in-plane (axial and/or hoop) properties increase; as the radial angle gets steeper, an increase in radial or dynamic strength is observed. The 45-degree FPA Omniweave may be viewed as a starting point for composite property assessment since a significant amount of test data and analyses on other materials systems have been obtained (Figure 4-8).

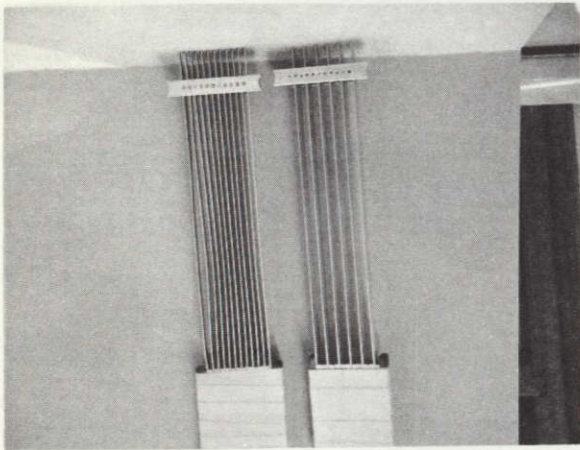




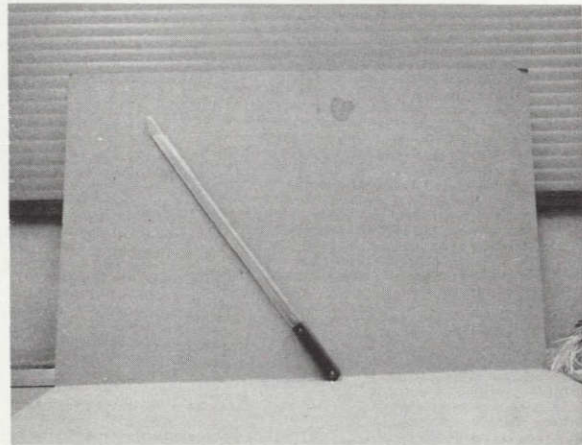
a. Full Width Blade Comb



b. Full Width Pin Tooth Comb

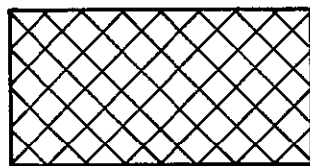


c. 12-blade Bayonet Comb (left)  
6-blade Bayonet Comb (right)

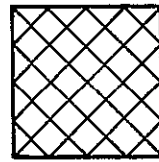
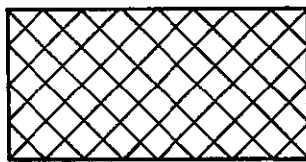


d. Single Blade Comb

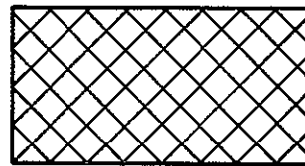
Figure 4-6. Omniweave Combing Devices



ORTHOGRAPHIC  
PROJECTION

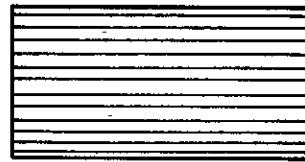


a. 45-degree FPA Geometry

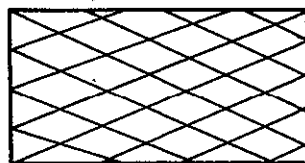


ORTHOGRAPHIC  
PROJECTION

[INTERLOCKED  
LAYERS]

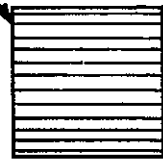
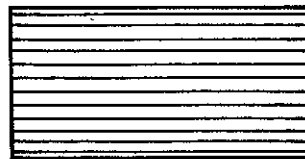


b. 45-degree LID Geometry

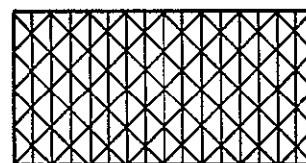


ORTHOGRAPHIC  
PROJECTION

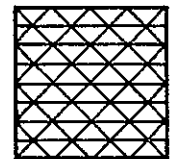
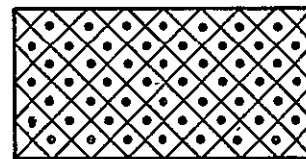
[INTERLOCKED  
LAYERS]



c. 18-degree LID Geometry



ORTHOGRAPHIC  
PROJECTION



d. 45-degree Triaxial Geometry

Figure 4-7. Selected Omniweave Geometries.

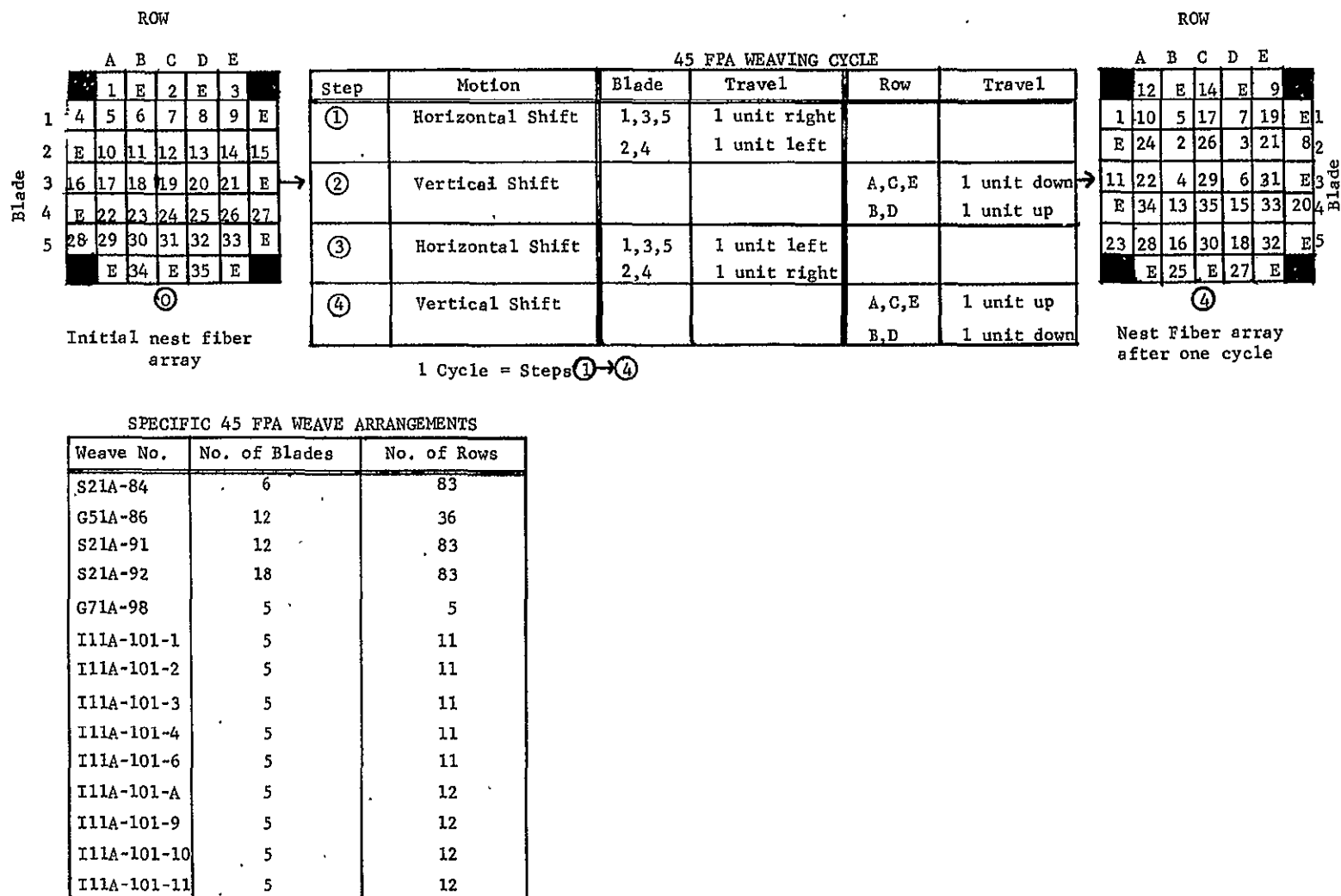


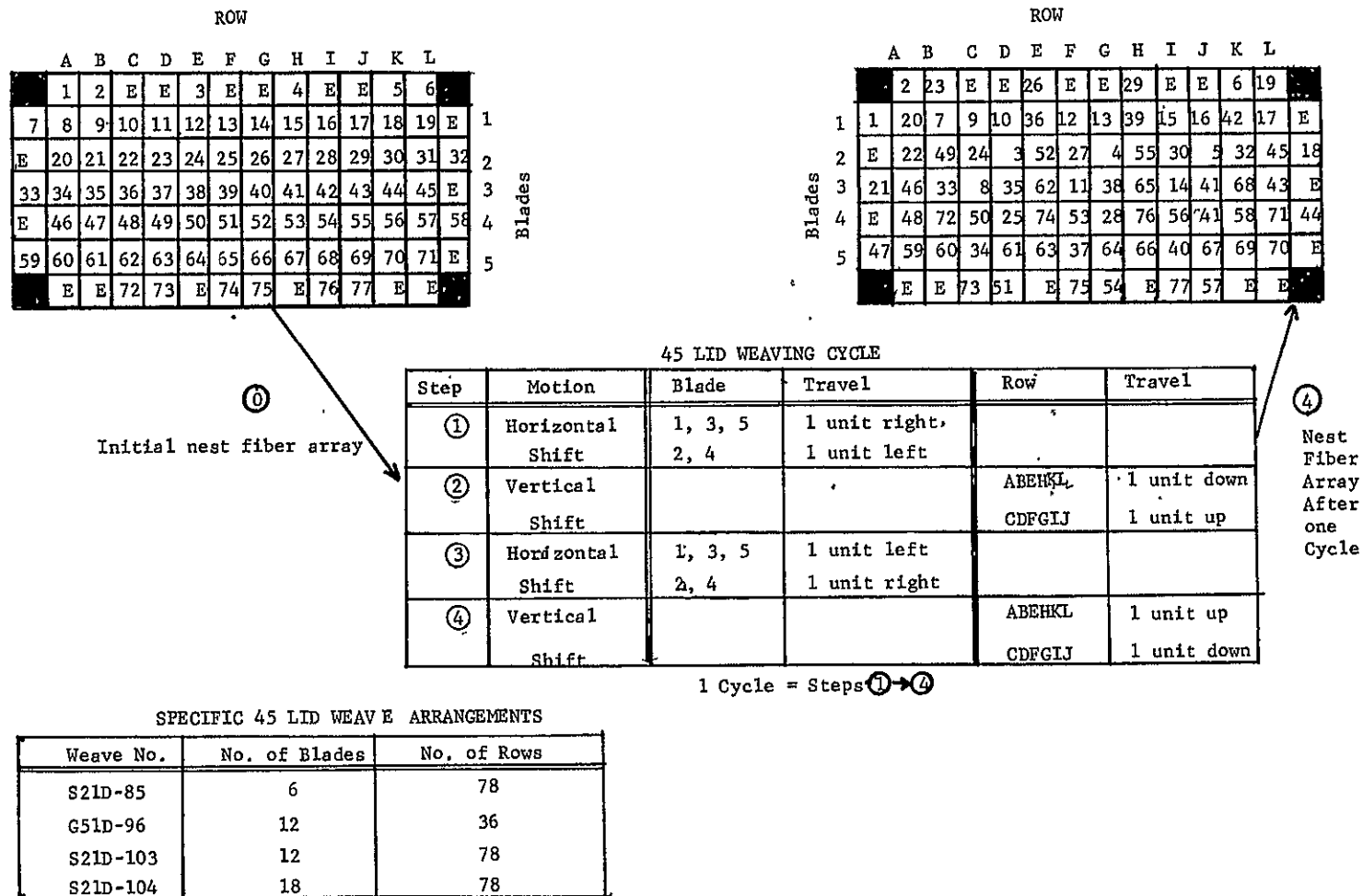
Figure 4-8. Yarn Movement Mechanism for 45-degree FPA Omniweave Geometry



An extremely attractive Omniweave configuration for the enhancement of in-plane structural properties is the 45-degree layered-in-depth (LID) construction. Nest yarn and cycling in the 45-degree LID geometry is similar to the 45-degree FPA design except that the vertical shifting sequence is changed from adjacent rows moving in opposite directions to a non-symmetrical shift sequence where two adjacent rows are moved in the same direction, while an adjacent single row is shifted in the opposite direction (Figure 4-9). This cycling scheme produced a highly interlocked planar weave in which fibers do not travel through-the-thickness but interlock with fiber layers in adjacent planes. (This weave may be compared to a bias-oriented laminated structure in which both warp and fill yarns travel in-depth to interlock with neighboring laminae). This geometry yields higher in-plane mechanical properties than a 45-degree FPA design. Due to the presence of many interlocking layers, interlaminar shear properties should be high.

The 18-degree LID Omniweave geometry is similar to the 45-degree LID construction, the major difference being that the weaving fibers are oriented at an angle more conducive to realizing greater hoop strength. This is achieved through the use of the yarn cycling sequence illustrated in Figure 4-10. However, due to fiber stiffness restraints and our current equipment limitations, yarn could not be effectively manipulated into this configuration.

The fourth Omniweave geometry produced for this study was a 45-degree FPA design with additional longitudinal fibers (triaxial fabric). This Omniweave design is affected by creating a 2-unit horizontal row shift pattern, creating non-moving rows in alternate vertical rows and by a change in the vertical shift cam (Figure 4-11). The fibers in the non-moving vertical rows weave in as longitudinals. This particular weave has fiber components travelling axially and in the bias direction. Its properties should be similar to those for the 45-degree FPA weave but with enhanced axial structural properties.



USE OR DISCLOSURE OF REPORT DATA IS SUBJECT TO THE RESTRICTION ON THE TITLE PAGE OF THIS REPORT

Figure 4-9. Yarn Movement Mechanism for 45-degree LID Omniweave Geometry

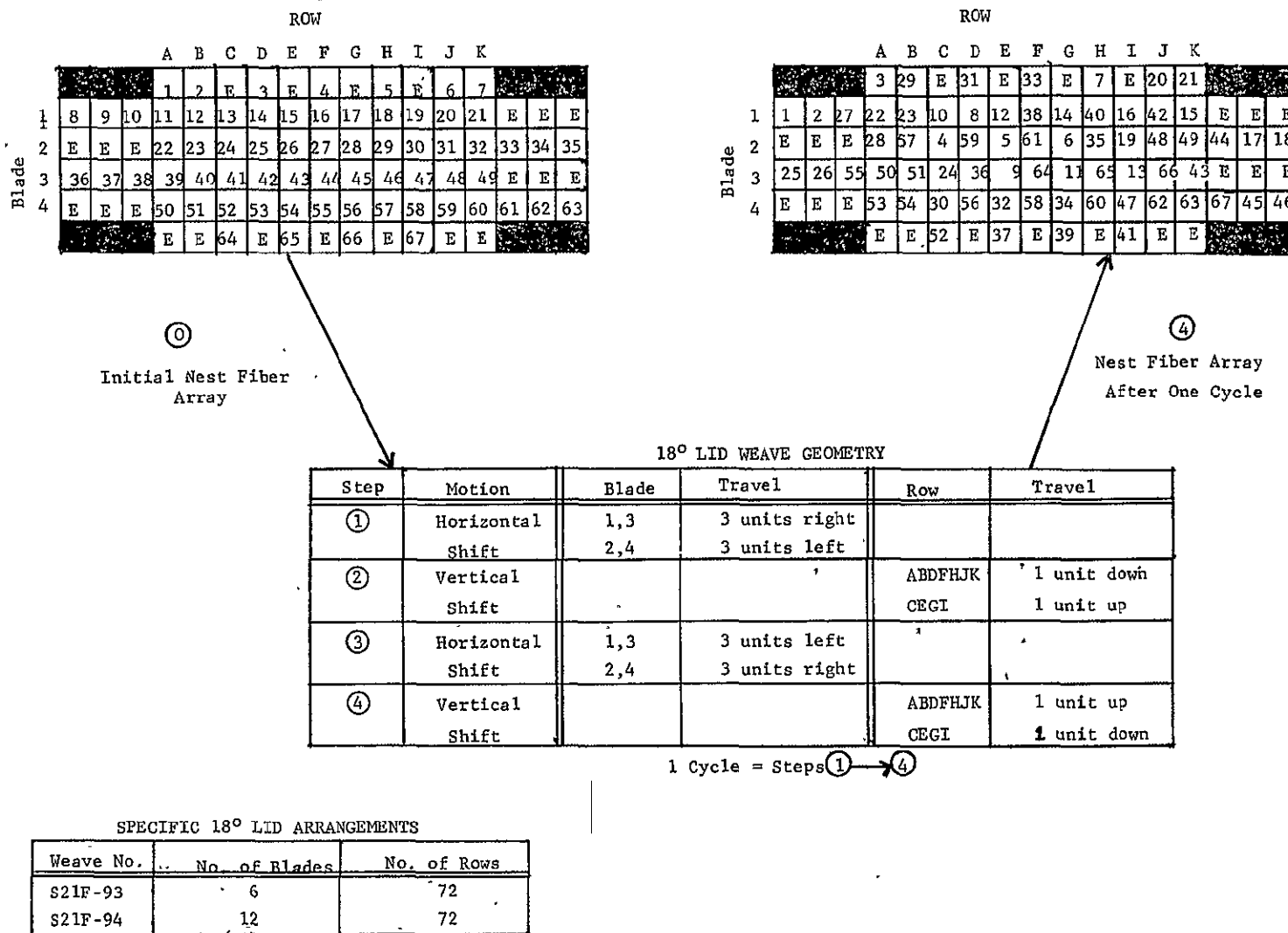


Figure 4-10. Yarn Movement Mechanism for 18-degree LID Omniweave Geometry

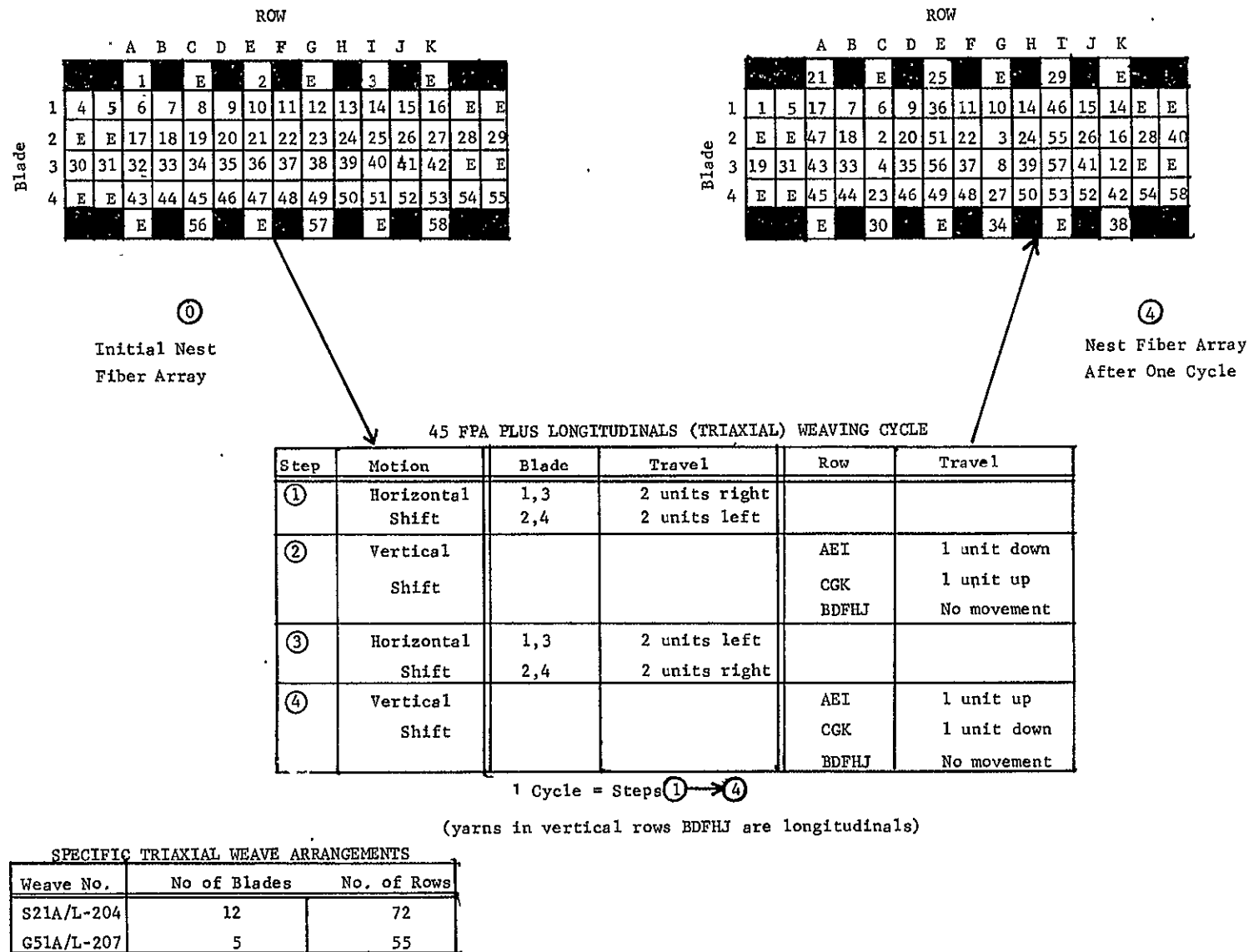


Figure 4-11. Yarn Movement Mechanism for Triaxial Omniweave Geometry

## 4.2 MATERIALS SELECTION

### 4.2.1 FIBER SELECTION

A relatively inexpensive reinforcement, S-glass 20-end roving, was selected as the baseline material to study the effect of weave geometry on composite performance and to prepare unidirectional and off-axis test coupons to study the degree of translation of fiber strength and modulus to Omniweave configurations.

Ten thousand filament end Morganite Type II roving was chosen for its high specific strength and moderate specific modulus character. Ten thousand filament end roving was the only form in which this fiber was available. Previous efforts had indicated its suitability for weaving.

Thornel 50S 2-ply yarn has a high specific modulus with moderate specific strength. It had never been processed on Omniweave equipment.

Boron (tungsten core) 1/8-inch wide filament tape was selected for its high specific strength and modulus. This contract initiated the first weaving of this prepreg.

All of the fibers selected for fabrication into Omniweave composites--S-glass, Morganite Type II, boron, and Thornel 50S--represent well characterized and commercially available materials which have high specific strength characteristics. In addition, boron (tungsten core) and Thornel 50S have high specific moduli which may prove to be beneficial for this and other structural applications. Table 4-1 summarizes the characteristics of the selected fibers. All reinforcement with the exception of boron\* were woven as prepreg using USP23 epoxy resin. Thus, the selected fibers exhibit a wide range of structural properties which are useful for the production of efficient structural composites.

### 4.2.2 RESIN SELECTION

USP23, a proprietary epoxy resin developed by the US Polymeric Company, Incorporated, Santa Ana, California, was selected as the resin prepreg for all the fiber reinforcements\*. USP23 was selected for use because of the following factors.

1. This resin material was reported to have good strength, modulus and toughness performance (Table 4-2).
2. USP23 epoxy can be utilized as a prepregging resin resulting in a coated fiber suitable for weaving on Omniweave process equipment. The prepreg is dry (non-tacky) flexible, and abrasion resistant.

---

\*Due to non-availability of boron filaments from vendor sources, HT424/boron was used to substitute for USP23/boron at a later date in the program.

TABLE 4-1. FIBER CHARACTERISTICS (2, 3)

Material	S-Glass	Morganite Type II	Thornel 50S	Boron(w) Core
Fiber Form	20 end roving	10,000 filament tow (continuous)	4 strands of 2 ply yarn	collimated 1/8" wide tape
Filament Diameter	10	7.5	6.6	100
Density, g/cc	2.49	1.78	1.68	2.62
Tensile Strength psi	500,000	400,000*	220,000	380 to 600 x 10 <sup>3</sup>
Tensile Modulus x 10 <sup>-6</sup> , psi	12.3	35 - 45*	50	60

\*Test data indicates that actual fiber modulus and strength were  $28.5 \times 10^6$  psi and 250,000 psi (See Section 7.2).

TABLE 4-2. RESIN CHARACTERISTICS

Property	USP23 Epoxy Resin <sup>(4)</sup>	HT424 Epoxy-Phenolic Resin <sup>(5)</sup>
Tensile Strength	12,000 psi	8,000 psi
Tensile Modulus	540,000 psi	500,000 psi
Flexural Strength	18,000 psi	—
Flexural Modulus	310,000 psi	—
Compressive Strength	17,600 psi	—
Compressive Modulus	580,000 psi	—
Specific Gravity	1.20 gm/cc	1.22 gm/cc
% Elongation (75° F)	3.5 - 4.5	—
Coefficient of Linear Expansion	$4.5-5.0 \times 10^{-5}$ in/in°F	—
Poisson's Ratio	0.40	—
Shear Strength	9,000 Johnson Shear	—

3. The resin has a long storage life at room temperature (approximately one year) making it possible to order all prepreg at the onset of the program and being able to use it at any time within the contract duration.
4. US Polymeric has had extensive experience with this resin system so that problems in non-uniformity and batch-to-batch variations in the prepreg could be minimized.

All prepreg, with the exception of boron, was processed using USP23 epoxy. HT424 epoxy-phenolic resin was used to coat the boron tape. This prepreg system was selected on the basis of its extensive development and characterization by GE-RES<sup>(5)</sup>. Table 4-3 summarizes the characteristics of all the prepregged reinforcement utilized in this study.

TABLE 4-3. Prepreg Fiber Characteristics<sup>(6)</sup>

Material	S-Glass 901 Epoxy/ USP-23 Prepreg		Morganite Type II/ USP23 epoxy prepreg	Thornel 50S USP23 epoxy Prepreg	Boron (Tungsten Core) Epoxy phenolic prepreg
US Polymeric Lot Number	W-1369	W-1441	W-1398	W-1404	W-1079    W-1083
Quantity, lbs.	70	15	14	12	5
Prepreg Form	20 end roving	20 end roving	10,000 filament continuous tow	4-Yarn tape	1/8" wide tape, 29 Filaments
Resin Content	20.0 to 23.1%	25.0 to 26.5%	33.4 to 38.0%	33.4 to 34.9%	38 - 42%
Volatiles	0.6 to 0.9%	0.0 to 1.2%	3.8 to 5.5%	3.9 to 5.5%	< 10%
Time	10 min.	10 min.	10 min.	9 min.	10 min.
Temp.	325° F	325° F	325° F	325° F	325° F
Weave Use	S21A-84 S21D-85 S21A-91 S21A-92 S21D-103 S21D-104 I11A-101-9 I11A-101-10 I11A-101-11	S21F-92 S21F-93 S21A/L-204	G51A-86 G51D-96 G51A/L-207 I11A-101-A I11A-101-10	G71A-98	I11A-101-1 I11A-101-2 I11A-101-3 I11A-101-4 I11A-101-A I11A-101-6 I11A-101-9 I11A-101-10



### 4.3 FABRICATION OF UNIDIRECTIONAL TEST COUPONS

In order to arrive at more realistic estimates of Omniweave composite properties, it is necessary to determine the resin/fiber shear interface properties. These data were obtained from a series of off-axis instrumented tensile tests on unidirectional composites. These data served as a basic input to the "OMNI" computer code (See Section 6.1) to determine the constants in the equations used for analytical prediction of composite properties. Unidirectional test coupons oriented at 0, 20, 45, 60 and 90-degrees were prepared using the following procedure (test data appear in Section 5.1):

The S-glass/USP23 prepreg was circumferentially wound on an 11-inch diameter by 12-inch long cylindrical mandrel. The feed advance was adjusted to the average width of the prepreg (2/25-inch advance/revolution) to minimize overlap and gaps while winding. When a layer of circumferentials was completed, it was removed from the mandrel and flattened into a 12-inch by 34-inch sheet. The sheet was then cut into 8-inch by 10-inch plies which were stacked 11 deep in an 8-inch x 10-inch compression mold. The panel was then given the cure cycle shown in Table 4-4b. This cure cycle yielded panels which were essentially transparent in the 1/8-inch thickness. The panels were characterized (Table 4-5) and tensile samples machined at the desired orientations.

TABLE 4-4. OMNIWEAVE CURE CYCLES FOR USP23 EPOXY COMPOSITES

a. Original Cure Cycle		
Time (min.)	Temperature (°F)	Pressure (psi)
8-10	R.T. to 150	100
30	150	100
10-12	150-250	100
30	250	100
30	250	1000
5-6	250-300	1000
60	300	1000
Air Cool	300 - R.T.	1000
b. Modified Cure Cycle		
Time (min.)	Temperature (°F)	Pressure (psi)
5	R.T.	1000
30	R.T. to 250	100
30	250	100
30	250	1000
15	250-300	1000
60	300	1000
30	300 to R.T.	1000

TABLE 4-5. S-GLASS/USP23 UNIDIRECTIONAL COMPOSITE  
CHARACTERIZATION

Parameters	Panel #1 0°, 20°	Panel #2 90°	Panel #3 60°	Panel #4 45°
Density	1.98	1.97	1.94	1.90
Wt. % Resin	24	27	25	27
Wt. % Fiber	76	73	75	73
Porosity	0	0	1	2
Vol. % Resin	40	44	40	43
Vol. % Fiber	60	56	59	55

#### 4.4 PRELIMINARY PROCESSING STUDIES

##### 4.4.1 S-GLASS/USP23 PREPREG

The S-Glass/USP23 prepreg was highly uniform, non-tacky and flexible. It was utilized immediately to provide full size Omniweave panels. Portions of the S-Glass/USP23 Omniweave S21A-84 and S21D-91 were molded in accordance with a cure cycle furnished by US Polymeric (Table 4-4a). These composites were non-uniform in appearance due to the dominance of resin-rich and resin-starved areas, and poor fiber wetting. This non-homogeneity was rectified by the installation of a new cure cycle (Table 4-4b) which did not provide for a time dwell at 150° F. Most S-glass Omniweave panels were fabricated using this cure cycle.

##### 4.4.2 MORGANITE TYPE II/USP23

The Morganite prepreg was processed by US Polymeric in a similar manner to the S-glass prepreg so that weaving and curing parameters would be similar. The resin content of the Morganite prepreg was higher yet this did not adversely affect processing characteristics. No significant problems were encountered in using this prepreg system.

##### 4.4.3 THORNEL 50S/USP23

The filaments were collimated into 8-ply bundles (4-strands) which were subsequently prepregged and staged in a similar manner to the Morganite and S-glass prepreg material. The individual Thornel bundles assumed a flat or ribbon configuration which was extremely sensitive to bending damage. The prepreg quality varied from spool to spool, none of it really suitable for weaving.

The Thornel 50S prepreg was received as a level wound prepreg separated by parting sheets on 6-inch diameter spools. The prepreg system was extremely difficult to remove from these spools and generally broke and fractured at the spool surface.

A 6- by 7-element Omniweave strip was successfully woven into a trial weave by exercising extensive care. Extremely low combing pressure was used and about 10 to 15 percent of the weaving elements shattered during the weaving trial.

Several attempts were made to prepare a 6-layer by 36-yarns/layer 45-degree FPA Omniweave strip using this Thornel 50S/USP23 prepreg. In the first attempt, the prepreg was loaded into the weaving nest without any pretreatment. During the first combing operation, about 10 percent of the weaving yarns broke in a brittle fracture mode. These loose yarns interfered strongly with oriented yarns on subsequent combing operations causing more extensive fiber fracturing. This weaving attempt was then aborted.

Prior to the second full size weaving attempt, several lengths of prepregged Thornel 50S were coated with various lubricant or diluent materials such as polyethylene glycol, water, acetone, methanol and combinations of these materials. Then the treated prepreg was handled and combed to note if any of these coatings could minimize fiber damage. The coating mixture of 25 parts Polyethylene Glycol and 75 parts water exhibited greater flexibility, toughness, and less tack than the others and another weaving attempt was made using this treated prepreg. Again, significant yarn damage and fracture occurred during combing due to the presence of brittle regions and varying tackiness along the fiber lengths. This weave was then aborted.

Efforts were then redirected to weaving non-prepregged Thornel 50 yarn. This yarn can bend around a 1-inch diameter rod without visible damage and when heavily coated with water and did not fray severely under several simulated combing trials.

The water-coated Thornel 50 yarn was being loaded into the carrier blades for another weaving attempt when a program change was made to delete Thornel 50 from the Omniweave material matrix. Consequently, all work stopped on the fabrication of Thornel 50 Omniweave materials.

#### 4.4.4 BORON (W) CORE/HT424 RESIN

A 1/8-inch wide Boron/HT424 prepreg tape was procured. The prepreg was in the form of a wide thin ribbon which had non-tacky characteristics and could tolerate only slight bending. The 1/8-inch tape was cut into 2-foot lengths and positioned into a 6 x 6 (36-element) 45-degree FPA weaving nest by a metal hook attachment through a heat shrinkable tubing coupling. Combing was done after each half-cycle using low comb pressure and little fiber damage was observed. This trial weave indicated that boron can be successfully woven on current finite length Omniweave equipment. Later attempts to weave thicker sections proved to be unsuccessful and all boron strips woven on the program were 6-layers wide by 11-units in width (0.050 - 0.060-inch molded thickness).

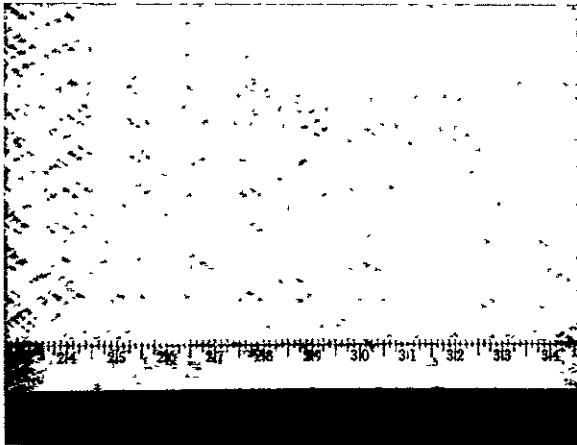


Figure 4-12. S21D-85 Omniweave Fabric

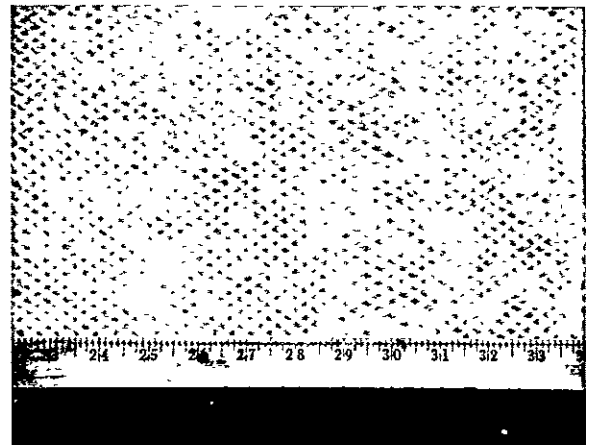
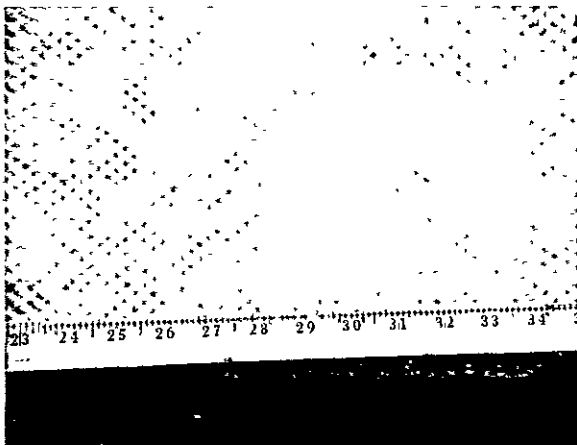
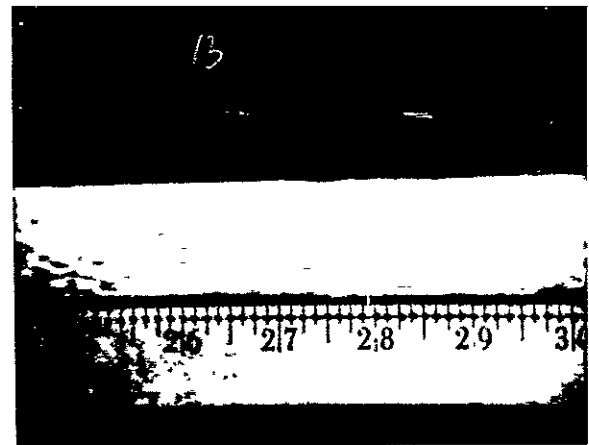


Figure 4-13. S21A-91 Omniweave Fabric



(a) Top View



(b) Side View

Figure 4-14. S21A-92 Omniweave Fabric

#### 4.5.1.5 Fabrics No. S21F-93, S21F-94

The weaving nest set-up for these weaves is shown in Figure 4-10. The fibers were skeined into 43-inch length units and attached to the carrier blades using the mono-filament coupling device. This first attempt to weave a fine textured 18-degree LID weave was relatively unsuccessful. The prepreg yarn had a tendency to spread and twist. Also, it had a rougher surface than yarns from the previous vendor batch. The weaves exhibited non-uniformity due to combing difficulties and the inability to approach the intended fabric geometry. Combing was accomplished using a single tooth comb which was sequentially positioned between every insert row. Individual stitches were forcibly pushed to the prewoven length where the interstitch region was spread by replacing the tooth comb with a 1/2-inch diameter rod, and applying downward force. The woven weight was unsupported. Figures 4-15 and 4-16 illustrate weave non-uniformity.

#### 4.5.1.6 Fabric No. S21D-103

The weaving nest set-up for S21D-103 fabric is illustrated in Figure 4-19. It was woven simultaneously with S21D-85 and was processed in an identical manner. Figure 4-17 is a photograph of this fabric.

#### 4.5.1.7 Fabric No. S21D-104

The weaving nest set-up for S21D-104 is shown in Figure 4-9. This weave was processed using techniques developed for S21D-85. Figure 4-18 is a photograph of a segment of this fabric.

#### 4.5.1.8 Fabric No. S21A/L-204

The weaving nest set-up for S21A/L-204 is shown in Figure 4-11. Weave S21A/L-204 was the first attempt to weave a triaxial fabric, i.e., a 45-degree FPA fabric with woven longitudinals. Using techniques similar to those employed on certain weaves such as S21A-84 resulted in loose packing density due to interference from the longitudinal yarns, whose vertical drape drastically affected combing procedures. Figure 4-19 is a photograph of this fabric.

The first half of the woven length (3-1/2-inch) was combed using singular teeth to comb each stitch row. The weave weight was unsupported. High combing force with fiber spreading was employed. The weaving technique was then changed to one in which higher fiber packing and an equiaxial fiber network was produced. The weave was supported approximately 1-inch below the prewoven length, and, after combing with the single tooth blade, fibers on either side of the blade were tensed to remove fiber slack and crimp from the prewoven lengths. This new weaving approach, while assuring greater uniformity and packing density, was extremely time-consuming. For economic reasons, this weave was stopped after only a 7-inch total length was woven. A limited amount of test data was obtained from this geometry. Figure 4-20 illustrates the various regions of this triaxial fabric.

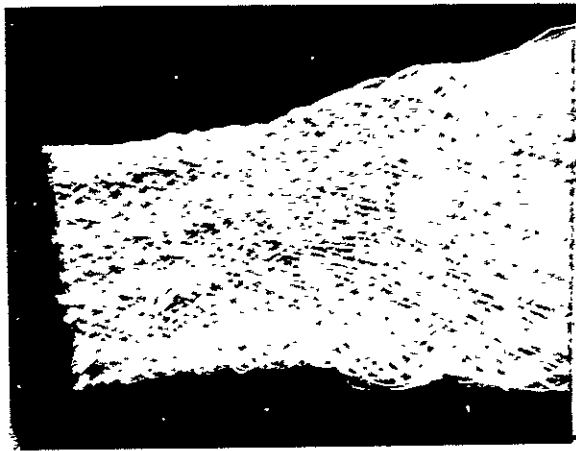


Figure 4-15. S21F-93 Omniweave Fabric      Figure 4-16. S21F-94 Omniweave Fabric

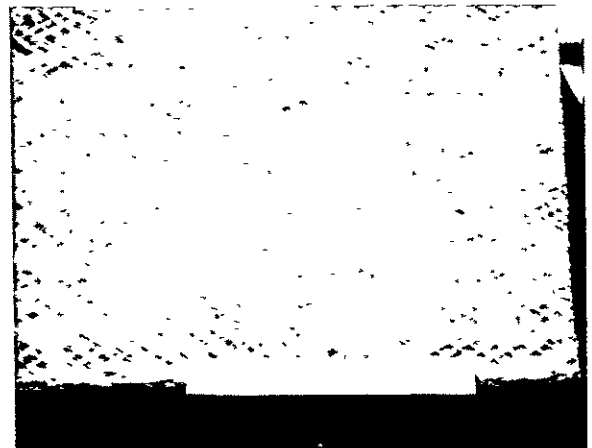
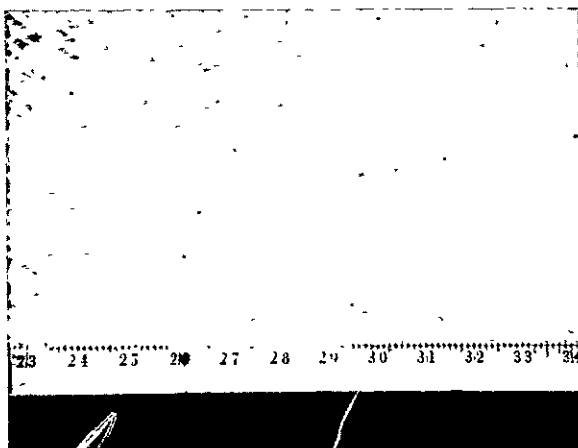


Figure 4-17. S21D-103 Omniweave Fabric      Figure 4-18. S21D-104 Omniweave Fabric

#### 4.5.2 MORGANITE TYPE II/USP23 OMNIWEAVE FABRICS

Three Morganite epoxy Omniweave fabrics were produced:

1. G51A-86 -- 12 layer 45-degree FPA Fabric
2. G51D-96 -- 12 layer, 45-degree LID Fabric
3. G51A/L-207 -- 5 layer 45-degree FPA and Longitudinals Fabric

##### 4.5.2.1 Fabric No. G51A-86

The weaving nest array for the G51A-86 prepreg fabric is illustrated in Figure 4-8. Morganite/USP23 was skeined into 43-inch length units and loaded into the insert carrier blades using a monofilament loop coupling. A six-blade bayonet comb was used to carry the weave crossovers to the prewoven length after each half-cycle. The weave was unsupported. A large fixed blade comb was inserted to ensure uniformity across the width after every cycle. Figure 4-21 is a photograph of this prepreg weave.

##### 4.5.2.2 Fabric No. G51D-96

The fiber movement mechanism for G51D-96 is shown in Figure 4-9. Morganite/USP23 was skeined into 43-inch lengths and loaded into the carrier blades using a monofilament loop coupling. The prepreg had many irregular regions along its length which prevented the use of a full size comb. After each half-cycle, a single tooth blade was inserted between each insert row and the weave crossovers were sequentially brought down to the prewoven length. Next, a six-blade alternate stitch comb was used to compact the weave followed by a 12-blade bayonet combing. The weave was unsupported.

##### 4.5.2.3 Fabric No. G51A/L-207

G51A/L-207 was woven as a shallow axial 45-degree FPA weave with additional woven longitudinal fibers. The yarn motions are described in Figure 4-11. The weave was unsupported during the entire weaving cycle. After each half-cycle, the weave crossovers were sequentially combed using a single tooth blade. Low combing pressure was utilized to affect a shallow axial fiber orientation with minimal fiber damage. Figure 4-22 presents a view of this particular fabric.

#### 4.5.3 THORNEL 50S/USP23 OMNIWEAVE FABRIC

Only one Thornel prepreg fabric, G71A-98, was produced. This was due primarily to weaving difficulties as discussed in Section 4.4.3. Also a change in program scope occurred after the first fabric was produced which resulted in Thornel 50S/USP23 being removed from the materials matrix. One tensile test was performed on this Thornel Omniweave composite.

##### 4.5.3.1 Fabric No. G71A-98

The nest arrangement for G71A-98 is shown in Figure 4-11. Four 2-ply prepreg yarn ends were attached to the nest using heat-shrinkable tubing coupled through a metal





Figure 4-19. S21A/L-204 Omniweave Fabric Weaving Conditions (Note vertical yarn drape during weaving)



Figure 4-20. S21A/L Omniweave Fabric (Note high and low fiber packing regions)

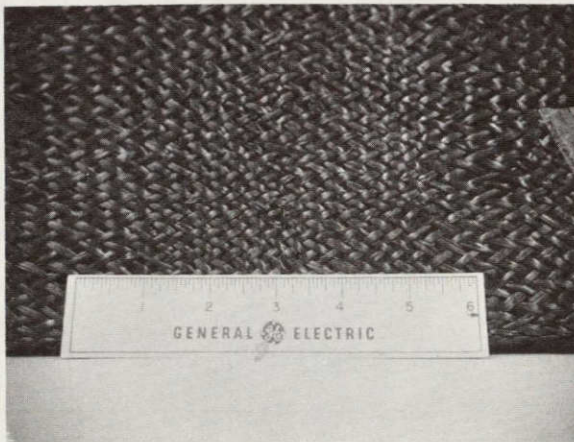


Figure 4-21. G51A-86 Omniweave Fabric

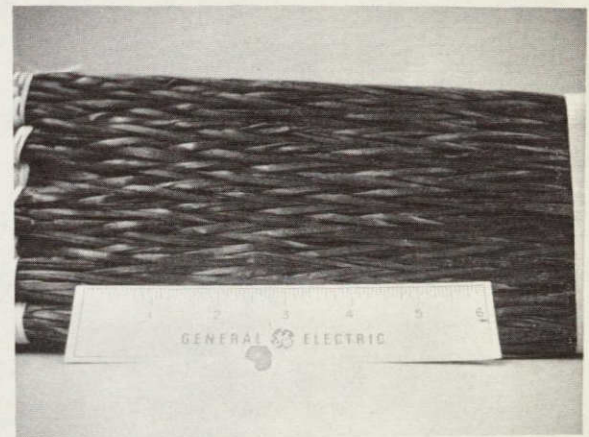


Figure 4-22. G51A/L-207 Omniweave Fabric



hook attachment. Combing was done using a singular tooth comb with weave packing proceeding after each half cycle. Low combing pressure was utilized to affect a shallow axial angle weave with minimal fiber damage.

#### 4.5.4 BORON/HT424 PREPREG OMNIWEAVE FABRICS

Five boron/HT424 Omniweave fabrics were woven:

- |               |   |                               |
|---------------|---|-------------------------------|
| 1. I11A-101-1 | } | 6 layer, 45-degree FPA Fabric |
| 2. I11A-101-2 |   |                               |
| 3. I11A-101-3 |   |                               |
| 4. I11A-101-4 |   |                               |
| 5. I11A-101-5 |   |                               |

All of these were made using the same weaving nest cycling sequence as illustrated in Figure 4-11 and identical weaving techniques.

The boron prepreg tape was attached to the weaving nest by a heat-shrinkable coupling to a nylon monofilament loop. A single tooth comb was utilized to sequentially comb weave crossovers after each half cycle. Special efforts were made during combing to prevent tape breakage. The yarn ends were held under mild tension and minimal combing pressure was exerted.

The original objective for weaves I11A-101 was to produce 4 to 6-inch wide, 6 and 12-layer boron Omniweave composites. Many attempts to do so were aborted because of excessive tape damage due to snarls, premature crossovers and entanglements of this brittle prepreg tape system. Since a wide strip could not be obtained on our present finite length equipment, it was decided to prepare many narrow strips of boron alone and boron in combination with other fibers to determine if there was a synergistic effect introduced in tensile properties. Subsection 4.5.5 discusses mixed fiber Omniweave fabric production.

#### 4.5.5 MIXED FIBER OMNIWEAVE FABRICS

Four mixed fiber narrow Omniweave fabrics were prepared:

1. I11A-101-A -- 50/50 Boron/HT424/Morganite Type II/USP23
2. I11A-101-9 -- 50/50 Boron/HT424/S-Glass/USP23
3. I11A-101-10 -- 25/75 Boron/HT424/S-Glass/USP23
4. I11A-101-11 -- 50/50 Morganite Type II/USP23/S-Glass/USP23

#### 4.5.5.1 Fabric No. I11A-101-A:

The nest set up for this mixed boron/Morganite system is shown in Figure 4-23a. Both fiber types were attached to the nest through a heat-shrinkable coupling to a monofilament loop attachment. The weave was combed in a manner similar to the techniques employed for weave I11A-101-1.

#### 4.5.5.2 Fabric No. I11A-101-9:

The nest set-up was identical to that employed for weave I11A-101-A except that S-glass replaced Morganite in the nest array. (Figure 4-23b). The boron was attached by the same technique as in I11A-101-1 with the S-glass prepreg looped through a monofilament attachment loop. Combing procedures was the same as that used for Weave I11A-101-1.

#### 4.5.5.3 Fabric No. I11A-101-10:

The nest set up for this weave is shown in Figure 4-23c. Methods of attachment and weaving procedures are the same as those used with weave I11A-101-9. Figure 4-24 is a photograph of this mixed fiber Omniweave fabric.

#### 4.5.5.4 Fabric No. I11A-101-11:

The weaving nest arrangement is illustrated in Figure 4-23d. Both filaments were attached to the nest inserts by looping through a nylon monofilament attachment. A single tooth comb was sequentially employed after each half-cycle while the weave yarn ends were maintained under moderate tension.



	M	E	M	E	M	E	M	E	M	E	M	E	
M	B	M	B	M	B	M	B	M	B	M	B	M	E
E	M	B	M	B	M	B	M	B	M	B	M	B	M
M	B	M	B	M	B	M	B	M	B	M	B	M	E
E	M	B	M	B	M	B	M	B	M	B	M	B	M
M	B	M	B	M	B	M	B	M	B	M	B	M	E
	E	B	E	B	E	B	E	B	E	B	E	B	

(a) Weave I11A-101A

	S	E	S	E	S	E	S	E	S	E	S	E	
S	M	S	M	S	M	S	M	S	M	S	M	S	E
E	S	M	S	M	S	M	S	M	S	M	S	M	S
S	M	S	M	S	M	S	M	S	M	S	M	S	E
E	S	M	S	M	S	M	S	M	S	M	S	M	S
S	M	S	M	S	M	S	M	S	M	S	M	S	E
	E	M	E	M	E	M	E	M	E	M	E	M	

(d) Weave I11A-101-11

	S	E	S	E	S	E	S	E	S	E	S	E	
S	B	S	B	S	B	S	B	S	B	S	B	S	E
E	S	B	S	B	S	B	S	B	S	B	S	B	S
S	B	S	B	S	B	S	B	S	B	S	B	S	E
E	S	B	S	B	S	B	S	B	S	B	S	B	S
S	B	S	B	S	B	S	B	S	B	S	B	S	E
	E	B	E	B	E	B	E	B	E	B	E	B	

(b) Weave I11A-101-9

	S	E	S	E	S	E	S	E	S	E	S	E	
S	S	S	B	S	S	S	B	S	S	S	B	S	E
E	S	S	S	B	S	S	S	B	S	S	S	B	S
S	B	S	S	S	B	S	S	S	B	S	S	S	E
E	S	B	S	S	S	B	S	S	S	B	S	S	S
S	S	S	B	S	S	S	B	S	S	S	B	S	E
	E	S	E	B	E	S	E	B	E	S	E	B	

(c) Weave I11A-101-10

M = Morganite Type II/USP23

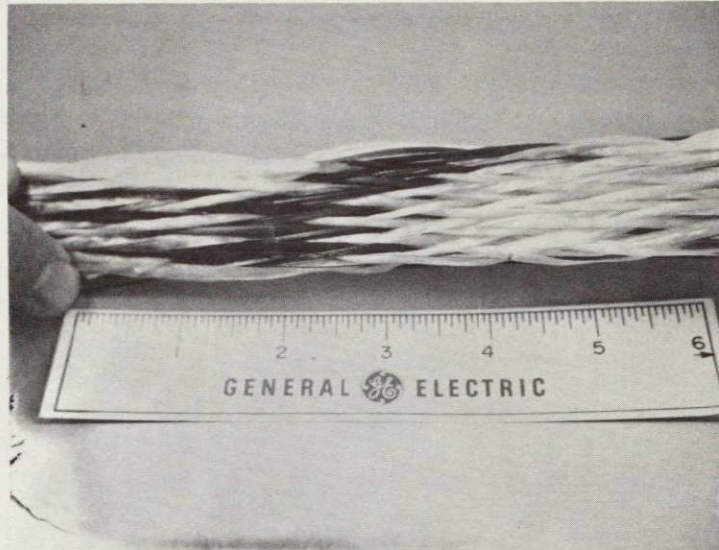
B = Boron (W Core) HT424

S = S-Glass/901/USP23

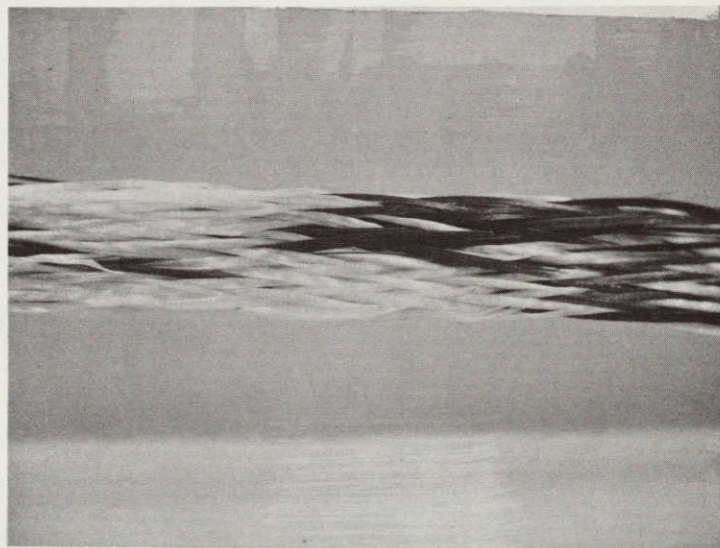
■ = Corner stop

E = Vacant yarn slot

Figure 4-23. Nest Fiber Arrays for Mixed Fiber 45-degree FPA Geometries



(a) Top Surface View



(b) Bottom Surface View

Figure 4-24. I11A-101-10 25/75 Boron/S-Glass Omniweave Fabric



## 4.6 OMNIWEAVE COMPOSITE FABRICATION

### 4.6.1 GLASS/USP23 OMNIWEAVE COMPOSITES

The resin and volatile contents of the prepregged glass Omniweave fabrics were determined prior to molding. The volatile content of the prepreg was determined by curing at 300°F for twenty minutes and measuring the weight loss. The resin content was determined by soxhlet extraction of the prepreg with dimethylformamide. The resin content of the prepregged Omniweave varied between 19 and 25 percent, and volatile contents averaged about one percent. Several trial Omniweave panels were molded at various conditions to determine the optimum cure cycle. (The manufacturer's recommended cure cycle produced poor quality panels). Cure cycles A and B (Table 4-7) yielded molded panels having high density and low porosity values. The resin content was determined by measuring panel weight loss after exposure to 1100°F for 8 hours. Densities of the molded parts ranged from 1.93 to 2.02 g/cc and resin contents from 20 to 26 weight percent. Table 4-8 presents a molding summary for the S-glass Omniweave composites.

### 4.6.2 MORGANITE/USP23 OMNIWEAVE COMPOSITES

The Morganite/USP23 prepreg Omniweave fabrics were characterized using the same methods as used for the glass fabrics. Resin contents varied between 33 and 38 weight percent, and volatiles averaged about one percent. Cure cycles A and B (Table 4-7) were used to mold the Morganite Omniweave panels. Densities of the molded parts were 1.44 to 1.48 g/cc with resin contents between 34 and 38 percent. The resin content of the Morganite panels was calculated by measuring the weight loss during molding and using procedures outlined in Section 10.1. Table 4-9 presents a molding summary for the Morganite Omniweave composites.

### 4.6.3 BORON, THORNEL AND MIXED FIBER OMNIWEAVE COMPOSITES

The molding conditions were modified to each Omniweave composite system. Eight inch lengths of these Omniweave strips were molded at their woven width (3/4-inch to 1-inch) in a steel slot mold. No prepreg analysis was performed due to the limited amount of material available. (Vendor figures on resin, volatile content were used). Table 4-10 presents a molding summary for these composites. Calculations used to determine resin/fiber contents are listed in Section 10.2.

TABLE 4-7. CURE CYCLES UTILIZED IN FABRICATING  
OMNIWEAVE COMPOSITES

Time (min)	Temperature (°F)	Pressure (psi)
(A)		
5	RT	1000
15	R.T. - 250°	100
30	250°	100
30	250°	1000
5	250 - 300°	1000
60	300°	1000
(B)		
Time (min)	Temperature (°F)	Pressure (psi)
5	R.T.	1000
15	R.T. - 300°	100
90	300°	1000
(C)		
Time (hr)	Temperature (°F)	Pressure (psi)
1	300°	100
8	350°	0
(D)		
Time (hr)	Temperature (°F)	Pressure (psi)
3	300°	1000
(E)		
Time (min)	Temperature (°F)	Pressure (psi)
20	R.T. - 250°	100
15	250°	100
15	250°	1000
5	250 - 300°	1000
60	300°	1000

TABLE 4-8. MOLDING AND CHARACTERIZATION OF S-GLASS/USP23 OMNIWEAVE COMPOSITES

Omniweave Fabric No.	Panel No.	Mold Cycle Table (4-7)	Molded Thickness (in)	Density (gm/cc)	Resin Content (wt. %)	Fiber Content (wt. %)	Porosity (vol. %)	Resin Content (vol. %)	Fiber Content (vol. %)	Test Samples
S21A-84	1	A	0.074	2.02	20	80	1	34	65	flexure
S21A-84	2	B	0.075	1.99	20	80	3	33	64	tensile, shear, compression
S21A-91	2	A	0.140	2.00	21	79	2	35	63	flexure
S21A-91	3	B	0.145	2.00	21	79	2	35	63	structural skin demonstration item
S21A-92	1	A	0.192	1.99	22	78	2	36	62	flexure
S21A-92	2	B	0.187	2.01	22	78	0	37	63	structural skin demonstration item
S21D-85	1	A	0.092	2.01	21	79	1	35	64	flexure
S21D-85	2	B	0.087	2.00	21	79	2	35	63	structural skin demonstration item
S21D-103	1	A	0.158	1.99	24	77	0	40	60	flexure
S21D-104	1	A	0.213	1.93	26	74	1	42	57	flexure
S21D-104	2	B	0.185	1.98	24	76	0	40	60	tensile, shear, compression
S21D-104	3	B	0.188	1.93	24	76	2	39	59	structural skin demonstration item
S21A/L-204	1	B	0.147	1.72	25	75	12	36	52	tensile, flexure
S21A/L-204	2	B	0.201	1.63	25	75	17	34	49	tensile, flexure



TABLE 4-9. MOLDING AND CHARACTERIZATION OF MORGANITE/USP-23 OMNIWEAVE COMPOSITES

Omniweave Fabric No.	Panel No.	Mold Cycle (Table 4-7)	Molded Thickness (in)	Density (gm/cc)	Resin Content (wt. %)	Fiber Content (wt. %)	Porosity (vol. %)	Resin Content (vol. %)	Fiber Content (vol. %)	Test Samples
G51A-86	1	A	0.235	1.47	38	62	2	47	51	flexure
G51A-86	2	B	0.193	1.48	36	64	3	44	53	
G51D-96	1	A	0.218	1.47	34	66	3	42	55	flexure
G51D-96	2	B	0.269	1.47	36	64	3	44	53	tensile, compression, shear
G51D-96	3	B	0.250	1.46	36	64	4	44	52	tensile, compression, shear
G51D-A/ L-207	1	B	0.336	1.47	36	64	3	44	53	flexure
G51DA/ L-207	2	B	0.231	1.48	36	64	3	44	53	tensile, compression, shear
G51DA/ L-207	3	B	0.180	1.44	36	64	5	43	52	tensile, compression, shear
G51D-A/ L-207	4	B	0.180	1.44	36	64	5	43	52	

TABLE 4-10. MOLDING AND CHARACTERIZATION OF BORON, THORNEL AND MIXED FIBER OMNIWEAVE COMPOSITES

Omniweave Fabric No.	Materials	Panel	Mold Cycle (Table 4-7)	Molded Thickness (in)	Density (g/cc)	Resin Content (wt. %)	Fiber Content (wt. %)	Porosity (vol. %)	Resin Content (vol. %)	Fiber Content (vol. %)
I11A-101-1	Boron/HT424	A	C	0.056	1.90	26	74	4	41	55
I11A-101-1	Boron/HT424	B	C	0.057	1.92	26	74	4	41	55
I11A-101-2	Boron/HT424	A	C	0.053	1.79	26	74	10	39	51
I11A-101-2	Boron/HT424	B	C	0.100	1.03	26	74	48	22	30
I11A-101-3	Boron/HT424	A	C	0.051	1.91	26	74	4	41	55
I11A-101-3	Boron/HT424	B	C	0.052	1.90	26	74	4	41	55
I11A-101-4	Boron/HT424	A	C	0.053	1.92	26	74	4	41	55
I11A-101-4	Boron/HT424	B	C	0.053	1.96	26	74	0	43	57
I11A-101-A	Morganite/USP23 Boron/HT424	A	D	0.115	1.41	22	41	14	26	32
						13	24		15	13
I11A-101-A	Morganite/USP23 Boron/HT424	B	D	0.117	1.30	22	41	20	24	30
						13	24		14	12
I11A-101-6	Boron/HT424	A	C	0.062	1.51	26	74	24	33	43
I11A-101-6	Boron/HT424	B	C	0.050	1.87	26	74	6	40	54
I11A-101-9	Boron/HT424 Glass/USP23	A	D	0.090	1.86	11	21	5	18	15
						14	53		23	39
I11A-101-9	Boron/HT424 Glass/USP23	B	D	0.084	1.90	11	21	3	18	15
						14	53		24	40
I11A-101-10	Boron/HT424 Glass/USP23	A	D	0.093	1.81	7	12	10	11	6
						19	62		28	45

TABLE 4-10. MOLDING AND CHARACTERIZATION OF BORON, THORNEL AND MIXED FIBER OMNIWEAVE COMPOSITES (Continued)

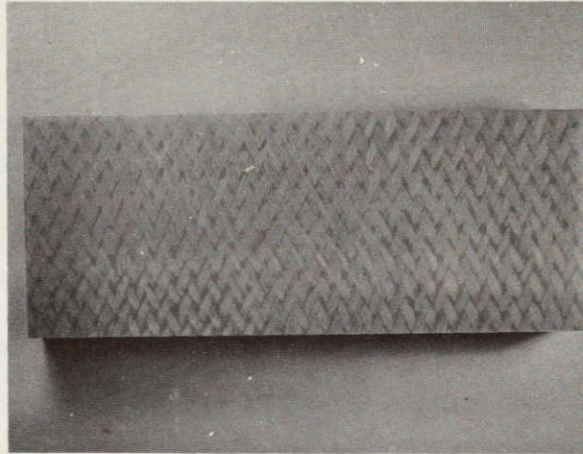
Omniweave Fabric No.	Materials	Panel	Mold Cycle (Table 4-7)	Molded Thickness (in)	Density (g/cc)	Resin Content (wt. %)	Fiber Content (wt. %)	Porosity (vol. %)	Resin Content (vol. %)	Fiber Content (vol. %)
I11A-101-10	Boron/HT424 Glass/USP 23	B	D	0.109	1.56	7 19	12 62	20	25	7 39
I11A-101-11	Morganite/USP23 Glass/USP23	A	E	-	1.72	27	27 46	12	38	18 32
I11A-101-11	Morganite/Glass/USP23	B	E	-	1.72	27	27 46	12	38	18 32
I11A-101-11	Morganite/Glass/USP23	C	E	-	1.70	27	27 46	13	38	18 31
G71A-98	Thornel 50/USP23	A	D	0.036	1.45	35	65	5	43	52

#### 4.7 FABRICATION OF OMNIWEAVE/HONEYCOMB DEMONSTRATION ITEMS

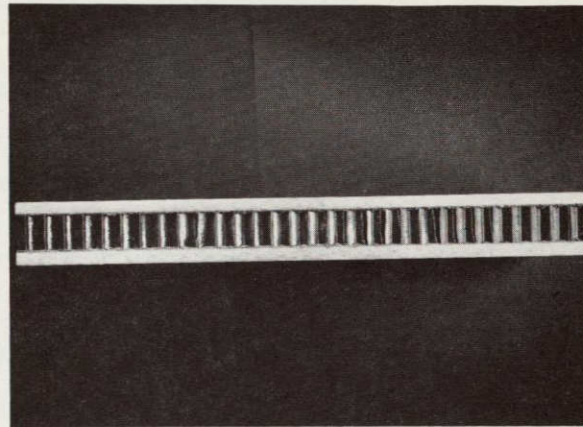
Part of the contractual requirements of this study was the delivery of several demonstration Omniweave structural skin/honeycomb sandwich constructions to the NASA Marshall Space Flight Center. The materials utilized were not optimized for the application and were provided solely for demonstrative purposes.

Two 8-inch x 3-inch glass-epoxy Omniweave/honeycomb composites were fabricated by bonding the Omniweave panels onto the honeycomb faces with HT435 film adhesive. The Omniweave bond surfaces were sand blasted followed by acetone wiping prior to adhesive application. The adhesive was cured under low pressure at 350° F for one hour.

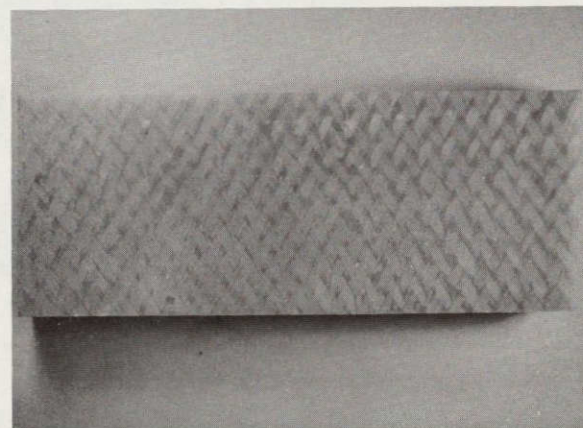
Omniweave/honeycomb composite A (Figure 4-25) consisted of two standard construction glass/epoxy Omniweave panels number S21A-91-3 (density = 2.00 g/cc; thickness = 0.145-inch) and S21A-92-2 (density = 2.01 g/cc; thickness = 0.187-inch) bonded to 1/2-inch thick, 1/4-inch cell size phenolic honeycomb. Composite B consisted of two layered-in-depth construction glass/epoxy Omniweave panels number S21D-85-2 (density = 2.00 g/cc; thickness = 0.087-inch) and S21D-104-3 (density = 1.93 g/cc; thickness = 0.188-inch) bonded to 1/2-inch thick, 1/4-inch cell size aluminum honeycomb (Figure 4-26).



(a) S21A-91 Structural Skin

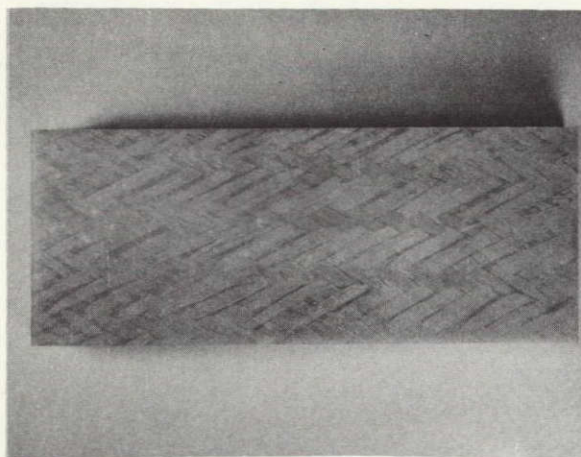


(b) Side View

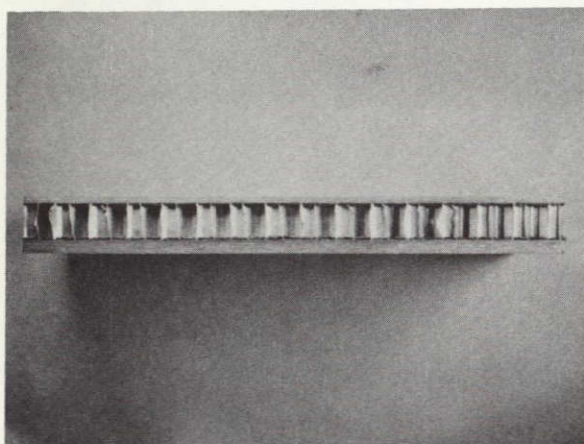


(c) S21A-92 Structural Skin

Figure 4-25. S21A-91/Plastic Honeycomb Core/S21A-92 Structural Sandwich Assembly (Overall Dimensions: 8" x 3" x 0.85")



(a) S21D-85 Structural Skin



(b) Side View

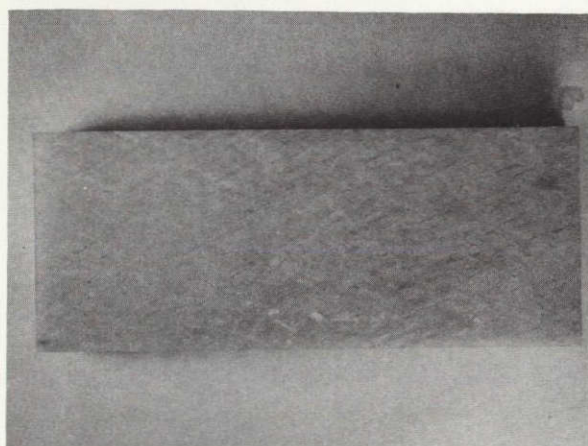


Figure 4-26. S21D85/Aluminum Honeycomb Core/S21D-104 Structural Sandwich Assembly (Overall Dimensions: 8" x 3" x 0.8")



#### 4.8 SUMMARY AND CONCLUSIONS

The work performed on this initial study demonstrates the feasibility of the Omniweave process to weave multidirectional fiber constructions using S-glass, Morganite Type II, Thornel 50S, and boron prepregged fibers. Also, mixed fiber systems (boron/S-glass, boron/Morganite and Morganite/S-Glass) were successfully fabricated.

S-Glass and Morganite prepreg were the easiest fibers to process; the more brittle Thornel 50S and boron presented severe weaving problems.

The 45-degree FPA and 45-degree LID Omniweave constructions may be processed more easily on the finite length Omniweave equipment than the 18-degree LID or isotropic triaxial fabric constructions. In all cases, the radial fiber pitch angle was maintained at 5-10-degrees to maximize in-plane properties.

Weaving improvements are needed to maximize weave uniformity, weave density and speed of production. Combing techniques need to be improved or eliminated since they can cause fiber abrasion damage and are extremely operator sensitive.

All moldings with USP23 prepreg were based on vendor recommended conditions<sup>(6)</sup>. Several cure modifications were performed to note the effect on composite properties. Boron/HT424 Omniweave moldings followed cure cycles recommended by a previous GE-RESID study<sup>(5)</sup>.

All S-glass composites, with the exception of the isotropic triaxial construction S21A/L-204, had low porosity (0-3 percent) and relatively uniform fiber content (57 to 65 percent). All Morganite composites had approximately equal fiber contents (51 to 55 volume percent) and moderate porosity (3-5 percent). The boron and mixed fiber composites exhibited a wide range of fiber contents and porosity levels.

Two demonstration Omniweave/honeycomb composites were assembled and delivered to NASA-MSFC per contract requirements. These assemblies were to be used only for demonstration purposes.

**SECTION 5**  
**MECHANICAL EVALUATION OF OMNIWEAVE COMPOSITES**



## SECTION 5

### MECHANICAL EVALUATION OF OMNIWEAVE COMPOSITES

The data presented in this section represent preliminary values for Omniweave structural composites. The weaving and processing procedures have not been optimized, nor have test specimen configuration studies been performed to ensure the validity of the data. In most cases, standard ASTM test procedures have been employed, several of which may not be meaningful for multidirectionally reinforced composite materials such as Omniweave.

The experimental data presented in this section exhibit, in general: (1) a rather large degree of scatter; and, (2) somewhat lower strength and stiffness (modulus) values than anticipated. The former is probably due to the fact that weaving and processing parameters have not yet been optimized, while the latter may also be related to test specimen geometry. In view of these considerations, the mechanical property data presented herein for various Omniweave composites are generally considered to be lower limits for the property levels which can be anticipated in the near future.

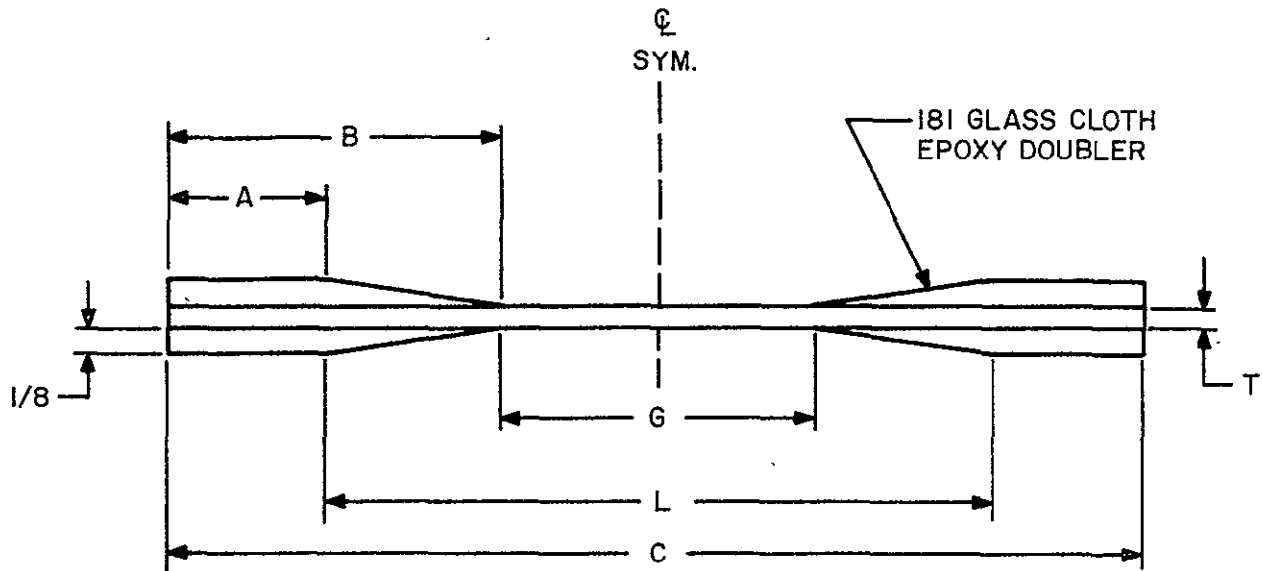
#### 5.1 TESTING OF UNIDIRECTIONAL TEST COUPONS

Tensile tests were performed on unidirectional S-glass/USP23 epoxy composites at 0, 20, 45, 60, and 90-degree angles to the fibers. Data obtained from these tests were used to establish the elastic constants ( $E_1$ ,  $E_2$ ,  $G_{12}$  and  $\nu_{12}$ ) and strength parameters ( $F_1$ ,  $F_2$  and  $F_{12}$ ) of this composite material system as described in Section 6.2. These composite properties are required as inputs for the OMNI computes code which was used to predict the thermostructural performance of Omniweave (Section 6.1, Appendix 10.4).

Test specimens were fabricated to the configurations shown in Figure 5-1. The physical characteristics of panels from which these specimens were cut are shown in Table 5-1. These data were established from the known fiber and resin densities, measured panel densities and fiber weight fraction data obtained from resin burnout experiments. End reinforcement doublers were made from a 181 glass cloth/Epon 828 layup and bonded to test specimens with Epon 828 (See Appendix 10.3)

The physical dimensions of all test specimens were measured and the nominal fiber angles were checked. Strain gages were then applied as shown in Figure 5-2. The test procedure for each specimen included the following:

1. Install specimen in grips of Instron test machine and connect all strain gages to a BLH SR-4 switching box and strain gage readout meter.
2. Apply load in four equal increments up to a preselected maximum load level.



Fiber Angle (degrees)	C (in)	L (in)	Width (in)	L/W	G (in)	T (in)	A (in)	B (in)
0	9	5	0.50	10.0	3	0.05	2.0	3.0
20	10	8	0.75	10.6	4	0.10	1.0	3.0
45	10	8	0.75	10.6	4	0.10	1.0	3.0
60	10	8	0.75	10.6	4	0.10	1.0	3.0
90	8	6	0.75	8.0	2	0.10	1.0	3.0

Figure 5-1. Unidirectional Tensile Specimen Geometry

TABLE 5-1. PHYSICAL CHARACTERISTICS OF UNIDIRECTIONAL S-GLASS/USP23 EPOXY TEST PANELS

Specimen	Density (gm/cc)	Resin Weight (percent)	Fiber Weight (percent)	Porosity (percent)	Resin Volume (percent)	Fiber Volume (percent)
0°, 20° Panel 1	1.98	24	76	0	40	60
45° Panel 2	1.90	27	73	2	43	55
60° Panel 3	1.94	25	75	1	40	59
90° Panel 4	1.97	27	73	0	44	56

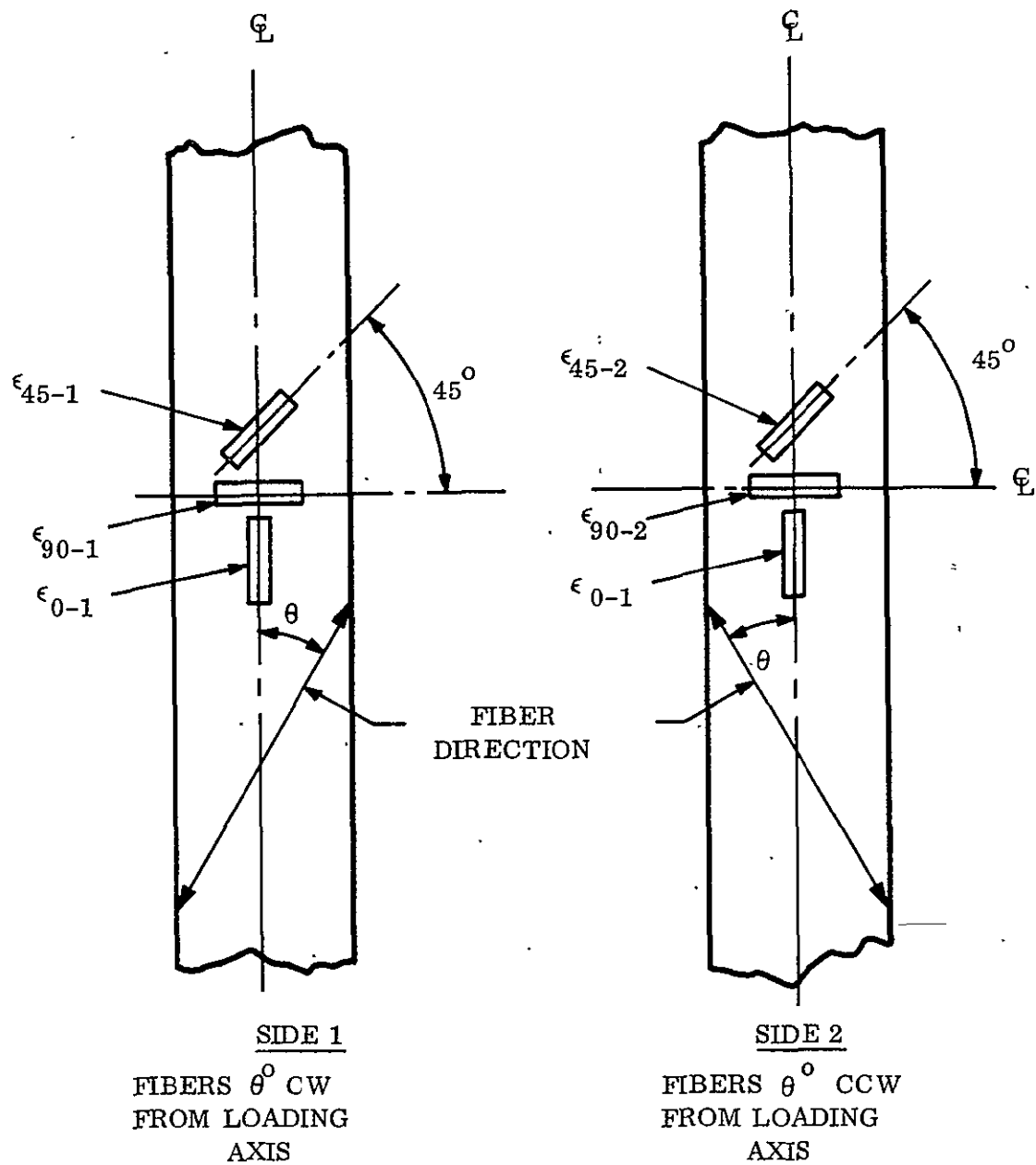
3. Repeat the above twice for each specimen yielding a total of 12 stress-strain data points for each strain gage.
4. Load the specimen to failure recording average axial strain as a function of load in an X-Y recorder.

The equations used to derive elastic constants from unidirectional test data contain terms having the form:

$$\frac{\epsilon_n}{\sigma_x}$$

where  $\epsilon_n$  is a given strain gage reading at the axial stress level  $\sigma_x$ . In order to obtain the best value for this term from each strain gage on a given specimen, the 12 independent stress-strain data points were used to obtain a least squares fit of the data. Values of  $\epsilon_n/\sigma_x$  terms thus obtained are given in Table 5-2 along with ultimate axial strength ( $F_x^n$ ) data. Additional 90-degree strength data, obtained in an earlier series of tests, is given in Table 5-3. A photograph illustrating the failure modes for these off-axis test series is shown in Figure 5-3. Strength data for 0° and 90° fiber orientations are compared to literature reported values in Table 5-4. This table shows that the data obtained in this program are lower than anticipated indicating the need for improved processing techniques.

Literature reported values for 0 and 90-degree unidirectional tensile strength of Morganite Type II/Epoxy composites are shown, for reference, in Table 5-5.



NOTE:  $45^\circ$  GAGES ON OFF AXIS SPECIMENS ( $\theta = 20^\circ, 45^\circ, 60^\circ$ ) ONLY...  
 $0^\circ$  AND  $90^\circ$  GAGES ON  $\theta = 0^\circ$  AND  $90^\circ$  SPECIMENS LOCATED  
 SYMMETRICALLY ABOUT HORIZONTAL  $C_L$

Figure 5-2. Strain Gage Location and Identification

TABLE 5-2. S-GLASS/USP23 UNIDIRECTIONAL TENSILE DATA

Specimen Number	Angle (degrees)	$\epsilon_{0-1}/\sigma_x$ ( $10^{-6}$ in <sup>-2</sup> /lb)	$\epsilon_{0-2}/\sigma_x$ ( $10^{-6}$ in <sup>-2</sup> /lb)	$\epsilon_{45-1}/\sigma_x$ ( $10^{-6}$ in <sup>-2</sup> /lb)	$\epsilon_{45-2}/\sigma_x$ ( $10^{-6}$ in <sup>-2</sup> /lb)	$\epsilon_{90-1}/\sigma_x$ ( $10^{-6}$ in <sup>-2</sup> /lb)	$\epsilon_{90-2}/\sigma_x$ ( $10^{-6}$ in <sup>-2</sup> /lb)	F <sub>x</sub> (ksi)
0-1	0	0.1387	0.1389	—	—	-0.04038	-0.03889	129.6
0-2		0.1400	0.1398	—	—	-0.03832	-0.04301	148.4
0-3		0.1308	0.1400	—	—	-0.03702	-0.04024	168.1
Average		0.1365	0.1396			-0.03857	-0.04071	148.7
20-1	20	0.2476	0.2355	-0.08238	0.1734	-0.1175	-0.0967	16.72
-2		0.2517	0.2598	-0.05872	0.1999	-0.1078	-0.1073	16.26
-3		0.2487	0.2505	-0.06760	0.2203	-0.1071	-0.1025	17.33
Average		0.2493	0.2486	-0.06957	0.1979	-0.1108	-0.1022	16.77
45-1	45	0.4576	0.5010	0.05095	0.2726	-0.1822	-0.1765	8.23
-2		0.4862	0.5296	0.03459	0.2606	-0.1608	-0.1794	6.71
-3		0.5015	0.4734	0.02659	0.2779	-0.1859	-0.1904	7.04
Average		0.4830	0.5013	0.03738	0.2704	-0.1763	-0.1821	7.33
60-1	60	0.4584	0.5178	0.1327	0.1944	-0.1448	-0.1466	4.82
-2		0.5229	0.4614	0.1196	0.1974	-0.1308	-0.1308	5.05
-3		0.5358	0.4247	0.1395	0.2105	-0.1400	-0.1244	5.10
Average		0.5057	0.4680	0.1306	0.2008	-0.1385	-0.1339	4.99
90-1	90**	*	*	*	*	*	*	*
-2		0.4542	0.3974	—	—	-0.03560	-0.03560	2.83
-3		0.4027	0.4114	—	—	-0.03444	-0.03444	6.17
Average		0.4284	0.3994			-0.03502	-0.03502	4.50

\* Specimen 90-1 failed in handling

\*\* See Table 5-3 for additional data



TABLE 5-3. TENSILE STRENGTH OF S-GLASS / USP23 EPOXY COMPOSITE 90-DEGREES TO FIBERS

Specimen Number	Tensile Strength, $F_x$ (psi)	Source
90-2	2830	Table 5-2
90-3	6170	Table 5-2
2-90-1	2990	Earlier data
2-90-2	2890	Earlier data
2-90-3	3430	Earlier data
Average	3660	



Figure 5-3. Post-Test Photographs Off-Axis Unidirectional Test Specimens

TABLE 5-4. COMPARISON OF UNIDIRECTIONAL S-GLASS/EPOXY DATA  
WITH LITERATURE REPORTED VALUES

Fiber Orientation (degrees)	Fiber Volume (percent)	Tensile Strength (psi)	Reference
0	60-65	268,000	7
	60-65	350,000	8
	60-65	294,000	8
	60-65	305,000	8
	60	148,700	GE data
90	60-65	3,300	7
	60-65	8,000	8
	60-65	6,100	8
	60-65	10,200	8
	60	3,660	GE data

TABLE 5-5. UNIDIRECTIONAL TENSILE PROPERTIES OF  
MORGANITE TYPE II/EPOXY COMPOSITES  
(Literature Data)

Fiber Orientation (degrees)	Fiber Volume (percent)	Tensile Strength (psi)	Tensile Modulus ( $10^6$ psi)	Reference
0	—	150,000	—	7
	60	165,000	21.2	9
	51	125,000	18-22	10
	58*	88,500*	17*	11
	55	100,000	35	11
	55	80,000	24	11
	67.5	167,000	23.5	12
	55	175,000	19.5	12
90	—	8,000	—	7
	60	5,200	1.2	9
	52	8,700	1.2-1.5	10
	58	10,000	—	11
	67.5	8,400	—	12

\*Used in analysis (Section 6) to obtain best fit of Omniweave data.

## 5.2 FLEXURAL TEST DATA

All flexural tests were performed on an Instron testing machine at a cross-head speed of 0.05 in/min. A standard 3-point flexure test fixture was used and large span-to-span ( $l/d$ ) ratios were selected to provide flexural stress failure with minimal shear interaction. Tables 5-6 and 5-7 summarize flexural property values obtained for S-glass and Morganite Type II Omniweaves. Additional flexural data for the S-glass material was obtained from the short beam shear tests (Table 5-14), since flexural (tension) failures occurred in these specimens (rather than shear failures) in spite of the small  $l/d$  ratios employed. This is discussed further in Section 5.5.

### 5.2.1 S-GLASS/EPOXY OMNIWEAVE FLEXURAL DATA

Results of the S-glass/epoxy Omniweave flexure tests are shown in Table 5-6. The effect of fiber orientation on flexural strength and modulus is graphically summarized in Figures 5-4 and 5-5. The data slope closely follows the analytical predictions of tensile strength, but the absolute flexural strength values are significantly lower than anticipated. These low values are probably due to poor fiber wetting and interfacial strength since unidirectional composites of identically processed materials exhibited about half of the expected values when tested in tension (Section 5.1).

Figure 5-6 presents curves showing the effect of Omniweave construction reinforcement geometry and composite thickness on flexural strength for  $\pm 30$ -degree and  $\pm 60$ -degree oriented Omniweave materials. These data indicate that the fabric thickness does not affect ultimate strength values. The data do strongly indicate, however, that the layered-in-depth (LID) construction yields higher ultimate strengths at low axial fiber angles and lower ultimate strength at large axial fiber angles than the fiber pitch angle (FPA) construction.

Figures 5-7 and 5-8 present flexural strength and modulus data in the direction along the fiber axis for these S-glass Omniweave composites. The data trend indicates that weave geometry and composite thickness do not have a significant effect on flexural properties parallel to a fiber direction. The average strength values shown in Figure 5-7 are approximately 50 percent of those obtained on 0-degree unidirectional material in tension.

Several molding cycles, "A" and "B", were utilized to cure the composites (Table 4-7). Cure cycle "A" involved a significantly longer resin advancement dwell time during cure than did cure cycle "B". Significant improvement in strength values was noted for the panels processed using cure cycle "B". Figures 5-9 and 5-10 show this effect of cure cycle on flexural strength properties for panels S21A-84 (FPA construction) and S21D-104 (LID construction). These data indicate that improvements in composite properties can be made through optimization of the Omniweave molding process (Sections 7.2 and 8.2).



TABLE 5-6. FLEXURE TEST RESULTS: S-GLASS/USP23  
OMNIWEAVE COMPOSITES

Weave Geometry	Test Direction	Specimen No.	Fiber Angle (degrees)	Flexural Strength (ksi)	Flexural Modulus (10 <sup>6</sup> psi)	1/d Ratio
45° FPA 6 layers	Axial	S21A-84-A-1	±31	57.5	5.05	47.9
		-2	±32	55.8	5.08	47.3
		-3	±33	60.0	5.09	46.6
	Along Fiber	S21A-84-P-1	0-69*	65.5	5.02	46.0
		-2	0-65*	67.6	4.90	45.4
		-3	0-69*	61.2	4.79	44.9
	Transverse	S21A-84-T-1	±63	14.1	2.66	68.5
		-2	±63	16.1	2.55	44.9
		-3	±65	16.0	2.58	45.4
45° FPA 12 layers	Axial	S21A-91-A-1	±33	48.6	4.45	28.5
		-2	±32	48.7	4.59	28.4
		-3	±33	53.0	4.69	28.0
	Along Fiber	S21A-91-P-1	0-67*	62.4	4.95	24.0
		-2	0-67*	75.0	4.88	23.8
		-3	0-67*	68.0	4.96	23.8
	Transverse	S21A-91-T-1	±64	20.4	2.47	27.8
			±65	24.3	3.90	27.8
			±62	20.6	2.74	28.0
45° FPA 18 layers	Axial	S21A-92-A-1	±28	61.5	5.04	23.0
		-2	±26	60.2	4.79	22.8
		-3	±29	54.6	4.82	23.0
	Along Fiber	S21A-92-P-1	2-59*	71.8	4.85	23.2
		-2	2-58*	72.8	4.84	23.3
		-3	2-56*	77.6	4.91	23.2
	Transverse	S21A-92-T-1	±66	19.0	2.70	22.4
		-2	±69	19.2	2.75	22.2
		-3	±67	19.1	2.64	23.8

TABLE 5-6. FLEXURE TEST RESULTS: S-GLASS/USP23  
OMNIWEAVE COMPOSITES (Continued)

Weave Geometry	Test Direction	Specimen No.	Fiber Angle (degrees)	Flexural Strength (ksi)	Flexural Modulus (10 <sup>6</sup> psi)	l/d Ratio
18° LID 6 layers	Axial	S21F-93-A-1	±28	36.4	3.46	20.0
		-2	±30	49.8	4.69	20.2
		-3	±30	30.6	3.00	20.2
	Transverse	S21F-93-T-1	±61	18.2	2.10	19.9
		-2	±65	19.2	2.20	19.9
		-3	±60	16.4	2.27	19.9
18° LID 12 layers	Axial	S21F-94-A-1	±28	23.2	2.16	9.0
		-2	±25	17.7	1.51	8.0
		-3	±30	16.1	1.65	8.9
	Transverse	S21F-94-T-1	±66	13.9	1.31	9.1
		-2	±58	7.86	0.89	9.2
		-3	±63	7.01	0.74	9.2
45° LID 6 layers	Axial	S21D-85-A-1	±29	64.8	5.10	38.0
		-2	±27	63.9	5.07	38.3
	Along Fiber	S21D-85-D-1	5-59*	70.6	5.35	37.6
		-2	7-62*	64.4	4.69	37.6
		-3	5-66*	73.4	5.23	28.5
	Transverse	S21D-85-T-1	±61	15.4	2.88	53.8
		-2	±65	14.9	2.86	37.6
		-3	±64	15.2	2.68	39.3
45° LID 12 layers	Axial	S21D-103-A-1	±27	62.7	4.98	25.2
		-2	±27	64.8	4.82	25.0
		-3	±27	63.9	4.88	25.0
	Along Fiber	S21D-103-P-1	1-63*	78.5	4.62	24.8
		-2	7-54*	73.0	4.63	24.8
		-3	6-58*	68.1	4.79	25.0
		S21D-103-T-1	±63	13.8	2.50	25.0
		-2	±67	9.1	1.37	25.2
		-3	±63	15.1	2.44	25.3

TABLE 5-6. FLEXURE TEST RESULTS: S-GLASS/USP23  
OMNIWEAVE COMPOSITES (Continued)

Weave Geometry	Test Direction	Specimen No.	Fiber Angle (degrees)	Flexural Strength (ksi)	Flexural Modulus (10 <sup>6</sup> psi)	l/d Ratio
45° LID 18 layers	Axial	S21D-104-A-1	±24	69.6	4.84	20.7
		-2	±25	69.9	4.89	20.8
		-3	±25	65.1	4.49	20.9
	Along Fiber	S21D-104-P-1	2-57*	73.4	4.29	20.9
		-2	8-51*	69.8	4.15	20.8
		-3	6-51*	65.4	4.18	20.8
	Transverse	S21D-104-T-1	±63	12.2	2.16	20.9
		-2	±67	15.0	2.38	20.9
		-3	±70	13.0	2.07	20.8
Triaxial 12 layers	Axial	S21A/L-204-A-1		34.4	3.14	29.6
	Transverse	S21A/L-204-T-1 -2		33.0 23.2	3.40 2.76	22.6 24.6

\*Specimen tested with loading axis parallel to one fiber direction (0-degree)

Figure 5-11 presents photographs of typical post-test flexure specimens of S-glass Omniweave composites. The light areas within the specimens indicate the failure region and that damage occurred through local resin/fiber separations.

### 5.2.2 MORGANITE TYPE II/EPOXY FLEXURAL PROPERTIES

Flexure test results for Morganite Type II/USP23 Omniweave composites are given in Table 5-7. Figures 5-12 and 5-13 illustrate the effect of fiber orientation on the flexural strength and modulus of this Omniweave composite system. Again, the data slope appears to coincide well with tensile strength and modulus predictions. The low flexural modulus values indicate that a poor quality Morganite fiber was utilized. This is discussed in more detail in Section 7.2. Photographs of several typical failed specimens are shown in Figure 5-14.

## 5.3 TENSILE TEST DATA

### 5.3.1 S-GLASS/EPOXY OMNIWEAVE TENSILE PROPERTIES

Table 5-8 presents tensile test data on several S-glass/epoxy Omniweave composites. The tensile strength values are significantly lower than the flexural strength values indicating a need for improved processing. Figure 5-15 presents several post-test photographs of S-glass Omniweave tensile specimens.

### 5.3.2 MORGANITE TYPE II/EPOXY OMNIWEAVE TENSILE PROPERTIES

The tensile test data for this material system, Table 5-9, are significantly lower than the corresponding flexural properties indicating that: (a) test specimen configurations should be reevaluated; and, (b) resin material, and/or curing procedures should be

TABLE 5-7. FLEXURE TEST RESULTS:  
MORGANITE II/USP23 OMNIWEAVE COMPOSITES

Weave Geometry	Test Direction	Specimen No.	Fiber Angle (degrees)	Flexural Strength (ksi)	Flexural Modulus (10 <sup>6</sup> psi)	I/d Ratio
45° FPA 6 layers	Axial	G51A-86-A-1	±35	24.7	3.43	17.3
		-2	±36	23.8	3.36	17.4
		-3	±34	30.4	3.99	17.4
	Along Fiber	G51A-86-P-1	4-67*	40.5	5.20	17.1
		-2	1-77*	35.3	4.49	17.2
		-3	2-77*	29.9	4.52	17.2
	Transverse	G51A-86-T-1	±59	17.2	1.88	16.7
		-2	±60	19.8	1.81	16.7
		-3	±53	15.6	1.73	16.7
45° LID 12 layers	Axial	G51D-96-A-1	±22	69.4	8.53	18.4
		-2	±23	48.8	7.17	18.3
		-3	±27	51.0	8.10	16.0
	Along Fiber	G51D-96-P-1	4-46*	44.6	7.08	18.2
		-2	2-62*	42.8	7.22	18.2
		-3	—	56.4	7.85	18.2
	Transverse	G51D-96-T-1	±63	10.3	1.24	18.1
		-2	±60	16.2	1.57	18.1
Triaxial 6 layers	Axial	G51A/L-207-A-1	±15	96.7	10.1	17.7
		-2	±16	107.9	11.2	17.8
		-3	±19	105.7	11.9	17.7
	Transverse	G51A/L-207-T-1	±78	5.54	1.76	10.2
		-2	±72	3.86	1.03	16.7
		-3	±75	4.74	1.06	16.9

\*Specimens tested with loading axis parallel to one fiber direction (0-degree)

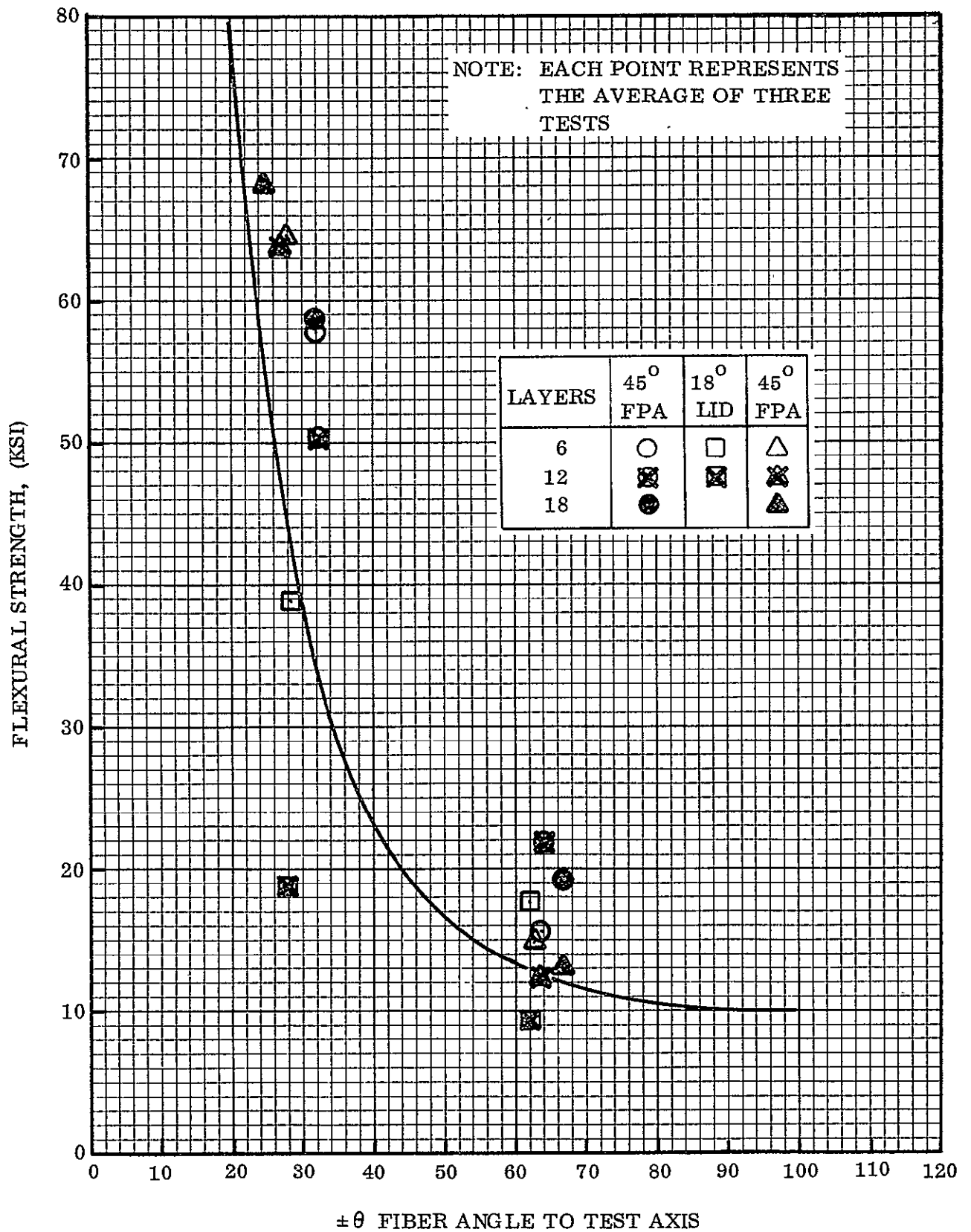


Figure 5-4. The Effect of Fiber Orientation on Flexural Strength of S-Glass/USP23 Omniweave Composites

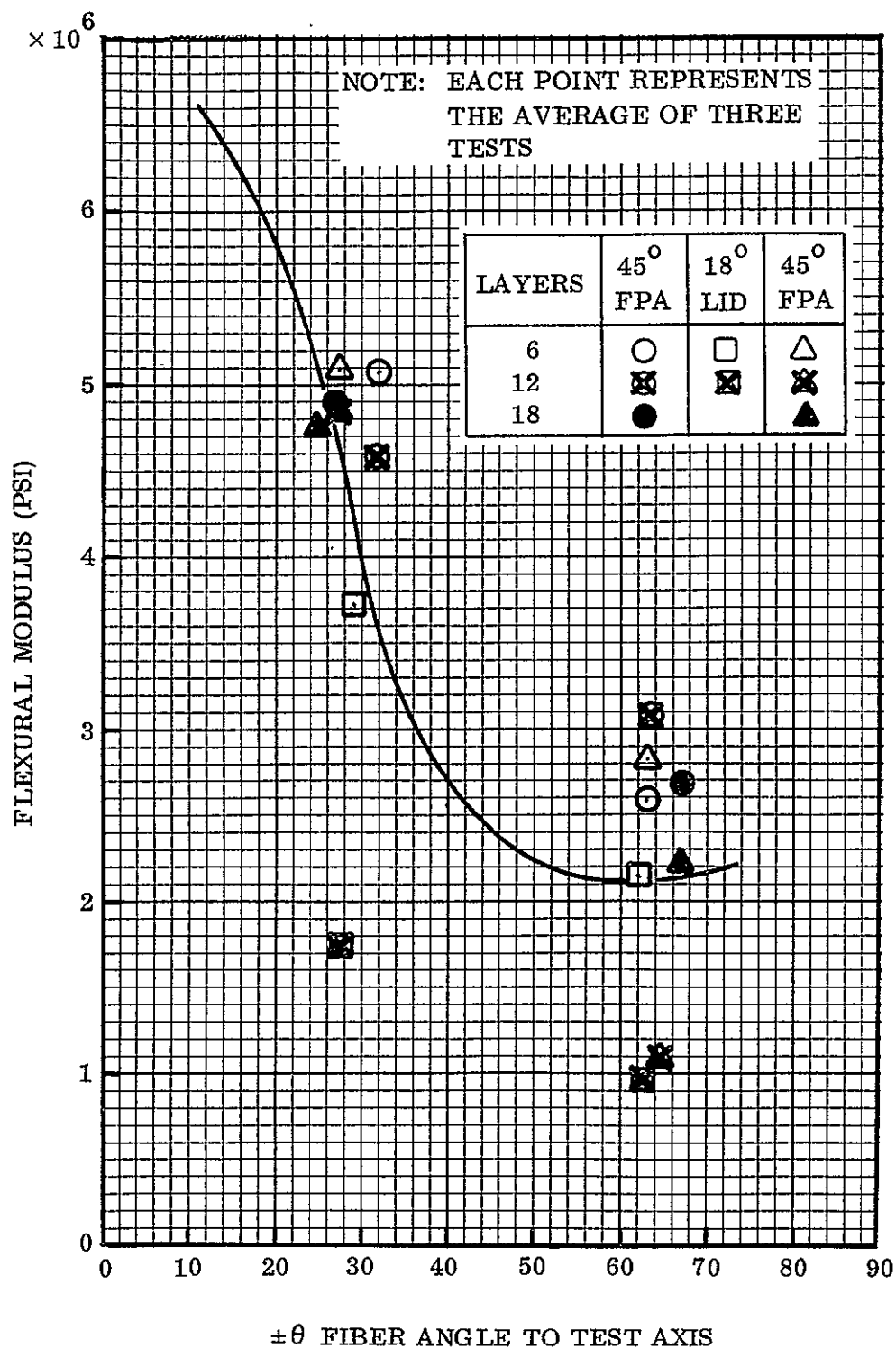


Figure 5-5. The Effect of Fiber Orientation on Flexural Modulus of S-Glass/USP23 Omniweave Composites

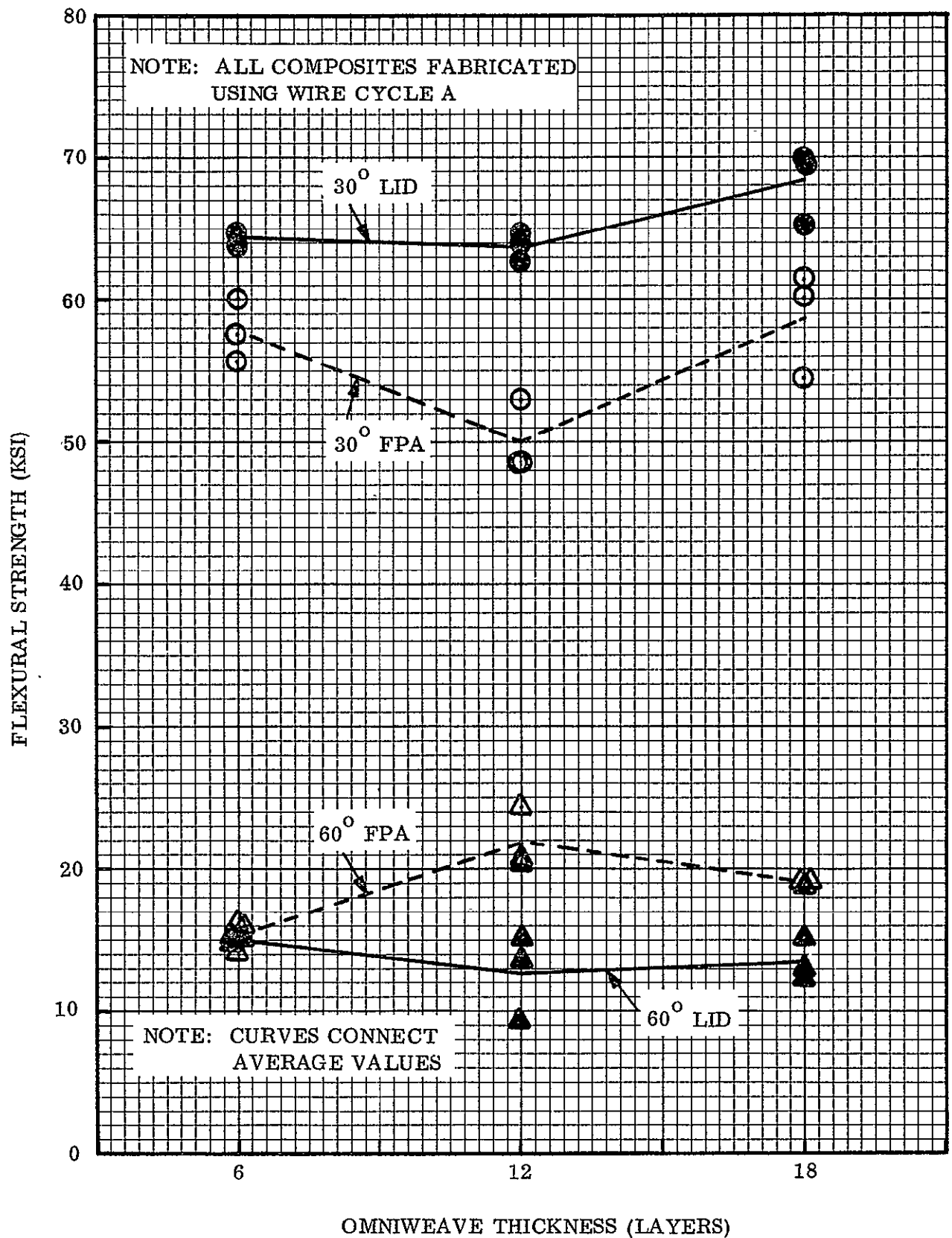


Figure 5-6. Effect of Omniweave Construction and Weave Thickness on Flexural Strength of S-Glass/USP-23 Composite

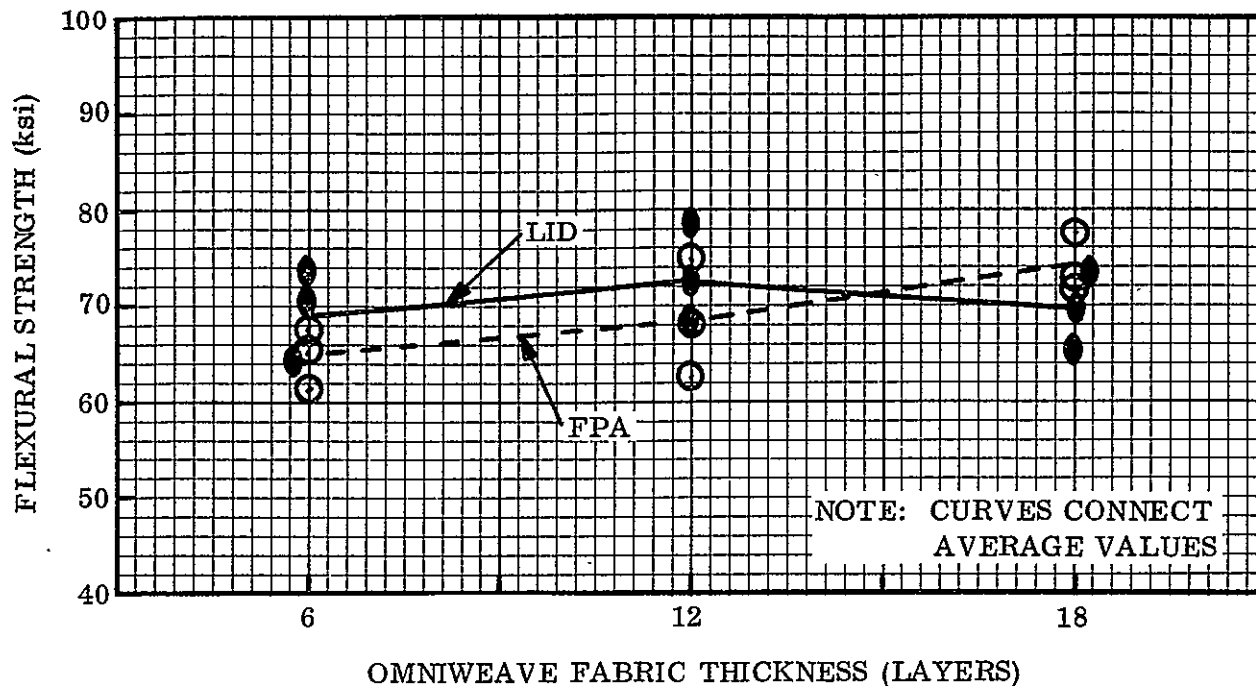


Figure 5-7. Flexural Strength of S-Glass/USP23 Omniweave Composites Tested along Fiber Axis

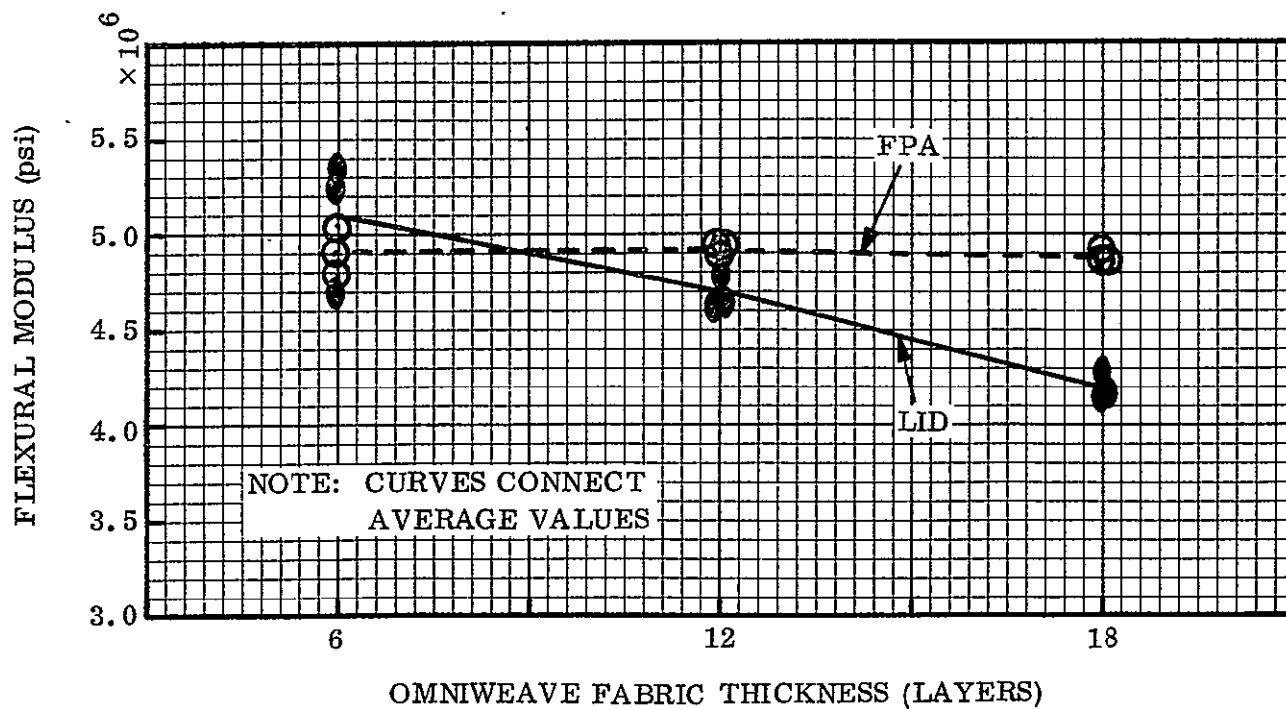


Figure 5-8. Flexural Modulus of S-Glass/USP23 Omniweave Composites Tested along Fiber Axis



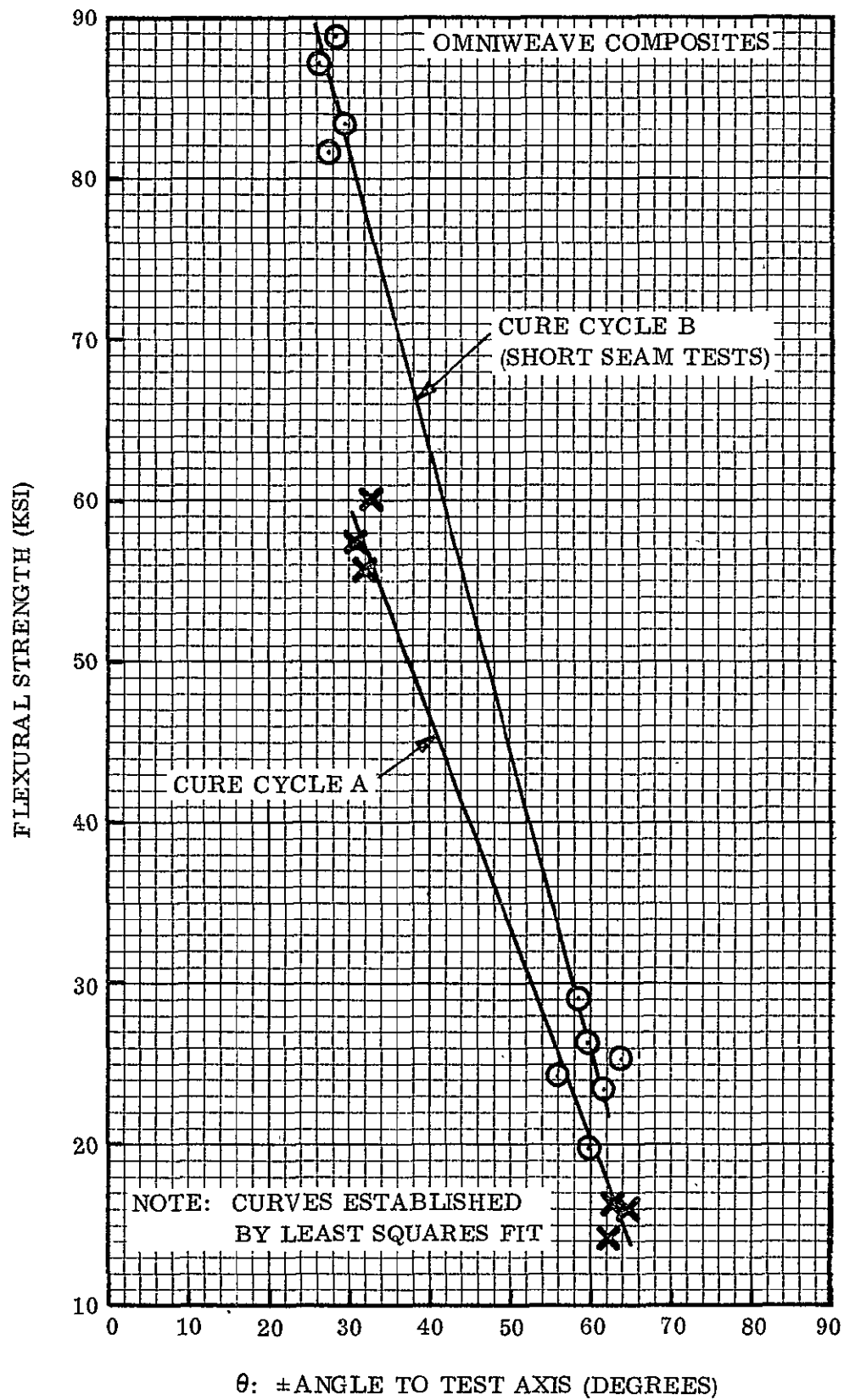


Figure 5-9. The Effect of Cure Cycle on Flexural Strength of S21A-94 S-Glass/USP23 Omniweave Composites

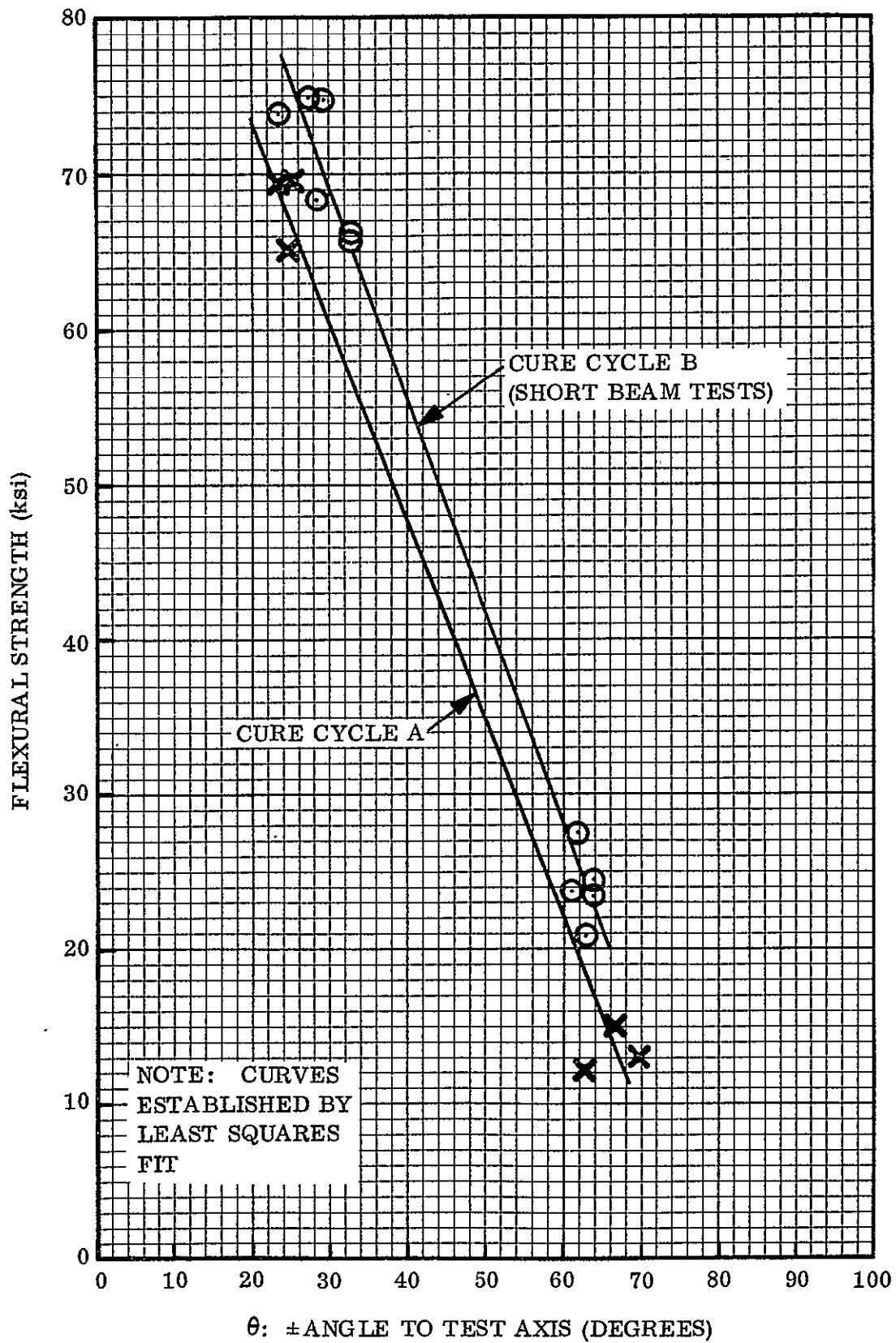


Figure 5-10. The Effect of Cure Cycle on Flexural Strength of S21D-104 S-Glass/USP23 Omniweave Composites

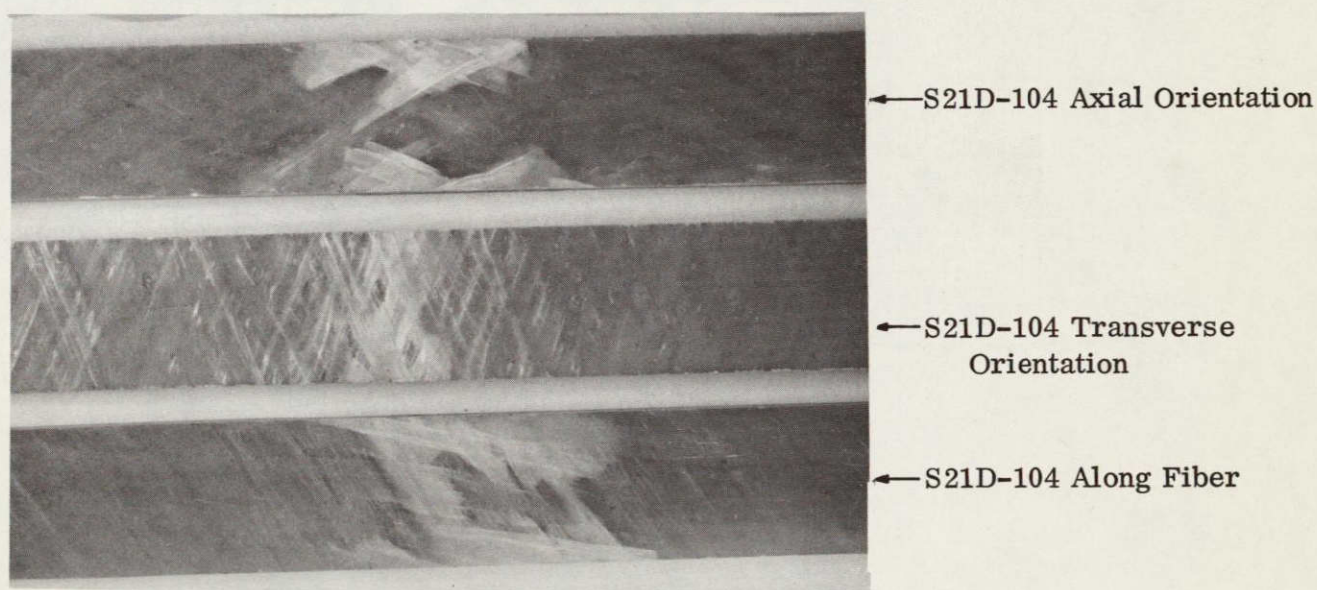
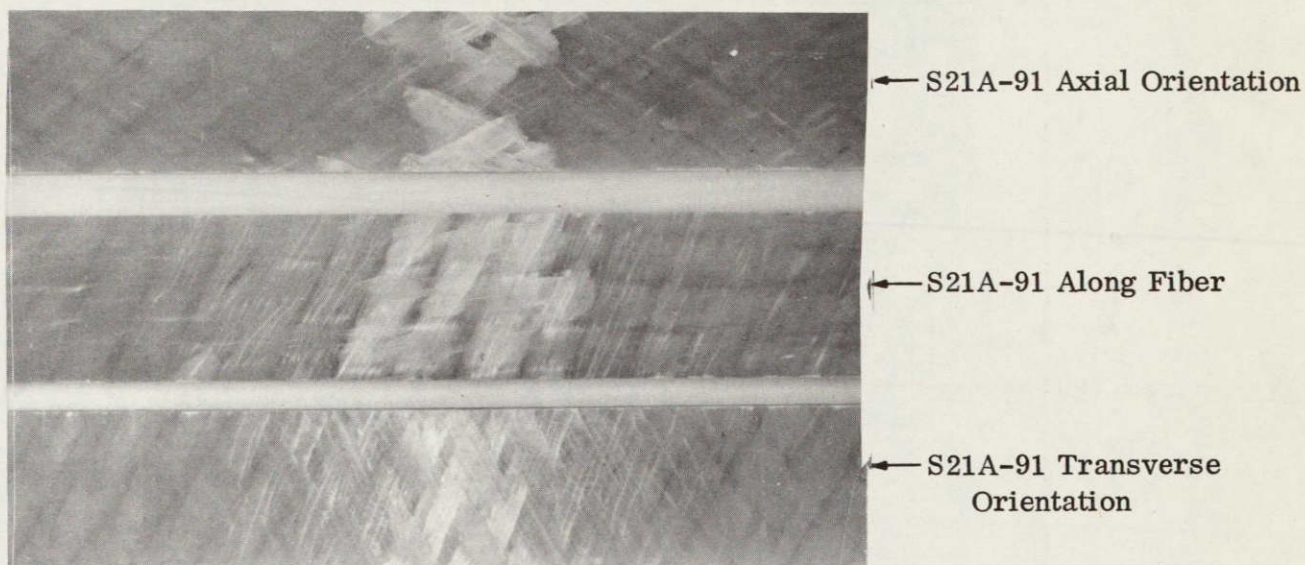


Figure 5-11. Typical S-Glass/Epoxy Flexure Specimens after Testing



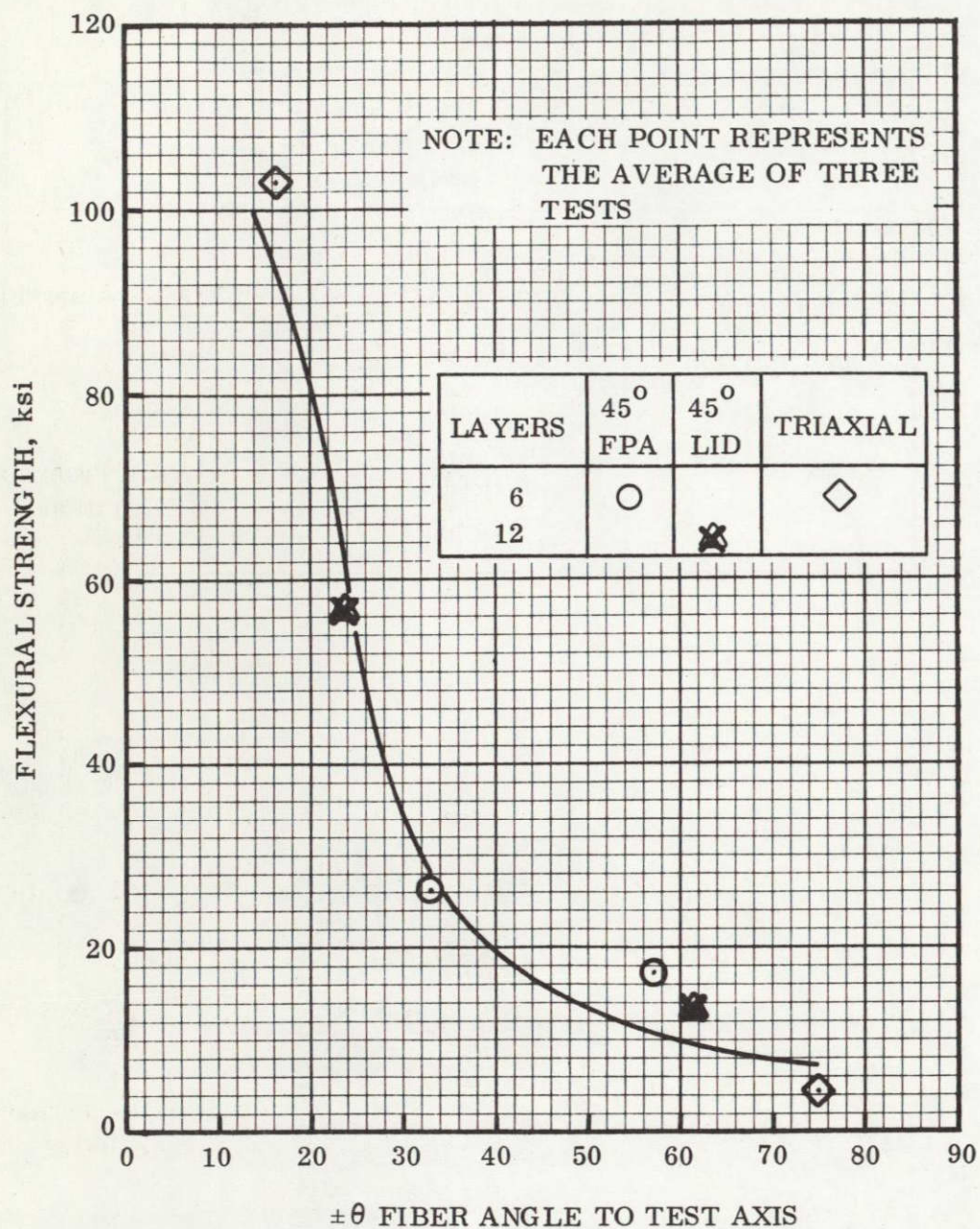


Figure 5-12. The Effect of Fiber Orientation on Flexural Strength of Morganite II/USP23 Omniweave Composites



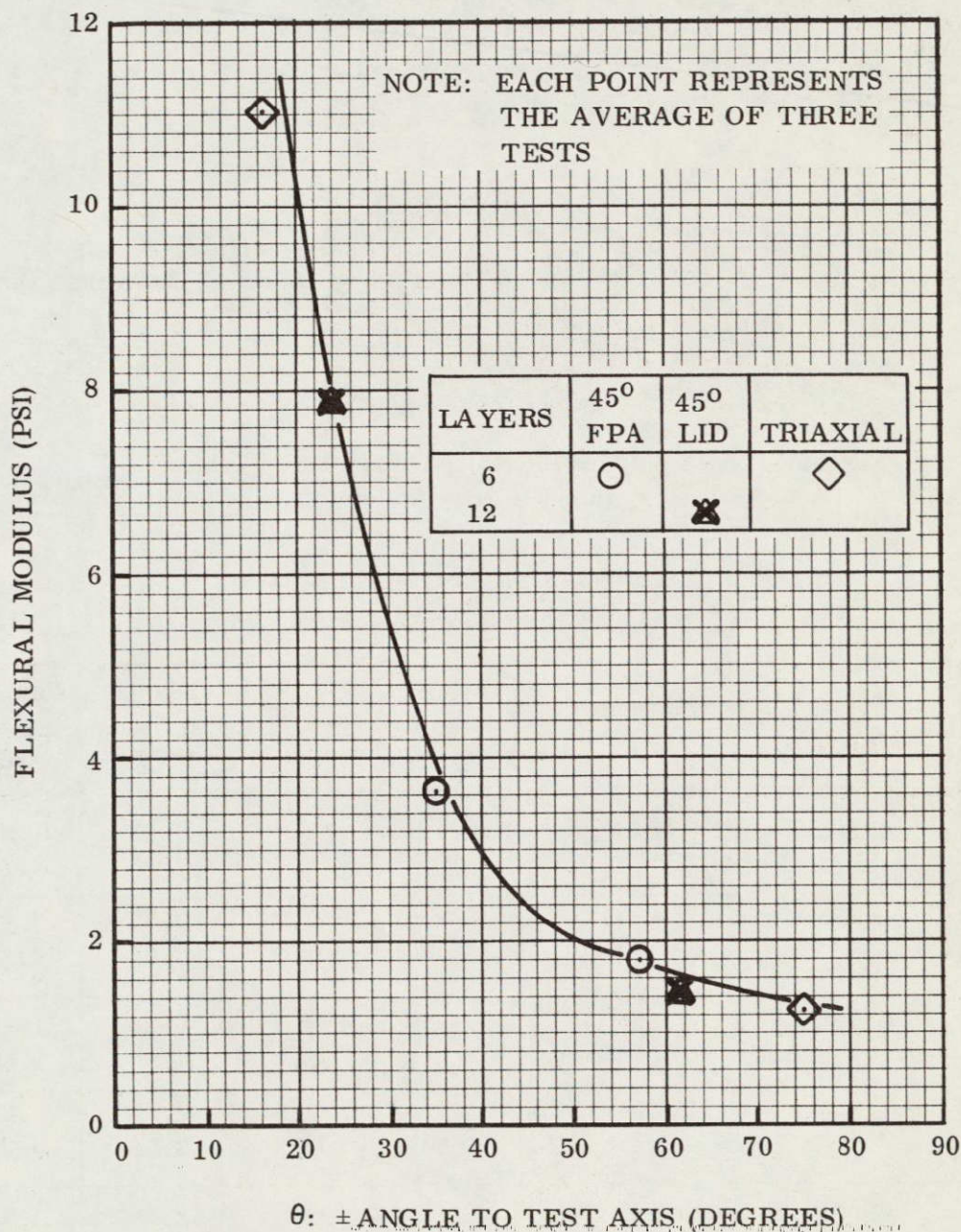


Figure 5-13. The Effect of Fiber Orientation on Flexural Modulus of Morganite II/USP23 Omniweave Composites



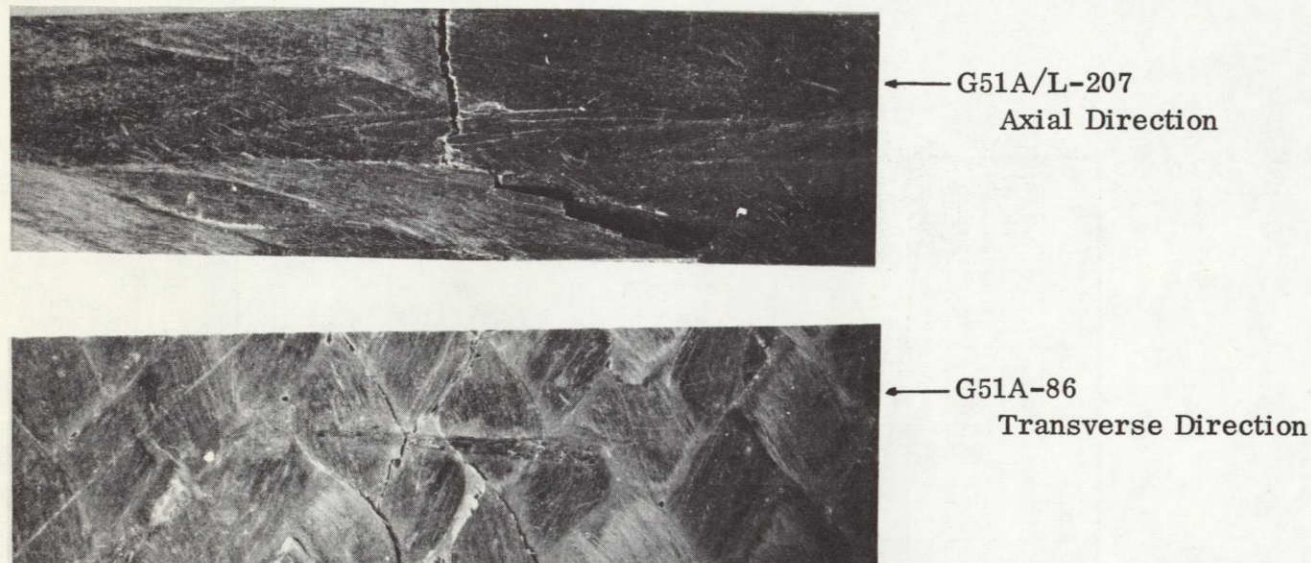
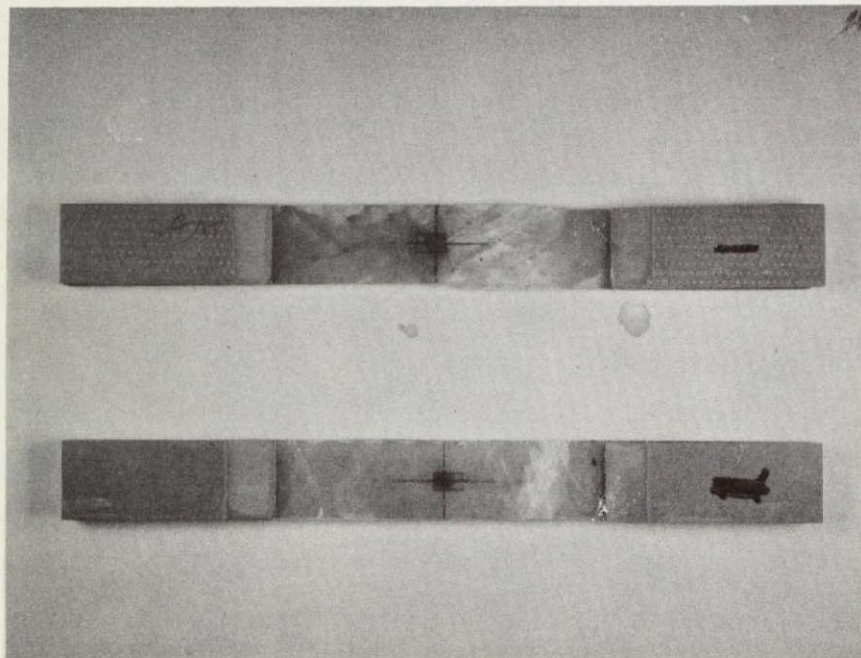


Figure 5-14. Typical Morganite Omniweave Flexure Specimen Failure Modes

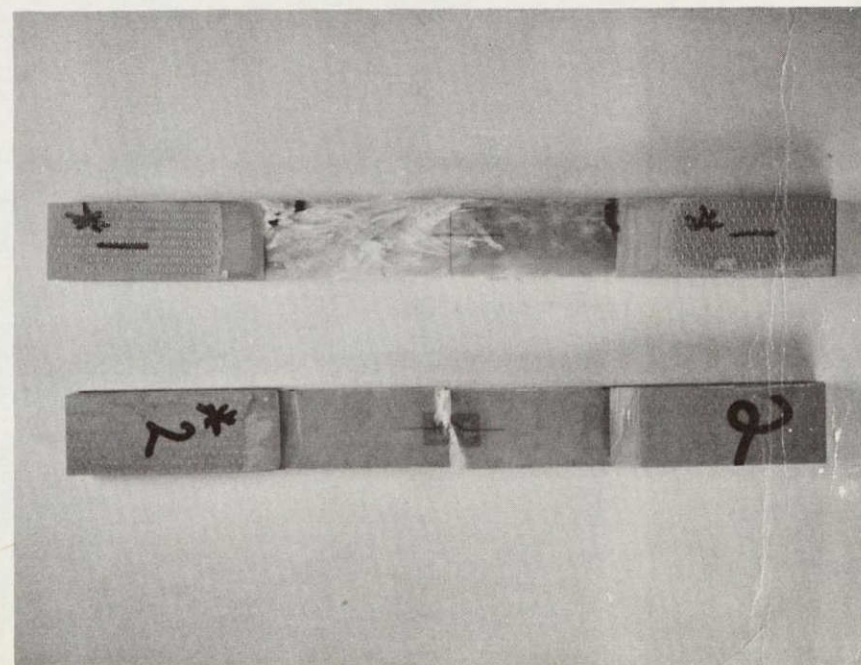
TABLE 5-8. TENSION TEST RESULTS:  
S-GLASS/USP23 OMNIWEAVE COMPOSITES

Weave Geometry	Test Direction	Specimen No.	Fiber Angle (degrees)	Tensile Strength (ksi)	Elastic Modulus ( $10^6$ psi)	Failure Strain (percent)
45° FPA 6 layers	Axial	S21A-84-A-1 -2	$\pm 24$ $\pm 33$	33.7 28.6	4.83 4.45	1.30 1.70*
	Transverse	S21A-84-T-1 -2	$\pm 63$ $\pm 64$	7.7 7.9	3.37 3.31	0.25 0.28
45° LID 18 layers	Axial	S21D-104-A-1 -2	$\pm 33$ $\pm 29$	47.4 52.2	4.96 4.74	1.49 1.56*
	Transverse	S21D-104-T-1 -2	$\pm 65$ $\pm 65$	8.5 7.2	2.71 2.58	0.37 0.31
Triaxial 12 layers	Axial	S21A/L-204-A-1	$\pm 54$	22.6	3.1	0.73*
	Transverse	S21A/L-204-T-1	$\pm 46$	14.5	2.9	0.68*

\*Strain extrapolated to failure.



(a) S21A-84 Axial Orientation (Top)  
S21A-84 Transverse Direction (Bottom)



(b) S21D-104 Axial Orientation (Top)  
S21D-104 Transverse Orientation (Bottom)

Figure 5-15. Failure Modes of S-Glass Omniweave Tensile Specimens



TABLE 5-9. TENSION TEST RESULTS: MORGANITE II/USP23  
OMNIWEAVE COMPOSITES

Weave Geometry	Test Direction	Specimen Number	Fiber Angle (degrees)	Tensile Strength (ksi)	Elastic Modulus (10 <sup>6</sup> psi)	Failure Strain (%)
40° LID 12 layers	Axial	G51D-96-A-2-1 -2	± 28 ± 32	39.6 30.6	8.67 5.46	0.55 0.60
	Trans-verse	G51D-96-T-3-1 -2	± 66 ± 62	4.28 6.04	1.38 1.51	0.32* 0.50*
Triaxial 6 layers	Axial	G51A/L-207-A-1 -2	± 13 ± 12	>58.6 <sup>(1)</sup> 56.5	14.2 13.4	0.42 <sup>(1)</sup> 0.42
	Trans-verse	G51A/L-207-T-1 -2	± 82 ± 80	1.83 2.89	1.06 1.08	0.18 0.27

\*Strain Extrapolated to Failure

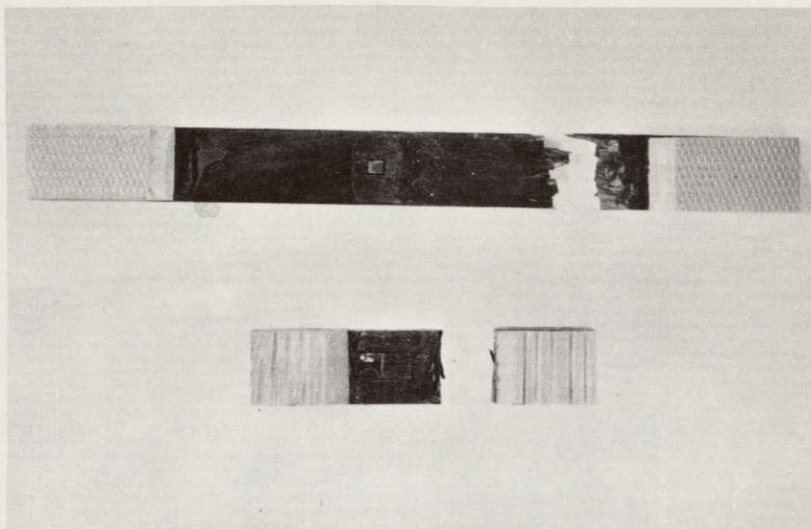
<sup>(1)</sup>Sample Did Not Fail

optimized to affect better interfacial strengths. The data trend indicates that the triaxial orientation construction is superior to the layered-in-depth construction (primarily due to the pronounced axial orientation of the fibers.) Figure 5-16 shows the mode of tensile failure of several Morganite/USP23 epoxy Omniweave composites.

### 5.3.3 BORON, THORNEL 50S, AND MIXED FIBER OMNIWEAVE TENSILE SPECIMENS

Boron, Thornel 50S, and boron/Morganite, boron/S-glass, and S-glass/Morganite Omniweave tensile properties were obtained for composites molded from woven-to-size narrow fabrics. By weaving and molding strips to the 1-inch wide configuration used for tensile specimens, discontinuous fibers (cut by machining operations) at specimen edges were eliminated. This specimen preparation technique was utilized in an attempt to establish a tensile specimen configuration which would yield meaningful tensile ultimate strength values by virtue of maintaining physical continuity of reinforcing fibers in the direction of applied load. The validity of this approach can ultimately be verified only by comparison of results with strength data obtained from cylinder tests (See Section 8.3). Tensile data for those systems is presented in Table 5-10.

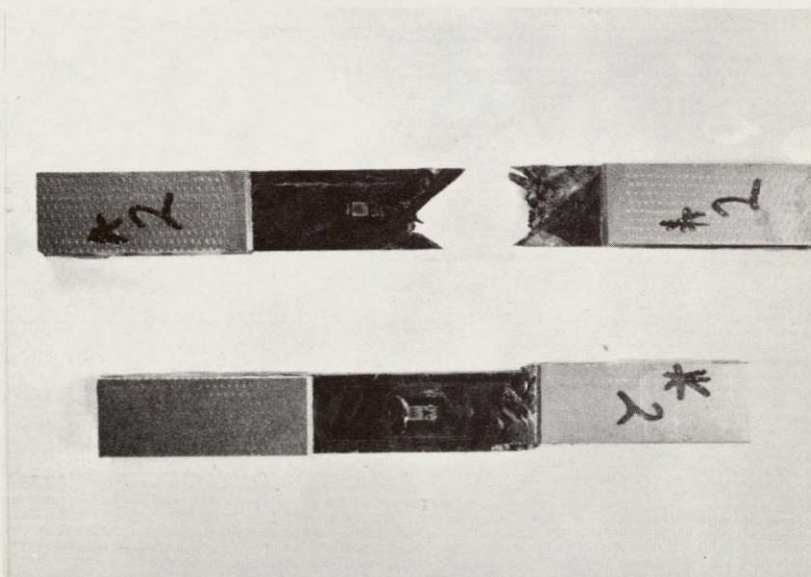




Axial Orientation

G51A/L-207

Transverse Orientation



Axial Orientation

G51D-96

Transverse Orientation

Figure 5-16. Morganite Omniweave Tensile Specimens After Test

TABLE 5-10. TENSION TEST RESULTS: BORON, THORNEL 50S  
AND MIXED FIBER OMNIWEAVE SYSTEMS

Test Direction: Axial

Weave Geometry: 45 degree FPA, 6 Layers

Material	Specimen Number	Fiber Angle (degrees)	Tensile Strength (ksi)	Elastic Modulus (10 <sup>6</sup> psi)	Failure Strain (%)
Boron/HT424 Epoxy-Phenolic	101-1A	± 6	137.3	25.3	0.53
	-1B	± 8	103.5	27.2	0.39
	-2A	± 6	88.4	23.2	0.38
	-2B**	± 8	32.2	17.4	0.20
	-3A	± 8	76.4	25.4	0.30
	-3B	± 7	66.7	26.7	0.26
	-4A	± 7	90.8	25.0	0.36
	-4B	± 7	86.8	26.5	0.34
	-6A	± 7	75.3	19.1	0.39
	-6B	± 10	85.8	24.2	0.36
Thornel 50S/USP23 Epoxy	G71A-98-1	± 8	61.6	23.4	0.26
Boron/HT424 Epoxy-Phenolic, Morganite II/USP23 Epoxy <sup>(1)</sup>	101-AA-1	± 9	42.4	11.3	0.38
	-2	± 10	51.9	11.8	0.45
Boron/HT424 Epoxy-Phenolic, S-Glass/USP23 Epoxy <sup>(2)</sup>	101-9A	± 7	84.6	11.0	0.76*
	-9B	± 6	98.3	10.4	0.96*
Boron/HT424 Epoxy-Phenolic, S-Glass/USP23 Epoxy <sup>(3)</sup>	101-10A	± 10	63.1	8.9	0.73*
	-10B	± 8	84.2	10.1	0.82*
Morganite II/USP23 Epoxy, S-Glass/USP23 Epoxy <sup>(4)</sup>	101-11A	± 8	86.2	12.2	0.68
	-11B	± 14	82.5	11.9	0.69*
	-11C	± 10	84.6	12.1	0.71

(1) 24% Boron/41% Morganite II by weight

(2) 21% Boron/53% S-Glass by weight

(3) 12% Boron/62% S-Glass by weight

(4) 27% Morganite II/46% S-Glass by weight

\* Strain Extrapolated to failure

\*\* 1.03 g/cc density, high void content



In general, the maximum modulus and strength properties measured for the boron/HT-424 system ( $E = 24 \times 10^6$  psi,  $F_{tu} = 137$  ksi) compare favorably with unidirectional tensile properties obtained for an identical materials system at similar volume fraction<sup>(5)</sup> ( $E = 25 \times 10^6$  psi,  $F_{tu} = 135$  ksi). The strength data scatter is quite wide indicating the difficulties in weaving and processing boron filaments into a uniform Omniweave composite. Figure 5-17 illustrates the range of failure modes experienced with the boron Omniweave composites.

The single modulus value for Thornel 50S/epoxy Omniweave is comparable with unidirectional values, but the strength value (also only one data point) indicates a poor translation of strength properties from the fiber to the composite. This is probably due to degradation of the Thornel 50S yarn during the impregnation, weaving and/or molding procedures.

Four mixed fiber Omniweave composite were produced solely for tensile evaluation: boron/Morganite (101-A), boron/S-Glass (101-9, 101-10), and S-glass/Morganite (101-11). With the exception of the boron/Morganite results, modulus and strength values appear to be realistic and can be approximated through knowledge of fiber volume fraction, fiber orientation, and unidirectional fiber data. Figure 5-18 represents post-test photographs of several mixed fiber Omniweave tensile specimens.

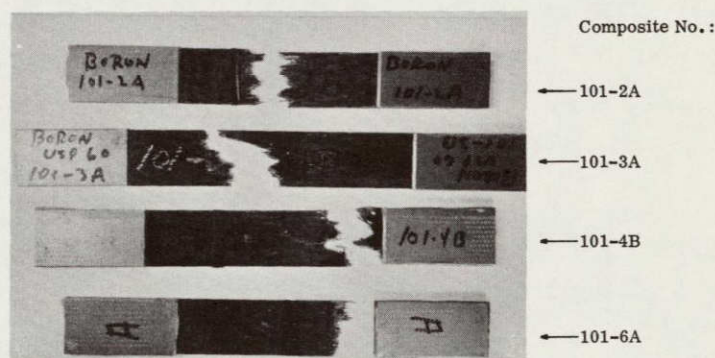


Figure 5-17. Tensile Failure Modes of Boron Omniweave Composites

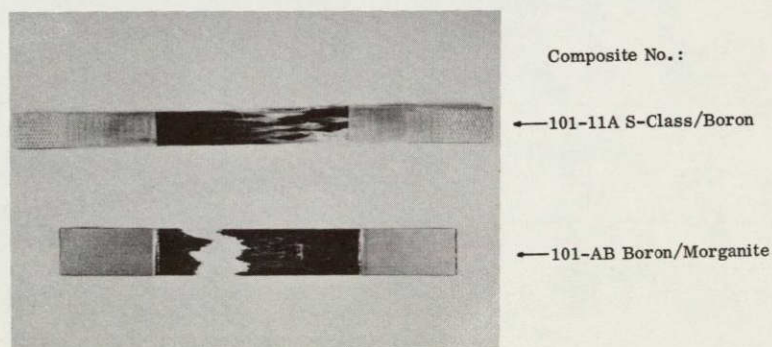


Figure 5-18. Post-Test Photograph of Mixed Fiber Omniweave Tensile Specimens



## 5.4 COMPRESSION TEST DATA

Compression tests were performed on selected S-glass and Morganite/USP23 epoxy Omniweave composites in an Instron test machine using a cross head speed of 0.05-inch/minute. A spherically seated loading head was used to insure good alignment of specimen and load train assembly. Test specimens were 3.00-inches long, 0.75-inch wide and the full thickness of the molded panel. These composites were tested using a restraining fixture (to prevent buckling) as described in Federal Test Method Standard Number 406, Method 1013. A Tinius Olsen LVDT compressometer having a 1-inch gage length was used for all strain measurements. Tables 5-11 and 5-12 summarize compression test results for S-glass and Morganite epoxy Omniweaves, respectively.

### 5.4.1 S-GLASS/EPOXY OMNIWEAVE COMPRESSION TESTS

The test data spread for these specimens is quite large, indicating a need for improved processing procedures and, perhaps, an improved test specimen configuration. The test data presented for S21D-104 (LID) composite is quite interesting. There appears

TABLE 5-11. COMPRESSION TEST RESULTS: S-GLASS/USP23 OMNIWEAVE COMPOSITES

Weave Geometry	Test Direction	Specimen Number	Fiber Angle (degrees)	Compressive Strength (ksi)	Elastic Modulus (10 <sup>6</sup> psi)
45° FPA 6 layers	Axial	S21A-84-A-1	± 33	27.7	5.21
		-2	± 30	25.0	4.54
		-3	± 26	33.2	—
	Trans-verse	S21A-84-T-1	± 62	16.5	2.53
		-2	± 56	16.2	2.60
		-3	± 59	9.0 <sup>(1)</sup>	2.77
		-4	± 60	14.5	—
	45° LID 18 layers	S21D104-A-1	± 25	37.1	5.07
			± 25	23.4	6.25
			± 27	35.5	3.83
			± 29	36.4	5.04
		S21D104-T-1	± 66	21.6	2.69
			± 62	30.0	3.66

(1)Top of specimen collapsed



TABLE 5-12. COMPRESSION TEST RESULTS: MORGANITE II/USP23  
OMNIWEAVE COMPOSITES

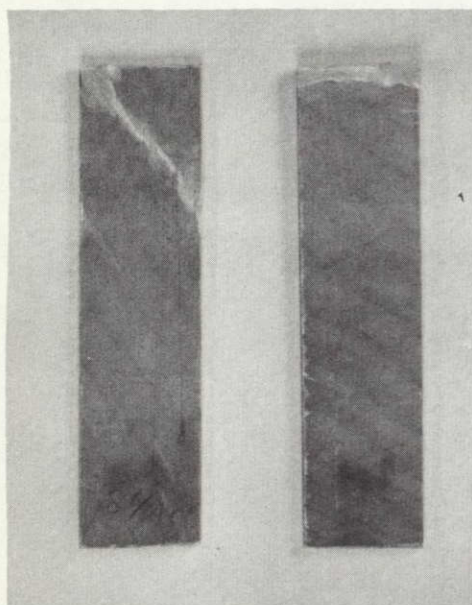
Weave Geometry	Test Direction	Specimen Number	Fiber Angle (degrees)	Compressive Strength (ksi)	Elastic Modulus ( $10^6$ psi)
45° LID 12 layers	Trans-verse	G51D963-19	± 55	19.2	2.00
		-20	± 58	>47.6*	1.95
		-21	± 71	21.9	1.56
Triaxial 6 layers	Axial	G51A/L207-A-1	± 11	48.9	14.9
		-2	± 11	57.6	—
		-3	± 20	51.2	—
	Trans-verse	G51A/L207-T-1	± 83	37.9*	1.19
		-2	± 84	40.0*	1.18
		-3	± 86	37.6	1.03

\*Sample did not fail

to be no trend established for compressive strength as a function of orientation. Further investigations are needed to determine if these data are meaningful since composite theory predicts a pronounced effect of filament orientation on modulus and strength properties. Figure 5-19 illustrates the failure modes of these compressive test specimens. Failure usually occurred along a fiber path.

#### 5.4.2 MORGANITE TYPE II/EPOXY OMNIWEAVE COMPRESSION TESTS

The test data spread for these specimens, Table 5-12, is also quite large again indicating the need for improved processing procedures and possibly new test specimen configurations. The compressive strength for the triaxial system appears to be insensitive to angular orientation. In addition, the transverse properties values are significantly higher than data reported in the literature for carefully processed unidirectional Morganite/epoxy composites (Table 5-13).



S21A-84: Axial Orientation (Left)  
Transverse Direction (Right)



S21D-104: Axial Orientation (Left)  
Transverse Orientation (Right)

Figure 5-19. Compressive Failure of S-Glass Omniweave Composites

TABLE 5-13. COMPARISON OF MORGANITE TYPE II/EPOXY OMNIWEAVE  
TRANSVERSE COMPRESSION DATA WITH LITERATURE REPORTED  
VALUES FOR UNIDIRECTIONAL MATERIAL

Fiber Orientation	Fiber Volume (percent)	Compressive Strength (psi)	Reference
90°	—	20,000	7
	65	27,500	13
	52	24,500	10
	67.5	31,700	12
± 85° Omniweave*	52	40,000	GE data

\*G51A/L-207



## 5.5 SHORT BEAM SHEAR TEST DATA

Short beam shear data was obtained using identical procedures to those employed for flexural tests except that lower l/d ratios were selected in an attempt to induce shear failures. Unfortunately, however, failure in all tests with the possible exception of the Morganite/Epoxy specimens G51A/L-207-2, 3, 4, was primarily outer fiber tension so that ultimate values of interlaminar shear strength were not obtained (Tables 5-14 and 5-15). It is interesting to note that relatively high shear stress levels were attained prior to failure in spite of the small l/d ratios used even though the processing procedures employed did not produce good interfacial bonding. It appears, therefore, that significant improvement in interlaminar shear strengths are feasible with the Omniweave method of composite manufacture. Figure 5-20 features post-test specimens indicating that tensile stresses induced the primary mode of failure.

TABLE 5-14. SHORT BEAM SHEAR TEST RESULTS: S-GLASS/USP23  
OMNIWEAVE COMPOSITES

Weave Geometry	Test Direction	Specimen Number	Fiber Angle (degrees)	Shear* Stress (psi)	Flexure* Stress (ksi)	l/d Ratio
45° FPS 6 layers	Axial	S21A-84-A-1	± 30	> 3130	83.5	13.3
		-2	± 28	> 3100	81.7	13.2
		-3	± 29	> 3240	88.7	13.7
		-4	± 27	> 3270	87.1	13.3
	Trans-verse	S21A-84-T-1	± 62	> 890	23.4	13.2
		-2	± 56	> 910	24.3	13.3
		-3	± 60	> 990	26.3	13.3
		-4	± 60	> 750	20.0	13.3
		-5	± 64	> 930	25.4	13.7
		-6	± 59	> 1060	29.0	13.7
	45° LID 18 layers	S21D-104-A-1	± 24	> 6690	74.0	5.5
			± 30	> 6740	74.9	5.6
			± 33	> 5840	66.0	5.6
			± 28	> 6710	75.0	5.6
			± 29	> 6540	68.2	5.2
			± 33	> 5040	65.7	5.7
		S21D-104-T-1	± 64	> 2270	24.6	5.4
			± 63	> 1930	20.8	5.4
			± 61	> 2170	23.5	5.4
			± 62	> 2390	27.3	5.7
			± 64	> 2140	23.2	5.4

\*Calculated at failure load — in most cases flexure stress values are ≥ flexural strength values (Table 5-4) indicating that specimens did not fail in shear.

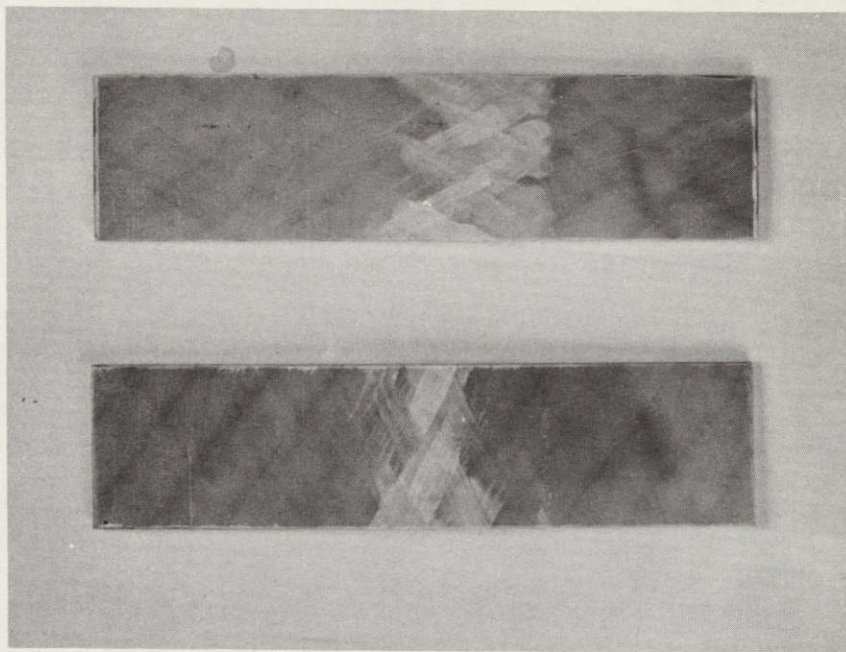
TABLE 5-15. SHORT BEAM SHEAR TEST RESULTS:  
MORGANITE II/USP23 OMNIWEAVE COMPOSITES

Weave Geometry	Test Direction	Specimen Number	Fiber Angle (degrees)	Shear* Stress (psi)	Flexure* Stress (ksi)	1/d Ratio
45° LID 12 layers	Axial	G51D-96-2-A-1	± 36	> 6520	52.2	4.0
		-2	± 32	> 6580	52.6	4.0
		-3	± 34	> 6860	54.0	3.9
		G51D-96-3-A-11	± 23	> 6070	46.5	3.8
		-12	± 29	> 6330	49.0	3.9
		-13	± 28	> 5920	44.4	3.7
		-14	± 25	> 6450	47.8	3.7
		-15	± 28	> 6790	51.6	3.8
	Trans-verse	G51D-96-2-T-1	± 63	> 2480	19.8	3.7
		-2	± 61	> 2540	19.0	3.7
		-3	± 63	> 1850	14.0	3.8
		-4	± 62	> 2380	17.7	3.7
		-5	± 61	> 2680	19.9	3.7
Triaxial 6 Layers	Axial	G51A/L-207-A-1	± 10	> 4790	109.6	11.4
		-2	± 20	7720**	88.5	5.7
		-3	± 11	7750**	65.7	4.2
		-4	± 14	9130**	79.0	4.3
	Trans-verse	G51A/L-207-T-1	± 84	> 880	5.30	3.0
		-2	± 84	> 760	4.58	2.0
		-3	± 81	> 990	5.49	2.8
		-4	± 81	> 1280	7.16	2.8
		-5	± 81	> 970	5.36	2.8

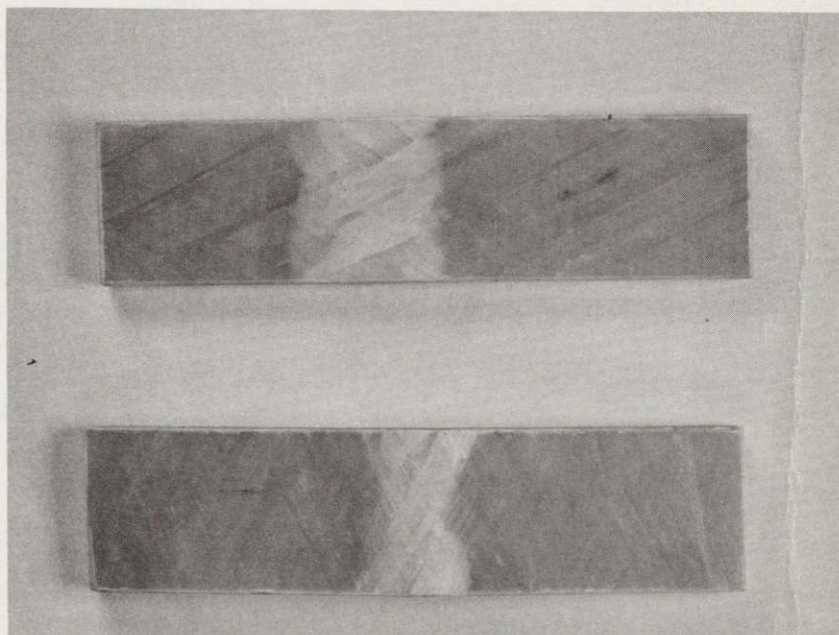
\*Calculated at failure load — in most cases strain values are  $\geq$  flexural strength values (Table 5-5) indicating that specimens did not fail in shear.

\*\*Flexure stress is  $<$  flexure strength, hence these values may represent measurable shear strengths.





S21A-84 Axial Orientation (Top) - Transverse Orientation (Bottom)



S21D-104 Axial Orientation (Top) - Transverse Orientation (Bottom)

Figure 5-20. Typical Short Beam Shear Failure Modes  
for S-Glass Omniweave Composites

## 5.6 CONCLUSIONS

The following conclusions have been made on the mechanical evaluation of Omniweave composites.

1. The measured effect of Omniweave fiber orientation on flexural properties appears to be realistic but the absolute strength and modulus values obtained are lower than anticipated. This is probably due to inadequate process optimization and/or test specimen configuration.
2. Data for the layered-in-depth (LID) construction indicate that it produced composites having greater in-plane properties than the fiber pitch angle (FPA) geometry.
3. The effect of cure cycle on flexural properties was shown to be significant and indicated that molding with the resin in a low stage of advancement improves fiber wetting and composite strength.
4. The tensile data for S-glass and Morganite Type II/epoxy Omniweave composites showed a wide scatter and lower strength values than would be predicted from unidirectional data for an optimum fiber-resin system. The data obtained, however, correlate well with predictions based on measured unidirectional properties for similarly processed fiber resin systems. This is encouraging in that it demonstrates the ability to predict Omniweave structural behavior, but it also points out the need for improved processing techniques to promote better fiber-resin adhesion.
5. The maximum property value achieved with the boron/HT424 FPA Omniweave was comparable with unidirectional boron/HT424 composite data.
6. Compressive test data on S-glass and Morganite exhibited significant data scatter. Transverse omniweave compressive strengths appeared to be significantly better than those reported in the literature for unidirectional materials.
7. Interlaminar shear modes of failure were not realized on short beam shear tests. Relatively high shear values are indicated for optimized Omniweave composites.

**SECTION 6**  
**OMNIWEAVE STRUCTURAL ANALYSES**



## SECTION 6

### OMNIWEAVE STRUCTURAL ANALYSES

Analyses were performed using the OMNI computer code to predict elastic moduli, coefficients of thermal expansion and approximate strengths as a function of the fiber angles for S-Glass, Morganite II, Boron, and Thornel 50 Omniweave composites. Off axis tests performed on unidirectional S-glass/epoxy composites were utilized to determine the elastic constants and strength parameters for a more realistic prediction of S-glass Omniweave composite properties. The utilization of Omniweave for launch vehicle structural skin application was analyzed with the general conclusions that significant weight savings (60 percent) can be realized in the unpressurized region and a 30% weight savings can be effected in the pressurized booster areas.

#### 6.1 INTRODUCTION TO THE OMNI COMPUTER PROGRAM

The Omniweave computer program (OMNI)<sup>(14)</sup> performs a thermoelastic analysis of fibrous composites with fibers in four directions symmetric with the composite coordinate system (Figure 6-1). Inputs consist of the defining fiber and binder isotropic moduli, binder volume fraction, and unidirectional composite axial, transverse, and shear strengths.

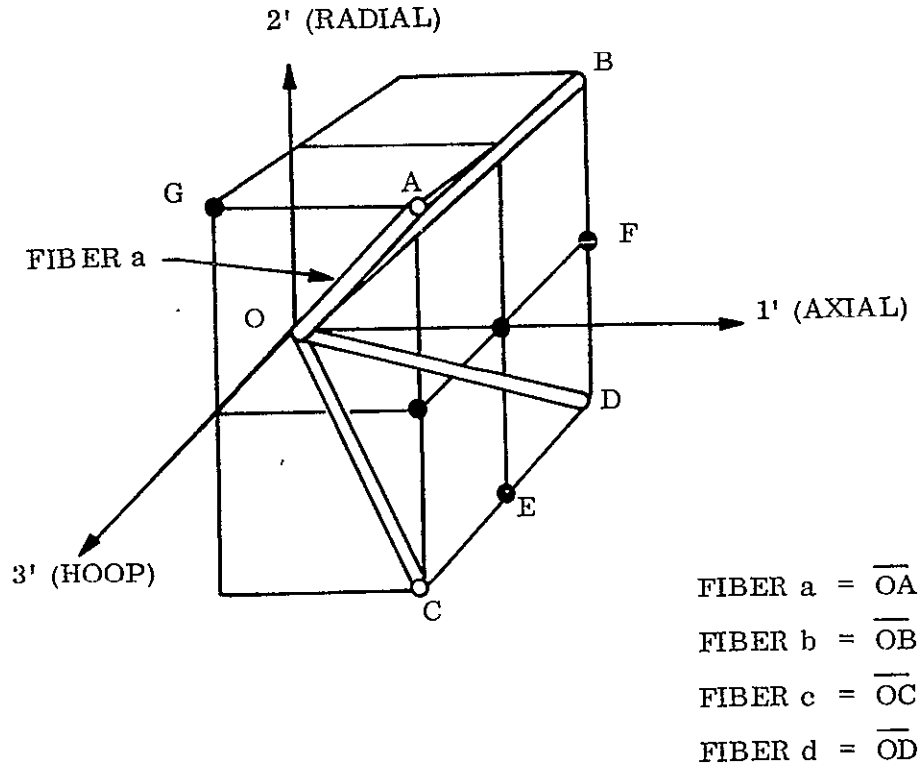
The analysis in OMNI utilizes an averaging technique where the 21 elastic stiffness or compliance restraints are determined by transformation from the four fiber directions to the composite direction and the average value is used:

$$C_{ijkl} \text{ (AVE)} = \frac{1}{4} \sum_{m=a}^d C_{ijkl} \quad (m)$$

where: a, b, c and d are the four fiber directions.

The composite co-ordinate system is shown in Figure 6-1 where the one foot axis can be visualized as the direction that Omniweave is manufactured or the axial direction. The three foot axis is the transverse or hoop axis, and the two foot axis is the thickness or radial direction.

A limits routine predicts the unidirectional composite elastic moduli ( $E_1$ ,  $E_2$ ,  $G_{12}$ ,  $G_{23}$ ,  $\nu_{12}$ ,  $\nu_{23}$ ,  $\alpha_1$  and  $\alpha_2$ ). The computer program then predicts the Omniweave composite orthotropic elastic moduli ( $E^*_1$ ,  $E^*_2$ ,  $E^*_3$ ,  $G^*_{12}$ ,  $G^*_{23}$ ,  $G^*_{31}$ ,  $\nu^*_{12}$ ,  $\nu^*_{23}$ ,  $\nu^*_{31}$ ,  $\nu^*_{21}$ ,  $\nu^*_{32}$ , and  $\nu^*_{13}$ ) and thermal expansion coefficients ( $\alpha^*_1$ ,  $\alpha^*_2$ , and  $\alpha^*_3$ ) as a function of the fiber angles (see Figure 6-2). Mechanical and thermal loads (temperature change from zero stress state) are then input; and Margins of Safety, stresses and strains determined. A summary of the inputs and outputs of OMNI is given in Table 6-1.

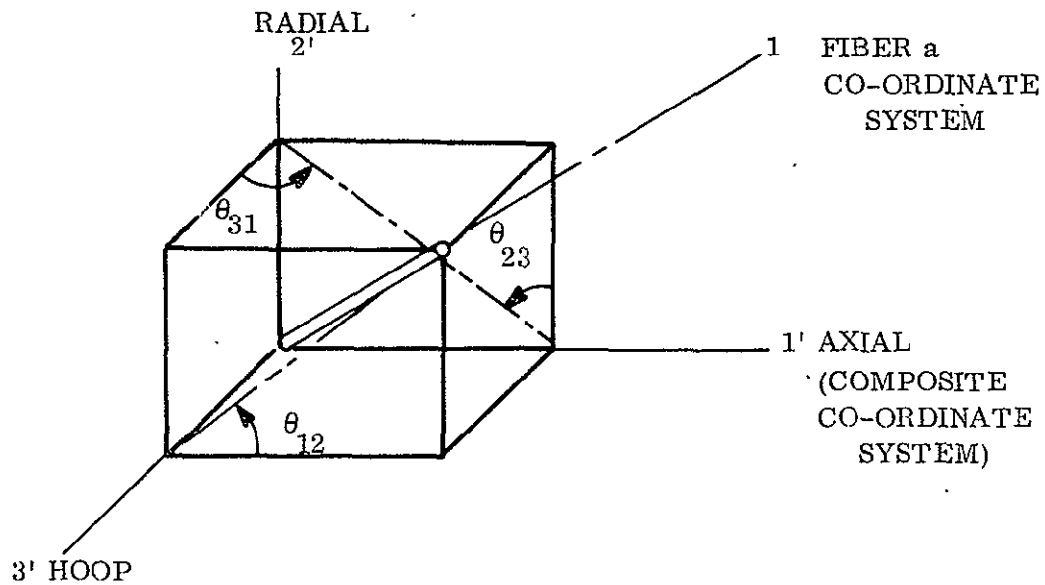


Composite Co-ordinate System

Omniweave is so constructed such that  $\overline{CE}$  equals  $\overline{DE}$  and  $\overline{BF}$  equals  $\overline{DF}$ , but there can be any variation in the relative lengths of AG, CD and BD changing the fiber angles. Figure 6-2 shows the projected angles  $\theta_{12}$ ,  $\theta_{23}$ , and  $\theta_{31}$  for fiber a and the angles from the composite axes 1', 2', and 3' as  $\phi_a$ ,  $\psi_a$  and  $\Omega_a$  respectively. The relationship between the projected angles and the direct angles are shown.

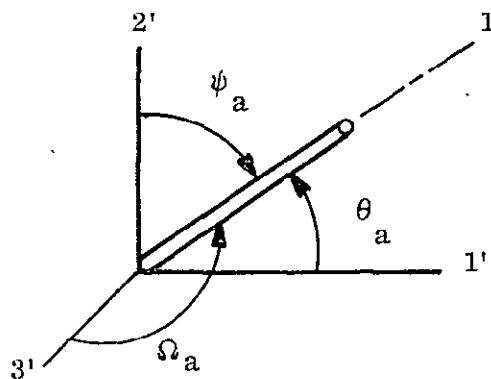
Figure 6-1. Description of Omniweave Fiber System

Maximum stress and Hill's modified failure criteria <sup>(15)</sup> were used to determine the margin-of-safety due to the applied load. From these values the strength allowables were determined. Hill's criteria showed the closest correlation to test data and will be used exclusively in the future to predict strength allowables in the Omniweave analysis. Also the max stress criteria does not yield a correct solution, because the OMNI computer program selects a specific fiber co-ordinate system to calculate the internal stresses. Therefore, the maximum stresses, which determine the Omniweave strength allowable, is not necessarily obtained. The correct maximum stresses could be obtained by rotating the co-ordinate system 360 degrees about the fiber axis, 1-axis



There are fibers b, c, and d in the other quadrants

Fiber orientation by angles from composite co-ordinates to fiber a



WHERE:

$$\text{TAN } \phi = \frac{\text{TAN } \theta_{12}}{\text{COS } \theta_{23}}$$

$$\text{TAN } \psi = \frac{\text{TAN } \theta_{23}}{\text{COS } \theta_{31}}$$

$$\text{TAN } \Omega = \frac{\text{TAN } \theta_{31}}{\text{COS } \theta_{12}}$$

Relationship between fibers a, b, c and d (Omniweave)

QUADRANT b:  $\phi_b = \phi_a$ ;  $\psi_b = \psi_a$ ;  $\Omega_b = 180^\circ - \Omega_a$ ;  $\theta_{12b} = \theta_{12a}$

QUADRANT c:  $\phi_c = \phi_a$ ;  $\psi_c = 180^\circ - \psi_a$ ;  $\Omega_c = \Omega_a$ ;  $\theta_{12c} = -\theta_{12a}$

QUADRANT d:  $\phi_d = \phi_a$ ;  $\psi_d = 180^\circ - \psi_a$ ;  $\Omega_d = 180^\circ - \Omega_a$ ;  $\theta_{12d} = -\theta_{12a}$

Figure 6-2. Omniweave Method of Analysis

TABLE 6-1. INPUTS AND OUTPUTS OF OMNI

Inputs	Outputs
1. Fiber orientation angles 2. Volume percent fiber 3. Fiber properties ( $E$ , $\nu$ and $\alpha$ ) 4. Matrix properties ( $E$ , $\nu$ and $\alpha$ ) 5. Composite stresses $\sigma_1'$ axial stress $\sigma_2'$ radial stress $\sigma_3'$ hoop stress $\sigma_{12}'$ , $\sigma_{23}'$ and $\sigma_{31}'$ (shear stresses) 6. Allowable Unidirectional Strengths $F_1$ parallel to fiber $F_2 = F_3$ transverse to fiber $F_{12} = F_{13}$ Shear $F_{23}$ = transverse shear 7. Temperature change from zero stress temperature	1. Unidirectional properties $(E_1, E_2 = E_3, G_{12} = G_{13}, G_{23}, \nu_{12} = \nu_{13}, \nu_{23}, \alpha_1, \alpha_2 = \alpha_3)$ 2. Composite properties Young's Moduli $E_1^*, E_2^*, E_3^*$ Shear Moduli $G_{12}^*, G_{23}^*, G_{13}^*$ Poisson's Ratios $\nu_{12}^*, \nu_{23}^*$ $\nu_{31}^*, \nu_{21}^*, \nu_{32}^*, \nu_{13}^*$ Thermal expansion coef. $\alpha_1^*, \alpha_2^*, \alpha_3^*$ 3. Composite Strains $\epsilon_1', \epsilon_2', \epsilon_3', \epsilon_{12}', \epsilon_{23}', \text{etc.}$ 4.* Strains in fiber coordinate directions $\epsilon_1, \epsilon_2, \epsilon_3, \epsilon_{12}, \epsilon_{23}, \text{etc.}$ 5.* Stresses in fiber coordinate directions $\sigma_1, \sigma_2, \sigma_3, \sigma_{12}, \sigma_{23}, \sigma_{13}$ 6.* Margins of Safety for the composite stresses $MS_1, MS_2, MS_3, MS_{12}, MS_{23}, MS_{13}$ (Max. Stress and modified Hill) *NOTE: The strains, stresses and Margins of Safety are given for mechanical stress loadings, residual stress loadings, and for combined mechanical and thermal loadings.

(See Figure 6-2) and determining the stresses for the co-ordinate systems at various increments. The maximum stress criteria does indicate the failure mode and was retained for this purpose.

Omniweave strength values are linearly dependent on the unidirectional strength corresponding to the failure mode, for the maximum stress criteria. This linear dependence is very nearly the case for Hill's criteria. It is therefore important that representative unidirection strength values, determined by tests, be input to obtain a correct computer analysis.

The OMNI computer code was specifically designed for standard FPA Omniweave, i.e., a fiber geometry where each fiber maintains a constant direction in space. The direction of each fiber for Layered in Depth Omniweave varies along the axial composite co-ordinate direction (see Figure 6-2) as a sinesoidal function. The angular displacement from the axial direction, i.e.,  $\theta_{12}$ , was approximated to vary between 0 and 15 degrees. Computer analysis indicated the Omniweave moduli and strength predictions varied only slightly between these two angles and that a value of  $\theta_{12} = 5^\circ$  yielded average values.

TABLE 6-2. BASIC MATERIAL PROPERTY INPUTS USED IN INITIAL ANALYSIS

Material	Modulus E ( $10^6$ psi)	Basic Axial Strength* (ksi)	Poisson's Ratio $\nu$	Coefficient of Thermal Expansion $\alpha$ ( $10^{-6}$ $F^{-1}$ )
Morganite II	40.0	400.0	0.25	2.0
Thornel-50	50.0	220.0	0.25	2.0
S-Glass	12.3	650.0	0.25	2.8
Boron	60.0	500.0	0.25	2.2
Resin (USP23 Epoxy)	0.54(K=1)	---	0.40	45.0

$$\text{*Unidirection Composite Strength} = \frac{\text{Fiber strength}}{1.3} \times \text{Fiber Volume}$$

Unidirectional shear and transverse tensile strength = 9000 PSI



## 6.2 PREDICTION OF OMNIWEAVE PROPERTIES AND COMPARISON WITH TEST DATA

### 6.2.1 PROPERTIES OF S-GLASS OMNIWEAVE COMPOSITES FROM UNIAXIAL TESTS

The off axis test data on unidirectional S-glass/USP23 composites reported in Section 5.1 was utilized to determine unidirectional elastic moduli and strength properties using the strain/elastic moduli equations presented in the Appendix Section 10.5.

From the  $0^\circ$  test data the parallel elastic modulus ( $E_1$ ) was determined to be  $7.25 (10)^6$  psi, the basic fiber elastic modulus ( $E_f$ ) was  $11.7 (10)^6$  psi with a resin elastic modulus of  $0.54 (10)^6$  psi. The transverse elastic modulus ( $E_2$ ) was determined to be  $2.42 (10)^6$  psi. The Poisson's Ratio  $\nu_{12}$  of 0.262 and finally the average shear modulus ( $G_{12}$ ) of  $0.744 (10)^6$  psi was determined. The individual values calculated for each test specimen using the OMNI computer program is listed for comparison (Table 6-3). The variation may be due to differences in fiber volume content from specimen to specimen. The correlation between predicted unidirectional moduli and that obtained from the OMNI computer code was very close except that the shear modulus test values were 10 percent higher than predicted. This correlation indicates that a K factor of 1.0 can be used in OMNI for S-glass composites. Previous data used a K factor of 1.9.

Using the unidirectional moduli, the axial modulus versus fiber angle was calculated and compared with the test data in Figure 6-3. All of the test data fell on the predicted modulus ( $E_X$ ) (except that for the  $45^\circ$  degree specimens) indicating that the unidirectional moduli determined are accurate. The axial modulus was also calculated using the basic fiber and matrix constituent properties with very little deviation from the test data. This close correlation was obtained using matrix modulus of elasticity of 540,000 psi with a K factor of 1.0.

The unidirectional strength was determined from the off axis tensile test specimens. The specific values calculated and the order of evaluation is shown in Table 6-4. The transverse tension and shear strength variation is partly due to the variation in volume percent fibers. The low values of  $F_2$  and  $F_{12}$  can be improved by process improvement.

Using these unidirectional strengths, the axial strength versus fiber angle was calculated using the Modified Hills Failure Criteria. This predicted strength versus the test data is shown in Figures 6-4 and 6-5. In Figure 6-4 it can be seen that there is very little change in the predicted strength if the transverse compression strength ( $F_{2C}$ ) is four times the transverse tensile strength ( $F_2$ ). As mentioned later it was decided to use the factor of four.

TABLE 6-3. S-GLASS UNIDIRECTIONAL MODULI FROM TEST DATA

Resin Modulus =  $0.54 (10)^6$  psi, = .35  
 Fiber Modulus =  $11.7 (10)^6$  psi, = .20

Fiber Orientation	Strain Reading	$E_1$ ( $10^6$ psi)	12	$E_2$ ( $10^6$ psi)	$G_{12}$ ( $10^6$ psi)
0°	Axial	7.25	0.288		
90°	Axial		0.237	2.42	
45°	Shear			(1.66)*	
(Average values used to obtain $G_{12}$ )			0.262	2.42	
45°	Axial				0.670
45°	Lateral				0.840
20°	Axial				0.722
20°	Lateral				0.765
20°	Shear				0.635
60°	Axial				0.722
60°	Lateral				0.865
60°	Shear				0.72
AVE					0.7436
DATA FROM OMNI COMPUTER CODE Using Constituent Properties					
$(E_b = 0.54(10)^6$ psi, $\nu_b = 0.40$ , $E_f = 11.5(10)^6$ psi, $\nu_f = 0.20$ )					
0 & 20		7.24	0.272	2.445	0.672
45		6.678	0.282	2.144	0.591
60		7.124	0.274	2.380	0.655
90		6.789	0.280	2.200	0.606
AVE.		6.957	0.277	2.292	0.631
VALUES USED TO CALCULATE AXIAL MODULUS					
TEST DATA		7.25	0.262	2.42	0.7436,

\*Value not used because 90° specimen gives best results.

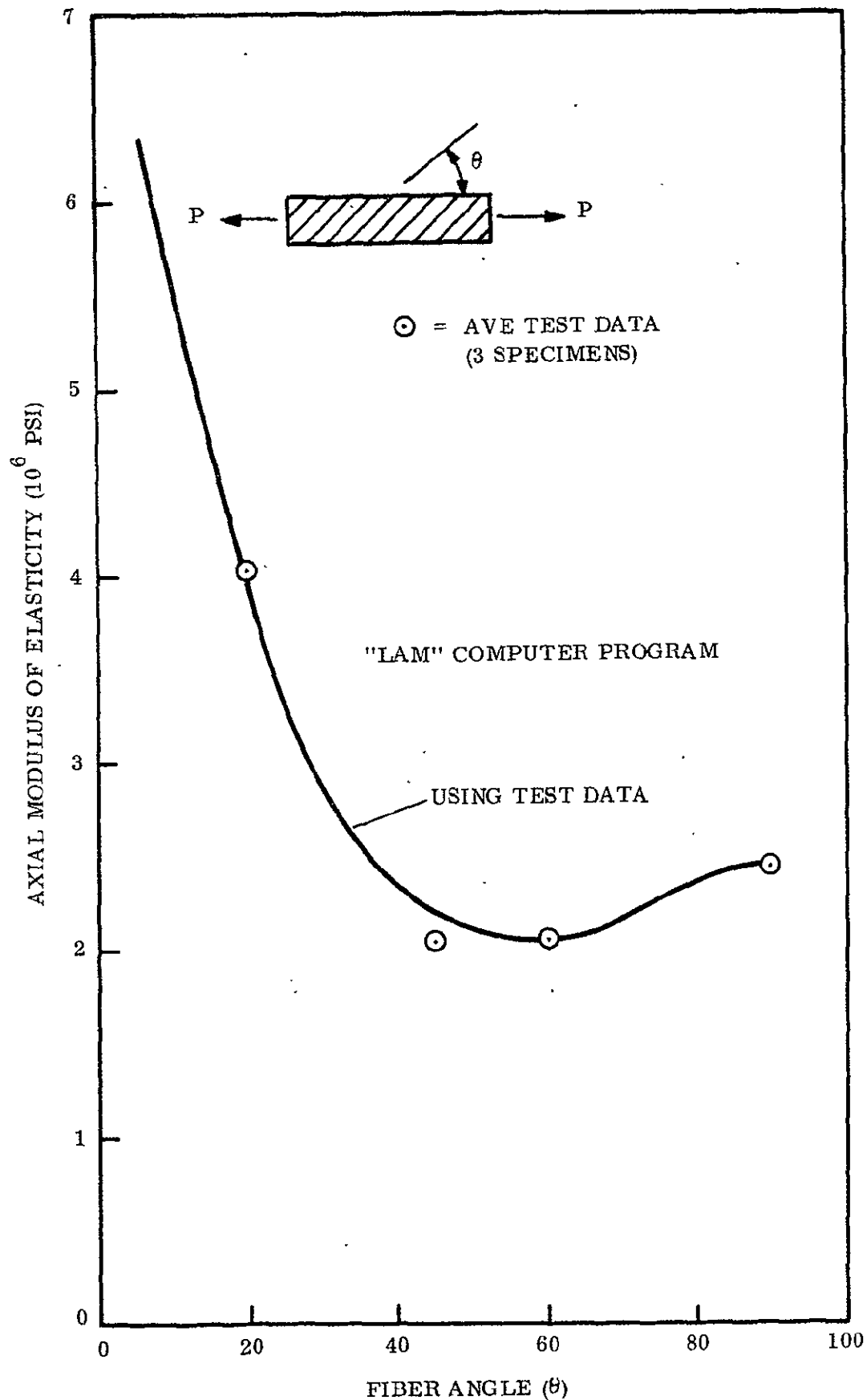


Figure 6-3. S-Glass Off-Axis Modulus Test Data

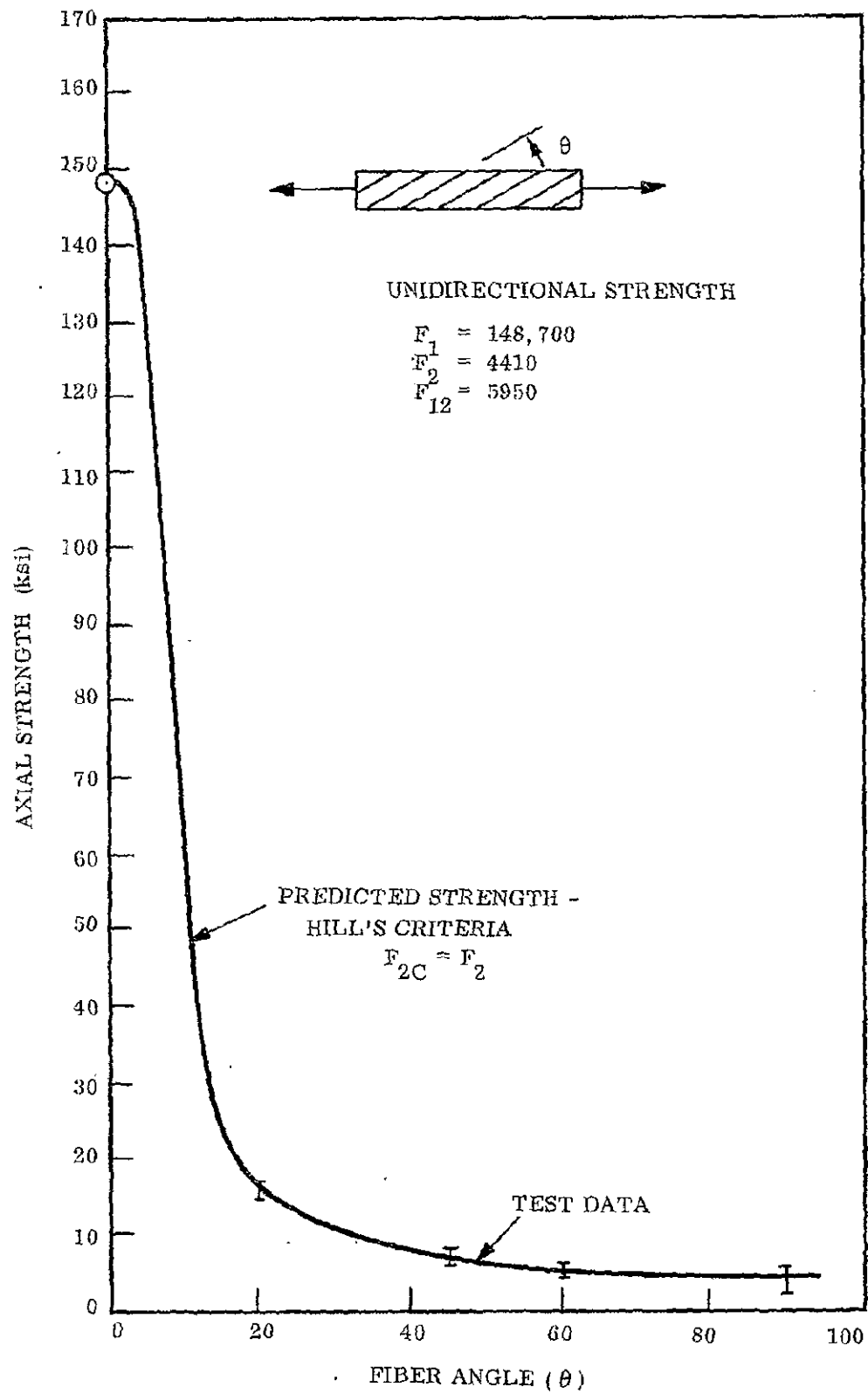


Figure 6-4. S-Glass Off-Axis Strength Test Data

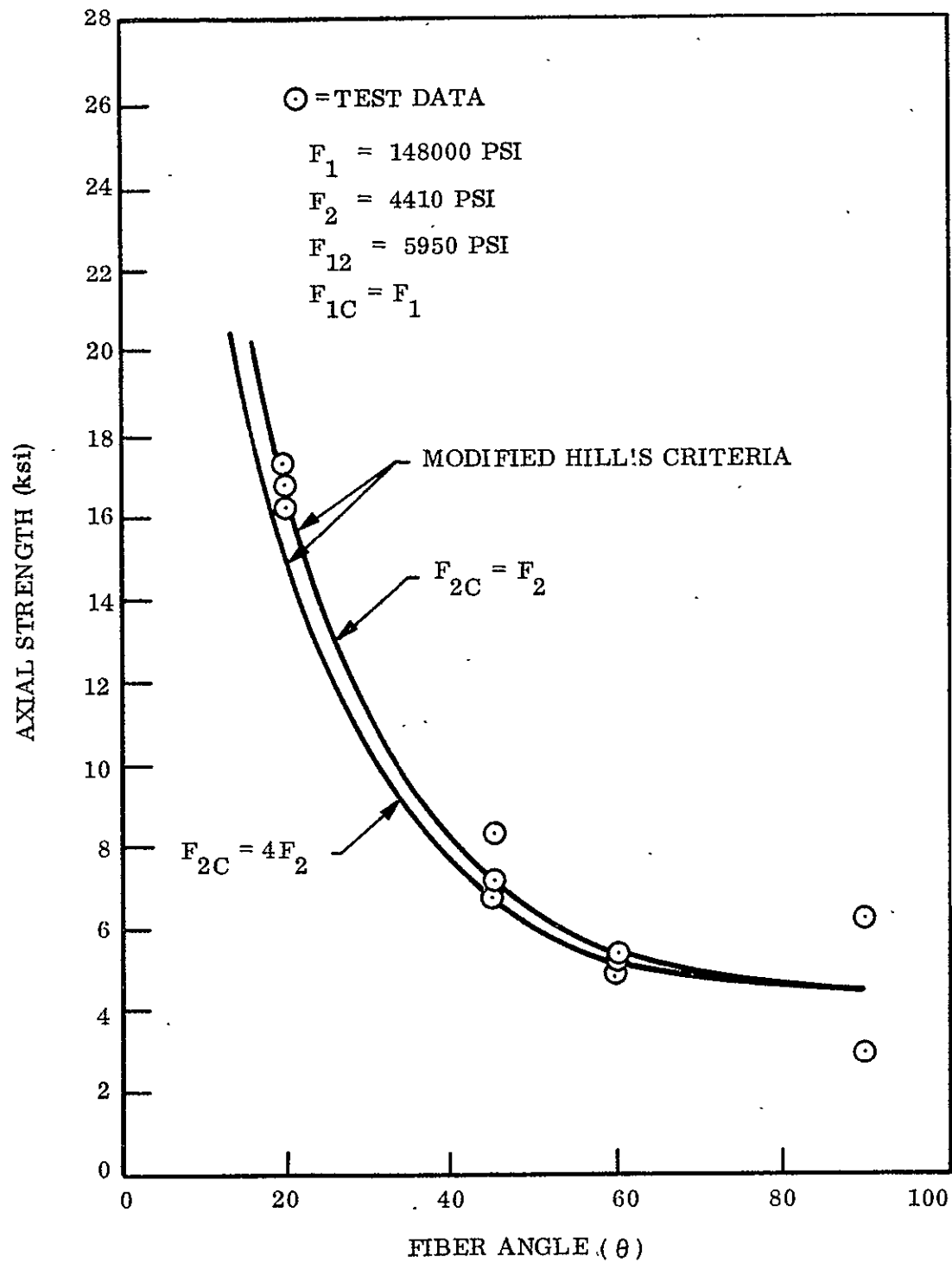


Figure 6-5. S-Glass Off-Axis Tensile Strength

TABLE 6-4. S-GLASS UNIDIRECTIONAL STRENGTH FROM TEST DATA

Test Fiber Orientation	Unidirectional Strength		
	<u>F<sub>1</sub></u> (psi)	<u>F<sub>2</sub>*</u> (psi)	<u>F<sub>12</sub>*</u> (psi)
0°	148,700	4500	
90°			
60°			3850
45°			6370
20°			5950
		AVE	5390
But 20° specimen gives best shear strength			5950
60°		4010	
45°		4650	
20°		4580	
		AVE	4413
Final Values Used	<u>148,700</u>	<u>4413</u>	<u>5950</u>

\*All of these values of transverse tensile and shear strengths are low and with process improvement we would expect a 100 percent improvement.

Using the unidirectional strength data, the predicted strength of the S-glass/epoxy Omniweave was determined using the OMNI computer program. Figure 6-6 shows the correlation between tensile test data and predicted values. Figure 6-7 shows the compression test data and Figure 6-8 the modulus of elasticity. The tensile test data values are significantly higher than the predicted strength when the uniaxial test data was used but was lower than the expected strength that can be obtained with process improvement. The two specimens in Figure 6-6 that fall outside the predicted range are considered to have an average fiber angle  $\theta$  of 20 degrees instead of the angles reported. The compression test data in Figure 6-7 is also in the range expected. As shown on this curve with the unidirectional transverse compressive strength ( $F_{2C}$ ) set equal to four times the transverse tensile strength ( $F_2$ ) results in a better fit of the test data.

The correlation of the composite elastic modulus test data is shown in Figure 6-8. In the steep part of the curve the discrepancy again could be due to the accuracy that the reported fiber angles have. Two prediction curves were generated with a volume

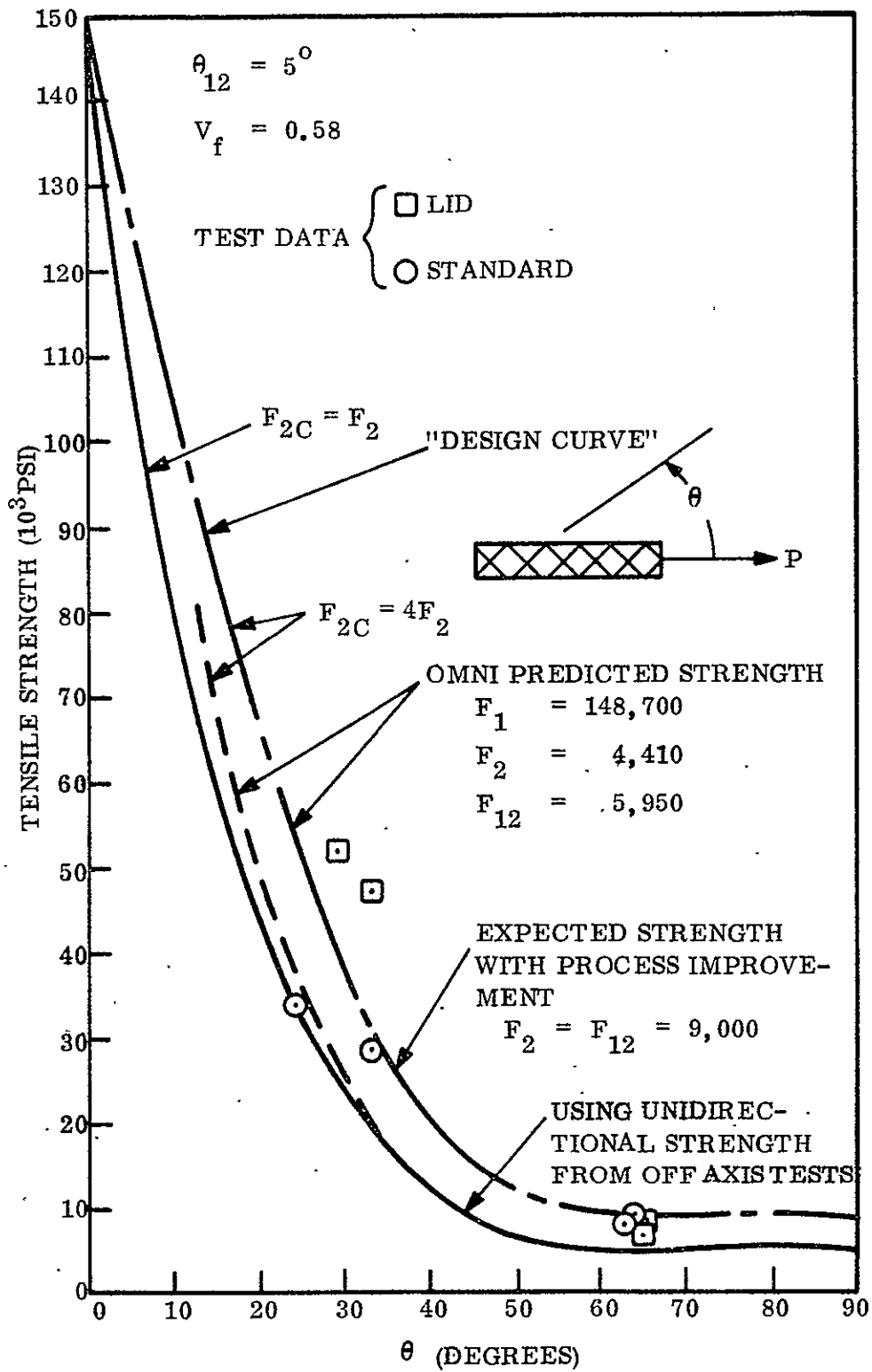


Figure 6-6. S-Glass Omniweave Tensile Strength

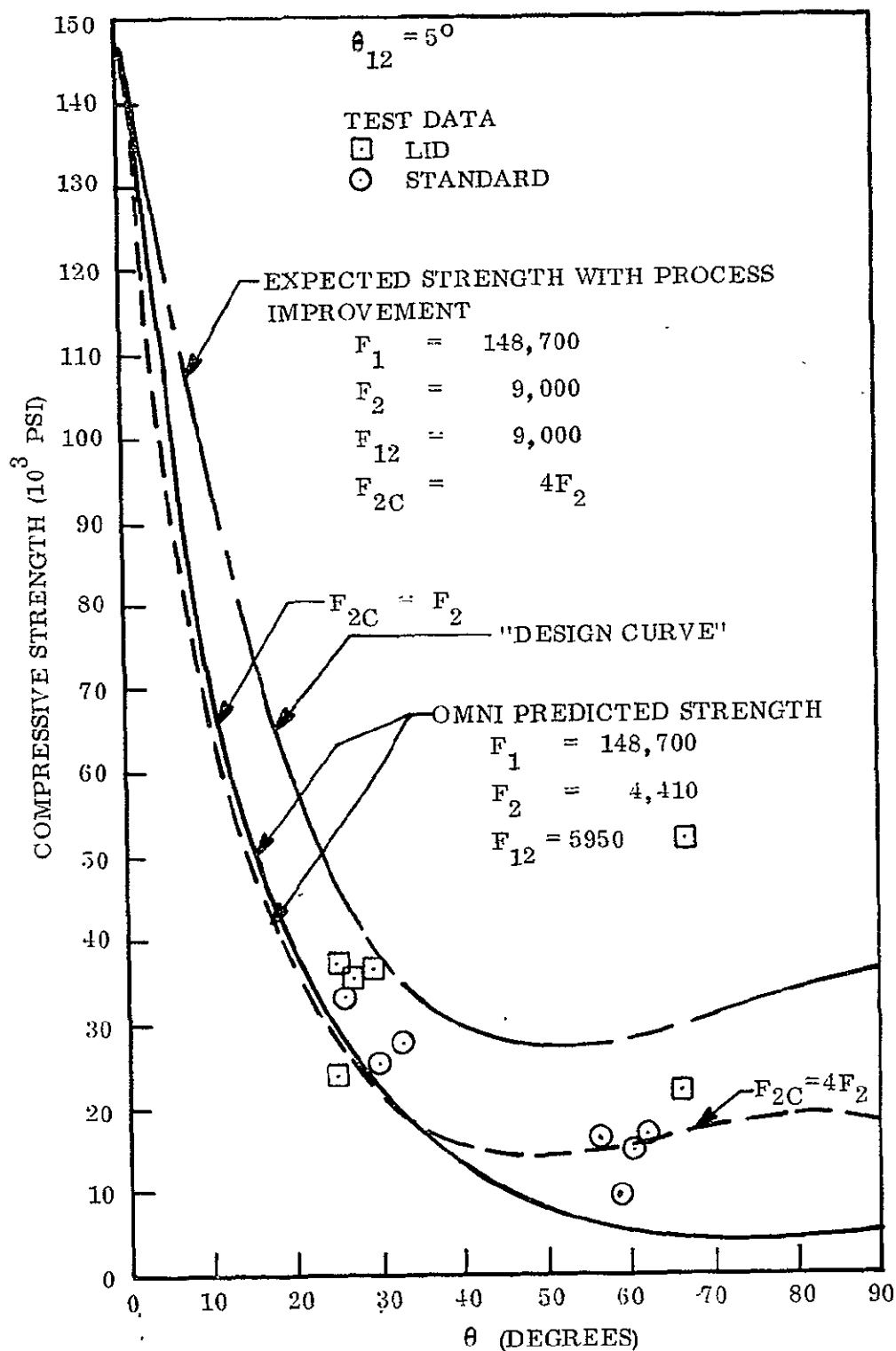


Figure 6-7. S-Glass Omniweave Compressive Strength



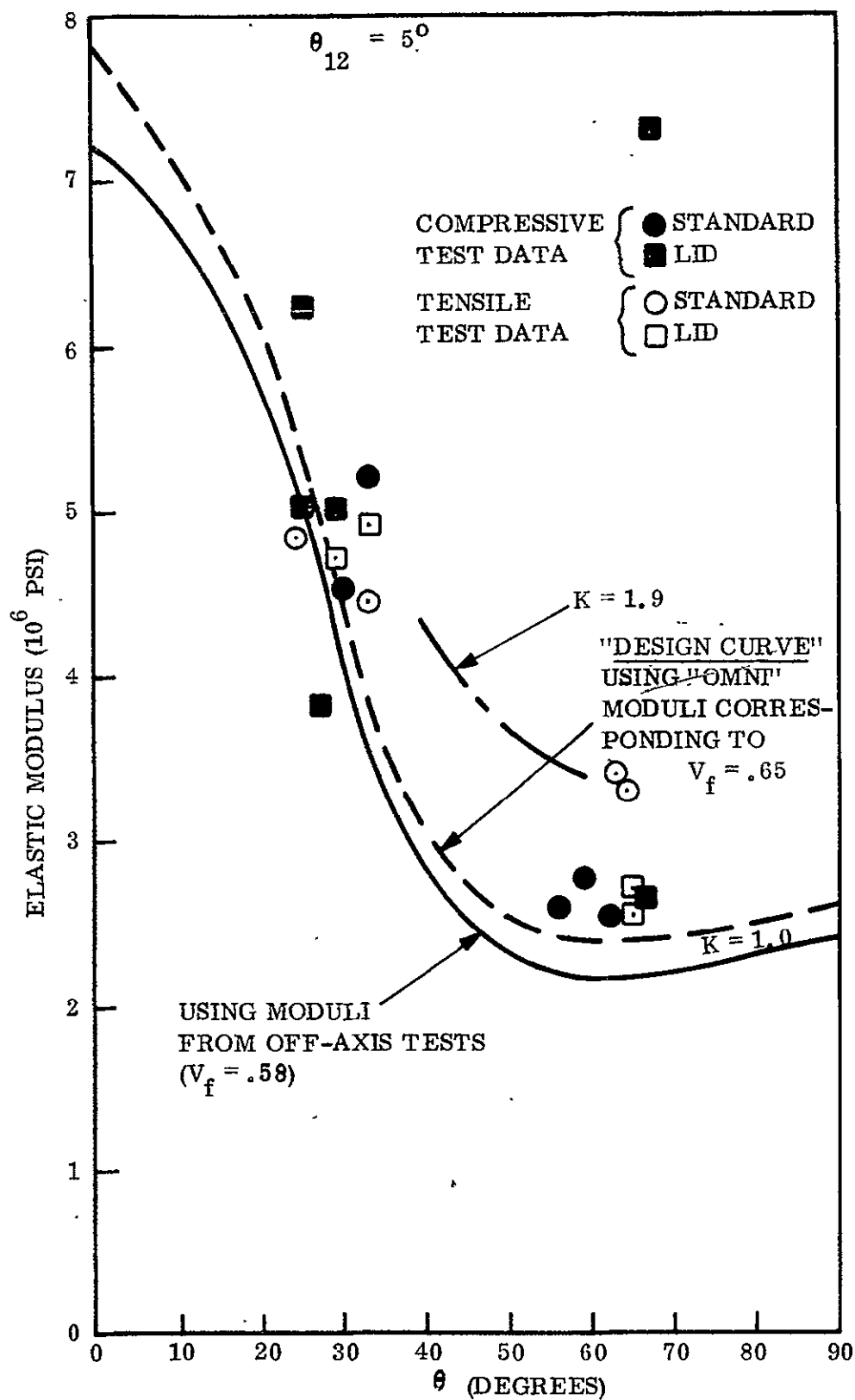


Figure 6-8. S-Glass Omniweave Modulus of Elasticity

percent fiber of 58 and 65 to correspond with the unidirectional moduli test values and the expected values with a higher volume fraction of fibers. The 65 percent fiber volume curve represents the predictions using the unidirectional moduli generated from the constituent moduli in the OMNI computer program. As determined from the off-axis test specimens the OMNI shear modulus is low by about 10 percent from the test data. If this increase were included in the analysis, the  $V_f = 0.65$  predicted composite modulus would be higher and closer to the test data. The final S-glass design curves of strength and modulus of elasticity are those labeled "Design Curve" in Figure 6-6, 6-7 and 6-8.

#### 6.2.2 FINAL DESIGN CURVES

The final "Design Curves" as predicted by the OMNI computer program for all of the layered-in-depth (LID) and the standard Omniweave configurations with a small edge projected angle ( $\theta_{12} = 5^\circ$ ) are shown in Figures 6-6 through 6-17. All of these properties are based on the percent fiber volume that was obtained in the fabrication of specimens. All of these predictions are based on a K factor of 1.0 and a transverse compression strength equal to four times the transverse tensile strength. Where considerable test data falls below the "Design curve", it has been judged that by process improvement, these values can be obtained.

#### 6.2.3 PRELIMINARY DESIGN CURVES

During the course of this program, the OMNI Computer Program was utilized to predict, not only strength and moduli properties but also Margins of Safety (under thermal or thermal plus mechanical loading), shear moduli, poisson's ratios, and coefficients of thermal expansion for Omniweave composites. These curves are presented in Appendix Section 10.6.

### 6.3 APPLICATION OF OMNIWEAVE TO LAUNCH VEHICLE BOOSTER SYSTEMS

There is not sufficient test data available to completely characterize and substantiate the failure criteria used. However, there is sufficient data so that an approximate prediction of strength can be made of the different Omniweave configurations to compare with metallic facing materials, currently being used as structural skins on launch vehicle booster systems. As shown in Figure 6-18, there is a good correlation of the test strength and predicted strength of the layered-in-depth configurations as a function of the fiber orientations. (This data on Quartz Omniweave was obtained through another program). This correlation was obtained using the Hill's modified failure criteria and assuming the values of the unidirectional transverse tensile strength and shear strength. The values that actually fit the test data best was for Quartz-Phenolic Omniweave, where the transverse tensile strength,  $F_2$ , was set equal to 10,000 psi and the shear strength,  $F_{12}$ , was set equal to 12,000 psi. Because the unidirectional strength of the other fiber systems with a different resin system could be below the values of 10,000 psi and 12,000 psi used in this correlation, both values were set equal to 9,000 psi for predicting the Omniweave strength in this study.

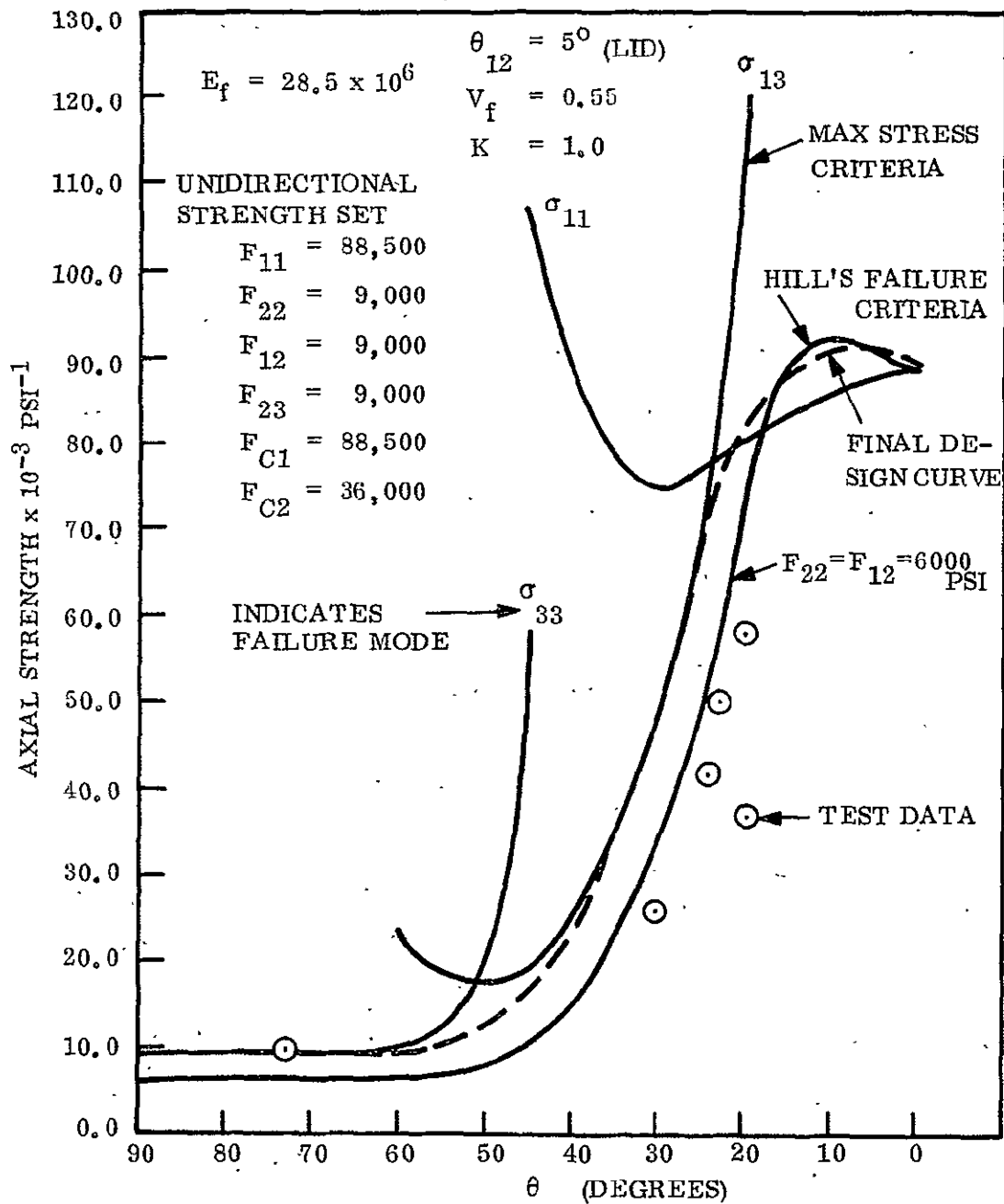


Figure 6-9. Axial Tensile Strength of Morganite II Omniweave

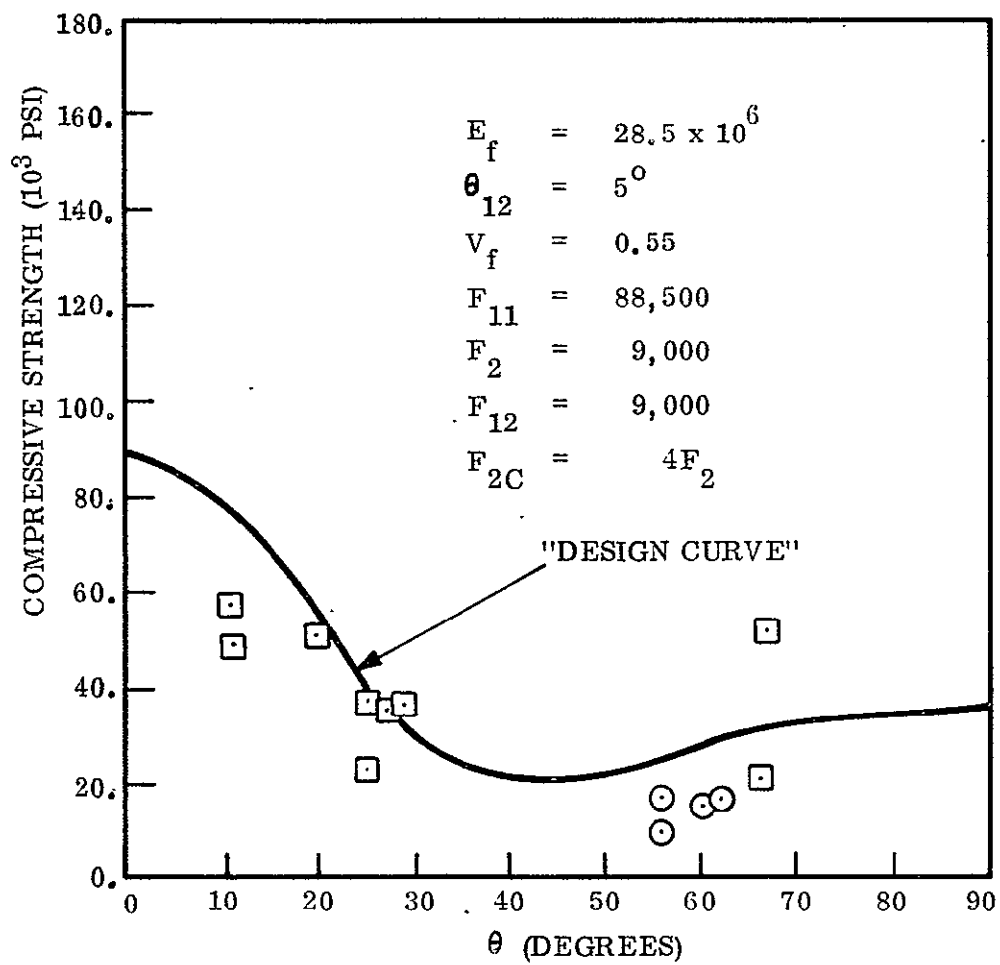


Figure 6-10. Morganite II Omniweave Compressive Strength

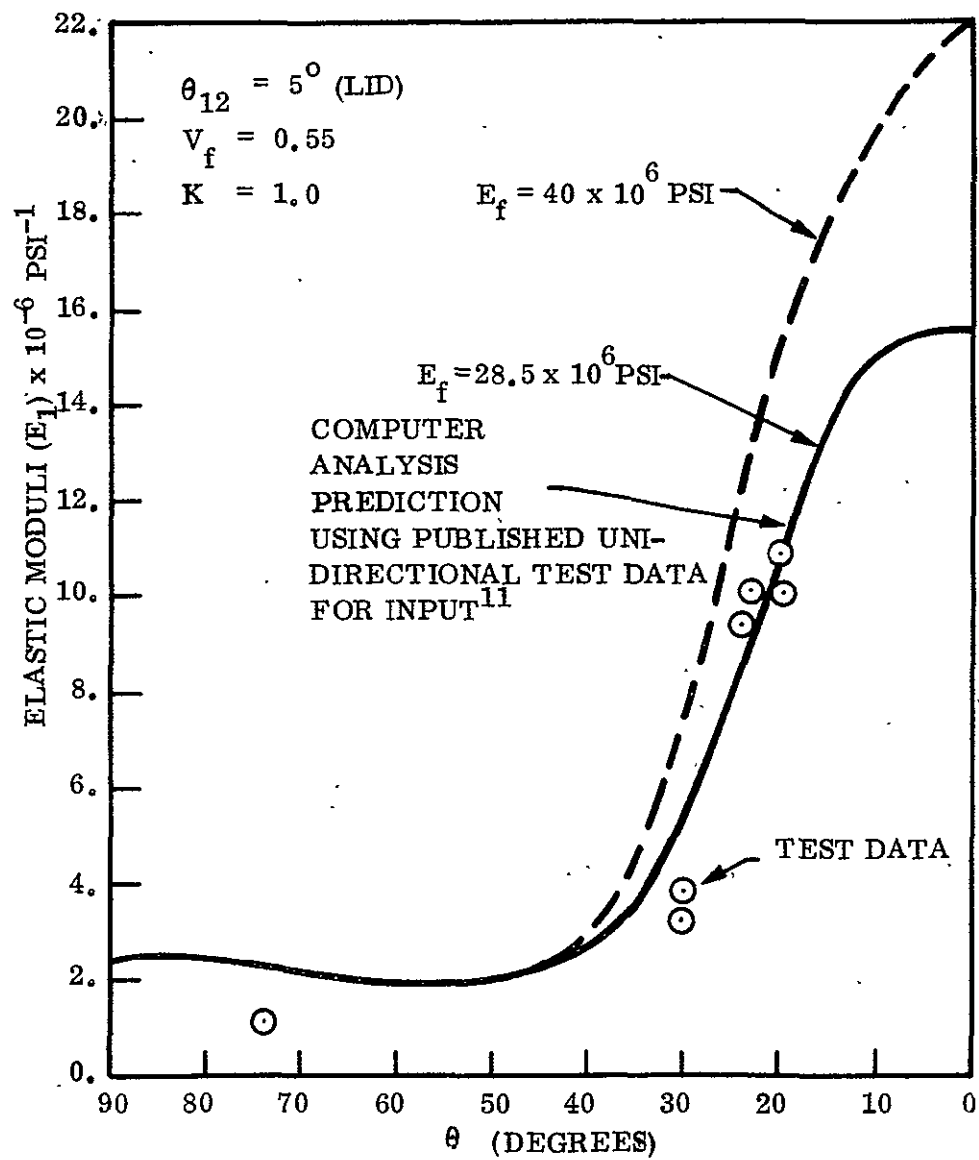


Figure 6-11. Longitudinal Elastic Modulus-Morganite II Omniweave

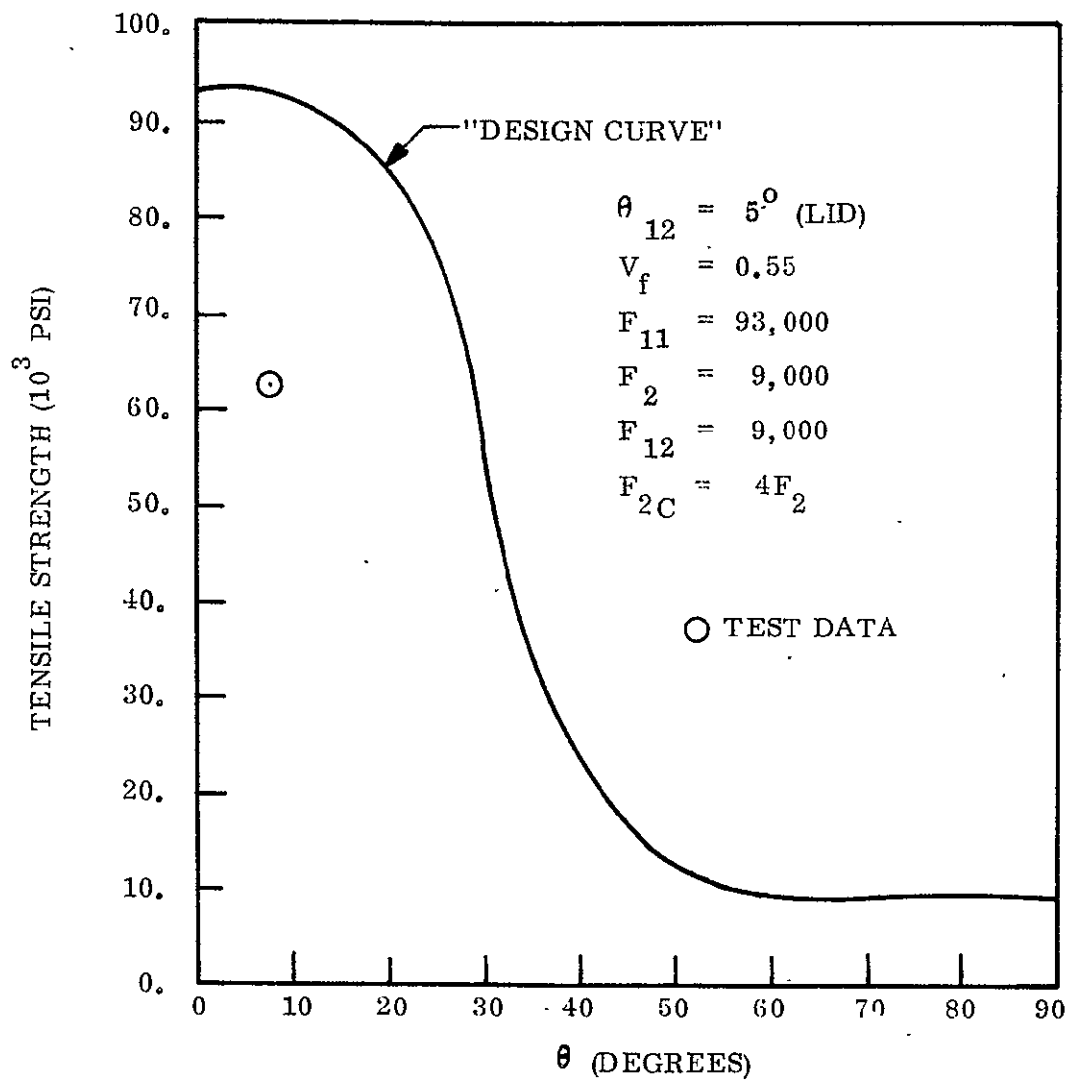


Figure 6-12. Thornel-50 Omniweave Tensile Strength Prediction

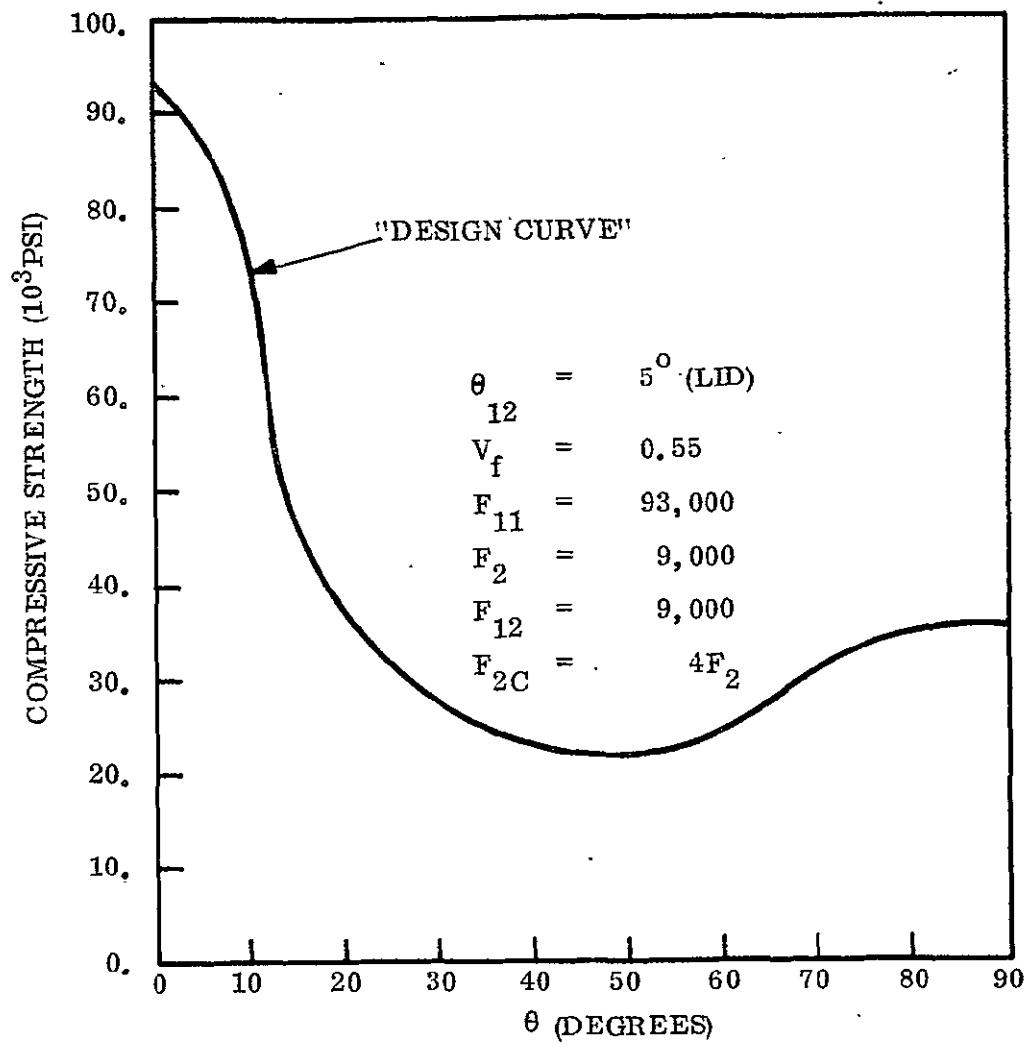


Figure 6-13. Thornel-50 Omniweave Compressive Strength Prediction

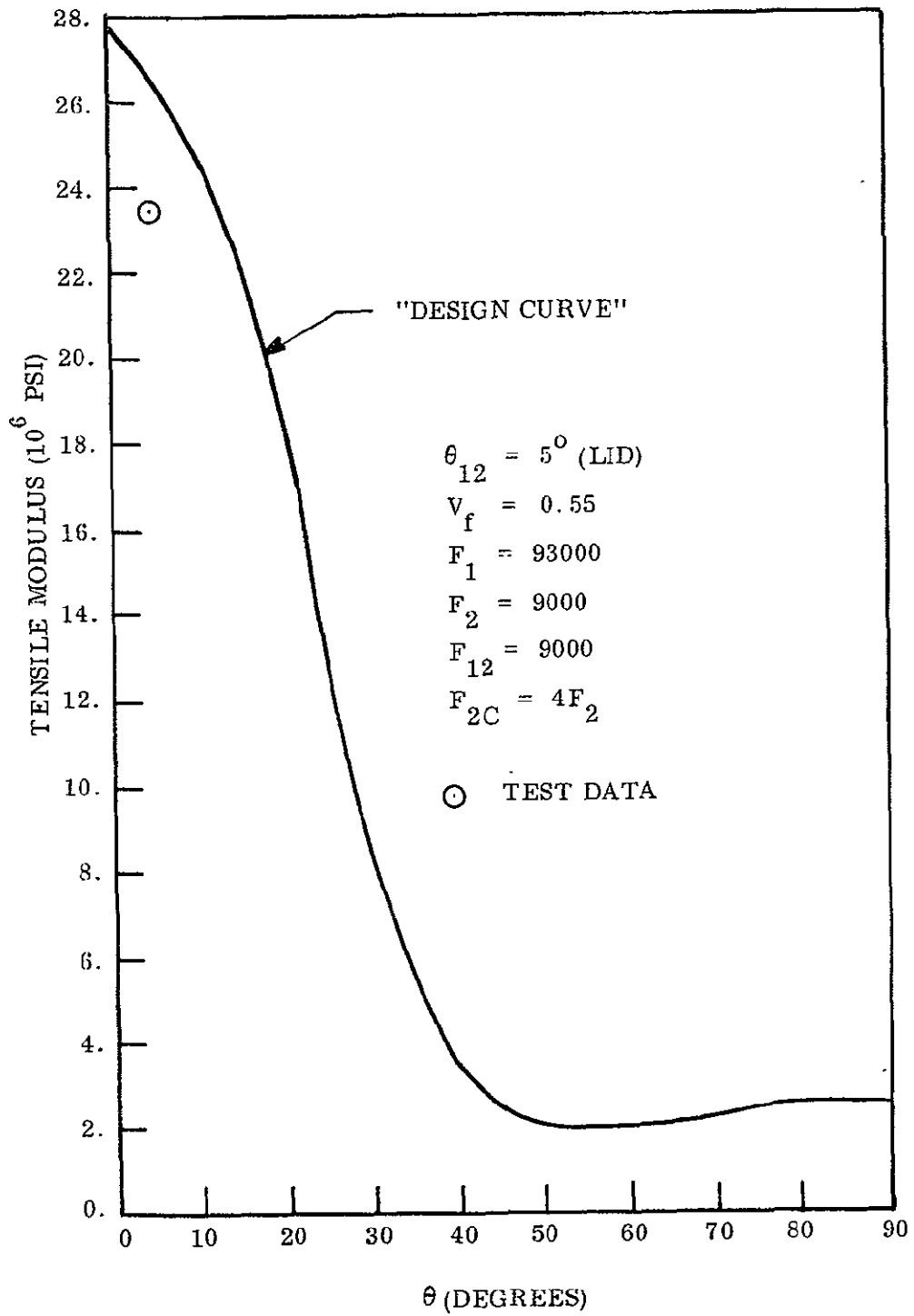


Figure 6-14. Thornel-50 Omniweave Tensile Modulus Prediction



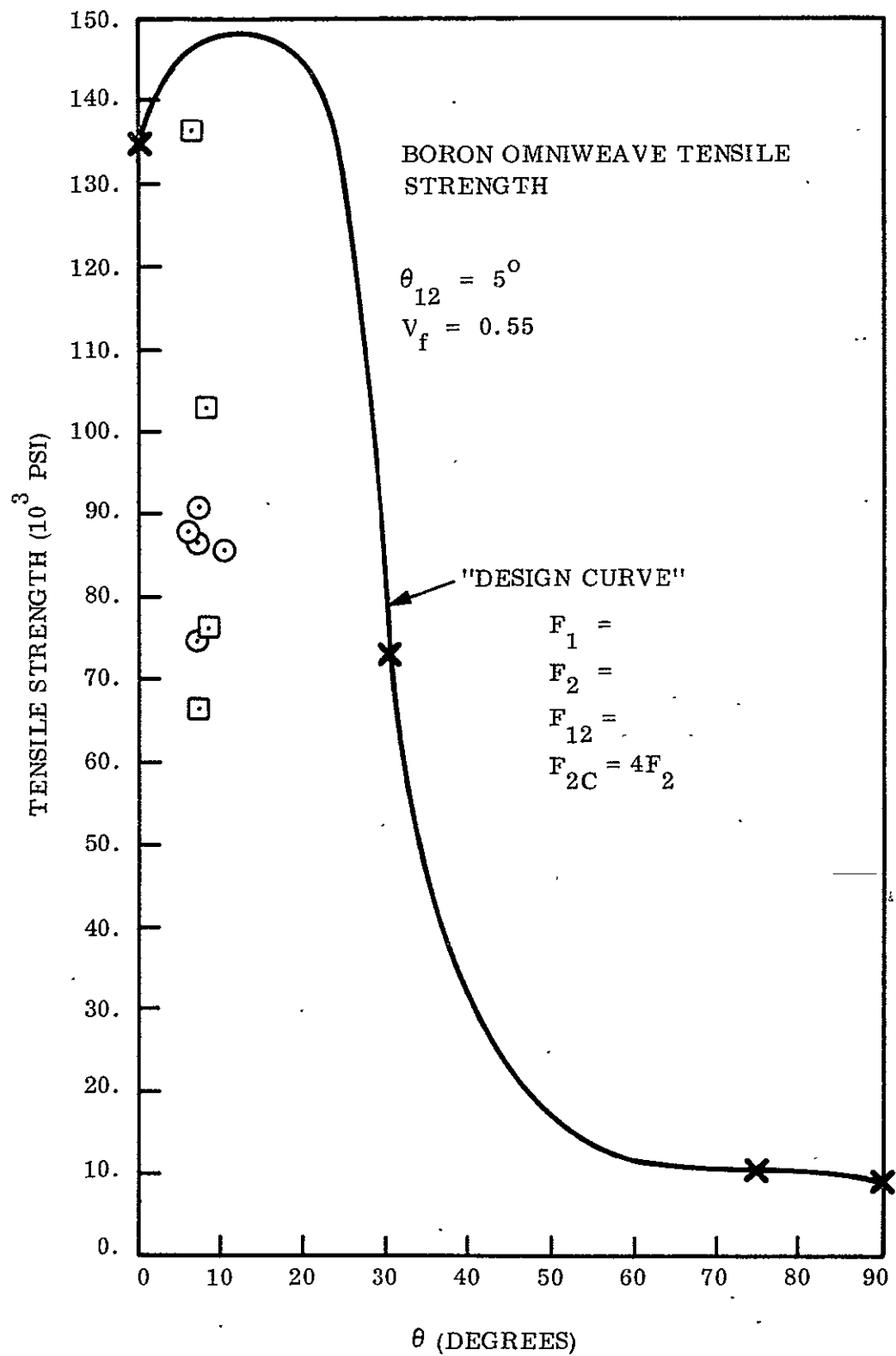


Figure 6-15. Boron Omniweave Tensile Strength

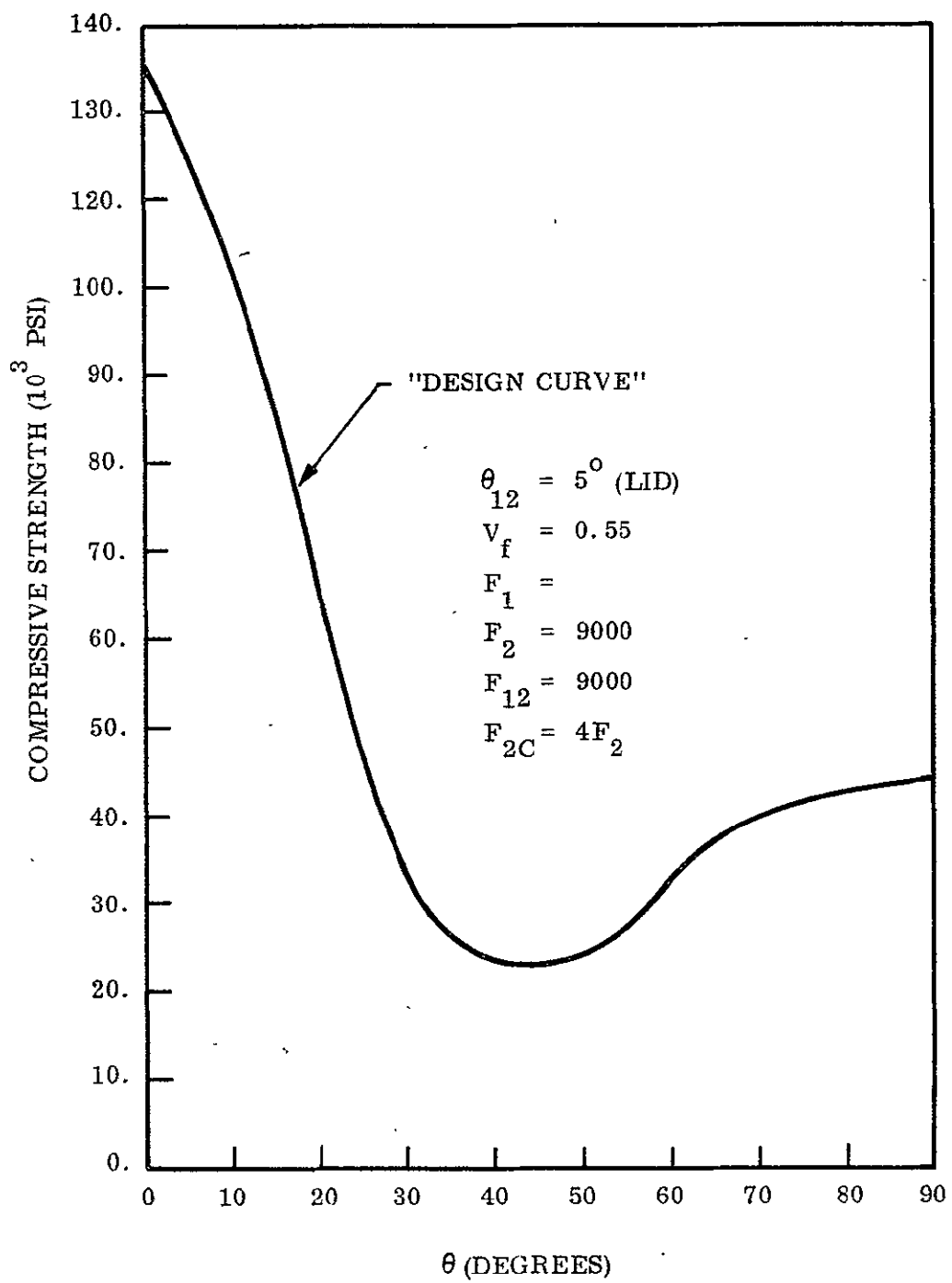


Figure 6-16. Boron Omniweave Compressive Strength

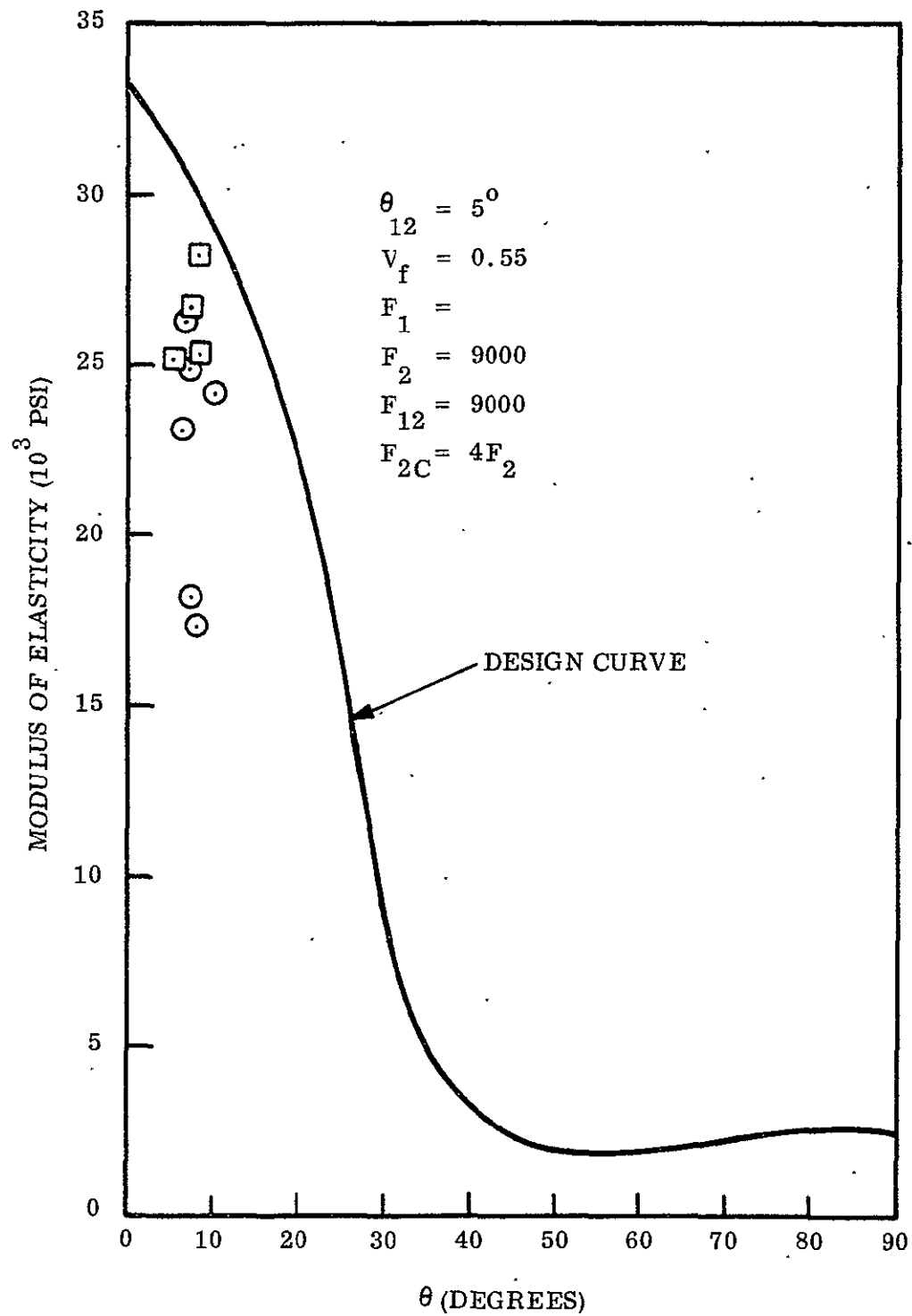


Figure 6-17. Boron Omniweave Tensile Modulus

$$\theta_{12} = 5^\circ \text{ (LID)}$$

$$V_f = 0.65$$

$$K = 1.9$$

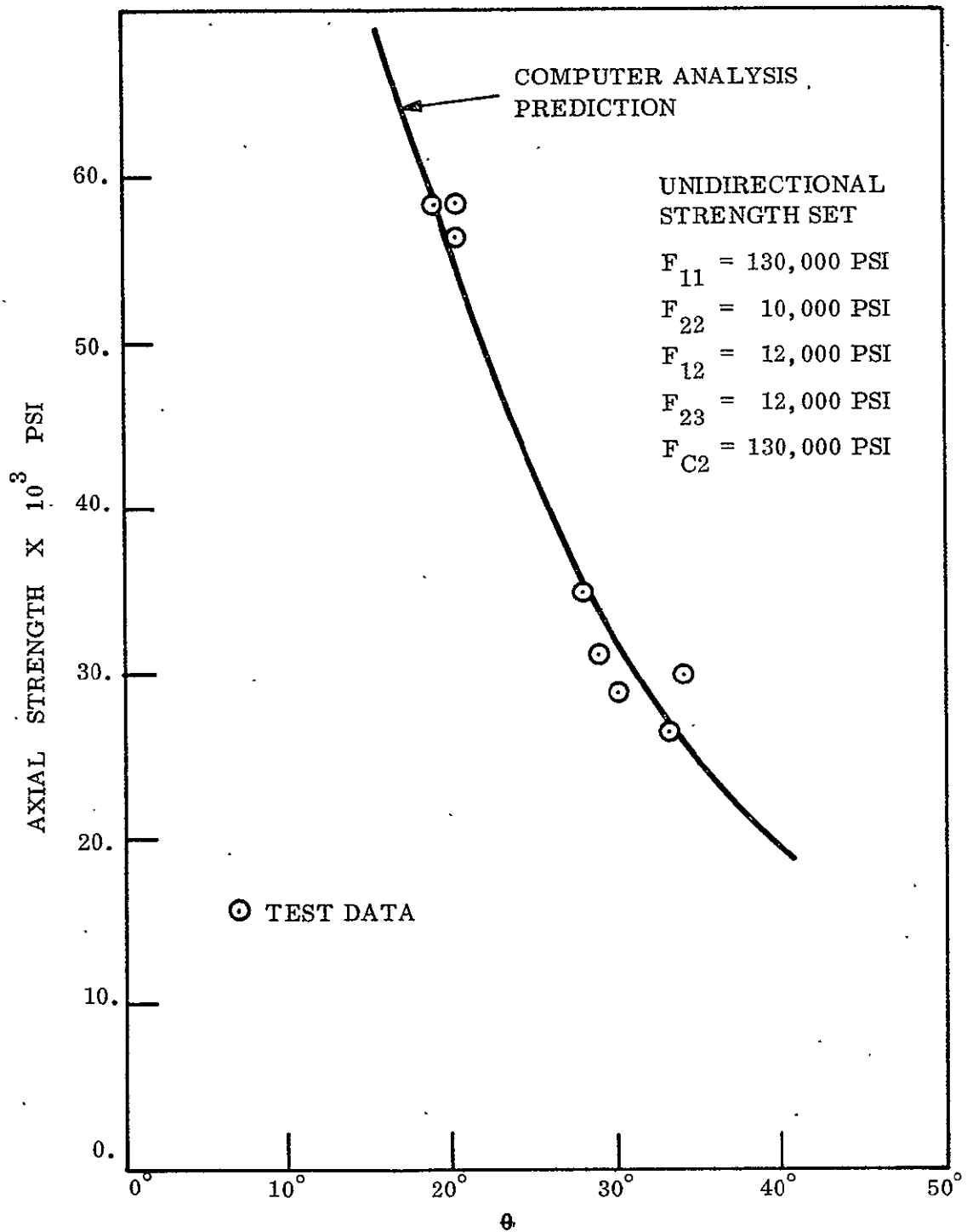


Figure 6-18. Axial Strength Using Hill's Modified Failure Criteria-Omniweave Quartz Phenolic

The configurations evaluated and the predicted strength are tabulated in Table 6-5. All configurations were for a fiber volume content of 65 percent. The axial and transverse strength of the 18 and 45 degree LID configurations are indicated. The third configuration, 18 and 72 degree LID, is two layers of 18 degree LID of equal thickness with one layer rotated 90° degree relative to the second layer. This results in a composite with equal strength in the axial and transverse directions.

TABLE 6-5. PREDICTED OMNIWEAVE STRENGTH  
(65% fiber volume content)

Material	Omniweave Angle to Axis (±θ)	Strength* (psi)		Density (lbs/in <sup>3</sup> )
		Axial	Transverse	
Morganite II	18° LID	120,000	10,000	0.0574
	45° LID	18,000	18,000	
	18°/72° LID	65,000	65,000	
S Glass	18° LID	64,000	10,000	0.0737
	45° LID	18,000	18,000	
	18°/72° LID	37,000	37,000	
Thornel 50	18°	86,000	10,000	0.0546
	45° LID	18,000	18,000	
	18°/72° LID	48,000	48,000	
Boron	18° LID	160,000	10,000	0.0702
	45° LID	18,000	18,000	
	18°/72° LID	85,000	85,000	

\* Unidirectional allowable strengths were conservatively assumed to be;

$$F_2 = 9000 \text{ psi and } F_{12} = 9000 \text{ psi}$$

From the data in Table 6-5 the specific strength of the various configurations was determined and tabulated in Table 6-6.

For launch vehicles, there are two critical loading conditions. The first is in the unpressurized areas where the critical shell loads are axial compression with low hoop loads. The second is in the pressurized areas where the axial compression is combined with hoop tensile loadings. Using honeycomb construction, the core thickness is varied to preclude buckling of the shell, so that the critical parameter is the strength to weight ratio (specific strength) of the facing materials. The Youngs modulus of the

TABLE 6-6. PREDICTED SPECIFIC STRENGTH COMPARISONS OF  
HONEYCOMB FACING MATERIALS  
AREAS OF LAUNCH VEHICLE NOT PRESSURIZED  
(Axial Strength Critical)

<u>Material</u>	<u>Omniweave Angle to Axis (<math>\pm \theta</math>)</u>	<u>Specific Strength (<math>10^3</math> inches)</u>	<u>Facing Weight Relative to 7075-T6</u>
Morganite II	18° (LID)	2080	36%
S Glass	18° (LID)	870	86%
Thornel 50	18° (LID)	1580	47.5%
Boron	18° (LID)	2270	33%
<u>Comparison Data</u>			
Ti-6Al-4V	Titanium	810	92.5%
17-7PH	Stainless Steel	650	115%
7075-T6	Aluminum	750	100%
Beryllium Sheet		1040	72%
AREAS OF LAUNCH VEHICLE PRESSURIZED (Both Axial and Hoop Strength Critical) (Axial Strength Equals Hoop Strength)			
Morganite II	45° (LID)	312	240%
	1/2 18°/1/2 72° (LID)	1130	66%
S Glass	45° (LID)	245	305%
	1/2 18°/1/2 72° (LID)	502	148%
Thornel 50	45° (LID)	330	227%
	1/2 18°/1/2 72° (LID)	880	85%
Boron	45° (LID)	256	292%
	1/2 18°/1/2 72° (LID)	1210	62%

facing material dictates the required core thickness with increased weight for lower modulus facing materials. This weight variation in general is of secondary importance to that of the facing weight. Therefore, specific strength of the facing materials is a good measure of the relative weight effectiveness of different facing materials for launch vehicle honeycomb construction.

As can be seen from Table 6-6, all of the shallow axial angle Omniweave configurations are very competitive with the metallic facing materials in the unpressurized area of the launch vehicle. The Boron Omniweave configuration indicates a facing weight 33 percent of an equivalent aluminum facing. Even when compared with beryllium facing the Boron Omniweave would be 46 percent of the beryllium weight.

In the pressurized area of the launch vehicle, the picture does not look as bright. All of the 45 degree LID Omniweave materials do not compare favorably with metal facing materials. The 18 and 72 degree Boron Omniweave indicates a weight savings of 62 percent of aluminum facings and is a little better than beryllium facing.

It should be pointed out that these are predicted values based on a conservative evaluation. Properties of optimized Omniweave materials are expected to be better than the assumptions in this evaluation so that even greater advantages are expected than those shown in Table 6-6. Other configurations should also improve these strength values. For the upressurized areas, the axial strength can be increased by going to 10 degree configurations. In the pressurized areas, the addition of fibers in the fifth direction, axial fibers added to the 45 or 60 degree Omniweave configuration looks promising.

#### 6.4 CONCLUSIONS

There were several significant data trends which occurred in all materials analyzed. Using the maximum stress criteria, strength prediction curves for 45 degrees FPA standard Omniweave indicates failure in the matrix material under axial loading. Shear failure occurs in the matrix for  $\theta_{12} = 0$  to 45 degrees and transverse tensile failure for  $\theta_{12}$  greater than 45 degrees. Axial strength increases with the modulus of the material and shows no dependence on the basic fiber strength for the high-strength fibers analyzed. Hill's failure criteria indicates a much lower axial strength than the maximum stress criteria for a 45 degree FPA fiber orientation. Strength is greatly reduced for  $\theta_{12}$  greater than 45 degrees as the result of the high transverse tensile stress produced.

Moduli prediction curves show  $E_1$ ,  $E_2$ , and  $E_3$  constant and approximately equal for  $\theta_{12}$  between 0 and 45 degrees.  $E_2$  increases sharply for  $\theta_{12}$  greater than 45 degrees.

Correlation between test data and the OMNI analysis for Morganite II and S-Glass Omniweaves yields the following results and conclusions:

1. The sharp increase in the strength predictions with an increasing  $\theta_{31}$  between 50 and 75 degrees has been verified by test. Predicting the exact strength

and moduli curves appears to be a matter of determining the correct unidirectional transverse shear and tensile strengths, the effective fiber modulus, and the effective binder modulus, i.e., K factor. Off axis tensile testing of unidirectional composites is recommended for obtaining these properties.

2. Preliminary evaluation indicates a substantial weight saving of 60 percent for Omniweave facing materials over the metallic facings in the unpressurized area of a launch vehicle.
3. A weight savings of 30 percent is indicated in the pressurized portion of the launch vehicle.



**SECTION 7**  
**DISCUSSION AND CONCLUSIONS**

## SECTION 7

### DISCUSSION AND CONCLUSIONS

The utilization of filamentary materials as structural composite reinforcements is directly related to: (a) the development of manufacturing technology which can provide weight-effective fiber configurations best able to meet the demands of the structural application; (b) generation of composites having consistently high and reproducible properties which can be predicted by analytical techniques; and, (c) better performance than state-of-the-art materials, e.g., metals, on a cost effective as well as on a weight effective basis.

Development of a composite material to the level where it can satisfy all of these requirements is a lengthy process. The Omniweave method of composite manufacture is in the initial phase of development from a laboratory item to a useful structural material. Table 7-1 summarizes the status of Omniweave development.

TABLE 7.1 OMNIWEAVE DEVELOPMENT STATUS

Criteria	Omniweave Status
Ability to Provide Weight Effective Fiber Configurations	Weaving design patterns have been devised to produce a multitude of fiber geometries and part shapes. Process needs improvements in loom operation and weaving techniques to maximize fabric uniformity and weave density.
Produce Composites Having High and Reproducible Mechanical Properties	Limited amount of test data indicates the need for improved processing. Test specimen configurations and methods should be reviewed and modified for evaluation of multidirectional reinforcement geometries.
Ability to Predict Composite Properties	The "OMNI" computer programs appears to be reliable for property predictions. Needs data obtained from off-axis testing of unidirectional composites to realize maximum reliability.
Interlaminar Strength without Sacrifice of Planar Properties	Preliminary property data indicates comparable in-plane properties to angle-plyed filamentary laminates with greater transverse compression and interlaminar shear strengths. Flexural fatigue properties are predicted to be higher than those obtained by laminate procedures.
Cost Effectiveness	Present processing costs are high. Development of continuous equipment will make Omniweave process less expensive than hand lay-up or filament winding procedures.

## 7.1 OMNIWEAVE WEAVING PROCESS

The Omniweave process has the potential to produce weight-effective structures since individual fibers can be oriented to meet the stress loads. High axial, high transverse or nearly isotropic fiber concentrations can be realized within the Omniweave fabric. In addition, these fibers are interlocked in-depth so that the high shear characteristics in the radial or thickness direction can be obtained since discrete laminae regions are not formed. Additional fibers can also be introduced into the weave along the orthogonal axes. Nearly any fiber, including tungsten-cored boron as this study showed, can be woven into an Omniweave configuration.

The Omniweave processing method is a new manufacturing technique which can be used to produce efficient filamentary composites. Up to now structural designs have been built around the fixed geometry and limitations of composites produced by hand lay-up, filament winding or standard warp/fill weaving. It is now possible to study the anticipated stress loads and to design the Omniweave which can best fit the structural requirements.

Weaving techniques have been devised to produce a multitude of fabric shapes, including structural tubes and struts, "I", "T" and channel beams, tapered shapes, and integrally ribbed cylinders. In addition, all constructions can eventually be built employing specific fibers in specific regions of the construction.

The weaving process that is now being used is in the very preliminary development stages. It utilizes a loom to affect the yarn cycling motions but weaves only finite length warp elements. Consequently, all yarn crossovers (weave stitches) have to be combed manually (if the weaving elements were fed from spools under proper tension, uniform, continuous fabric could be produced without any combing). The manual combing of weave crossovers produces fiber damage and non-uniformity in the woven fabric. It is believed that a major reason for the scatter in test data obtained in this study is directly related to premature failure initiated in distorted fabric regions. Recommendations for improving the weaving process are discussed in Section 8.1.

## 7.2 OMNIWEAVE MOLDING PROCESS

All materials were woven as prepreg in which the resin was advanced to the point where it was non-tacky. The woven prepreg fabrics were then molded either in a closed mold cavity or between metal plates. The test data obtained indicates that this molding procedure needs improvement and optimization. For example, the average tensile strength of the unidirectional S-glass/USP23 epoxy test coupons was about 150,000 psi, about half of the anticipated value. McLoughlin (16) has shown that the flexural strengths of S-glass/epoxy unidirectional composites are strongly influenced by the processing history. He obtained consistent flexural strengths of about 200,000 psi employing highly advanced prepreg. Upon using a less advanced prepreg material, McLoughlin raised the unidirectional flexural strength to over 400,000 psi (Table 7-2).

TABLE 7-2. EFFECT OF PREPREG CONDITIONS ON FLEXURAL PROPERTIES OF UNI-DIRECTIONAL S-GLASS/EPOXY COMPOSITES (16)

Prepreg Conditions	Molding Conditions	Flexure Strength (psi)	Flexural Modulus ( $\times 10^{-6}$ psi)	Interlaminar Shear Strength (psi)
33% Solids solution Impregnation, highly staged, non-tacky prepreg	1 hour at 120°C under 600 psi, vacuum 16 hours at 175°C Post-bake	202,000	6.9	10,2000
33% Solids solution Impregnation, Tacky high volatile content prepreg	1 hour at 150°C under 600 psi, vacuum 16 hours at 175°C Post-bake	425,000	8.5	13,400

This referenced study indicates that highly staged prepregged fibers, such as were used on this Omniweave program, prevents good fiber wetting and, therefore, results in composites having lower mechanical properties than anticipated. Variations of the cure cycle prior to final cure indicated significant property improvements may be realized using a more fluid resin condition (Table 7-3).

Cole and Mulvaney<sup>(8)</sup> have intensively studied the effect of cast epoxy resin properties on S-glass/epoxy unidirectional composite properties. Their data indicates that a two-fold increase in flexural strength can be realized by the judicious choice of the resin matrix (Table 7-4). It appears that the USP23 epoxy resin may not have been an optimum matrix for transference of stress loads to the Omniweave fibers. Recommendation leading to the improved molding of Omniweave composites are discussed in Section 8.2.

### 7.3 OMNIWEAVE TEST DATA AND STRUCTURAL ANALYSIS

The OMNI computer code was used throughout the program to predict Omniweave composite properties. In general, predictions agreed well with the generated data. It is interesting to note that the Omniweave mechanical property predictions for the S-glass/USP23 epoxy systems agreed very well when predictions were based on inputs obtained from the off-axis evaluation of unidirectional tensile coupons (See Figures 6-6 and 6-8).

The data and analysis on the Morganite Type II Omniweave composites indicates that the fiber properties were lower than reported in vendor data. It appears that the Morganite material had been derived from an early continuous process batch and had

TABLE 7-3. EFFECT OF CURE CYCLE ON FLEXURAL PROPERTIES OF S-GLASS/USP23 OMNIWEAVE COMPOSITES

Panel	Fiber Angle	Cure Cycle	Flexural Strength (psi)		
S21A-84	± 32	A	57,000		
	± 29	B	85,300		
	± 66	A	15,400		
	± 60	B	24,800		
S21D-104	± 25	A	68,200		
	± 30	B	70,600		
	± 67	A	13,400		
	± 63	B	23,900		
Cure Cycle "A"			Cure Cycle "B"		
Time, (min.)	Temp., (°F)	Pressure, (psi)	Time, (min.)	Temp., (°F)	Pressure, (psi)
5	RT	1000	5	RT	1000
15	RT to 250	100	15	RT to 300	100
30	250	100	90	300	1000
30	250	1000			
5	250 - 300	1000			
60	300	1000			

inferior properties to the meter length tow or recent continuously processed material. Table 7-5 illustrates the range of strength and modulus properties for Morganite II/epoxy unidirectional composites reported in the literature. If it is assumed that our fiber lot had properties comparable to those reported in Reference 11, the prediction curves closely approximate the values obtained through specimen testing (See Figures 6-9 and 6-11).

The boron Omniweave composites showed the greatest tensile test data scatter. Specimens failed classically (within the gage length at 90 degrees to load fracture), in a random jagged fracture near the doubler and within the doubler regions (See Figure 5-17).

The maximum tensile value for the boron/HT424 Omniweave system failed at a level higher than that obtained for a unidirectional composite of identical resin/fiber content (Table 7-6). An interesting point to note is that boron Omniweave tensile strengths for a ±5 - 20 degrees axial angle are predicted to be higher than that for a unidirectional boron/HT424 composite.

TABLE 7-4. THE EFFECT OF EPOXY RESIN MATRIX MATERIAL ON MECHANICAL  
PROPERTIES OF UNIDIRECTIONAL S-GLASS/EPOXY COMPOSITES  
(65% FIBER VOLUME FRACTION)(8)

Epoxy Resin Material	Resin Tensile Strength (psi)	Resin Modulus (x 10 <sup>-6</sup> psi)	Elongation Resin (%)	Resin Flexural Strength	Composite Tensile Strength, (psi) (90° Orientation)	Composite Modulus (x 10 <sup>-6</sup> , psi) (90° Orientation)	Composite Compressive Strength, (psi) (0° Orientation)	Composite Flexural Strength, (psi) (0° Orientation)	Composite Interlaminar Shear Strength (psi)
ERLA-4289	4900	0.23	18.5	10,800	3100	1.37	87,200	187,500	5500
Epon 828/Epon 1031	9100 - 11800	0.49	2.5	16,400	6100	2.19	192,000	344,700	11000
ERLA-4300	12900 - 16500	0.88	2.2	23,800	8000	3.11	228,000	380,700	12900
ERLA-0400	17500	0.69	4.6	27,600	10100	2.71	241,000	425,000	14300
USP23 (From Table 4)	12000	0.54	3.5 - 4.5	18,000	-----	-----	-----	-----	-----



TABLE 7-5. UNIDIRECTIONAL TENSILE PROPERTIES OF  
MORGANITE TYPE II/EPOXY COMPOSITES  
(Literature Data)

Fiber Orientation (degrees)	Fiber Volume (percent)	Tensile Strength (psi)	Tensile Modulus (10 <sup>6</sup> psi)	Reference
0	—	150,000	—	7
	60	165,000	21.2	9
	51	125,000	18-22	10
	58*	88,500*	17*	11
	55	100,000	35	11
	55	80,000	24	11
	67.5	167,000	23.5	12
	55	175,000	19.5	12
90	—	8,000	—	7
	60	5,200	1.2	9
	52	8,700	1.2-1.5	10
	58	10,000	—	11
	67.5	8,400	—	12

\*Used in analysis (Section 6) to obtain best fit of Omniweave data.

TABLE 7-6. BORON/HT424 OMNIWEAVE TENSILE STRENGTHS  
(55-FIBER VOLUME FRACTION) (EXTRACTED FROM FIGURE 6-15)

Test Configuration	Predicted Value, psi	Test Data, psi
Unidirectional layup	135,000	135,000
± 5° Omniweave	145,000	137,000
± 10° Omniweave	148,000	---
± 15° Omniweave	147,000	---
± 20° Omniweave	144,000	---

The majority of the mixed fiber Omniweaves failed by "brooming", e.g., individual fiber bundles were pulled out of the doubler regions, indicating that the test values obtained are conservative.

The compression tests and the corresponding predictive curves for all Omniweave materials indicate that significantly higher transverse compressive strengths may be realized with axially oriented Omniweave than with unidirectional materials (Table 7-7). This type of performance may have important bearing for certain structural applications (high axial tension coupled with high transverse compression).

TABLE 7-7. COMPARISON OF MORGANITE TYPE II/EPOXY  
OMNIWEAVE TRANSVERSE COMPRESSION DATA WITH LITERATURE  
REPORTED VALUES FOR UNIDIRECTIONAL MATERIAL

Fiber Orientation °	Fiber Volume (percent)	Compressive Strength (psi)	Reference
90°	—	20,000	7
	65	27,500	13
	52	24,500	10
	67.5	31,700	12
± 85° Omniweave*	52	40,000	GE data

\*G51A/L-207

Futile attempts were made to determine the interlaminar shear strength of the Omniweave composites. In all cases, with the possible exception of the test performed on one Morganite composite (G51A/L-207, 9000 psi interlaminar shear strength), specimen failure occurred at flexural strength levels indicating that the specimens did not fail in shear.

An area which may require investigation is the adequacy of the test specimen configurations. Omniweave is a multidirectionally reinforced composite which was evaluated using test techniques and configurations initially designed for isotropic materials and later modified for use with anisotropic laminates. It is probable that the test data may reflect the unsuitability of these test specimens. The test specimen width included few fiber crossovers since large fiber bundles were used as the weaving elements and most test specimens had a large thickness-to-width ratio implying that all tensile and compression data might be conservative. Whether these tests were realistic or not can only be determined through test specimen configuration studies (See Recommendations, Section 8.3).

**SECTION 8**  
**RECOMMENDATIONS**

## SECTION 8

### RECOMMENDATIONS

The work performed during this study has uncovered several key areas which will require intensive investigation in order to develop Omniweave composites for structural applications. Essentially, this recommended work effort is geared to upgrading the weaving process, optimizing the molding procedures and derivation of suitable testing configurations. In addition, several potential applications for the immediate use of Omniweave composites are outlined.

#### 8.1 WEAVING PROCESS OPTIMIZATION

Most of the problems associated with the weaving process have been discussed in Section 7.1. A concerted effort is needed to improve the quality of the Omniweave fabrics as well as explore techniques for implementing a continuous weaving operation. Some of the factors which should be investigated with the present finite length equipment are:

1. Combing techniques or fiber coatings which minimize fiber abrasion,
2. Yarn tensioning methods and packing techniques to remove fiber crimp and maximize fabric uniformity,
3. Techniques to enhance fabric density,
4. Techniques to improve Omniweave production rates.

In addition, a development effort should be initiated to determine the best means of producing continuous Omniweave flat fabrics and seamless cylinders:

1. Several preliminary continuous weaving designs should be scaled up to prototype models handling 36 to 100 weaving elements.
2. Spool tensioning techniques should be optimized through evaluation using these prototype models.
3. A wide range of fibers materials (e.g., glass, Morganite, boron) should be continuously woven into small strips to demonstrate feasibility.
4. Several weaving patterns should be woven sequentially within these small strips to demonstrate design feasibility.

#### 8.2 MOLDING PROCESS OPTIMIZATION

The test data obtained on this program showed that low mechanical values were obtained on S-Glass/USP23 epoxy resin Omniweave composites. These low values can

be traced back to the molding procedure and/or resin selection since test data for similarly processed unidirectional constructions were correspondingly low (See Section 7.2). In addition, Morganite test values were lower than anticipated but these appear to reflect the true fiber properties, e.g. ( $E = 28.5 \times 10^6$  psi, UTS = 200,000 psi). The boron and mixed fiber systems show fairly wide scatter indicative of the need for process improvement.

It is recommended that the variables in Omniweave molding be studied intensively to derive optimal procedures to produce composites having high and consistent mechanical property values. These studies should be performed using one Omniweave fabric design and one fiber material.

Several epoxy resins should be investigated as potential matrices for Omniweave composites. In all cases, post-weave impregnation with a low viscosity resin solution would be employed. Auxiliary vacuum pressure to remove volatiles during molding would be used for all process runs. Vendor recommended cure conditions would be utilized. Resin staging conditions, molding pressure and post cure cycle would be the prime variables studied. Off-axis data on similarly processed unidirectional composites would be used to generate predictive curves. Omniweave composites produced with these processing variations would be evaluated for flexural and tensile properties in both the axial and transverse directions.

The outcome of this effort would be a processing procedure which would produce Omniweave composites having significantly improved and reproducible properties.

### 8.3 EVALUATION OF TEST SPECIMEN CONFIGURATIONS

The relatively good correlation between some of the measured Omniweave tensile properties and predictions from the OMNI computer code is encouraging. Ultimately, however, computer code predictions must be verified by direct property measurements on structural shapes. Therefore, it is recommended that future Omniweave development efforts include mechanical testing of cylinders in tension, compression and torsion in order to provide strength and elastic constants data to compare with predictions from the OMNI program. When this has been accomplished, optimum test coupon configurations for simple mechanical property tests can be readily identified on a pragmatic basis.

### 8.4 OTHER APPLICATIONS FOR OMNIWEAVE COMPOSITES

Omniweave composites have shown the potential to be highly weight-effective as structural skins for honeycomb sandwich launch vehicle booster assemblies (Section 6.3). Omniweave materials can be efficient for many other structural application including:

1. beams, hollow thin wall struts for compressive and/or axial loadings
2. high temperature structural composites
3. structural members and components for airplanes, helicopters, launch vehicles, etc.

It is recommended that Omniweave composites be evaluated for potential use in applications such as those listed since it can produce components having similar in-plane properties to those of angle-plyed filamentary composites but with significantly enhanced interlaminar shear and fatigue characteristics. Moreover, the Omniweave manufacturing process has the potential for continuous production of structural members resulting in lower manufacturing costs than with the filament winding or hand lay-up method of production.



**SECTION 9**  
**BIBLIOGRAPHY**

## SECTION 9

### BIBLIOGRAPHY

1. Korb, L. J., "Advanced Composite Material Applications in Future Boosters and Spacecraft", 15th National SAMPE Symposium Proceedings, Volume 15, 1969.
2. "Modmor, High Modulus Carbon Fibers", New Products Data Sheet, Morganite Research and Development Limited, October 1968.
3. Dauksys, R. J. and Ray, J. D., "Properties of Graphite Fiber Non-Metallic Matrix Composites", J. Composite Materials, Volume 3, October 1969.
4. Private communication with US Polymeric Company, Santa Ana, California, July 1969.
5. Juneau, P. W., et al, "Optimization of a Boron Filament Reinforced Composite Matrix", Composite Materials: Testing and Design, ASTM STP460, American Society for Testing and Materials, 1969.
6. Vendor Data, US Polymeric Company, Santa Ana, California.
7. Chamis, C. C., "Failure Criteria for Filamentary Composites", Composite Materials: Testing and Design, ASTM STP460, American Society for Testing and Materials, 1969.
8. Mulvaney, W. P. and Cole, L. F., "Mechanical Property Correlations Between High Performance Composites and Cast Epoxy Resin Data", 22nd SPI ANTEC Proceedings, Section 4-C, February 1967.
9. Holmes, R. D., and Wright, I. W., "Creep and Fatigue Characteristics of Graphite/Epoxy Composites, AIAA Technical Conference and Symposium, June, 1970.
10. Harmon, E. J. et al, "Design, Fabrication and Evaluation of Graphite Fiber Reinforced Composite Structural Specimens", AFML-TR-69-189, September 1969.
11. Shockey, P. D., et al, "Structural Airframe Applications of Advanced Composite Materials", AFMT-TR-69-101, Volume IV, 1969.
12. Hayes, R. D., "Flight Worthy Graphite Reinforced Aircraft Primary Structure Assemblies", Northrup Quarterly Progress Report No. 2, Contract No. F33615-69-C-1490.

13. Elkin, R. A., et al, "Characterization of Graphite Fiber/Resin Matrix Composites", Composite Materials: Testing and Design, ASTM STP460, American Society for Testing and Materials, 1969.
14. Edighoffer, H. H., "Thermoelastic Analysis of Fibrous Composites with Fibers in Four Directions Symmetric with the Composite Co-Ordinate System (Omni-weave) using the OMNI Computer Code", GE Technical Memorandum TM 9335-RF3-0017, 1969.
15. Hoffman, V., "The Brittle Strength of Orthotropic Materials", J. Composite Materials, Volume 1, 1967.
16. McLoughlin, J. R., "Miniature Composite Sample Fabrication", GE R&DC, Schenectady, N.Y., Memo Report Number MO-69-0798, September 1969.
17. Dow, N. F., Rosen, B. W., "Zero Thermal Expansion Composites of High Strength and Stiffness", NASA Contract Report NASA CR-1324, 1969.

## **SECTION 10**

### **APPENDIX**

## SECTION 10

### APPENDIX

#### 10.1 FORMULAE USED IN CHARACTERIZING S-GLASS, MORGANITE II, BORON, AND THORNEL 50S COMPOSITES

- a) Determination of resin content of carbon composites

$$W_r = \frac{W_R - \Delta W}{100 - \Delta W}$$

Where:

$W_r$  = Weight (percent) resin in composite

$W_R$  = Weight (percent) resin, including volatiles, in prepreg

$\Delta W$  = Weight loss (percent) during cure

- b) Determination of fiber content

$$W_f = 100 - W_r$$

Where:

$W_f$  = Weight (percent) fiber in composite

$W_r$  = Weight (percent) resin in composite

- c) Determination of volume (percent) resin in composite

$$V_r = W_r \frac{(\rho_c)}{(\rho_r)}$$

Where:

$V_r$  = Volume (percent) resin in composite

$\rho_c$  = Composite density

$W_r$  = Weight (percent) resin in composite

$\rho_r$  = Resin density

- d) Determination of volume (percent) fiber in composite

$$V_f = W_f \frac{(\rho_c)}{(\rho_r)}$$

Where:

$V_f$  = Volume (percent) fiber in composite

$\rho_c$  = Composite density

$W_f$  = Weight (percent) fiber in composite

$\rho_r$  = Resin density

- e) Determination of composite porosity (volume percent voids)

$$P = 100 - \rho_c \left( \frac{W_r}{\rho_r} + \frac{W_f}{\rho_f} \right)$$

Where:

$P$  = Porosity

$\rho_c$  = Composite density

$W_r$  = Weight (percent) resin in composite

$\rho_r$  = Resin density

$W_f$  = Weight (percent) fiber in composite

$\rho_f$  = Fiber density

## 10.2 FORMULAE USED IN CHARACTERIZING MIXED FIBER OMNIWEAVE COMPOSITES

- a. The weight per unit length of each fiber-prepreg system ( $W_i$ ) was measured.
- b. The number of weaving elements ( $N_i$ ) of each fiber-prepreg system was determined from Figure 4-23.
- c. The resin weight percent of each fiber-prepreg system in composite form ( $R_i$ ) was assumed to be: 35 percent (Boron), 22 percent (S-glass) and 35 percent (Morganite II).



d. The following formulae were then employed:

$$\text{Weight percent resin } j = (W_r)_j = \frac{N_j W_j R_j}{\sum_{i=1}^n N_i W_i}$$

$$\text{Weight Percent fiber } j = (W_f)_j = \frac{N_j W_j (100 - R_j)}{\sum_{i=1}^n N_i W_i}$$

$$\text{Volume Percent Resin } j = (V_r)_j = \frac{(W_r)_j \rho_c}{(\rho_r)_j}$$

$$\text{Volume Percent Fiber } j = (V_f)_j = \frac{(W_f)_j \rho_c}{\rho_f}$$

$$\text{Volume Percent Porosity} = P = 100 - \sum_{i=1}^n (V_r)_i + (V_f)_i$$

Where:

$n$  = Number of fiber-prepreg systems in the composite

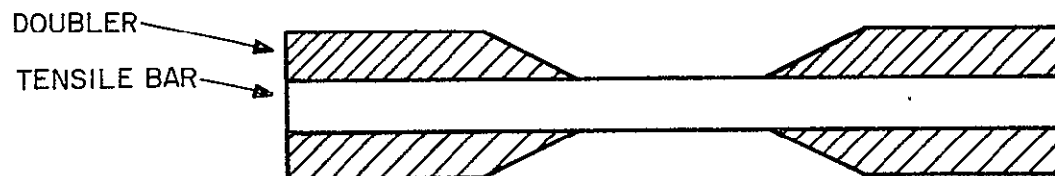
$\rho_c$  = Composite density

$\rho_r$  = Resin density

$\rho_f$  = Fiber density

### 10.3 TENSILE SPECIMEN PREPARATION

End reinforcement doublers were bonded onto the grip areas of all the tensile specimens. Bonding surfaces were given a light sanding, rinsed with acetone and coated with an



epoxy adhesive. The bond was cured between C clamps at 140°F for a minimum of two hours. The following table describes the doubler materials used on various tensile specimens.

Doubler Thickness (in)	Doubler Material	Test Specimens
0.100	181 glass/epoxy	glass/epoxy unidirectional
0.125	Paper/phenolic	glass/epoxy Omniweave
0.125	glass/epoxy	Morganite/epoxy Omniweave
0.50	Steel	Boron, thornel and mixed fiber Omniweaves

#### 10.4 ANALYSES OF OFF AXIS TENSILE TESTING OF UNIDIRECTIONAL COMPOSITES

The following relation steps were utilized to obtain the basic elastic modulli and strength constants input for use on the OMNI computer code.

##### A. Axial Strain/Axial Stress ( $\epsilon_o/\sigma_x$ )

$$\frac{\epsilon_o}{\sigma_x} = \frac{\epsilon_x}{\sigma_x} = \frac{m^4}{E_1} - 2 \frac{m^2 n^2}{E_1} \frac{\nu_{12}}{E_1} + \frac{n^4}{E_2} + \frac{m^2 n^2}{G_{12}} \quad (1)$$

##### B. Lateral Strain/Axial Stress ( $\epsilon_{90}/\sigma_x$ )

$$\frac{\epsilon_{90}}{\sigma_x} = \frac{\epsilon_x}{\sigma_x} = \frac{m^2 n^2}{E_1} - \frac{(m^4 + n^4)\nu_{12}}{E_1} + \frac{m^2 n^2}{E_2} - \frac{m^2 n^2}{G_{12}} \quad (2)$$

##### C. Shear Strain/Axial Stress ( $2 \epsilon_{45} - \epsilon_o - \epsilon_{90}/\sigma_x$ )

$$\frac{2 \epsilon_{45} - \epsilon_o - \epsilon_{90}}{\sigma_x} = \frac{\epsilon_{xy}}{\sigma_x} = - \frac{2 m^3 n}{E_1} - \frac{2(m^3 n - mn^3)\nu_{12}}{E_1} + \frac{2mn^3}{E_2} + \frac{m^3 n - mn^3}{G_{12}} \quad (3)$$

##### D. Axial Strength - Unidirectional Allowable

$$F_x = \frac{F_1}{\sqrt{m^4 + \left[ \left( \frac{F_1}{F_{12}} \right)^2 - 1 \right] m^2 n^2 + \left( \frac{F_1}{F_2} \right)^2 n^4}} \quad (4)$$

Where:

- $\epsilon_0$  = Axial reading of strain gage ( $0^\circ$ )
- $\epsilon_{90}$  = Lateral reading of strain gage ( $90^\circ$ )
- $\epsilon_{45}$  =  $45^\circ$  reading of strain gage ( $45^\circ$ )
- $\sigma_x$  = Stress in axial direction
- $F_x$  = Failing stress in axial direction
- $\theta$  = Angle from axial load direction to fiber direction
- $m$  =  $\cos \theta$
- $n$  =  $\sin \theta$
- $E_1$  = Unidirectional Young's Modulus parallel to fibers
- $E_2$  = Unidirectional Young's Modulus transverse to fiber direction
- $G_{12}$  = Unidirectional shear modulus
- $\nu_{12}$  = Unidirectional Poissons ratio (strain in transverse direction due to load in parallel direction)

when

$$\frac{\nu_{12}}{E_1} = \frac{\nu_{21}}{E_2}$$

- $F_1$  = Allowable unidirectional strength parallel to fiber direction
- $F_2$  = Allowable unidirectional strength transverse to fiber direction
- $F_{12}$  = Allowable unidirectional shear strength

#### E. Logic for Determining Unidirectional Moduli

1. Using Equations 1 and 2 the value of  $E_1$  and  $\nu_{12}$  are obtained from the  $0^\circ$  unidirectional test specimen.

$$n = 0; m = 1; \frac{\epsilon_0}{\sigma_x} = \frac{1}{E_1}; \frac{\epsilon_{90}}{\sigma_x} = -\frac{\nu_{12}}{E_1}$$

2. Using Equations 1 and 2, the value of  $E_2$  and  $\nu_{12}$  are obtained from the  $90^\circ$  unidirectional tests.

$$n = 1; m = 0; \frac{\epsilon_0}{\sigma_x} = \frac{1}{E_2}; \frac{\epsilon_{90}}{\sigma_x} = -\frac{\nu_{12}}{E_1}$$

3. Using Equation 3, the value of  $E_1$ , and  $E_2$  are substantiated using the  $45^\circ$  tests.

$$n = .707 ; m = .707 ; m^3 n = mn^3$$

$$\frac{2 \epsilon_{45} - \epsilon_0 - \epsilon_{90}}{\sigma_x} = 1/2 \left( \frac{1}{E_2} - \frac{1}{E_1} \right)$$

4. If correlation is not established in step 3,  $E_2$  is adjusted to give the best fit of the data in step 2 and step 3.

5. With  $E_1$ ,  $E_{12}$  and  $\nu_{12}$  established, the value of  $G_{12}$  is obtained from the  $20^\circ$  and  $60^\circ$  specimens. Equations 1, 2 and 3 are used to evaluate  $G_{12}$ . As can be seen from Figure 10-1 there is a high shear coupling in the  $20^\circ$  specimen and a very low shear coupling in the  $60^\circ$  specimen.

#### F. Logic for Allowable Strength Testing

1. Using the  $0^\circ$  specimens the unidirectional strength parallel to the fiber direction ( $F_1$ ) is obtained and correlated with the basic fiber strength.

$$n = 0, m = 0, F_x = F_1$$

2. Using the  $90^\circ$  specimen the strength transverse to the fiber direction ( $F_2$ ) is obtained:

$$n = 1, m = 1, F_x = F_2$$

This specimen is very prone to premature failure due to stress concentrations and bending due to misalignment and may have to be discarded.

3. The  $60^\circ$  specimen has close to zero shear coupling as shown in Figure 10-1 and will give the best strength results because of no shear deformation. The transverse strength ( $F_2$ ) is predominate.

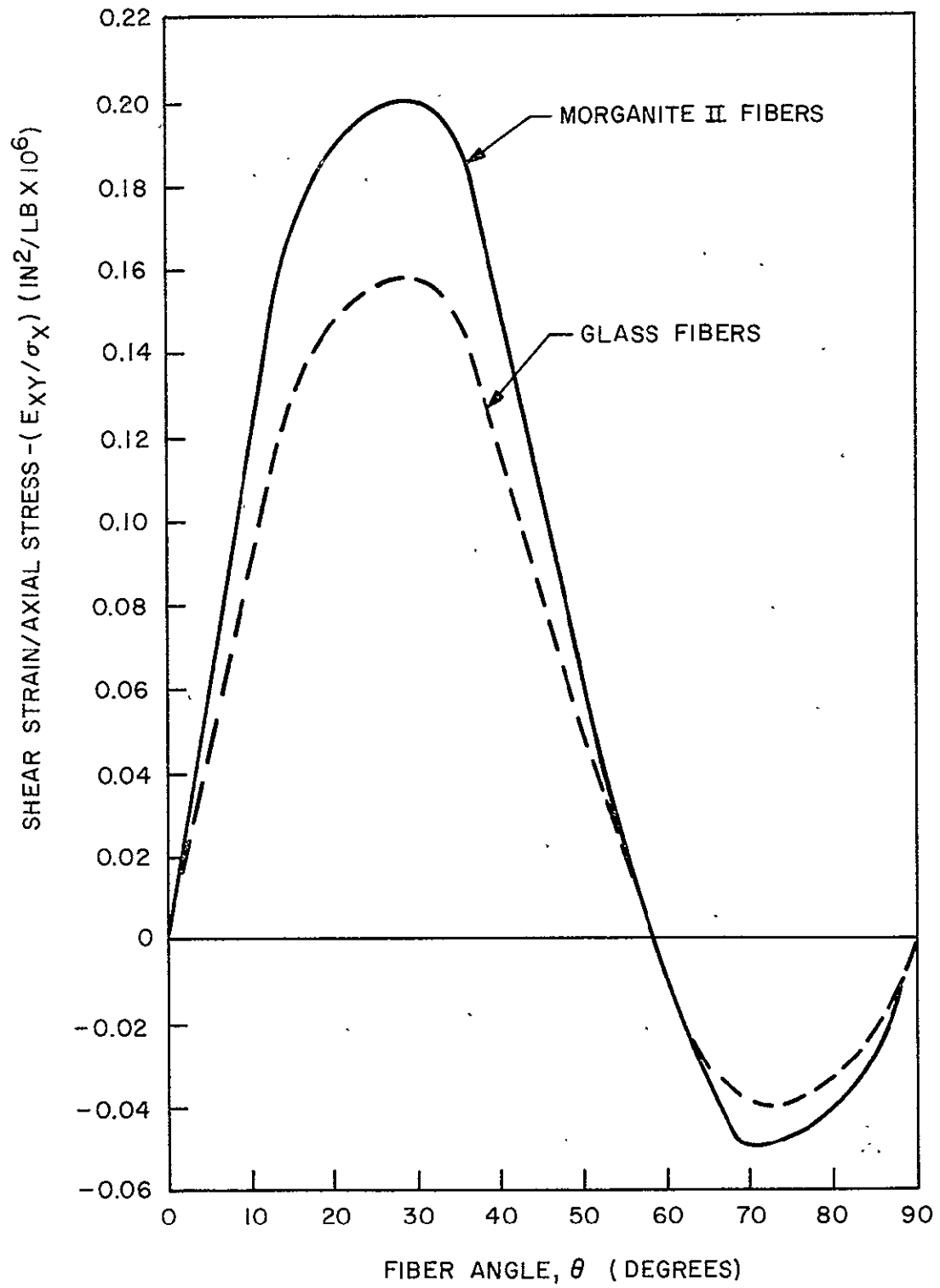


Figure 10-1. Shear Strain/Axial Stress Coupling

With  $\theta = 60^\circ$ ,  $n = 0.866$ ,  $m = 0.5$ ,  
 $n^2 = 0.75$ ,  $m^2 = 0.25$   
 $n^4 = 0.56$ ,  $m^4 = 0.0625$

$$\left(\frac{F_1}{F_x}\right)^2 = 0.0625 + 0.1875 \left[ \left(\frac{F_1}{F_{12}}\right)^2 - 1 \right] + 0.56 \left(\frac{F_1}{F_2}\right)^2$$

For  $F_1 \gg F_{12}$  &  $F_1 \gg F_2$

$$\frac{1}{F_x^2} = \frac{0.1875}{F_{12}^2} + \frac{0.56}{F_2^2} \quad (5)$$

4. The  $45^\circ$  specimen has a moderate amount of shear coupling (Figure 10-1) and the shear and transverse strength of equal importance.

With  $\theta = 45^\circ$ ,  $n = 0.707$ ,  $m = 0.707$   
 $n^2 = 0.5$ ,  $m^2 = 0.5$   
 $n^4 = 0.25$ ,  $m^4 = 0.25$

$$\frac{1}{F_x^2} = \frac{1}{4} \left[ \frac{1}{F_{12}^2} + \frac{1}{F_2^2} \right] \quad (6)$$

- f. The  $20^\circ$  specimen has a maximum amount of shear deformation and this test is used to find shear strength ( $F_{12}$ ).

$\theta = 20^\circ$ ,  $n = 0.34202$ ,  $m = 0.9397$   
 $n^2 = 0.117$ ,  $m^2 = 0.88$   
 $n^4 = 0.0136$ ,  $m^4 = 0.78$

$$\left(\frac{F_1}{F_x}\right)^2 = 0.78 + 0.103 \left[ \left(\frac{F_1}{F_{12}}\right)^2 - 1 \right] + 0.0136 \left(\frac{F_1}{F_2}\right)^2 \quad (7)$$

With this equation the shear allowable is predominate and a large error in the value  $F_2$  will have a small error in the value of  $F_{12}$  obtained.

6. With the data from the above tests, the shear and transverse strength ( $F_{12}$  and  $F_2$ ) can be determined.

### G. Shear Coupling

Equation 3 is the shear coupling equation and can be rewritten:

$$\frac{\epsilon_{xy}}{\sigma_x} = -\frac{2 m^3 n}{E_1} + \frac{2 m n^3}{E_2} + \left( -\frac{1}{G_{12}} - \frac{2 \nu_{12}}{E_1} \right) (m^2 - n^2) m n \quad (8)$$



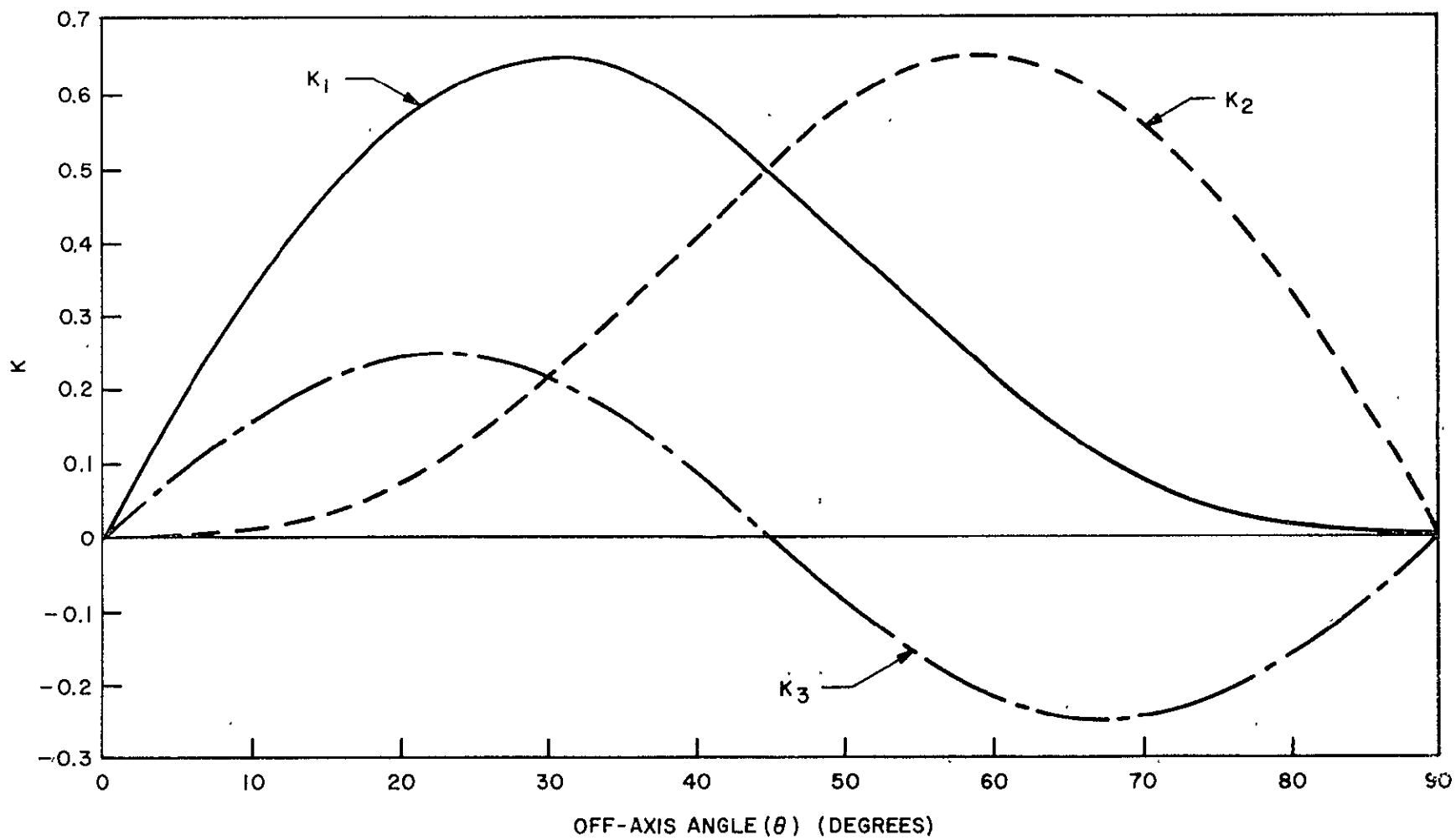


Figure 10-2. Shear Coupling Parameters

or

$$\frac{\epsilon_{xy}}{\sigma_x} = -\frac{1}{E_1} K_1 + \frac{1}{E_2} K_2 + \left( \frac{1}{G_{12}} - \frac{2\nu_{12}}{E_1} \right) K_3 \quad (9)$$

where

$$\begin{aligned} K_1 &= 2m^3 n \\ K_2 &= 2mn^3 \\ K_3 &= (m^2 - n^2)mn \end{aligned}$$

Looking at the plot of  $K_1$ ,  $K_2$  and  $K_3$  in Figure 10-2, it can be seen that depending on the unidirectional elastic moduli, there is some angle  $\theta$  where the shear coupling is zero. This point is at  $\theta = 58^\circ$  as shown in Figure 10-1. The shear strain/axial stress coupling in Figure 10-1 was obtained for Morganite II and Glass fibers using Equation 9 and the values of  $K$  in Figure 10-2. The values of the unidirectional moduli used in this evaluation is shown in Table 10-1.

TABLE 10-1. ESTIMATED UNIDIRECTIONAL MODULI OF MORGANITE II AND S-GLASS COMPOSITION

Morganite II	S - Glass
$E_1 = 22.4(10)^6$ psi	$E_1 = 5.96(10)^6$ psi
$E_2 = 3.8(10)^6$ psi	$E_2 = 2.95(10)^6$ psi
$\nu_{12} = 0.048$	$\nu_{12} = 0.143$
$\nu_{21} = 0.298$	$\nu_{21} = 0.29$
$G_{12} = 1.217(10)^6$ psi	$G_{12} = 1.01(10)^6$ psi

## 10.5 OMNIWEAVE TENSILE STRESS-STRAIN CURVES

Figures 10-1 through 10-20 present the tensile stress-strain curves obtained on Omniweave composites.

## 10.6 PRELIMINARY OMNIWEAVE PREDICTION CURVES

### 10.6.1 S-GLASS OMNIWEAVE

Figures 10-23 through 10-30 present preliminary predictions of the mechanical properties of S-glass Omniweave materials as a function of axial angle using a 45 degree projected radial fiber angle and predicted values not derived from the off-axis tests series. These curves are based on a  $K$  factor of 1.9 in contrast to 1.0 used in Section 6.2.1 and results in higher elastic moduli predictions with very little change in strength predictions.

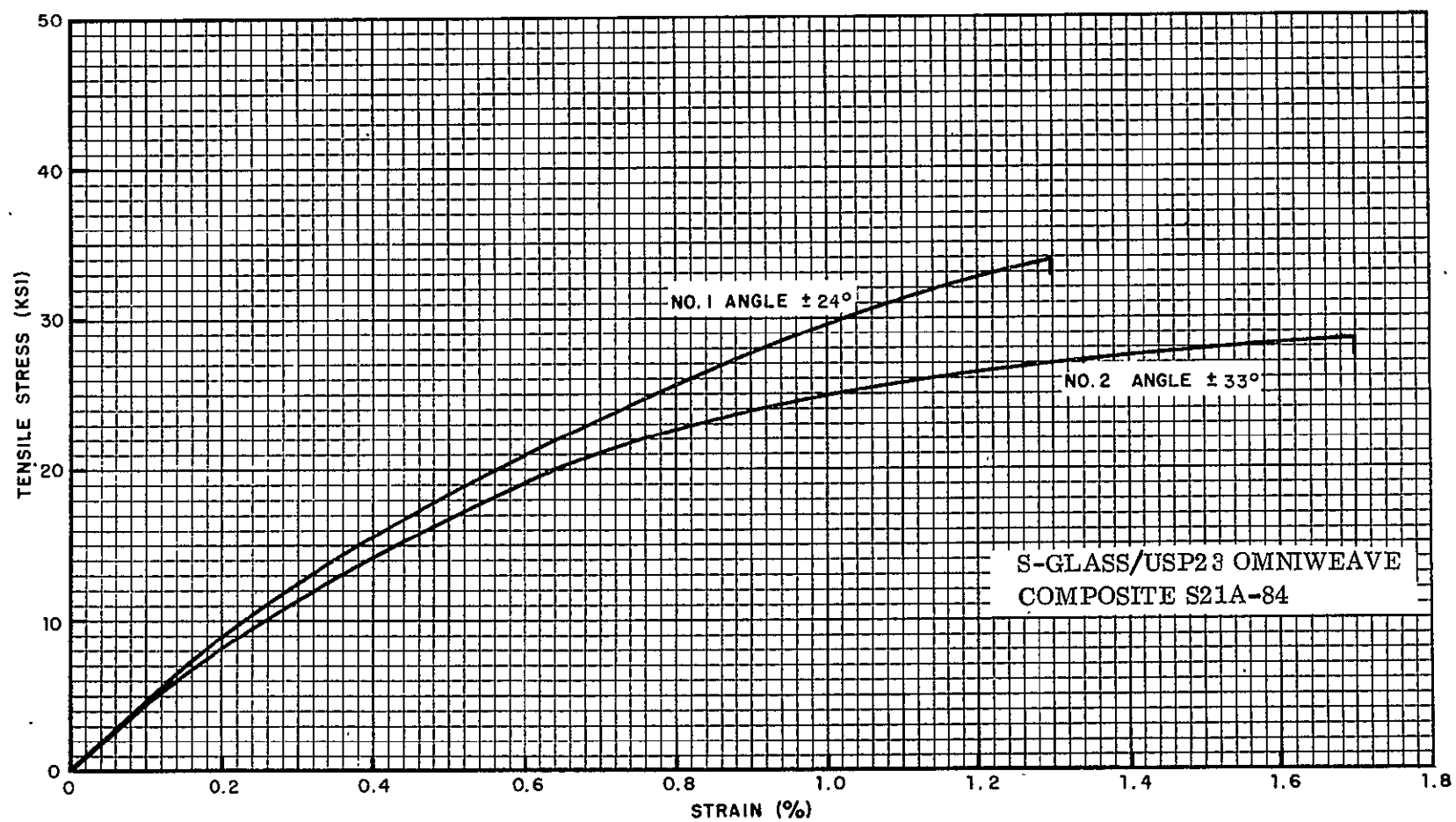


Figure 10-3. Tensile Stress-Strain Curves - S21A-84 Axial Direction

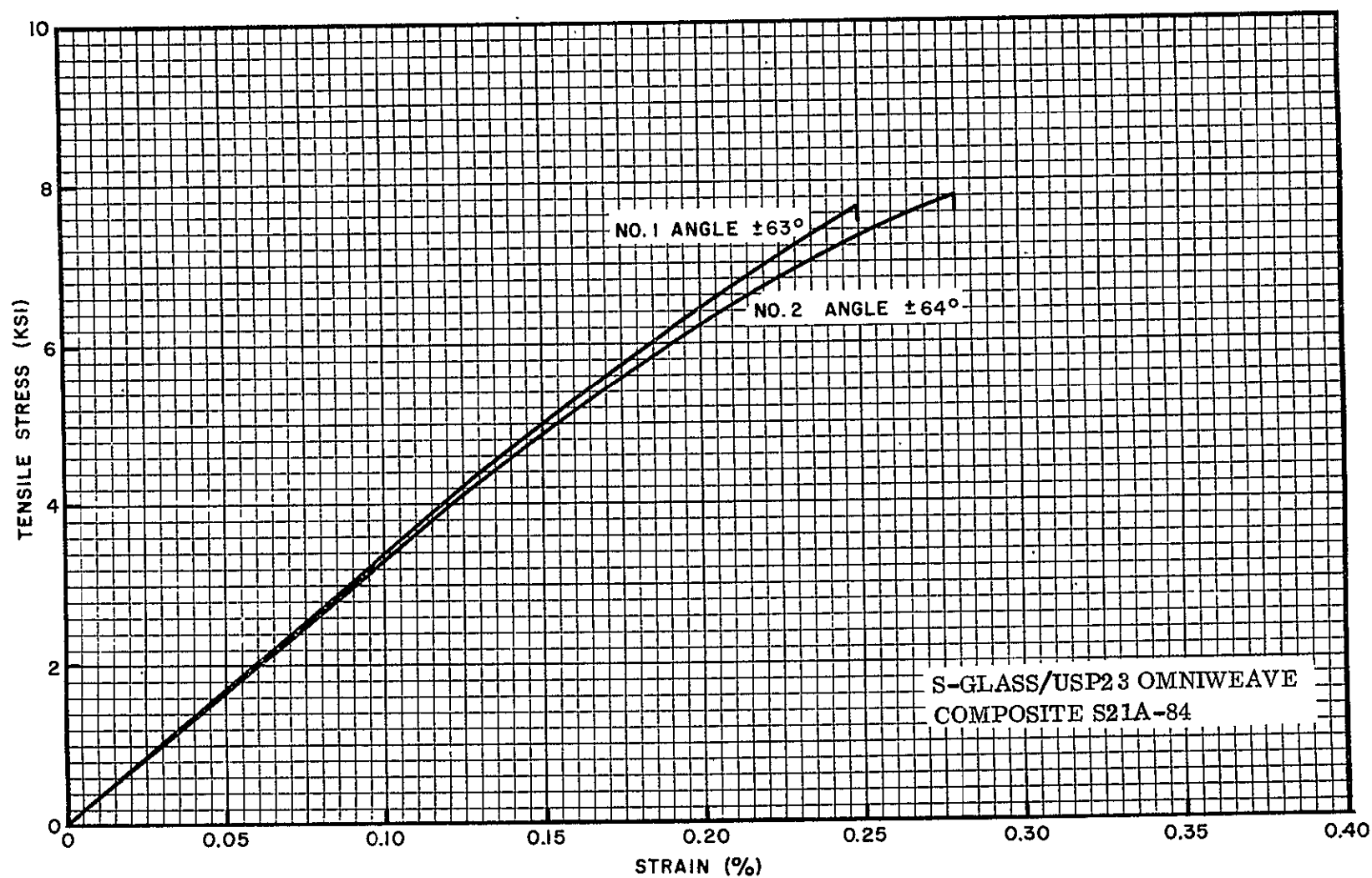


Figure 10-4. Tensile Stress-Strain Curves - S21A-84, Transverse Direction

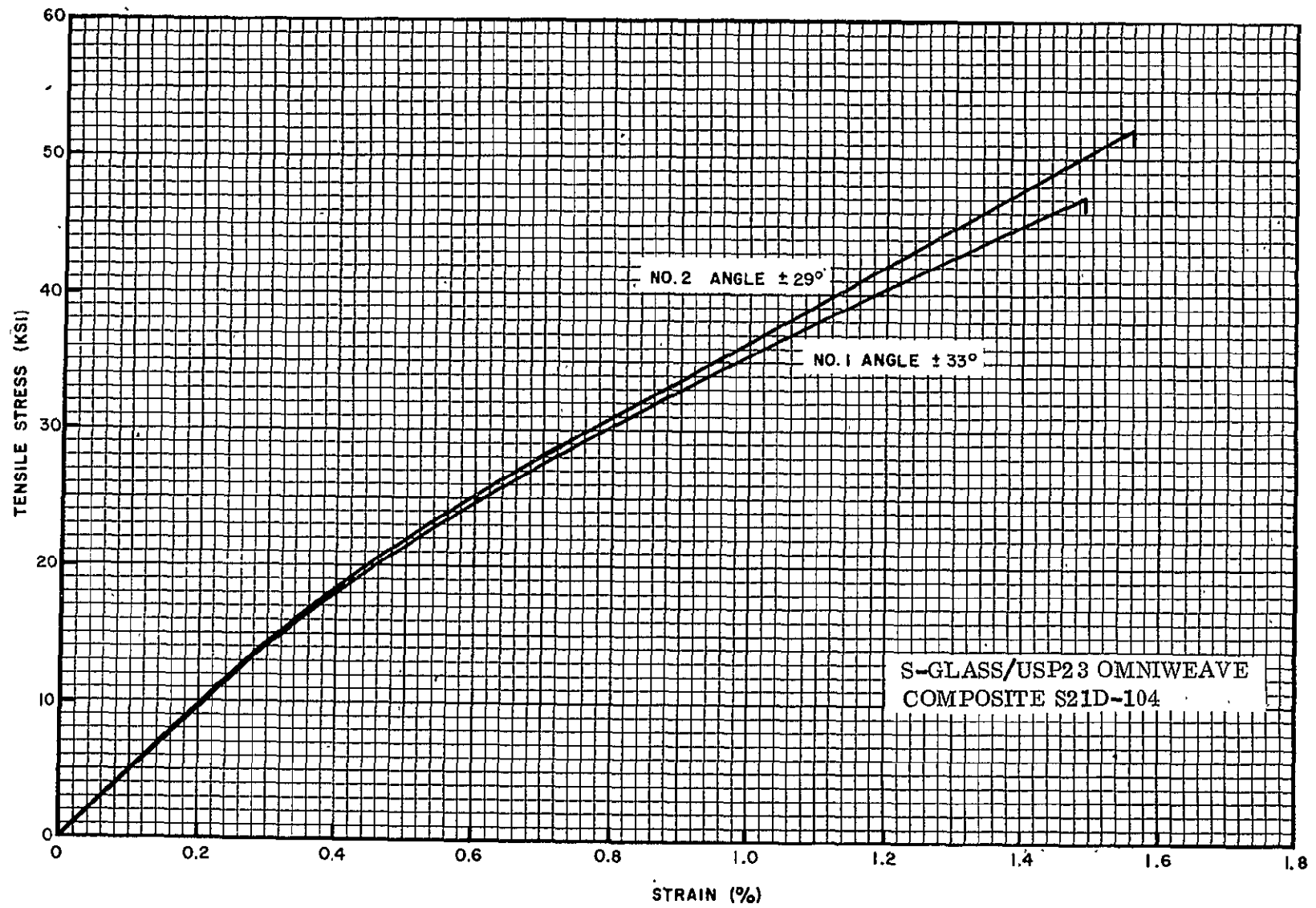


Figure 10-5. Tensile Stress-Strain Curves - S21D-104, Axial Direction

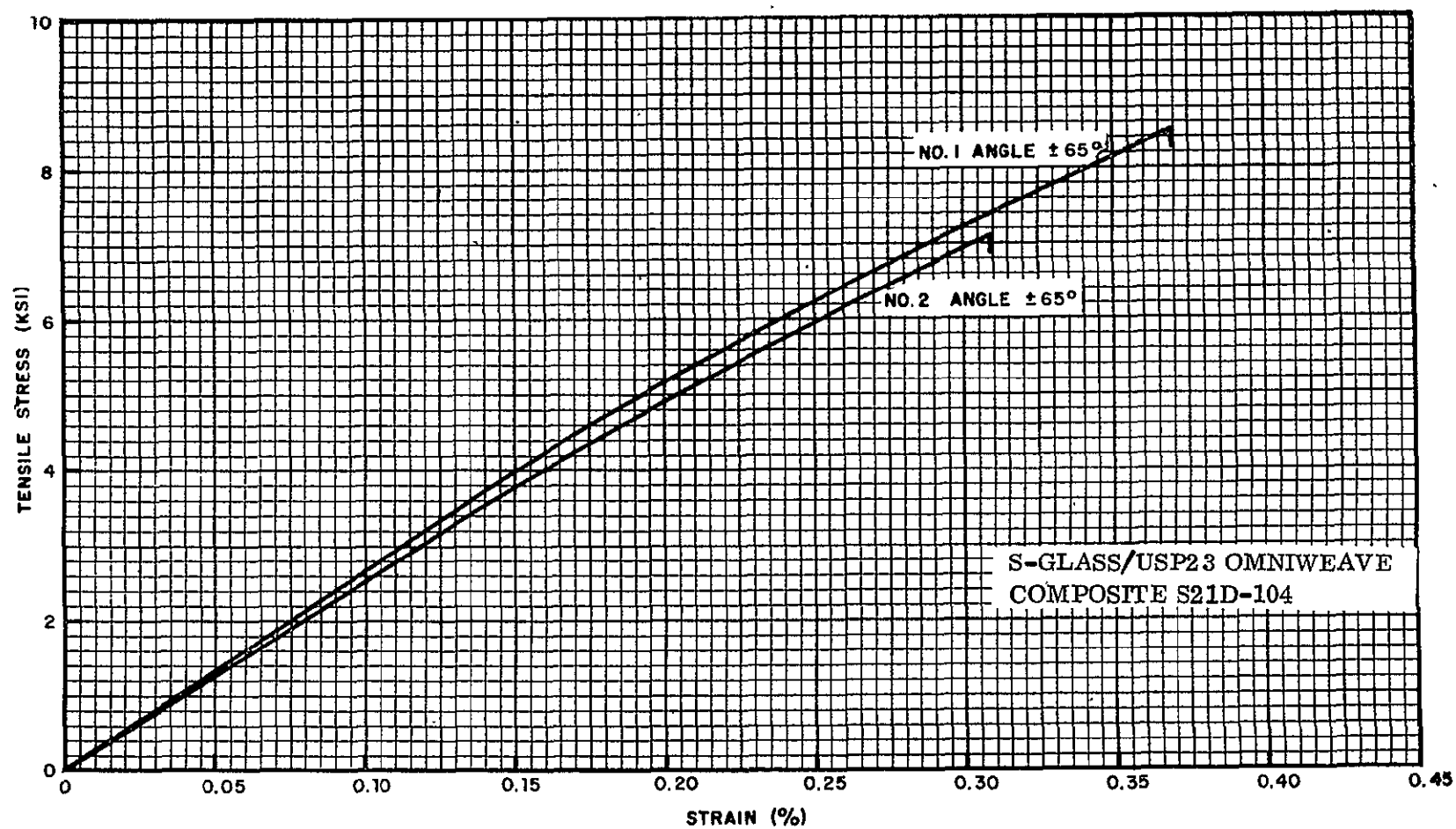


Figure 10-6. Tensile Stress-Strain Curves - S21D-104, Transverse Direction

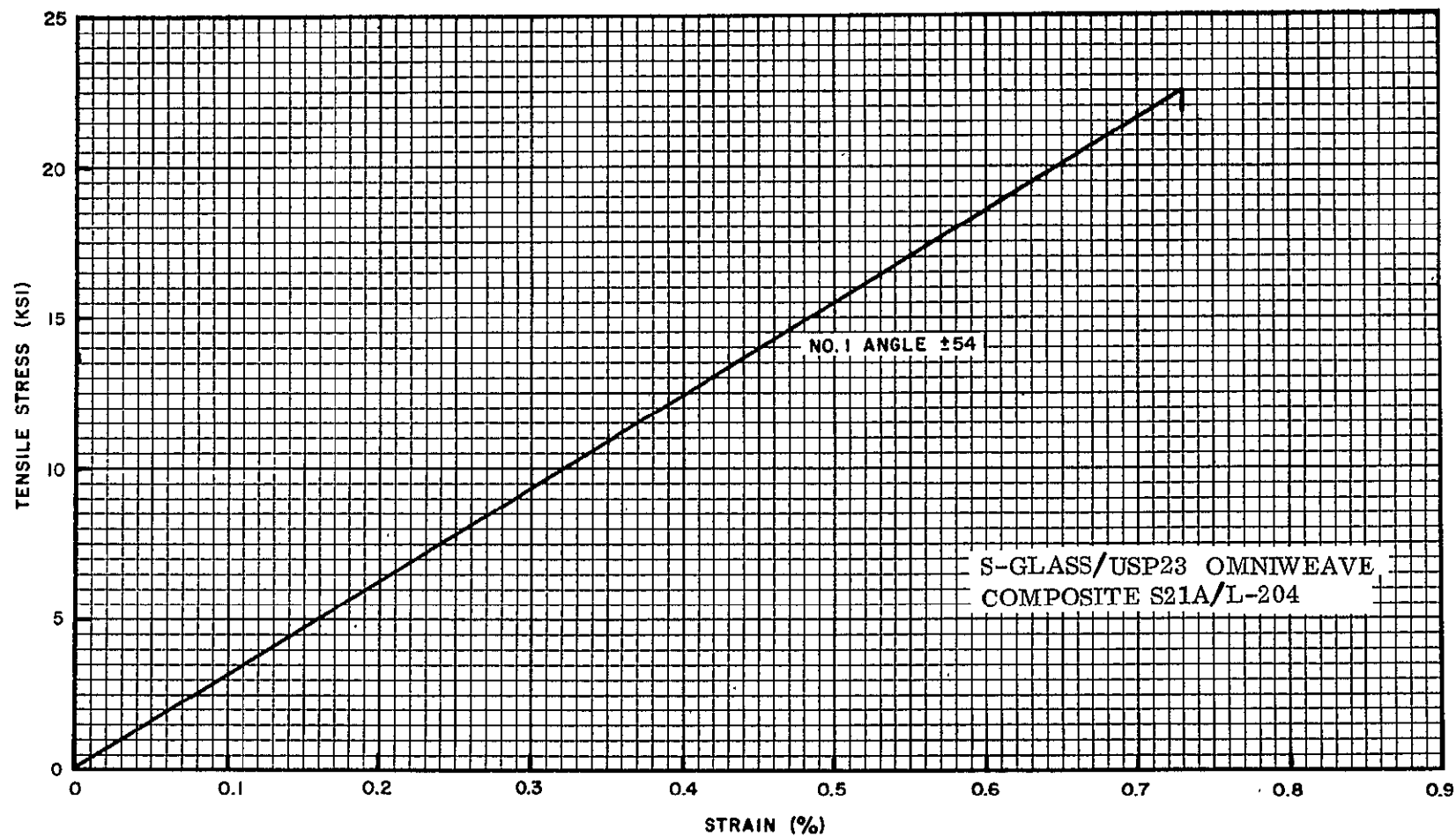


Figure 10-7. Tensile Stress-Strain Curves - S21A/L-204, Axial Direction



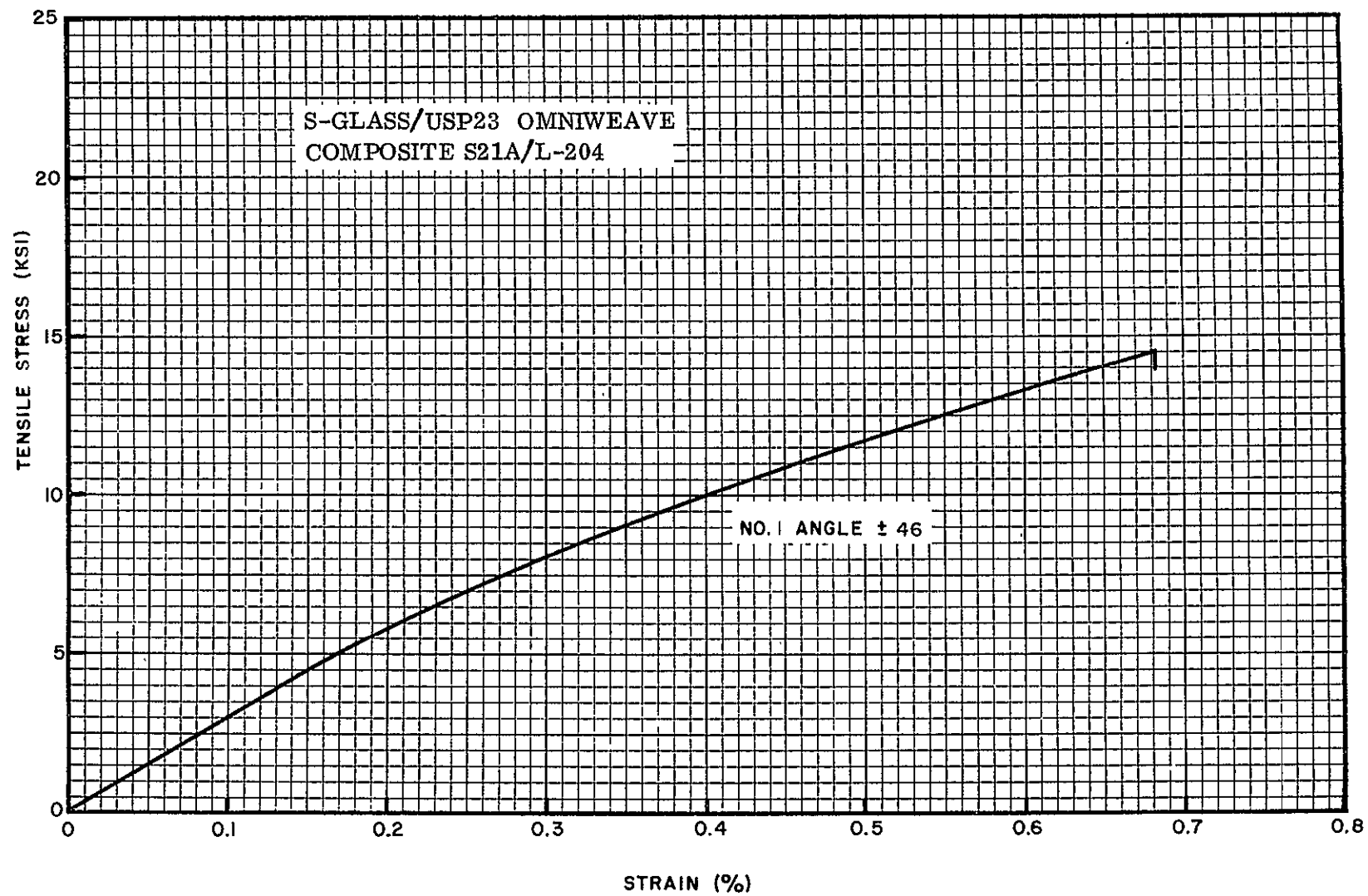


Figure 10-8. Tensile Stress-Strain Curves - S21A/L-204, Transverse Direction

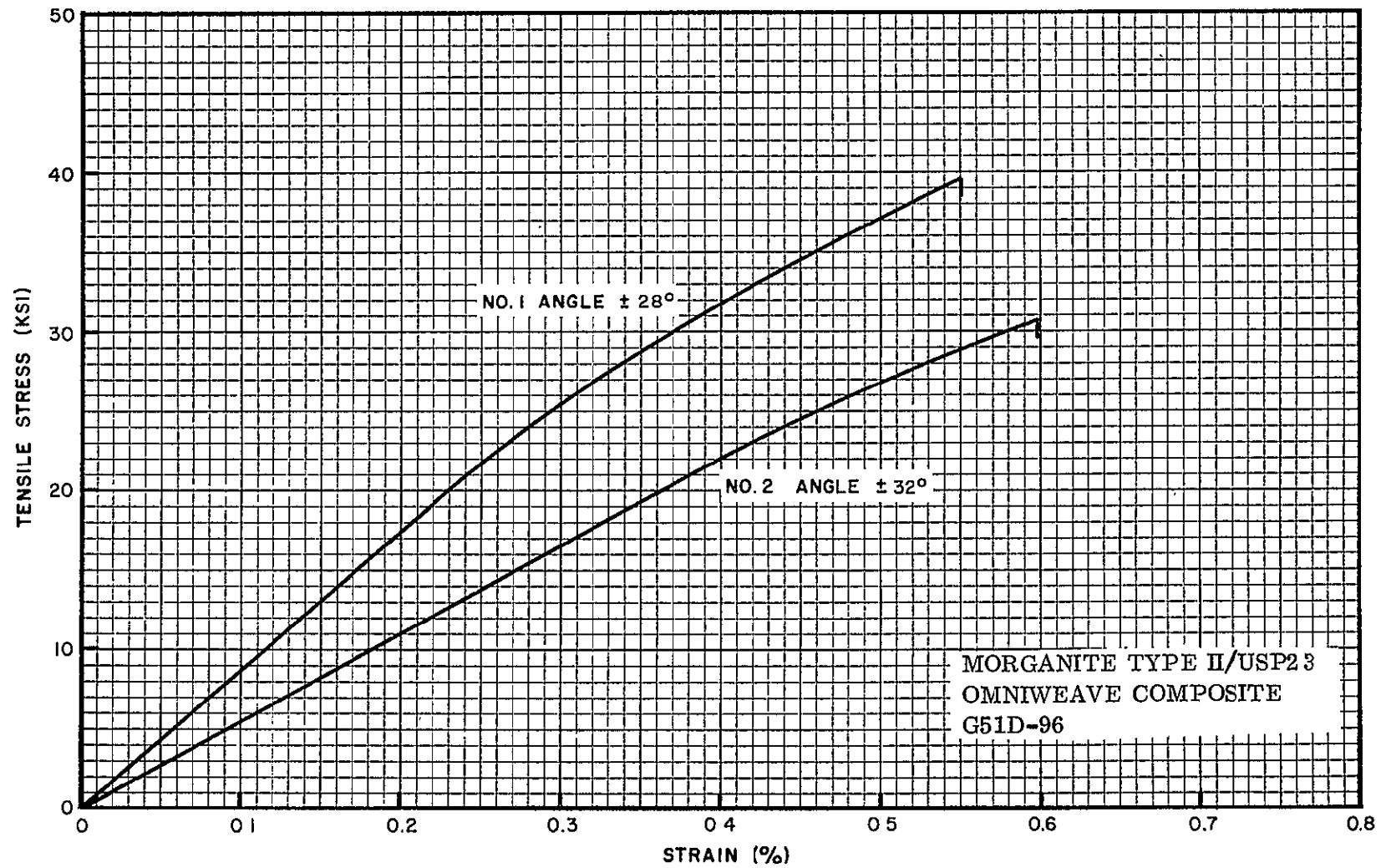


Figure 10-9. Tensile Stress-Strain Curves - G51D-96, Axial Orientation

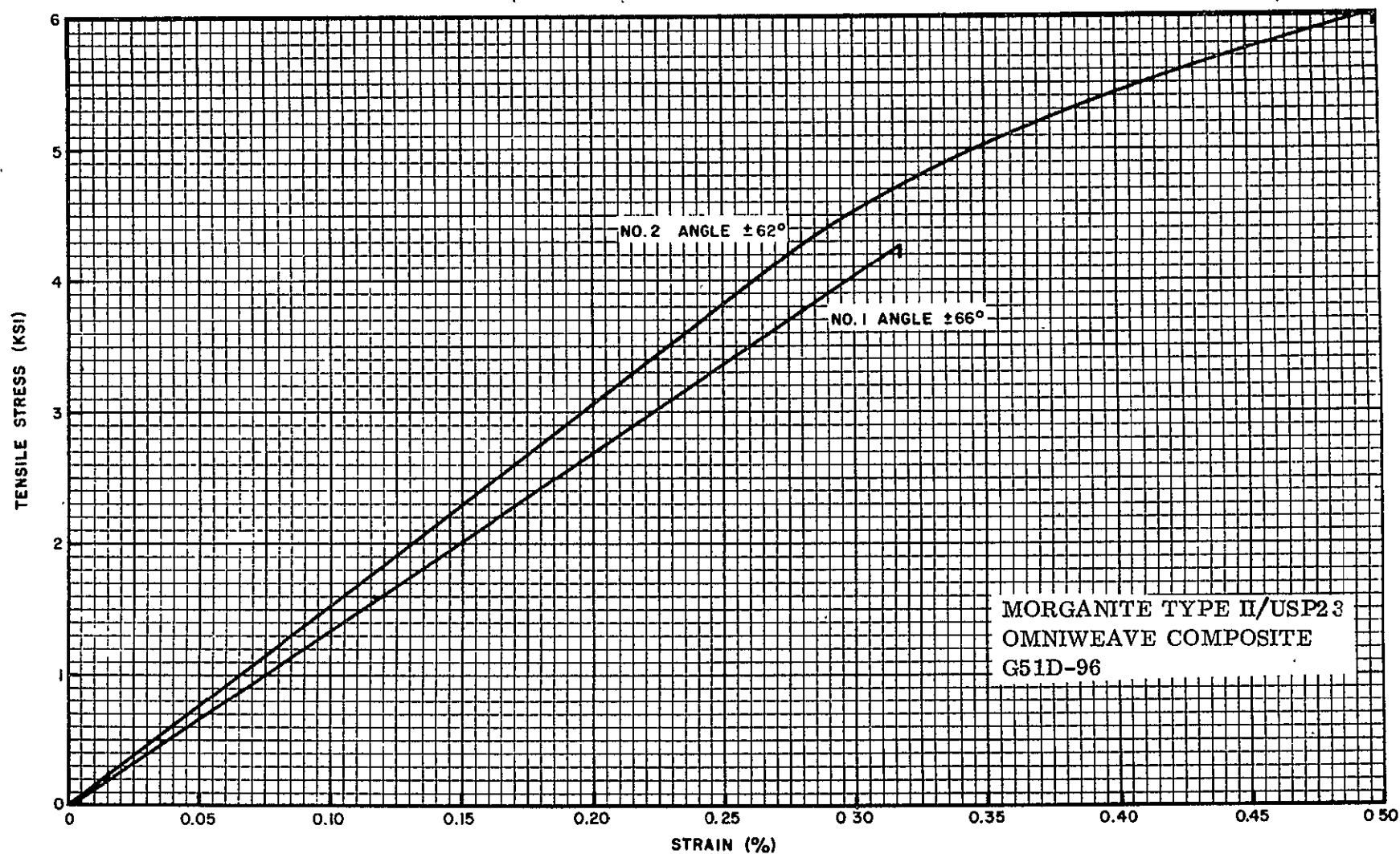


Figure 10-10. Tensile Stress-Strain Curves G51D-96, Transverse Direction

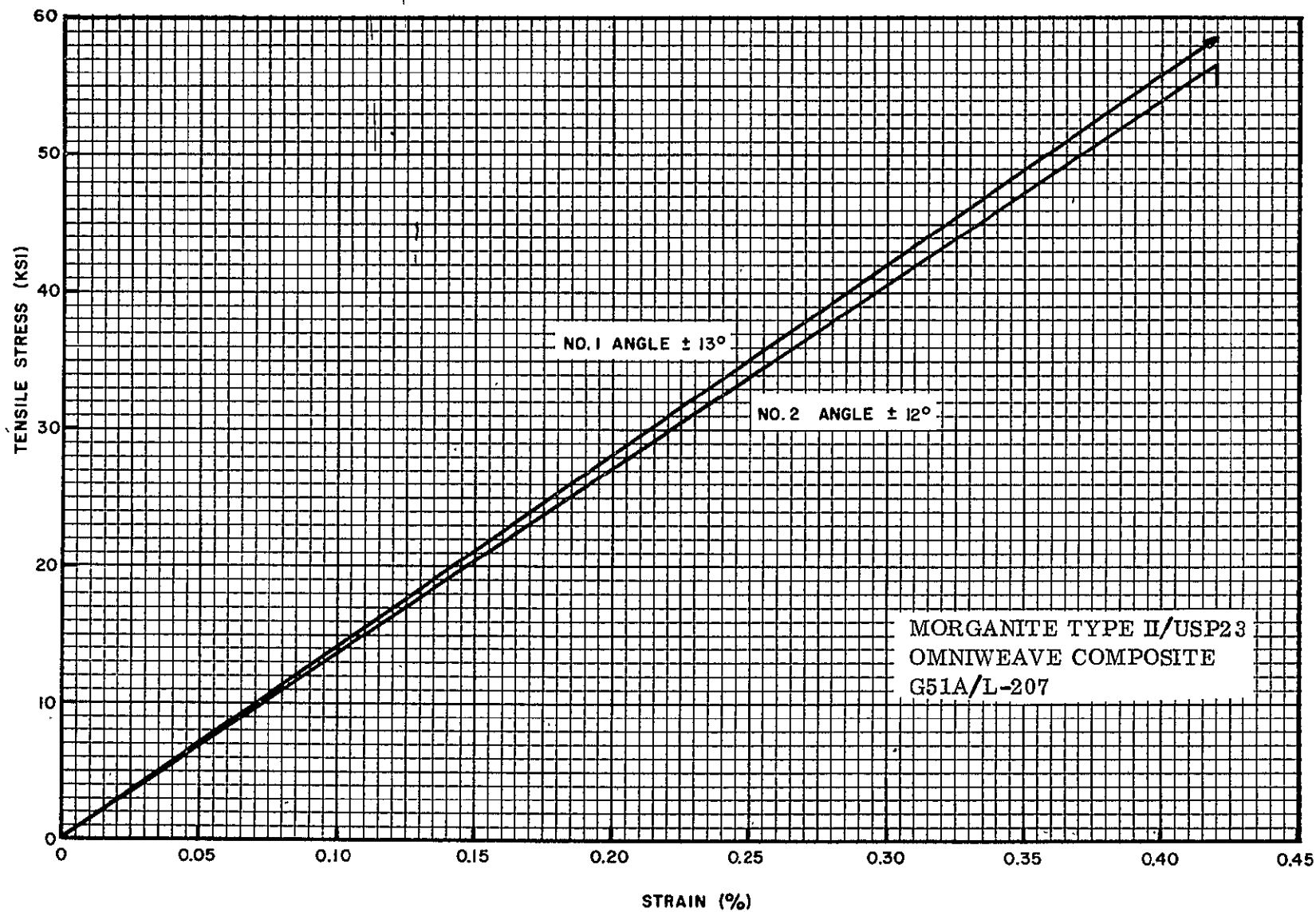


Figure 10-11. Tensile Stress-Strain Curves - G51A/L-207, Axial Direction

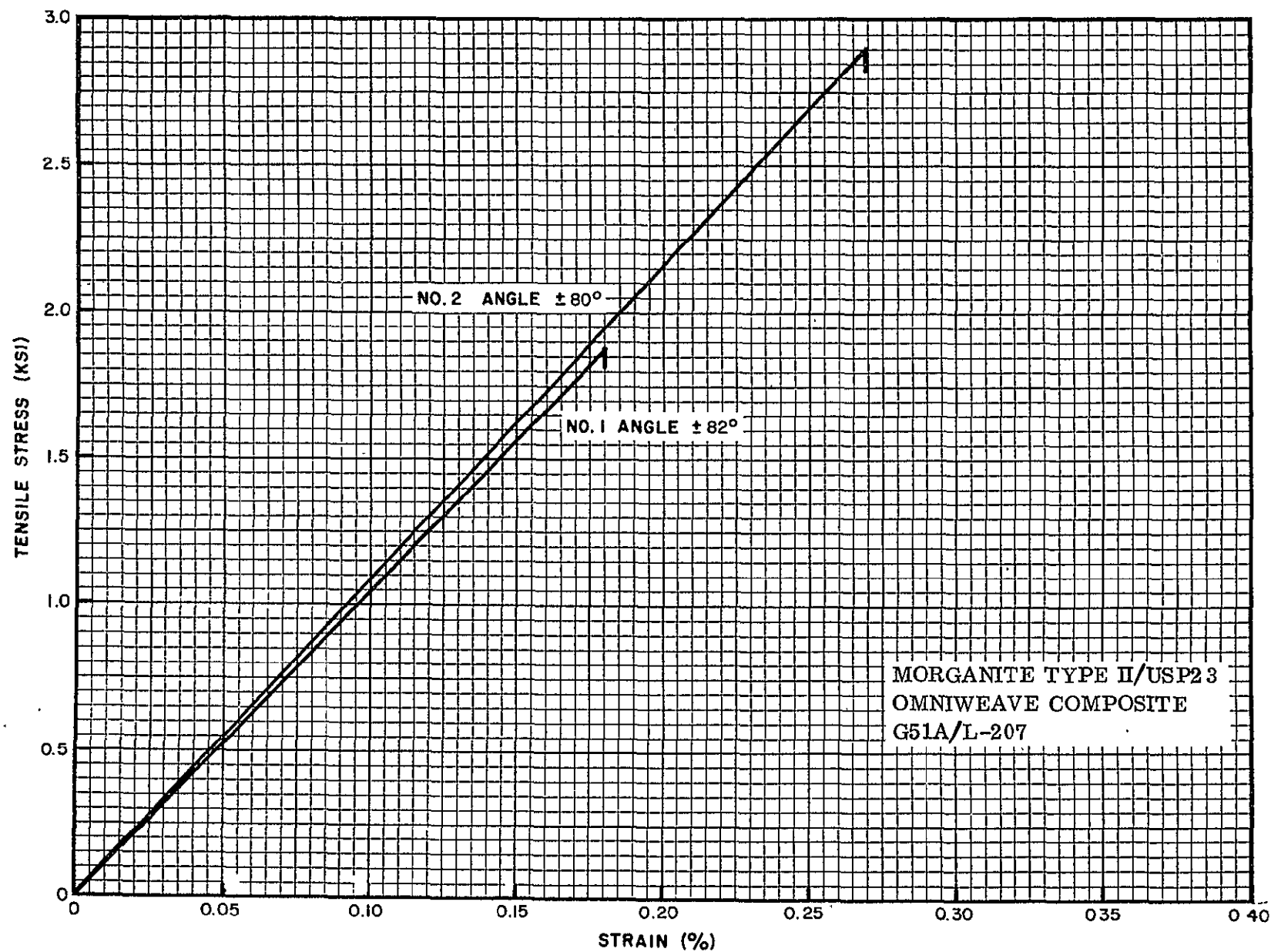


Figure 10-12. Tensile Stress-Strain Curves - G51A/L-207, Transverse Direction

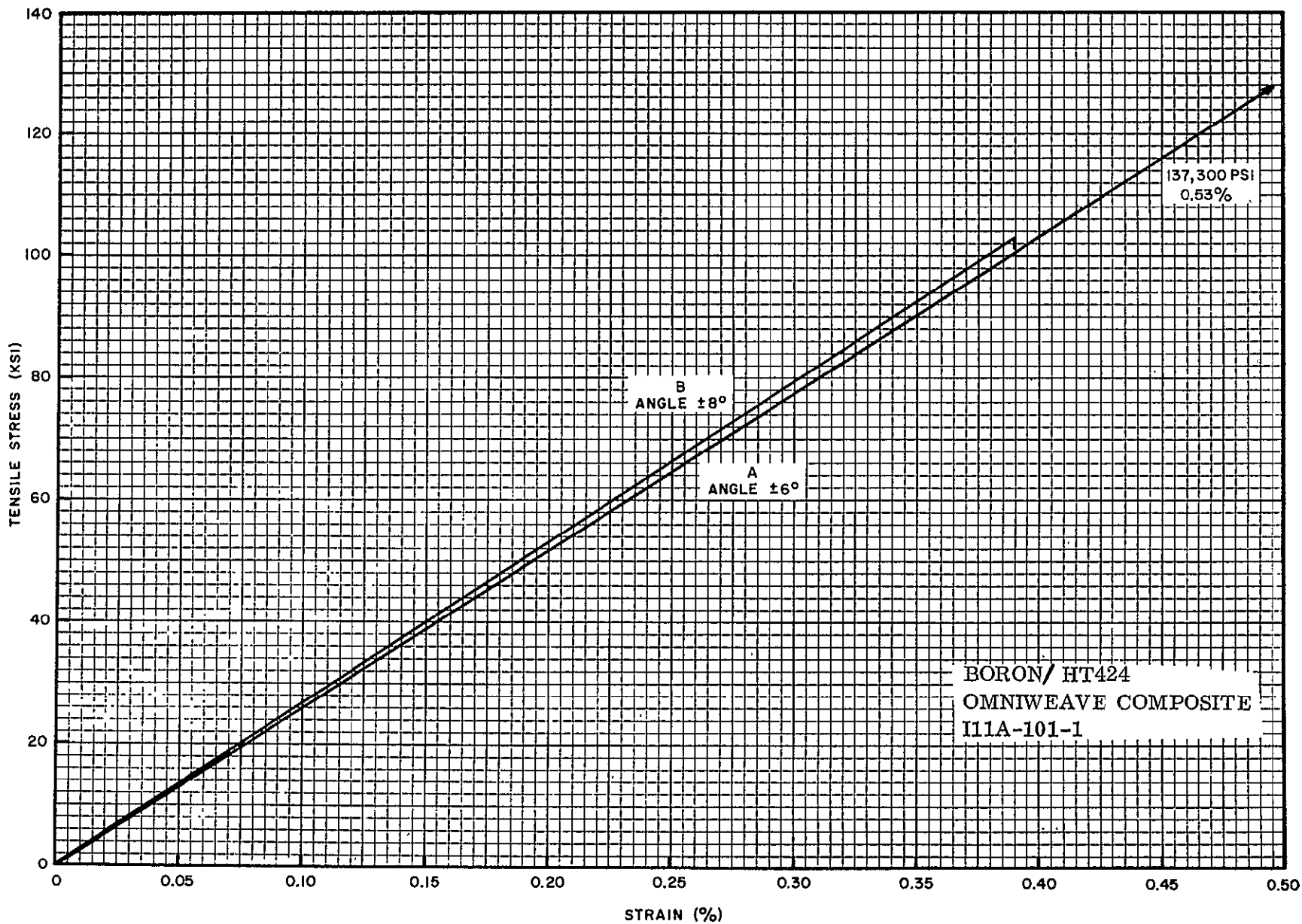


Figure 10-13. Tensile Stress-Strain Curves - I11A-101-1, Axial Direction

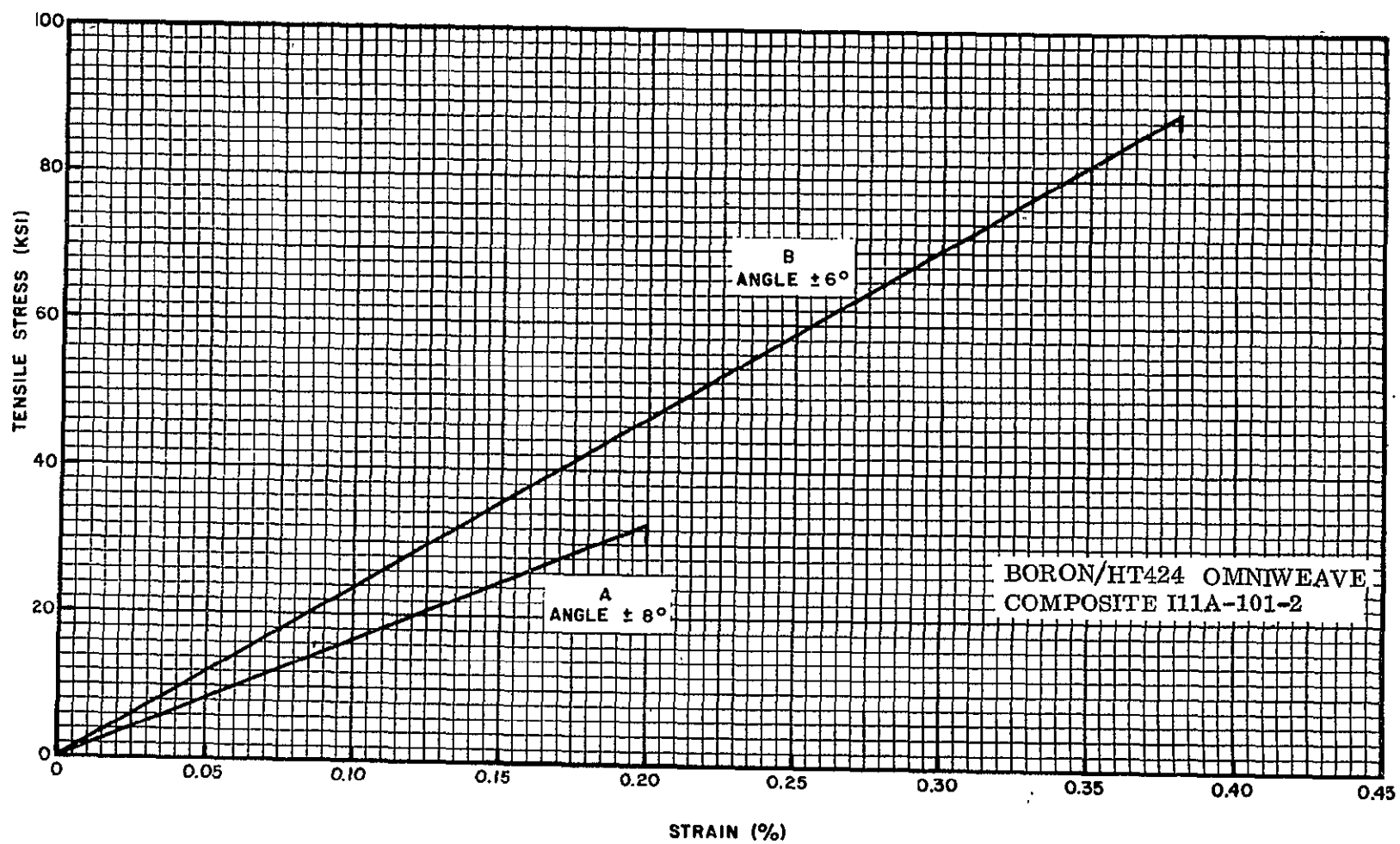


Figure 10-14. Tensile Stress-Strain Curves-I11A-101-2



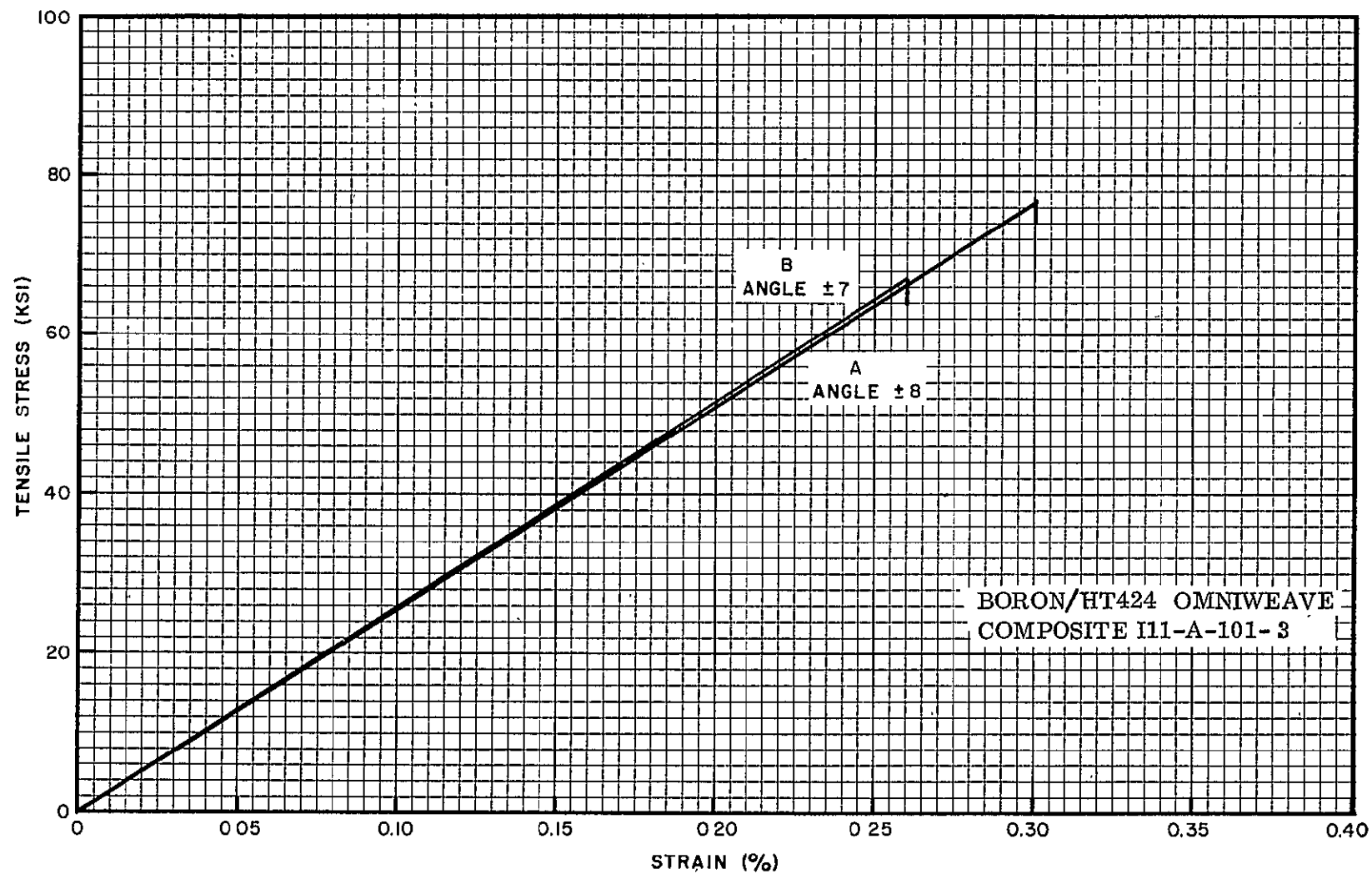


Figure 10-15. Tensile Stress-Strain Curves-I11A-101-3

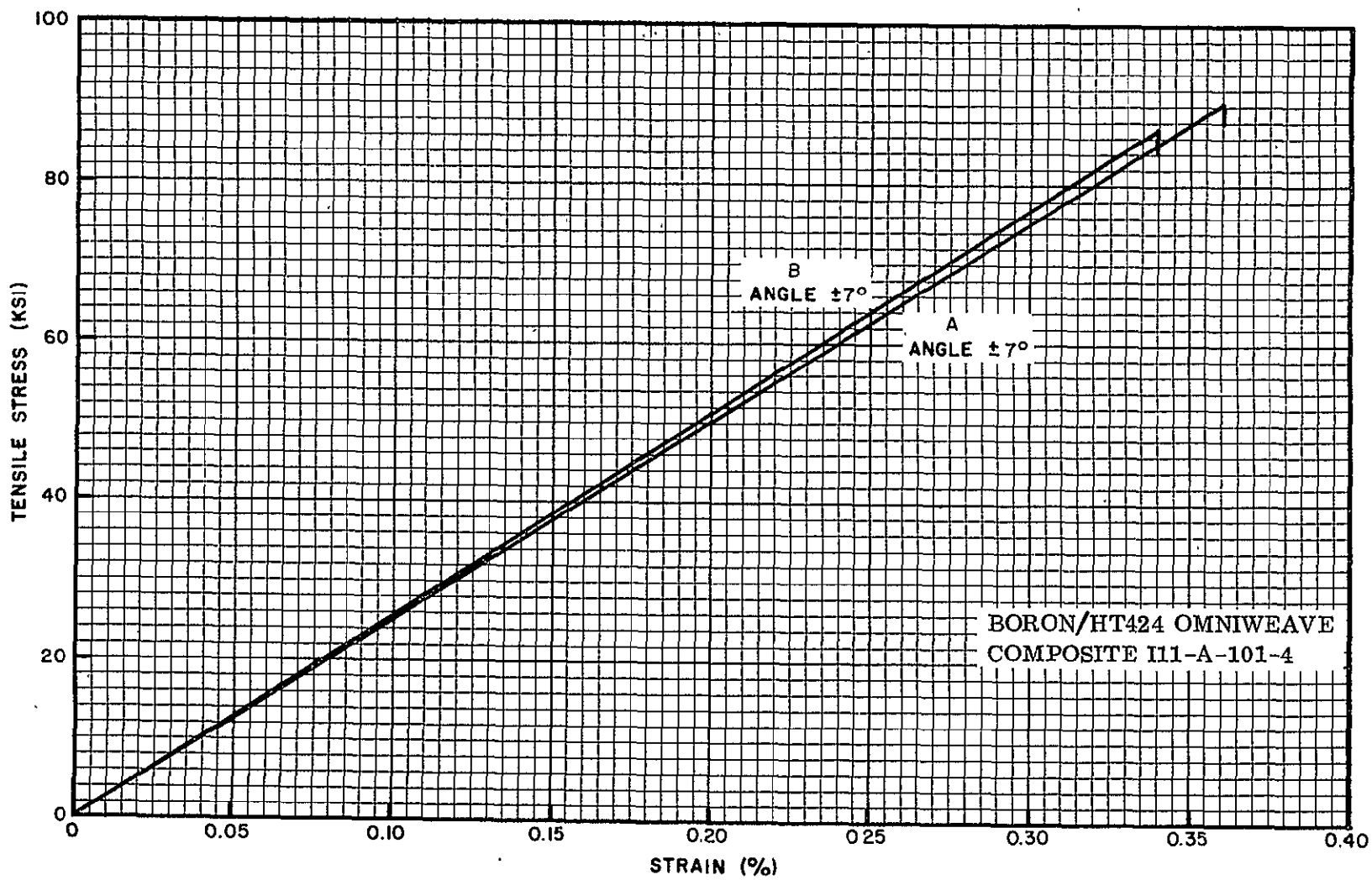


Figure 10-16. Tensile Stress-Strain Curves-I11A-101-4, Axial Direction

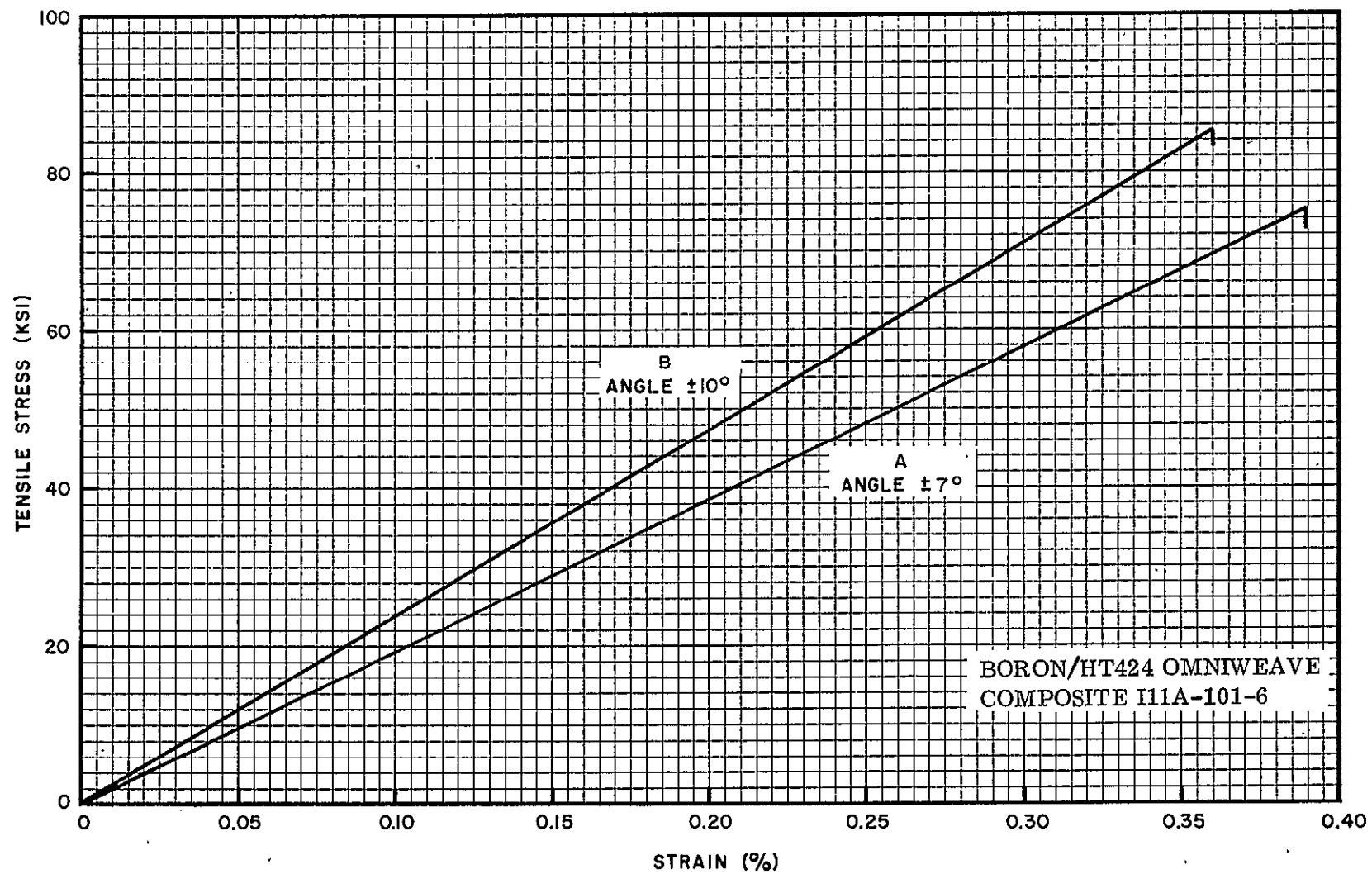


Figure 10-17. Tensile Stress-Strain Curves-I11A-101-6, Axial Direction

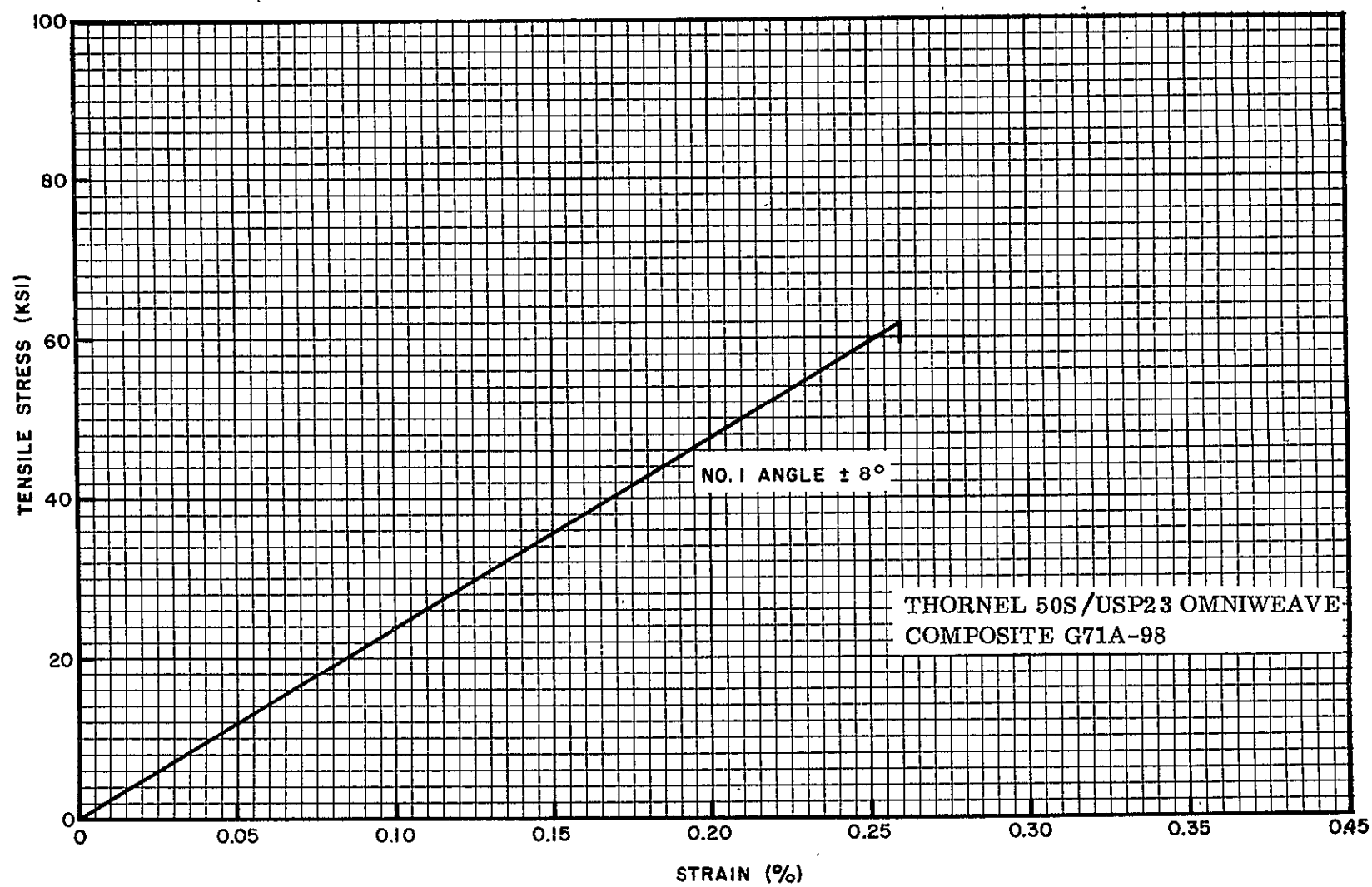


Figure 10-18. Tensile Stress-Strain Curves-G71A-98, Axial Direction

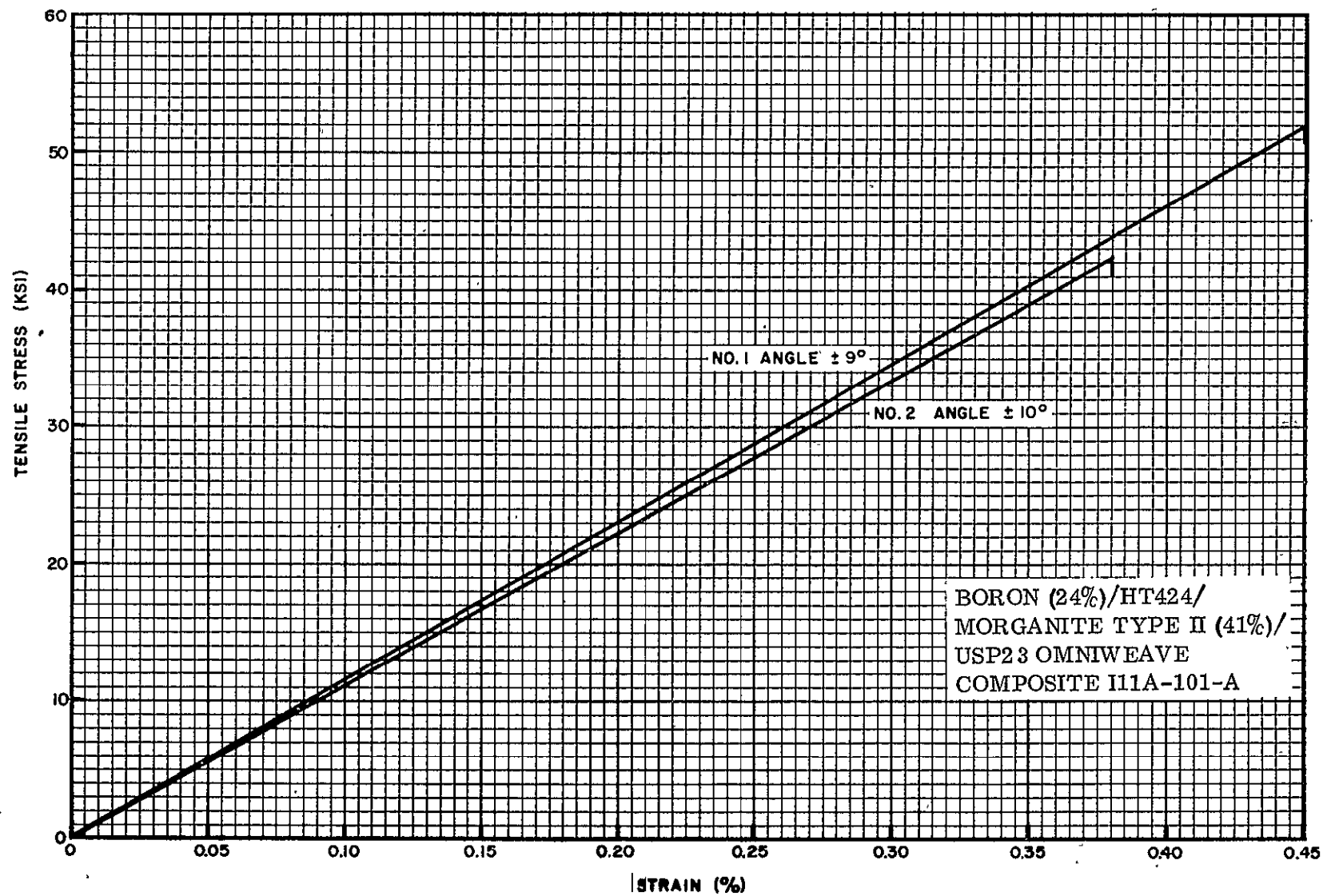


Figure 10-19. Tensile Stress-Strain Curves-I11A-101-A, Axial Direction

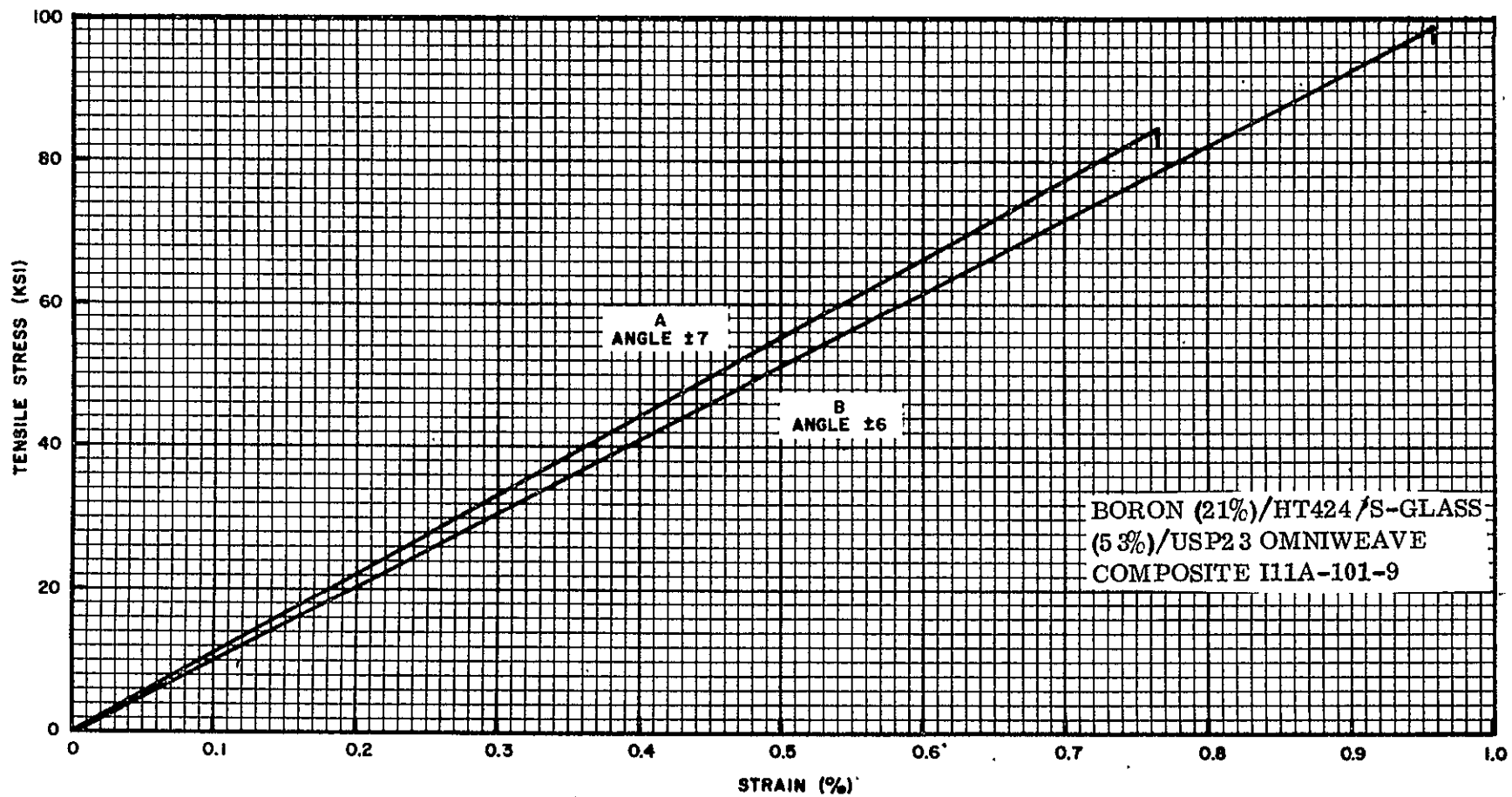


Figure 10-20. Tensile Stress-Strain Curves-I11A-101-9, Axial Direction

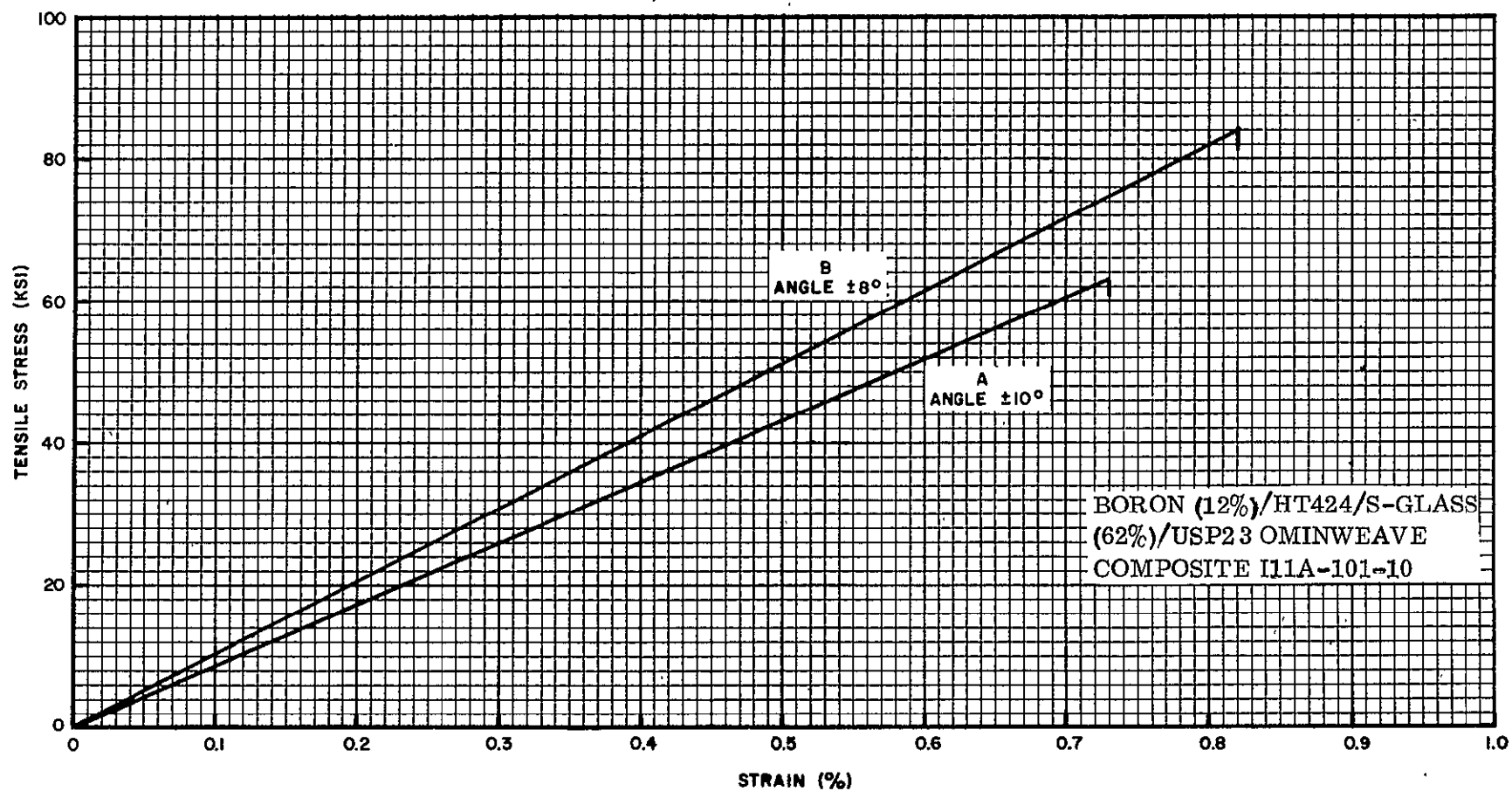


Figure 10-21. Tensile Stress-Strain Curves-I11A-101-10, Axial Direction



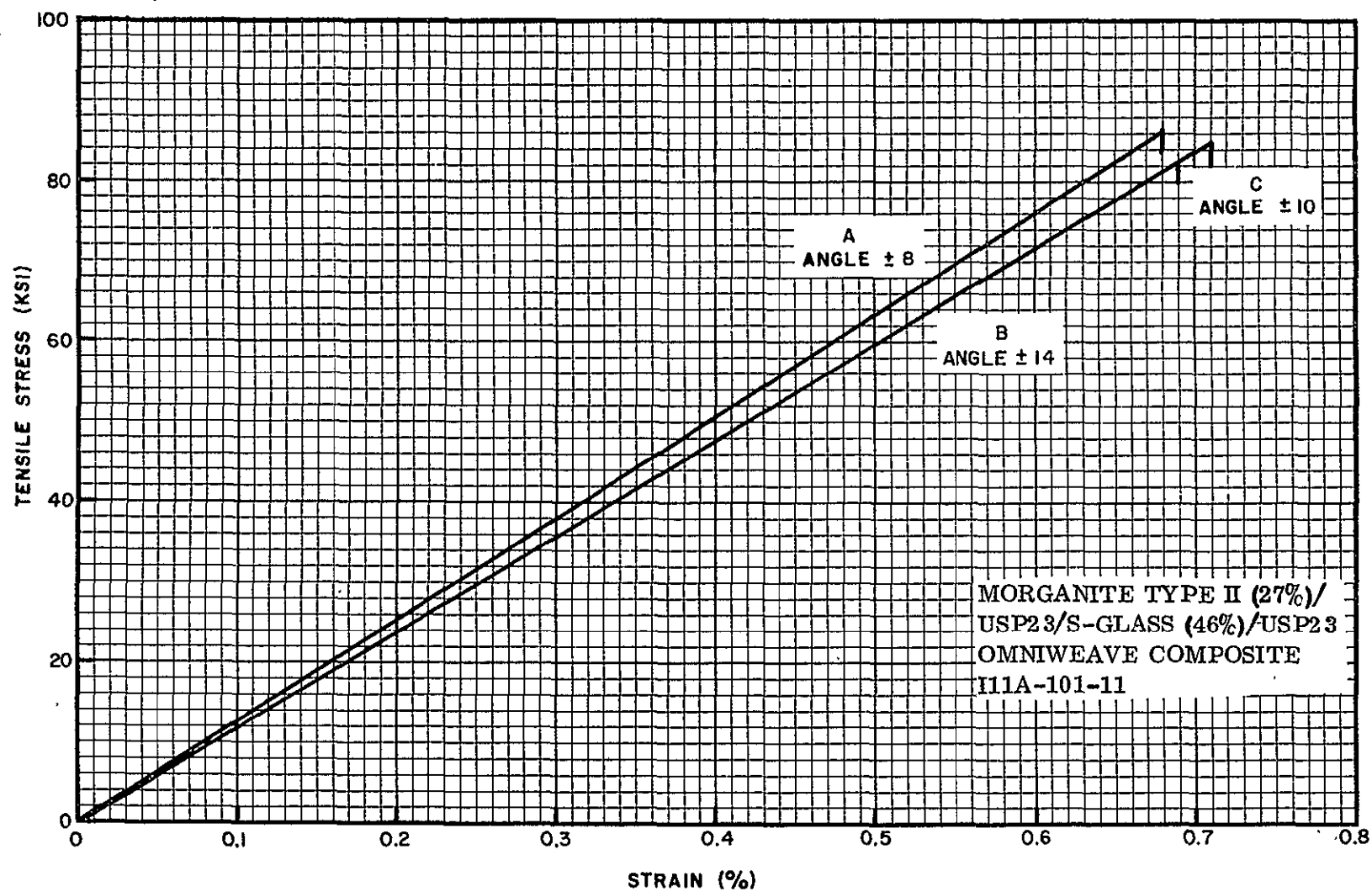


Figure 10-22. Tensile Stress-Strain Curves-I11A-101-11, Axial Direction

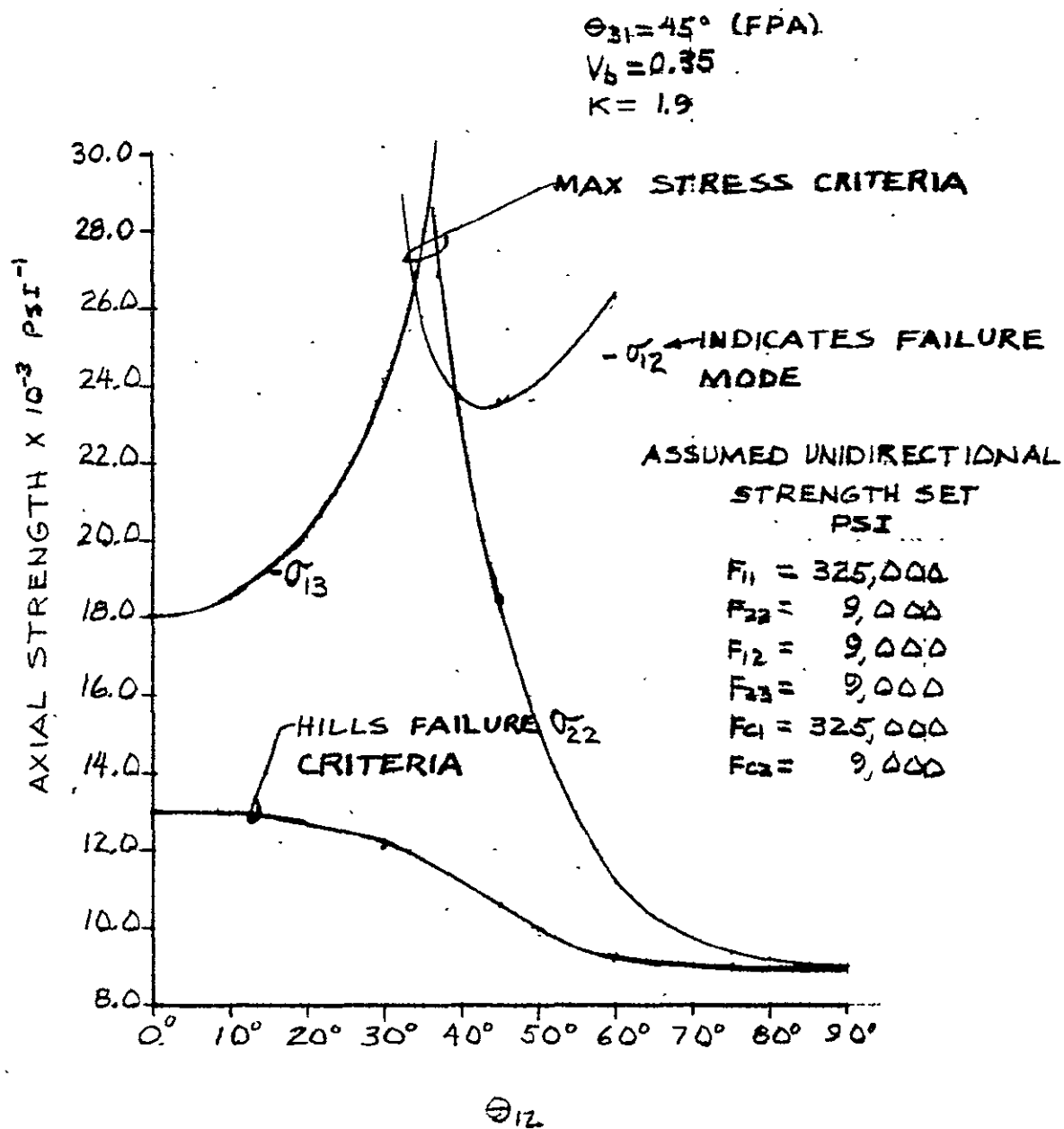


Figure 10-23. Axial Strength Predictions Using Max. Stress Criteria - S-Glass Omniweave Composites

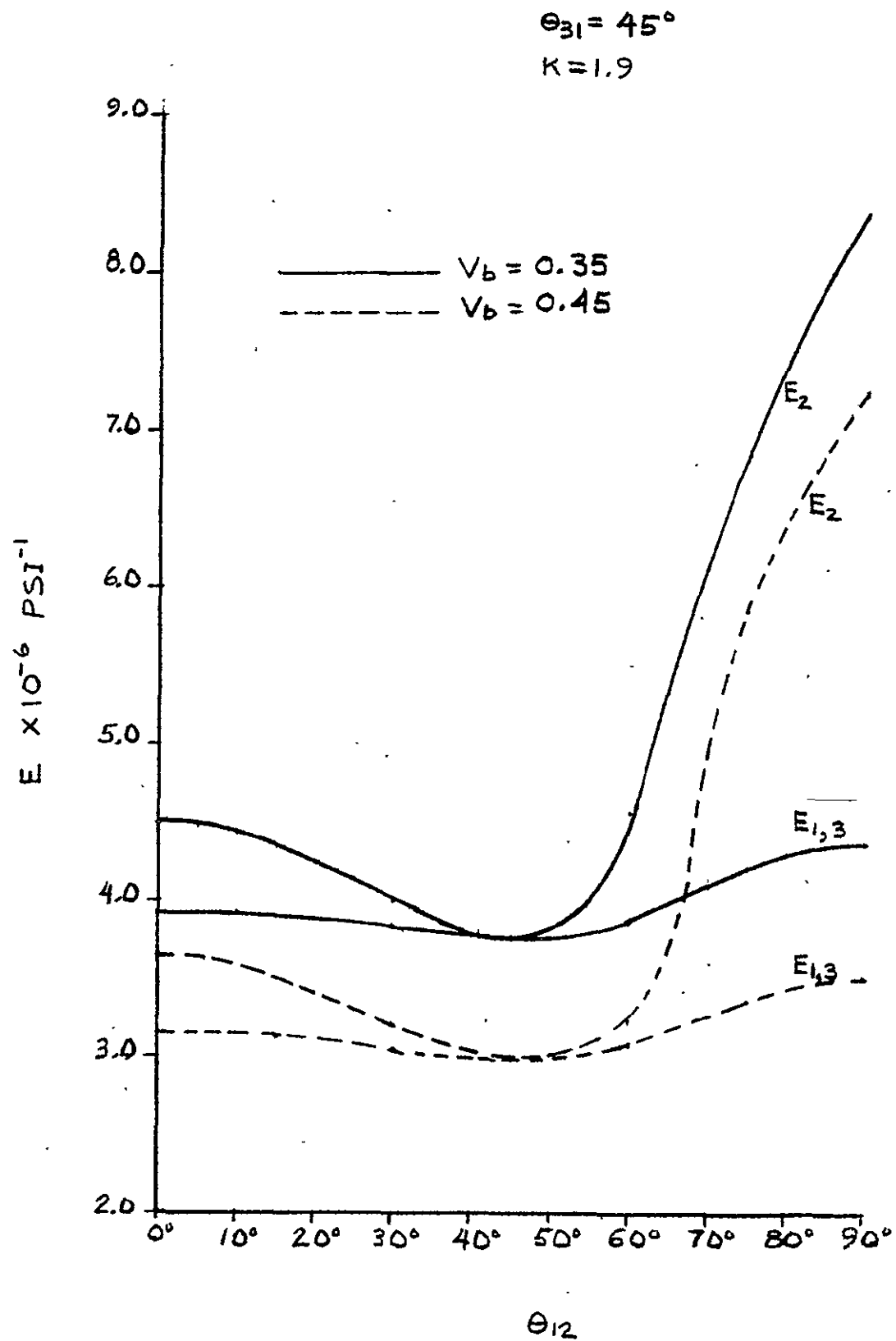


Figure 10-24. Elastic Moduli Prediction - S-Glass Omniweave Composites

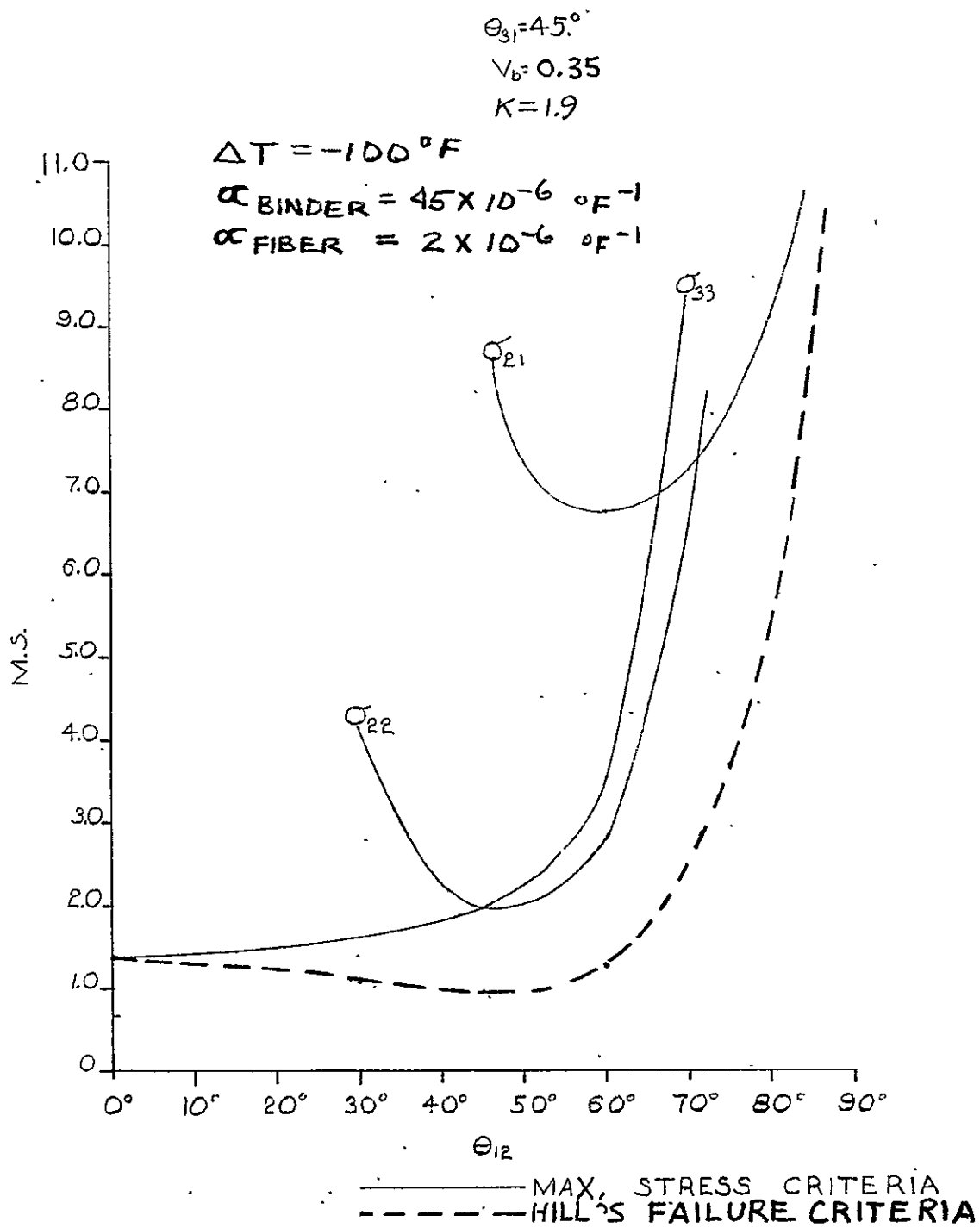


Figure 10-25. Margins of Safety (Thermal Loading Only) - S-Glass Omniweave Composites

$$\theta_{31} = 45^\circ$$

$$V_b = 0.35 \quad K = 1.9$$

LOADING

$$\sigma_{11} = 10,000 \text{ PSI}$$

$$\Delta T = -100^\circ \text{ F}$$

$$\alpha_{\text{FIBER}} = 2 \times 10^{-6} \text{ } ^\circ \text{ F}^{-1}$$

$$\alpha_{\text{BINDER}} = 45 \times 10^{-6} \text{ } ^\circ \text{ F}^{-1}$$

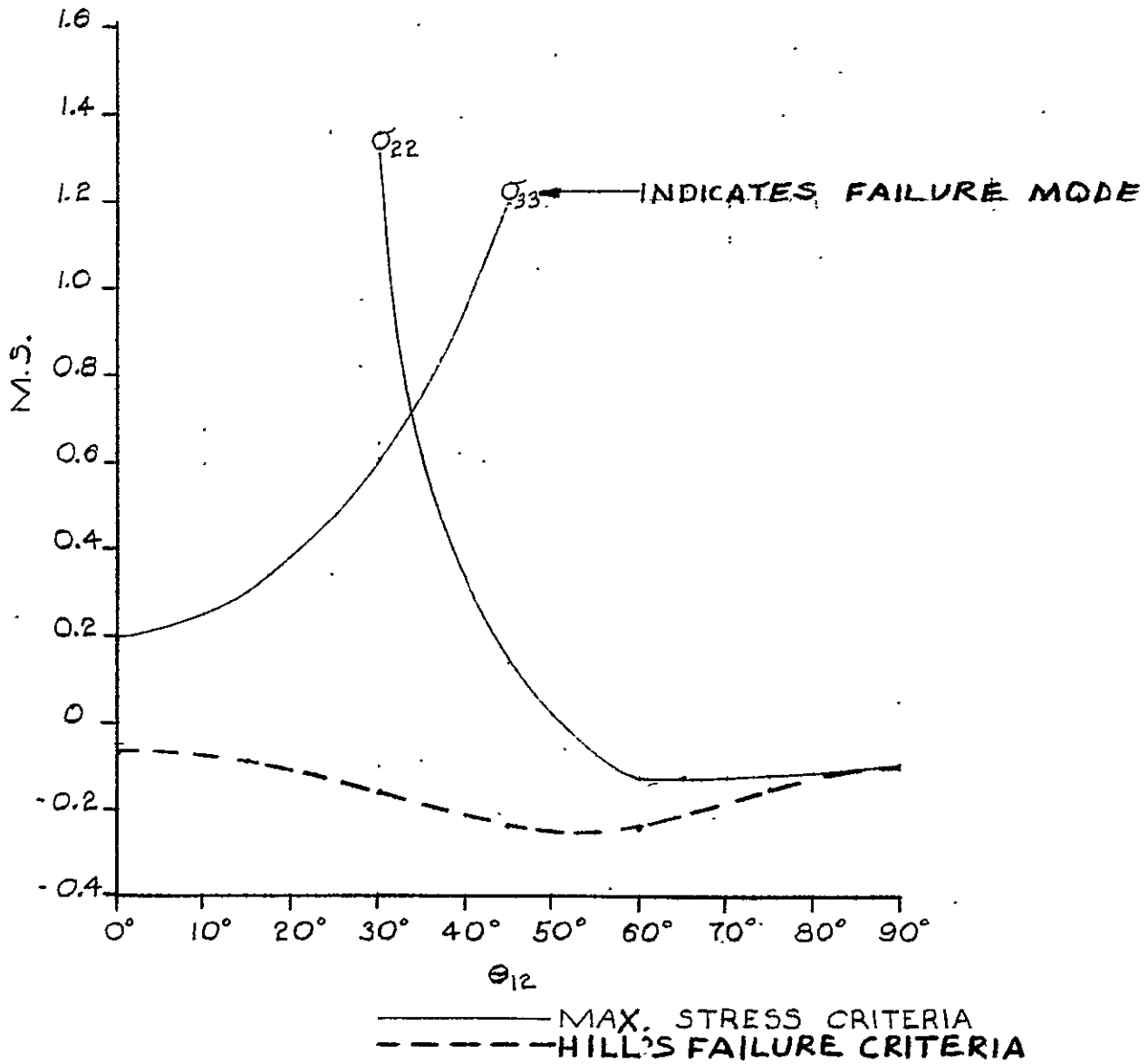


Figure 10-26. Margins of Safety (Thermal plus Mechanical Loading) - S-Glass Omniweave composites

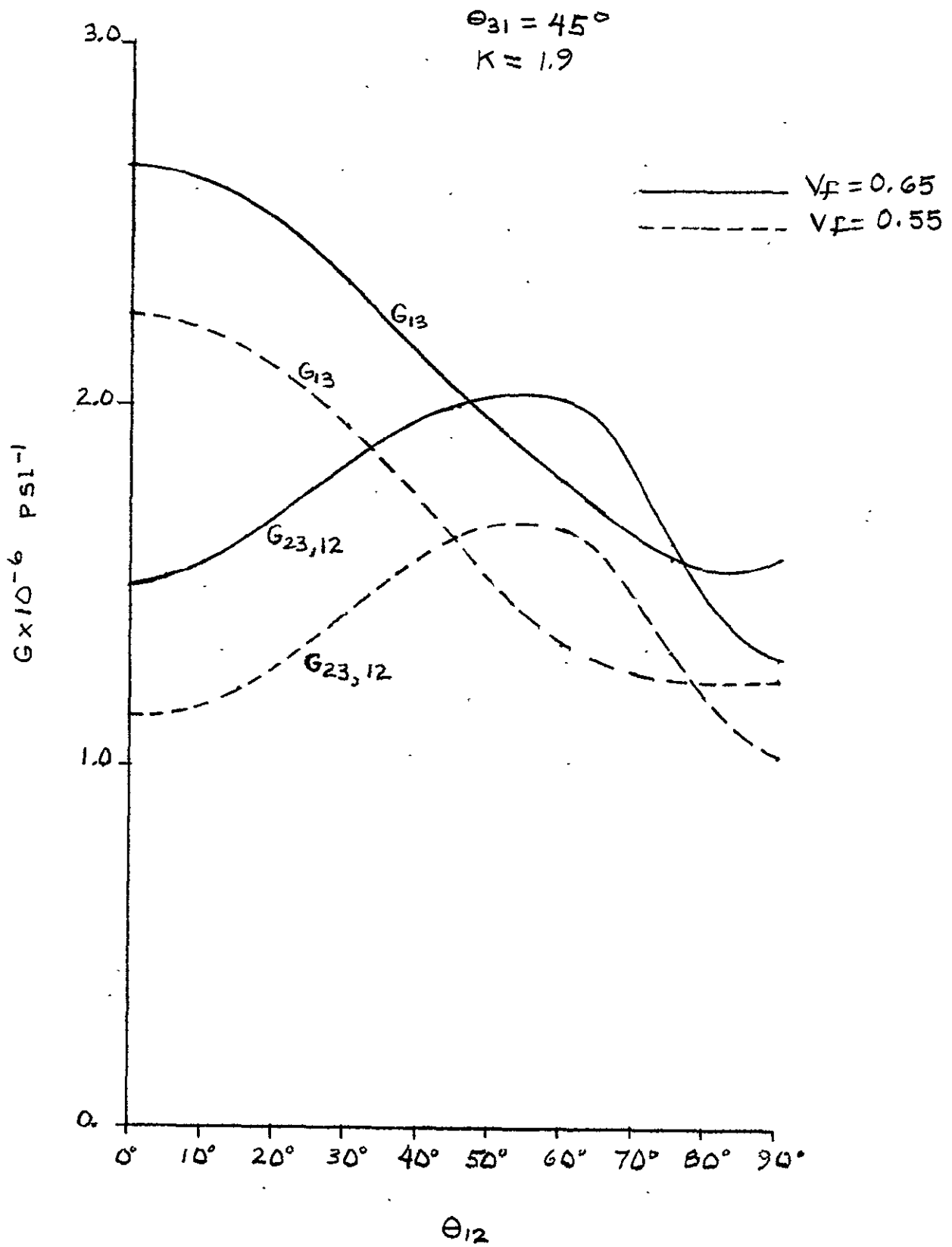


Figure 10-27. Shear Moduli - S-Glass Omniweave Composites

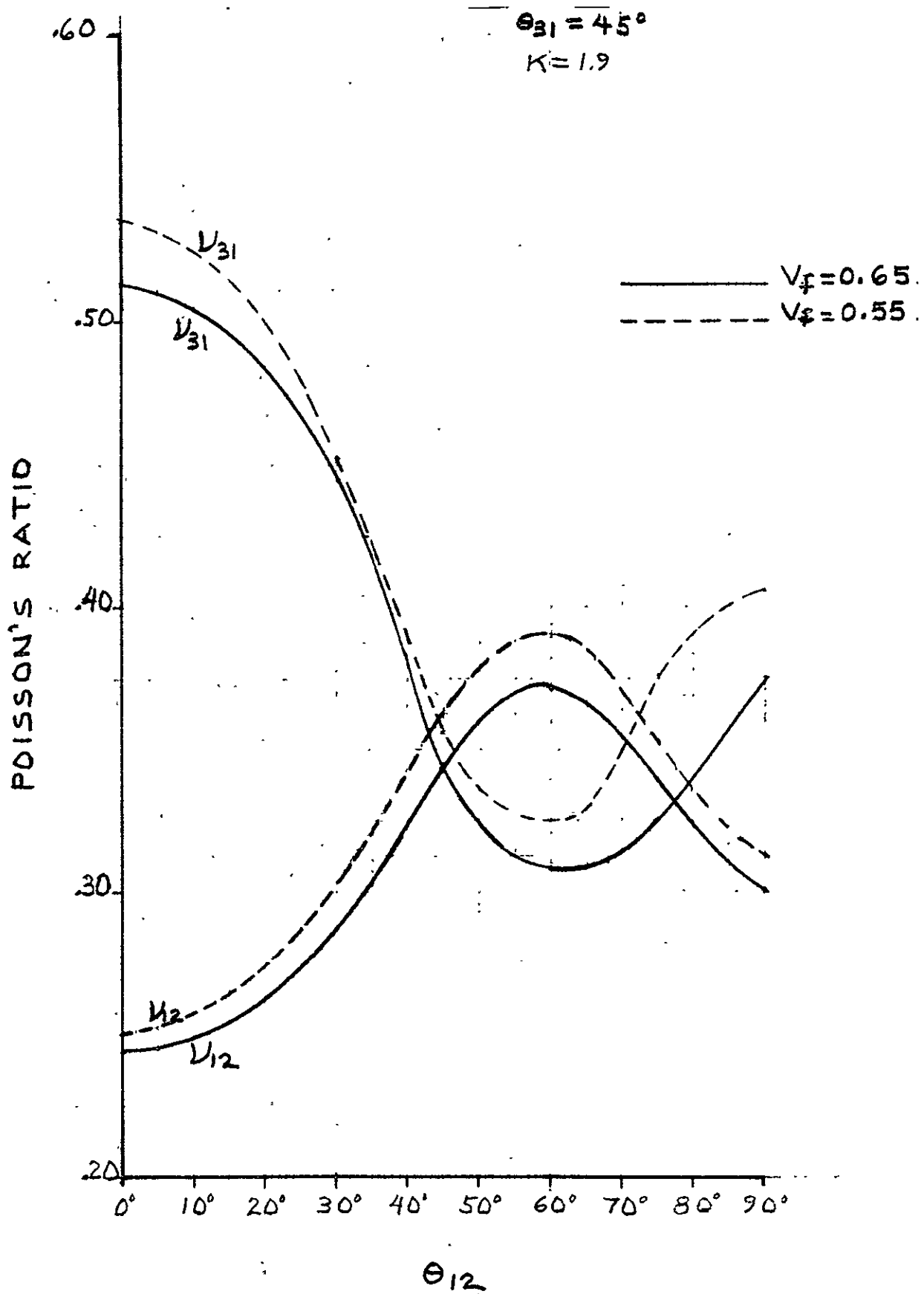


Figure 10-28. Poisson's Ratio for S-Glass Omniweave Composites



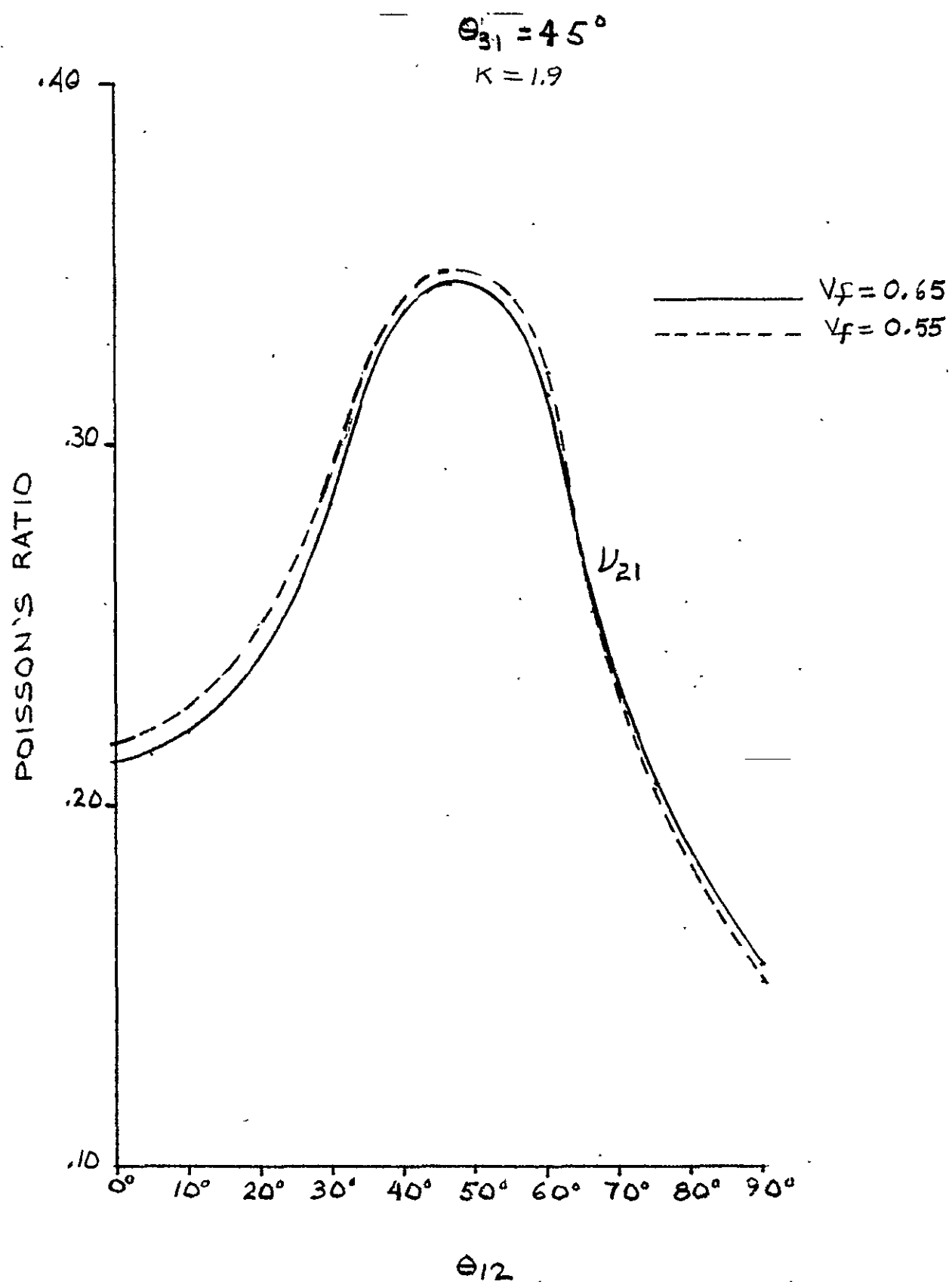


Figure 10-29. Poisson's Ratio for S-Glass Omniweave Composites

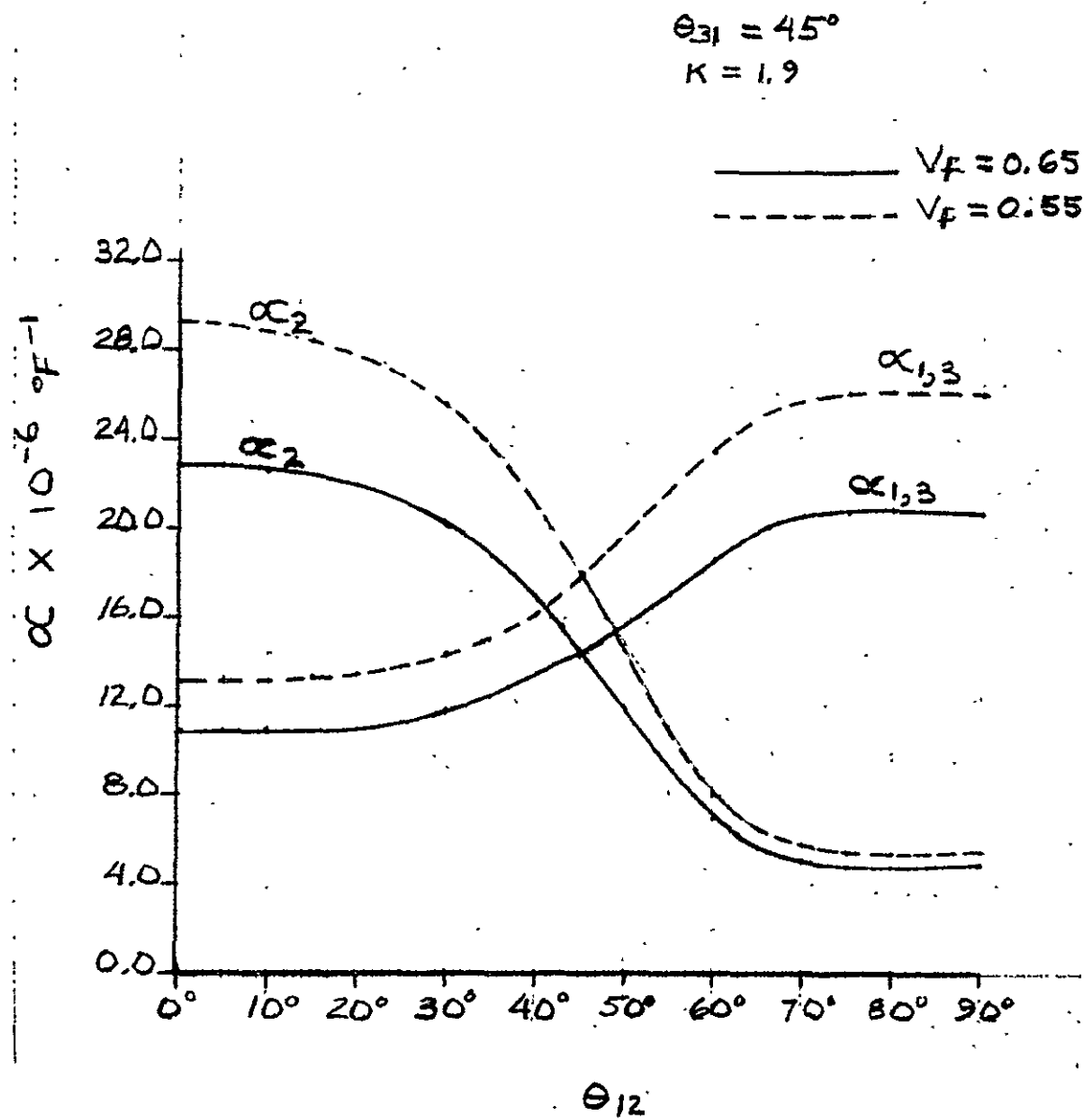


Figure 10-30. Coefficient of Thermal Expansion for S-Glass Omniweave Composites

### 10.6.2 MORGANITE II OMNIWEAVE

Preliminary Morganite II Omniweave strength prediction, modulus and thermal expansion curves for LID and 45 degree fiber pitch angle configuration are shown as functions of the defining fiber angle in Figures 10-31 through 10-54. Axial strength,  $v_{31}$  and  $E_1$  test values were plotted on those prediction curves for the LID configuration. Various sources of binder and fiber property inputs were then used to yield better test data correlation.

Figures 10-32 through 10-34 show the strength and moduli curves using the basic fiber and binder properties, given in Table 6-2, as input into OMNI for an LID configuration. A K factor (multiplying factor) of 1.9 for the binder modulus was used as the result of an evaluation study of laminated boron composites.

Figure 10-31 shows the strength prediction curves for a unidirectional transverse strength of 9,000 and 3,000 psi. The two curves form an envelope about the test points which indicates a true unidirectional transverse strength between 3,000 and 9,000 psi.

Analysis using basic fiber and binder properties (Figures 10-32 through 10-34) was then compared to analysis using published unidirectional composite test data (Figures 10-35 through 10-36) and a K factor of 1.9 for input into OMNI. Inputs used corresponding to each figure are given in Table 10-2. Better test data correlation was obtained using the published unidirectional test data for input. Further analysis of Morganite II using recently published data is presented.

Closer correlation was obtained using binder strength of 6000 psi, again indicating a binder strength of less than 9000 psi.

The results given above indicate the importance of determining, by test, unidirectional properties for input into OMNI to obtain a true prediction curve. Table 10-4 gives the critical factors in determining property values for Omniweave with a LID fiber configuration.

Figure 10-48 gives the axial, hoop and radial strength prediction for Morganite II LID Omniweave. As indicated, high strengths are obtainable in only 1 direction. Other moduli and thermal properties are shown in Figures 10-49 and 10-50 and are discussed under general data trends. A K factor of 1.9 was used in generating these property curves and also the curves for Morganite II 45 degree FPA standard Omniweave, shown in Figures 10-51 through 10-54.

### 10.6.3 THORNEL 50S OMNIWEAVE

Property Prediction curves for Thornel 50S for a standard 45 degree FPA configuration are shown in Figure 10-55 through 10-62. Basic fiber and binder properties (Table 6-2) were used as inputs to generate the prediction curves. Property predictions for a five degree radial angle 18 degree LID configuration are given in Table 10-3.

TABLE 10-2. BASIC FIBER AND BINDER PROPERTIES USED  
IN PRELIMINARY PREDICTIONS

Figure No.	Material Properties From Table 6-2 Used	K-Factor	Material Property Inputs Varied
10-31	All	1.9	$F_{22} = F_{12} = F_{23} = 3000 \text{ psi}$
10-32 to 10-34	All	1.9	None
10-35	ub, uf	1.9	Northrop basic fiber data <sup>12</sup> $E_f = 40 \times 10^6 \text{ psi}$ $F_{11} = 114,000 \text{ psi}$ $F_{12} = F_{22} = 10,000 \text{ psi}$
			AFML Unidirectional Test Data <sup>11</sup> $E_f = 28.5 \times 10^6 \text{ psi}$ $F_{11} = 88,500 \text{ psi}$ $F_{12} = F_{22} = 10,000 \text{ psi}$
10-30	ub, uf	1.9	$E_f = 28.5 \times 10^6$
10-37	ub, uf	1.0	AFML Unidirectional Test Data <sup>11</sup> $E_f = 28.5 \times 10^6$ $F_{11} = 88,500 \text{ psi}$ $F_{12} = F_{22} = 9000 \text{ psi}$ also $F_{22} = F_{12} = 6000 \text{ psi}$
10-38 through 10-54	All	1.9	None
10-55 through 10-70	All	1.9	None

\*NOTE: Except as noted, a unidirectional shear and transverse tension strength of 9,000 psi was used.  $E_b = 0.54 \times 10^6 \times K \text{ psi}$

TABLE 10-3. PROPERTY VALUES FOR OMNIWEAVE COMPOSITES WITH A  
18° LAYERED IN DEPTH FIBER CONFIGURATION

	$\theta_{12} = 5^\circ$	$V_f = 0.65$		
	Morganite II	S-Glass	Boron	Thornel-50
$E_1$ ( $10^6$ psi)	20.2	6.07	29.4	20.9
$E_2$ ( $10^6$ psi)	6.0	3.51	6.39	4.61
$E_3$ ( $10^6$ psi)	5.4	3.27	5.78	4.17
$G_{23}$ ( $10^6$ psi)	2.1	1.23	2.25	1.57
$G_{12}$ ( $10^6$ psi)	1.8	1.08	1.9	1.39
$G_{13}$ ( $10^6$ psi)	3.5	1.44	4.69	3.36
$\nu_{21}$	0.18	0.266	0.137	0.138
$\nu_{31}$	0.61	0.427	0.751	0.751
$\nu_{12}$	0.055	0.154	0.029	0.03
$\nu_{13}$	0.17	0.230	0.148	0.15
$\nu_{23}$	0.344	0.367	0.345	0.382
$\nu_{32}$	0.378	0.394	0.381	0.422
Axial Strength (psi)	120,000	64,000	86,000	160,000
<u>Margins of Safety</u>				
With Thermal Loading of $-100^\circ \Delta T$	4.4	6.64	3.98	4.22
$-100^\circ \Delta T + 10,000$ psi Axial Loading	2.8	2.49	2.80	2.9
$\alpha_1$ ( $10^{-6}$ IN./°F)	1.46	5.63	1.18	0.93
$\alpha_2$ ( $10^{-6}$ IN./°F)	21.2	25.9	21.4	27.3
$\alpha_3$ ( $10^{-6}$ IN./°F)	20.4	25.4	20.4	25.8

TABLE 10-4. CATALOG OF CRITICAL FACTORS FOR MORGANITE II  
OMNIWEAVE WITH A LID FIBER CONFIGURATION

1. K factor - Multiplying factor for binder modulus -

A K factor of 1.9 was used in the initial analysis.

A K factor of 1 yields the best correlation with test data.

2. Fiber Modulus - Two moduli were used in analysis -

a) Basic fiber modulus from published data<sup>2</sup> ( $E_f = 40 \times 10^6$ )

b) Unidirectional composite moduli from published  
data<sup>11</sup> ( $E_f = 28.5 \times 10^6$ )

Lower modulus yields lower strength allowable and better correlation with test data.

3. Binder strength -

A binder strength of 9000 PSI was used in the initial analysis. The actual binder strength appears to be about 6000 PSI.

4. Fiber strength -

The fiber strength is not critical for  $\theta_{31}$  greater than  $60-75^\circ$ , depending on binder strength and modulus used.

#### 10.6.4 BORON OMNIWEAVE

Property prediction curves for Boron Omniweave in a 45 degree FPA configuration is presented in Figures 10-63 through 10-70. Basic fiber and binder properties (Table 6-2) were used to generate the prediction curves. Property prediction values for an 18 degree LID configuration (radial angle  $\approx 5^\circ$ ) is given in Table 10-3.

#### 10.6.5 MARGIN-OF-SAFETY AND THERMAL EXPANSION PREDICTIONS

Margins-of-safety values for thermal loading only were determined for all materials for a 45 degree FPA fiber orientation. Near zero or negative margins of safety were predicted for values of  $\theta_{12}$  between 0 and 60 degrees. The high residual stresses resulting from thermal loading may be attributed to the high binder coefficient of

expansion ( $\alpha_{\delta} = 45 \times 10^{-6} \text{ }^{\circ}\text{F}$ ), which in reality is probably much less. The margin of safety curves show an extremum point at  $\theta_{12} = 50^{\circ}$  where failure is in transverse tension (see Figures 10-64, 10-57, and 10-65).

Analysis indicates a zero or negative coefficient of thermal expansion in one direction is possible for Omniweave constructions of certain fiber materials and specific fiber angle orientations. Figure 10-44 shows the effective thermal expansion coefficient as a function of  $\theta_{31}$  for Morganite II Omniweave with a LID fiber configuration. Negative values in the axial direction were obtained for  $\theta_{31}$  between 60 and 70 degrees. These results are similar to those given by Dow and Rosen<sup>17</sup> for laminate composites. Negative  $\alpha$  values in one direction were also obtained for Morganite II, Thornel-50, and Boron Omniweave composites with a  $45^{\circ}$  fiber pitch angle geometry (see Figures 10-48, 10-62 and 10-70).

As indicated, negative  $\alpha$  values were obtained in the radial direction only. As with 2-D composites the coefficient of thermal expansion decreases with increasing fiber modulus.

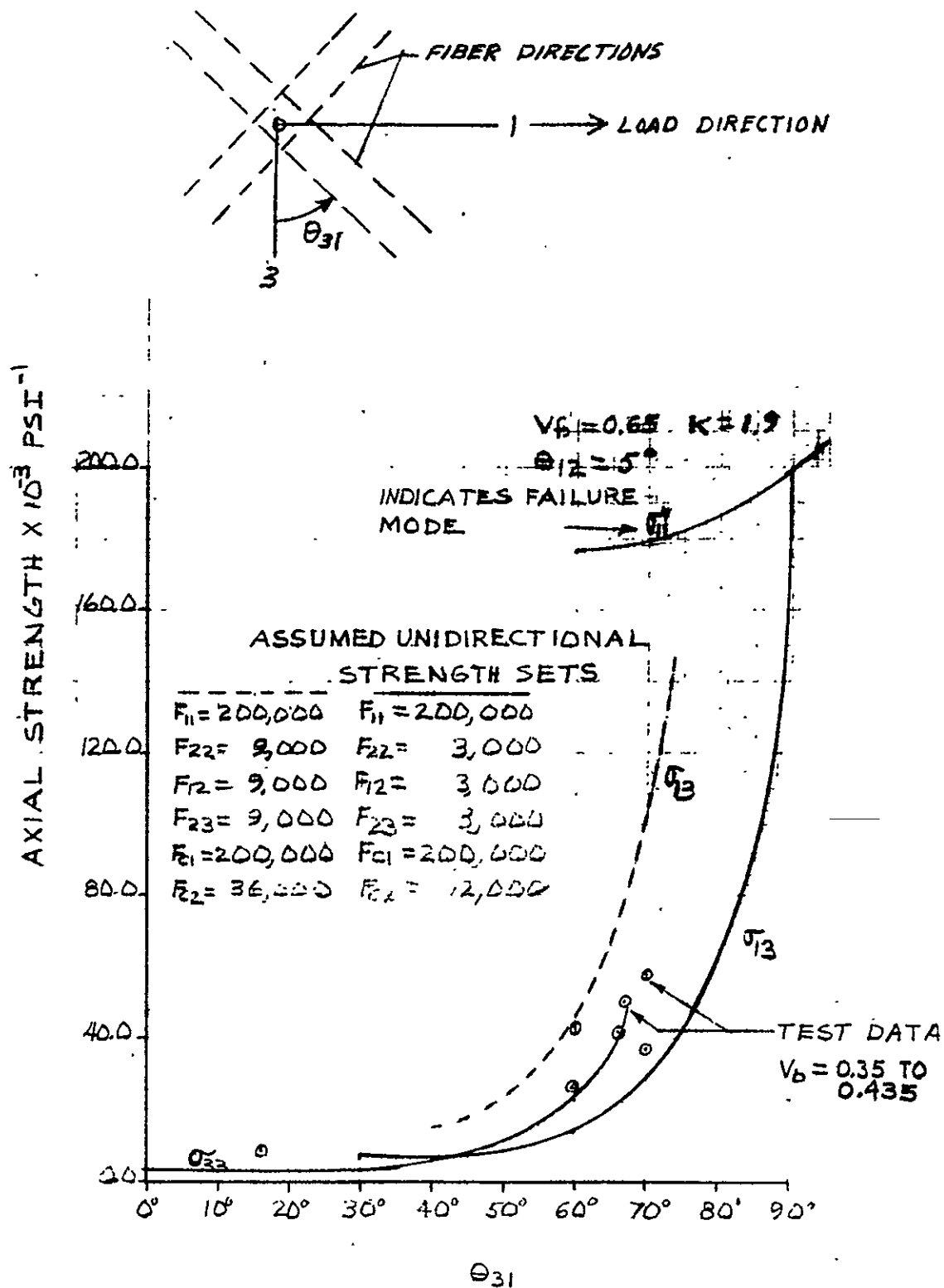


Figure 10-31. Axial Strength for Morganite II Omniweave Composites Using Max. Stress Criteria



$$\begin{aligned}\theta_{12} &= 5^\circ \text{ (LID CONF.)} \\ V_f &= 0.55 \\ K &= 1.9\end{aligned}$$

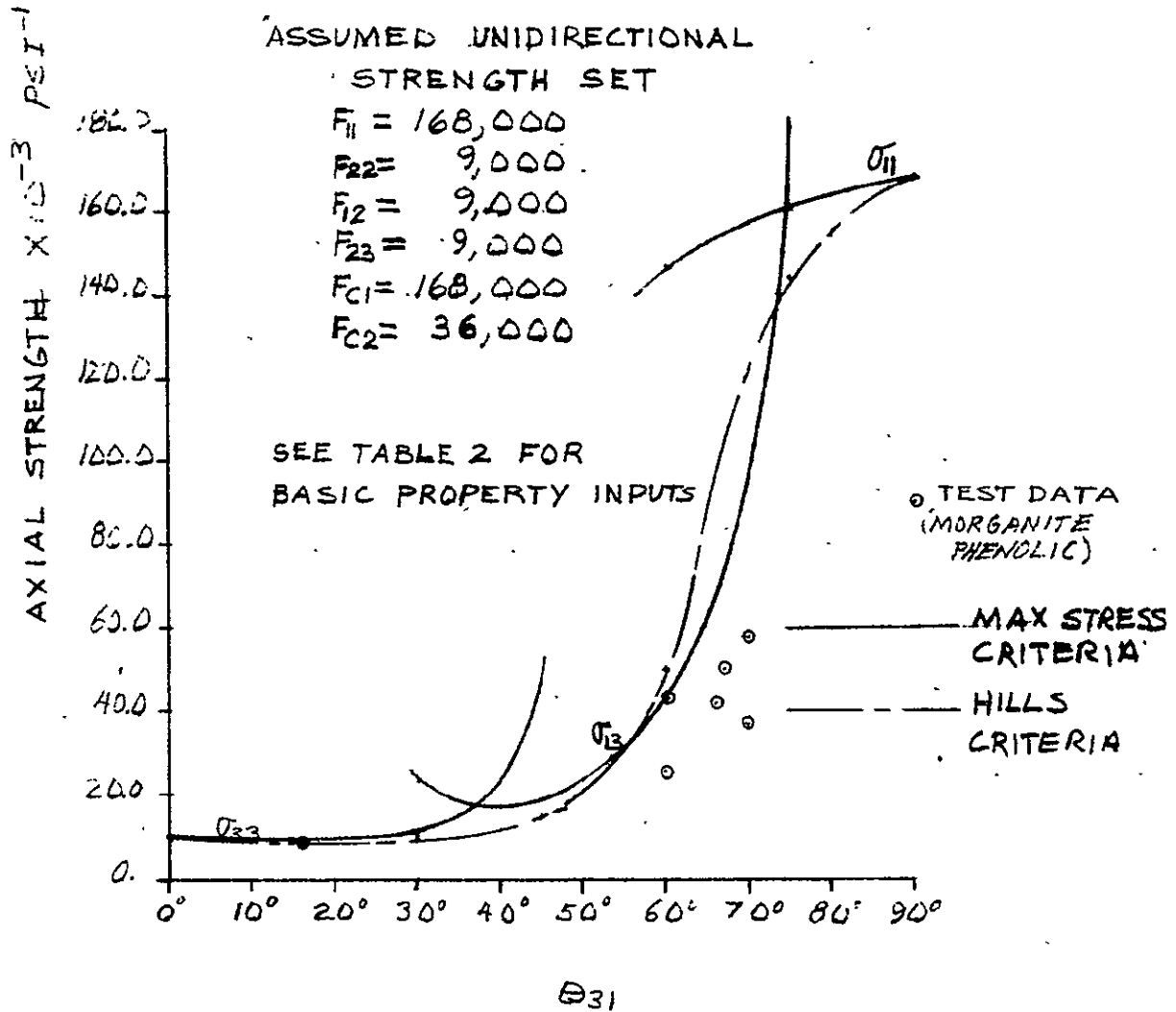


Figure 10-32. Axial Strength of Morganite II Omniweave Composites

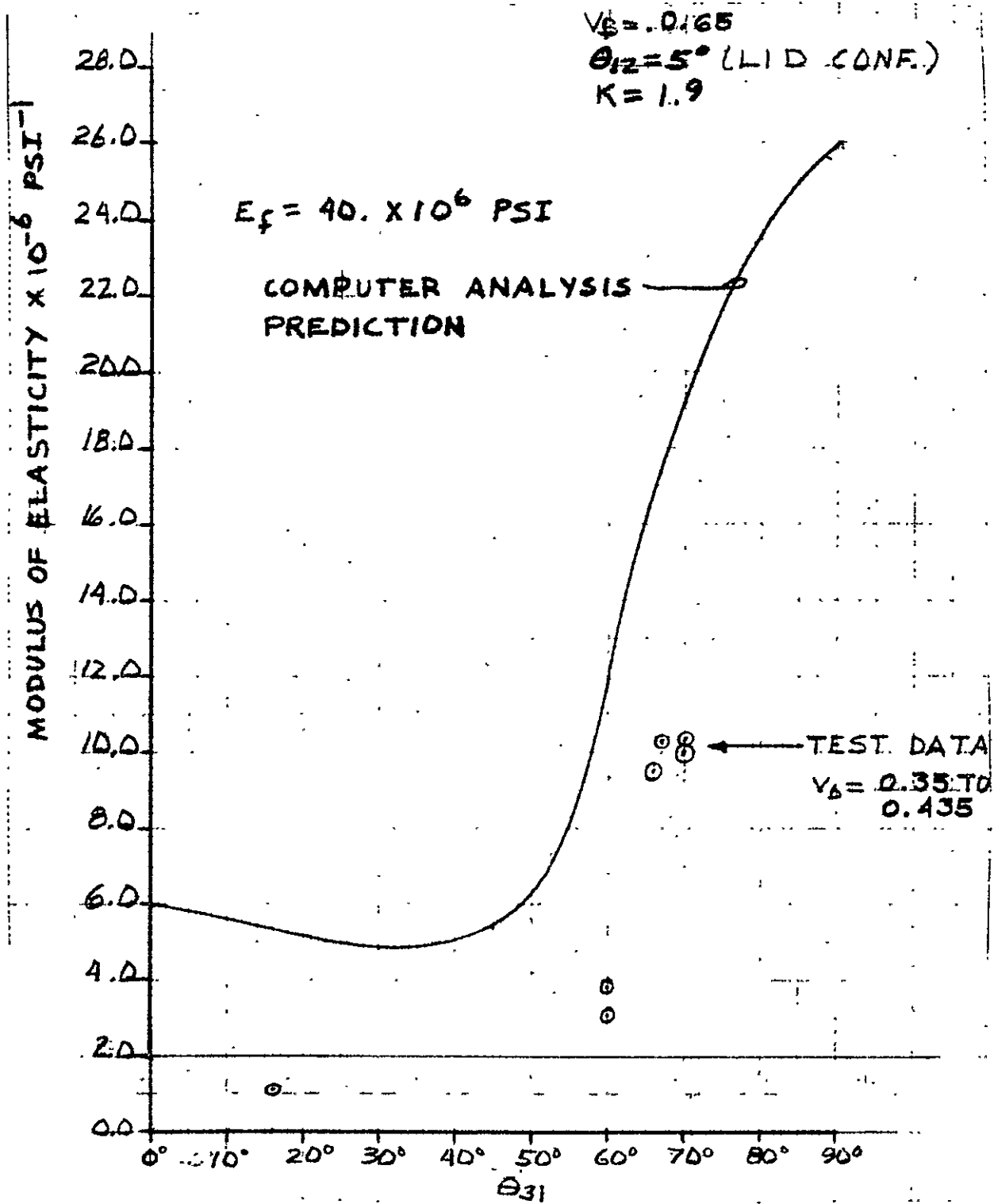


Figure 10-33. Elastic Moduli of Morganite II Omniweave Composites

$\Theta_{12} = 5^\circ$  (LID)  
 $V_f = 0.65$   
 $K = 1.9$  ← TEST DATA

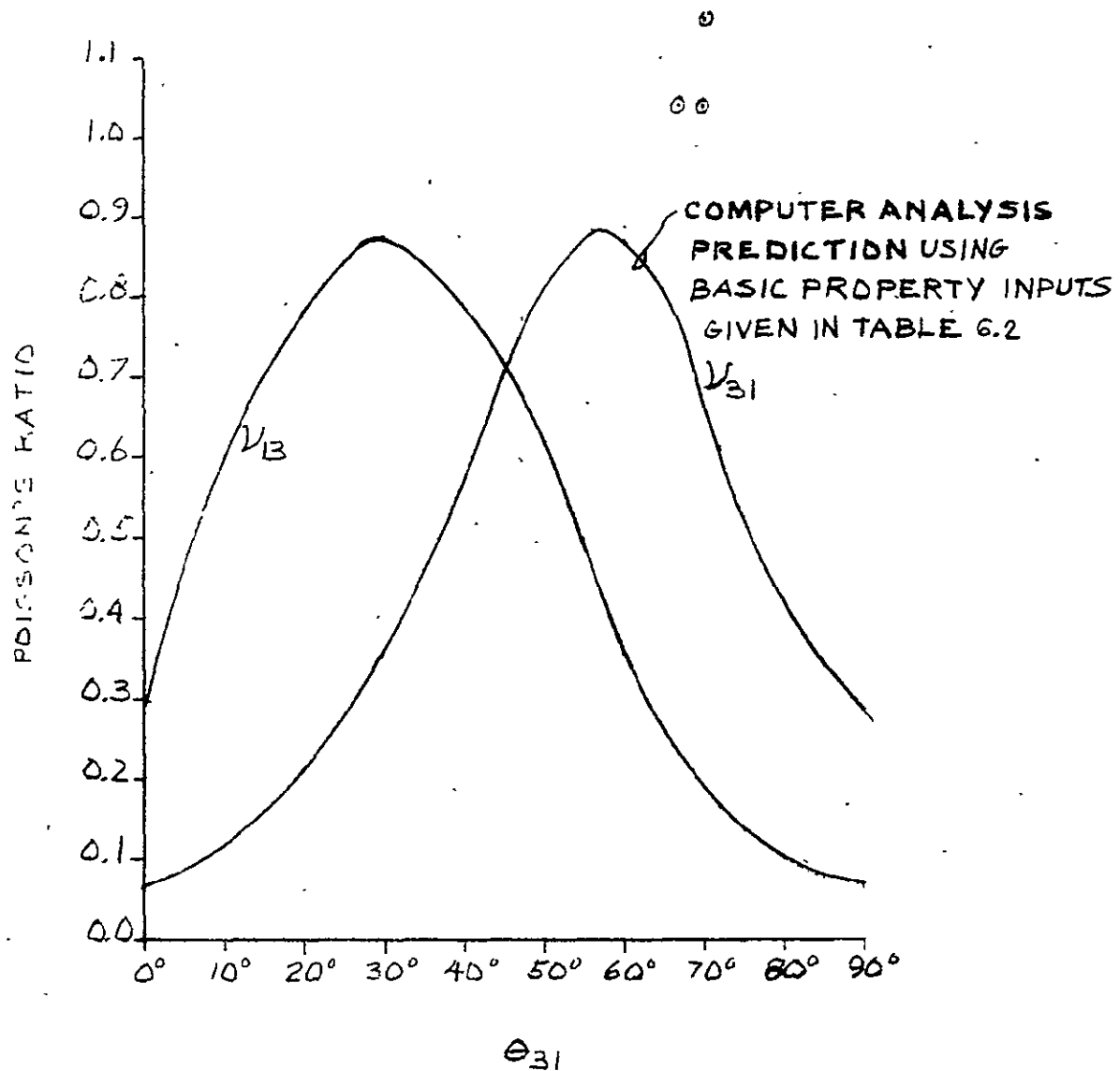


Figure 10-34. Poisson's Ratio of Morganite II Omniweave Composites

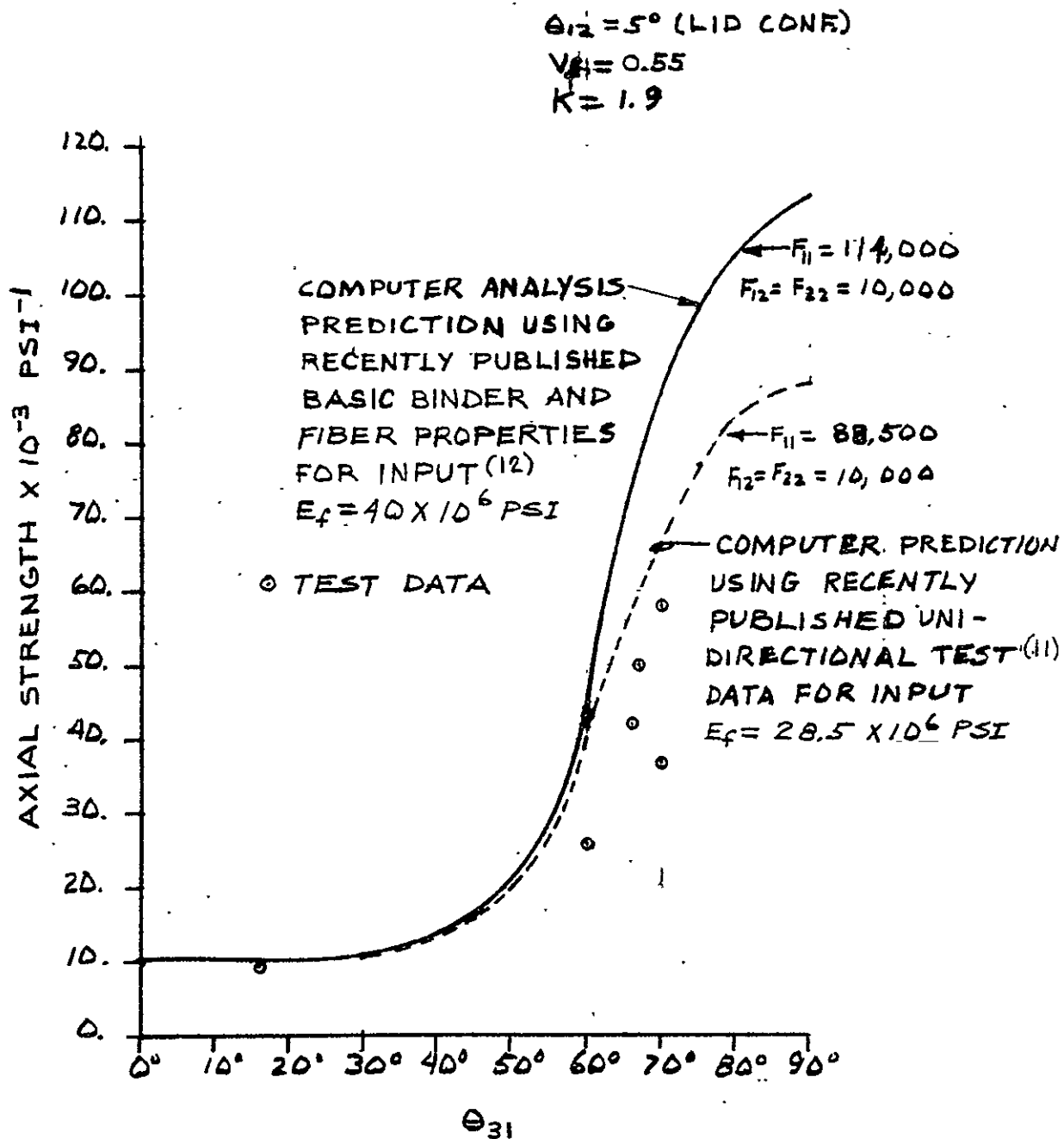


Figure 10-35. Axial Strength of Morganite II Omniweave Composites using Hill's Modified Failure Criteria

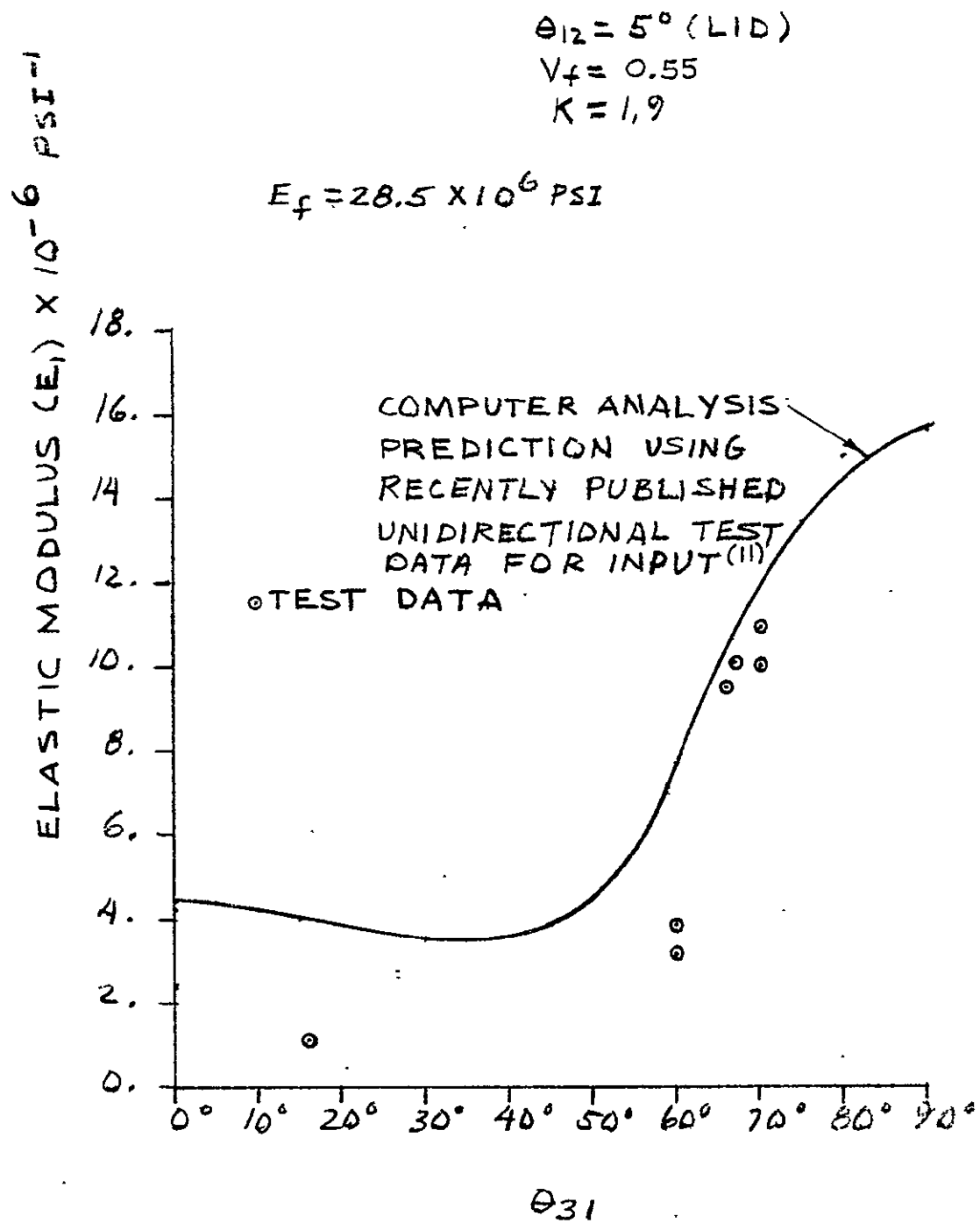


Figure 10-36. Longitudinal Elastic Modulus of Morganite II Omniweave Composites

$$\begin{aligned}\theta_{12} &= 5^\circ \\ V_f &= 0.55 \\ K &= 1.0\end{aligned}$$

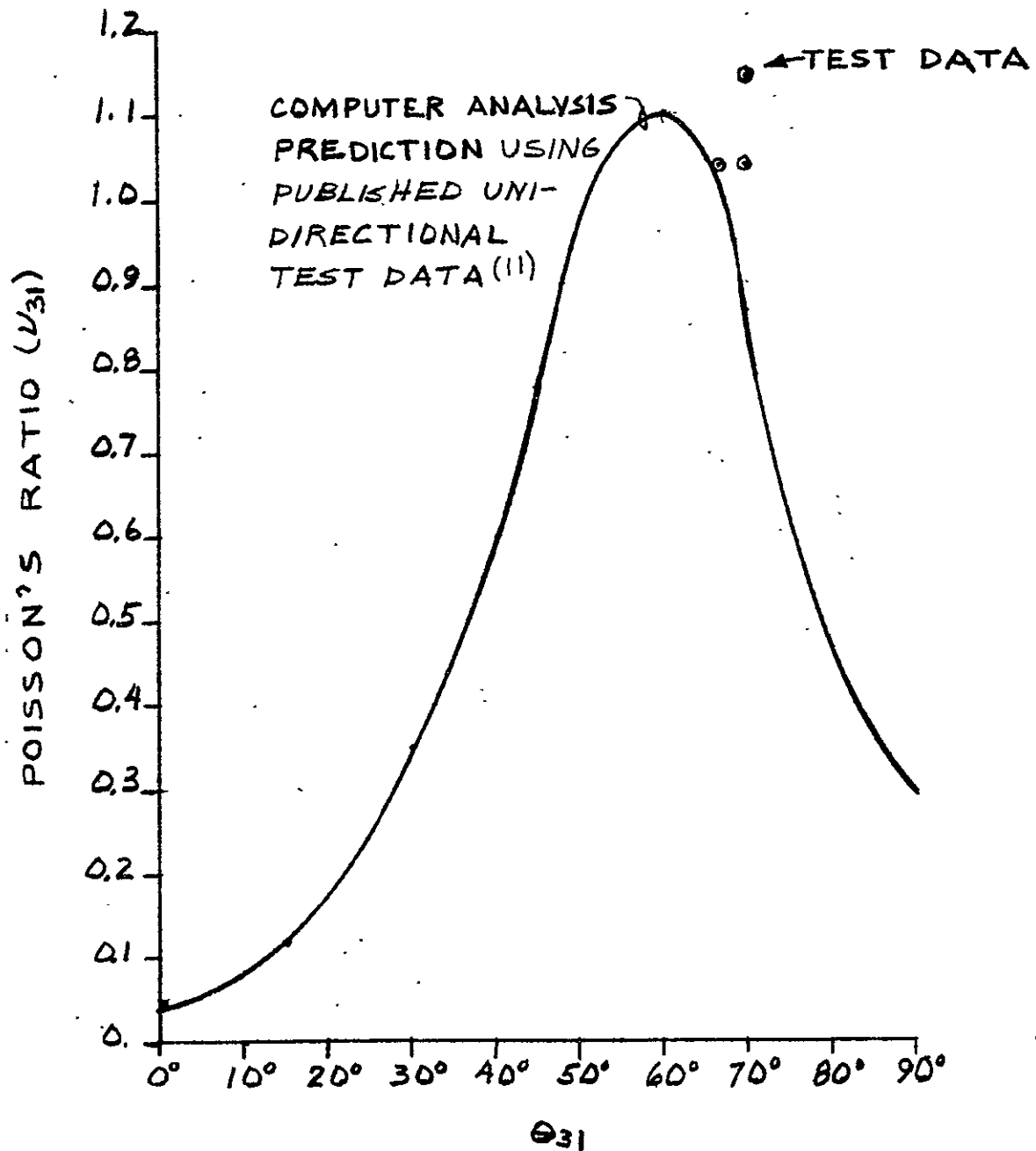


Figure 10-37. Poisson's Ratio of Morganite II Omniweave Composites

$$V_f = 0.55$$

$$\theta_{12} = 5^\circ \text{ (LID)}$$

$$K = 1.9$$

$$F_{11} = 164,000$$

$$F_{22} = 9,000$$

$$F_{12} = 9,000$$

$$F_{23} = 9,000$$

$$F_{c1} = 164,000$$

$$F_{c2} = 36,000$$

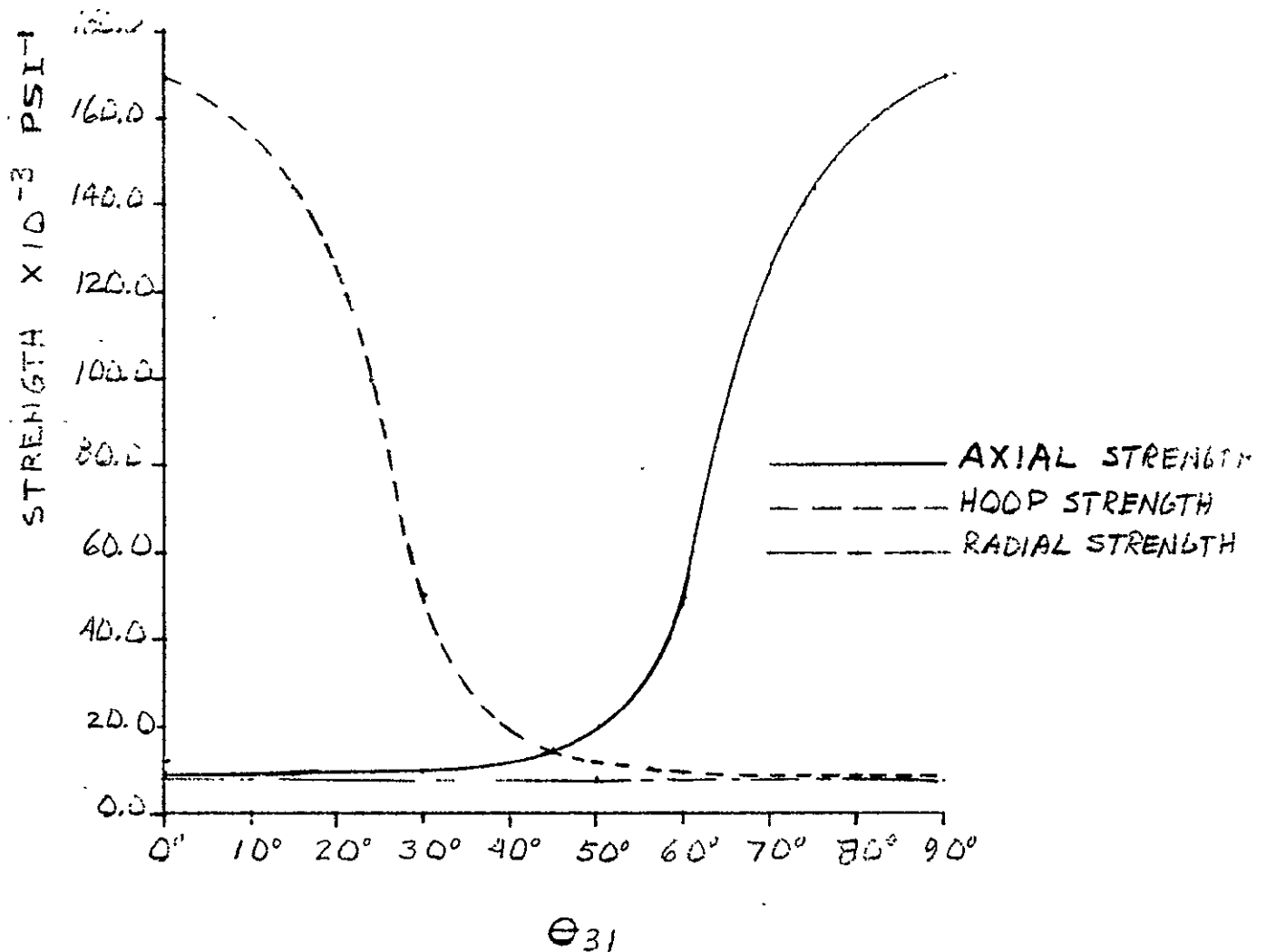


Figure 10-38. Strength Prediction Curves for Morganite II Omniweave Composites using Hills Failure Criteria

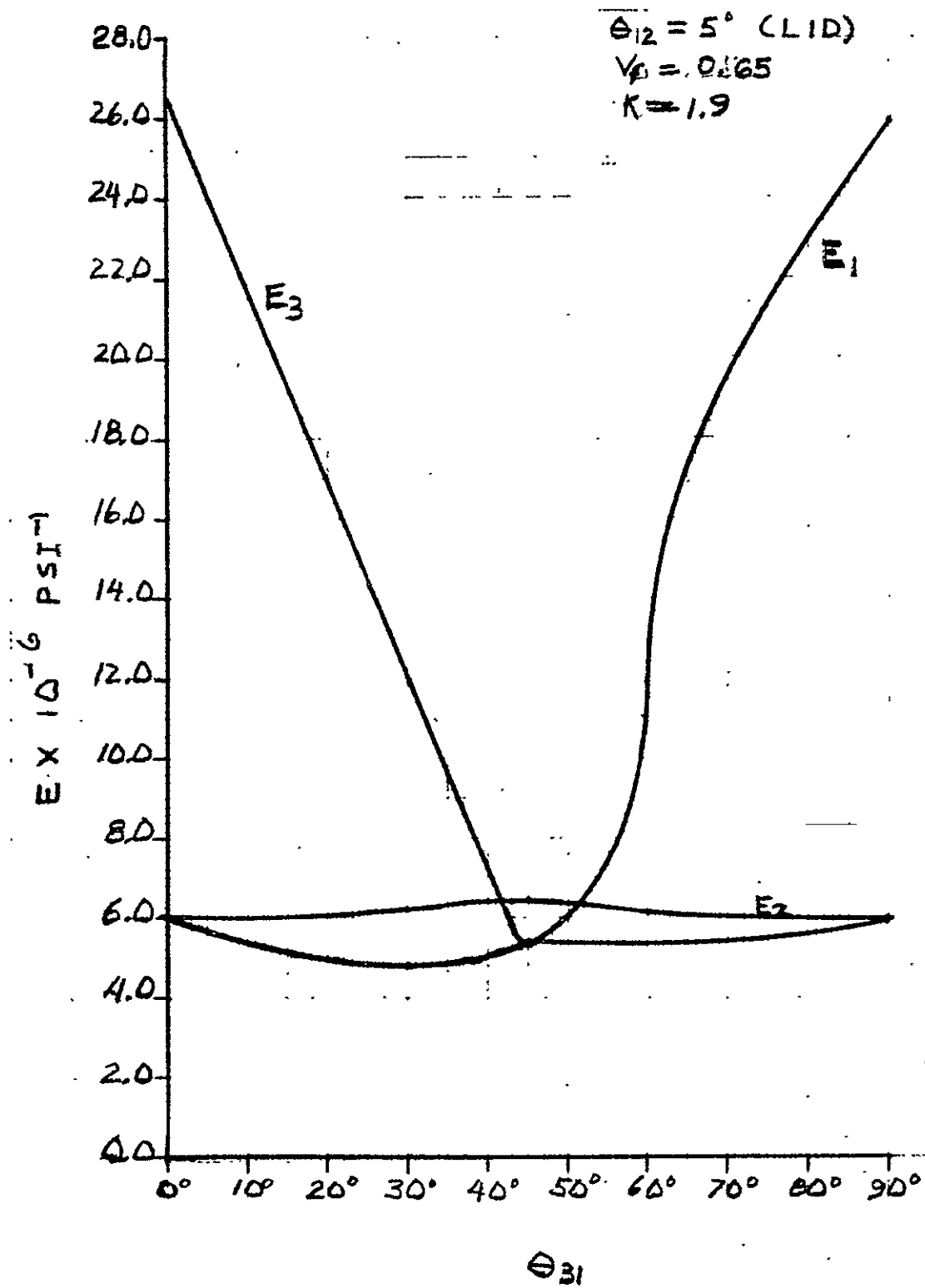


Figure 10-39. Elastic Module Prediction Curves for Morganite II Omniweave Composites



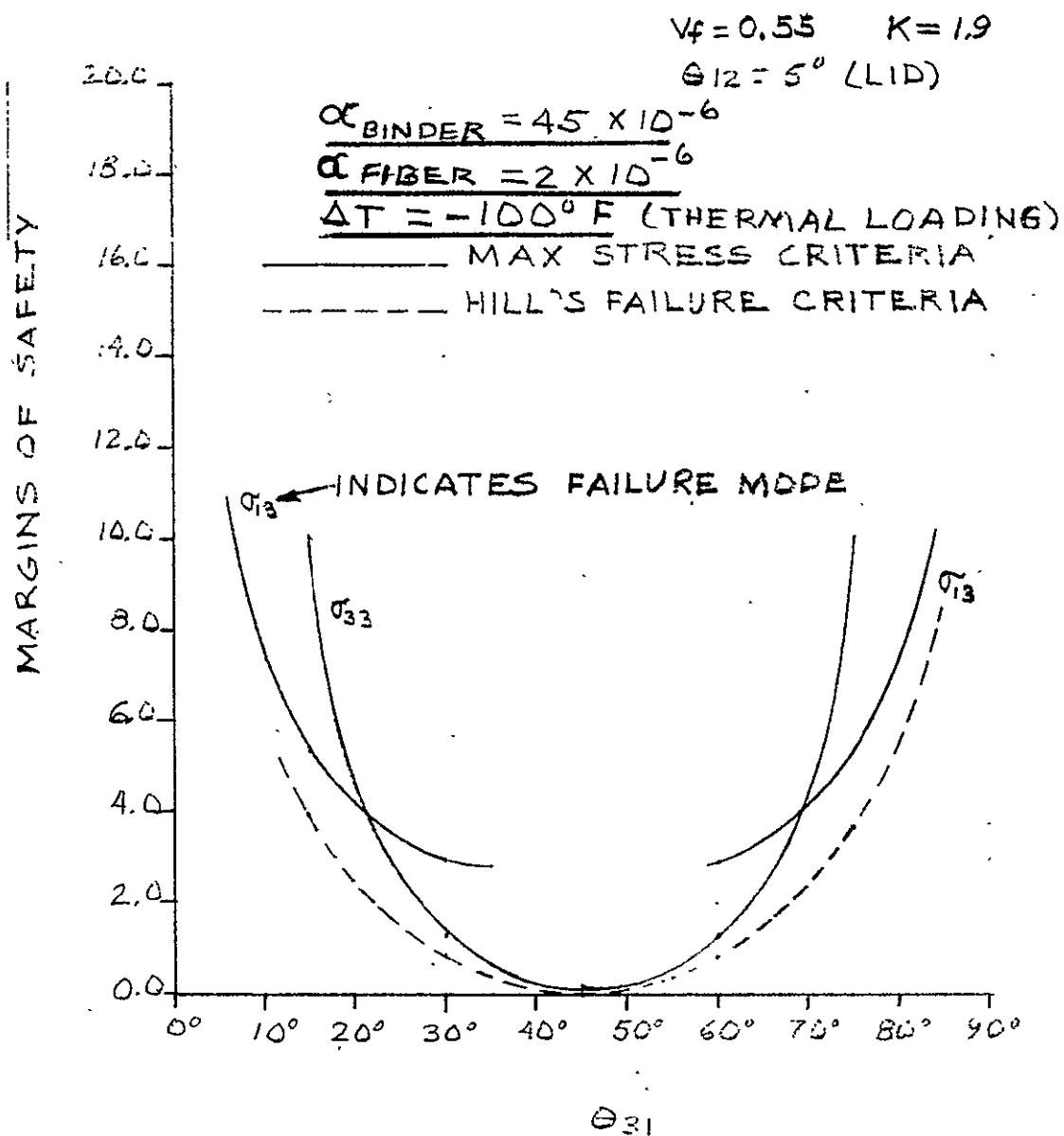


Figure 10-40. Margins of Safety (Thermal Loading Only) for Morganite II Omniweave Composites

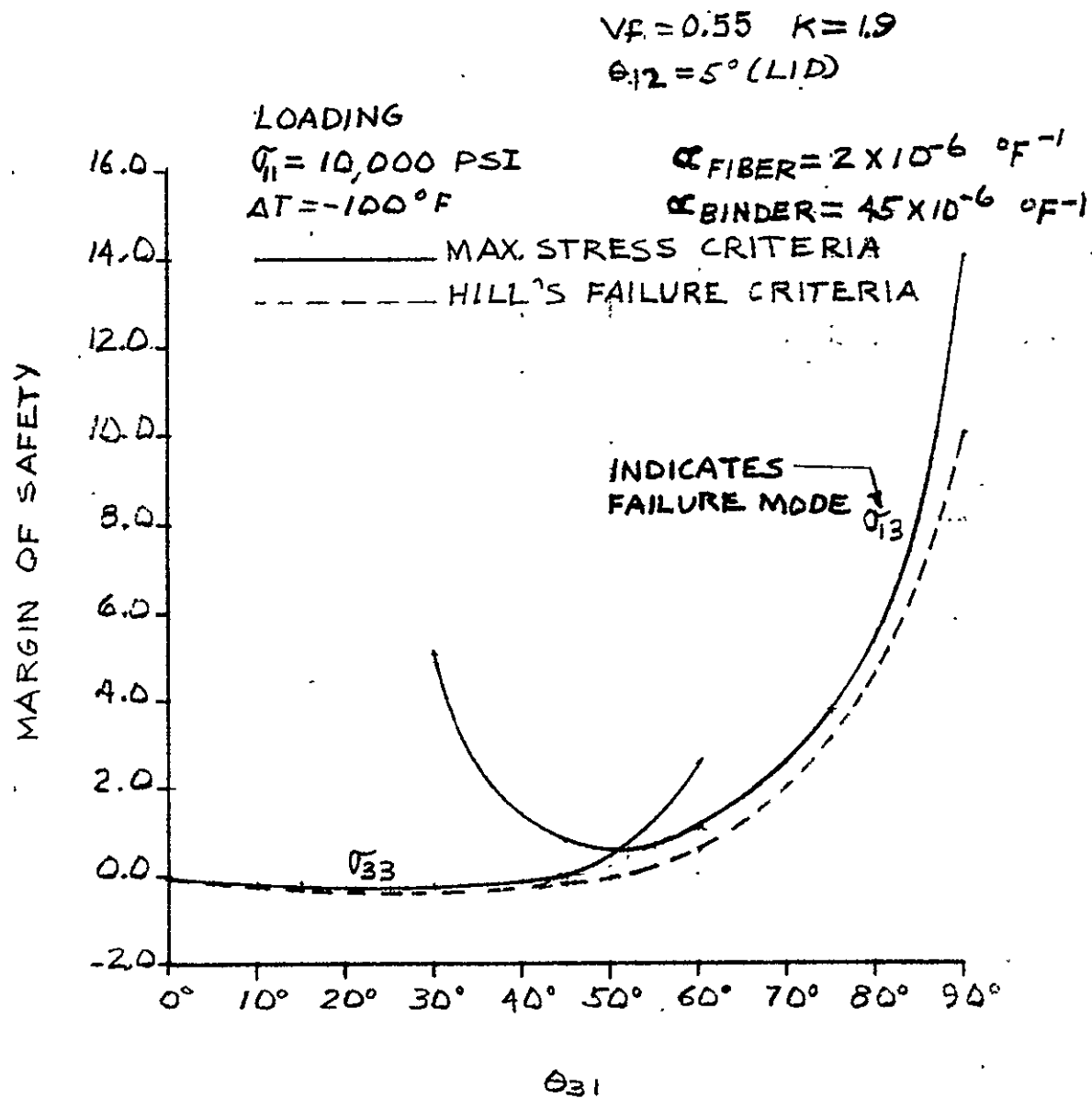


Figure 10-41. Margins of Safety (Thermal Plus Mechanical Loading for Morganite II Omniweave Composites

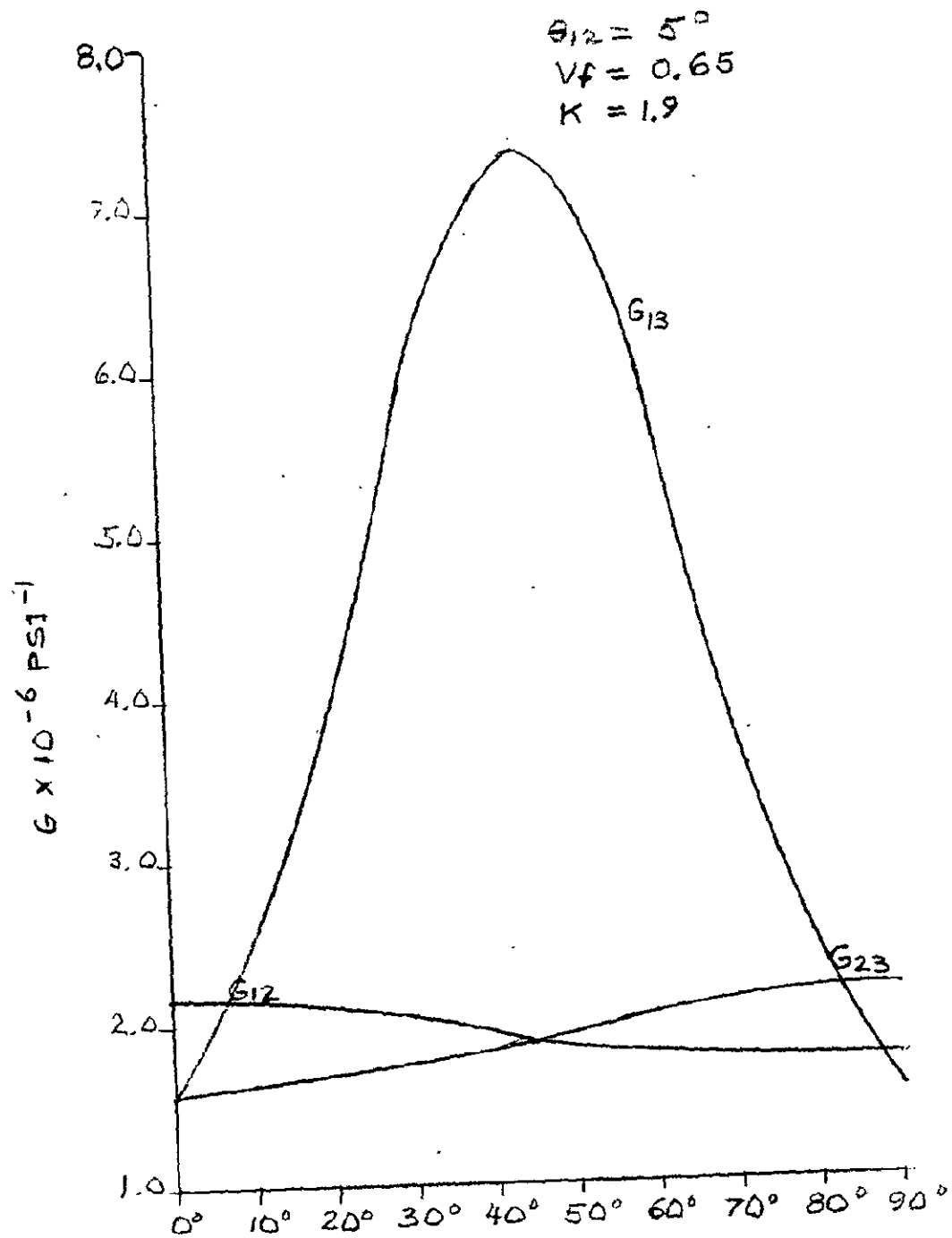


Figure 10-42. Shear Moduli of Morganite II Omniweave Composites

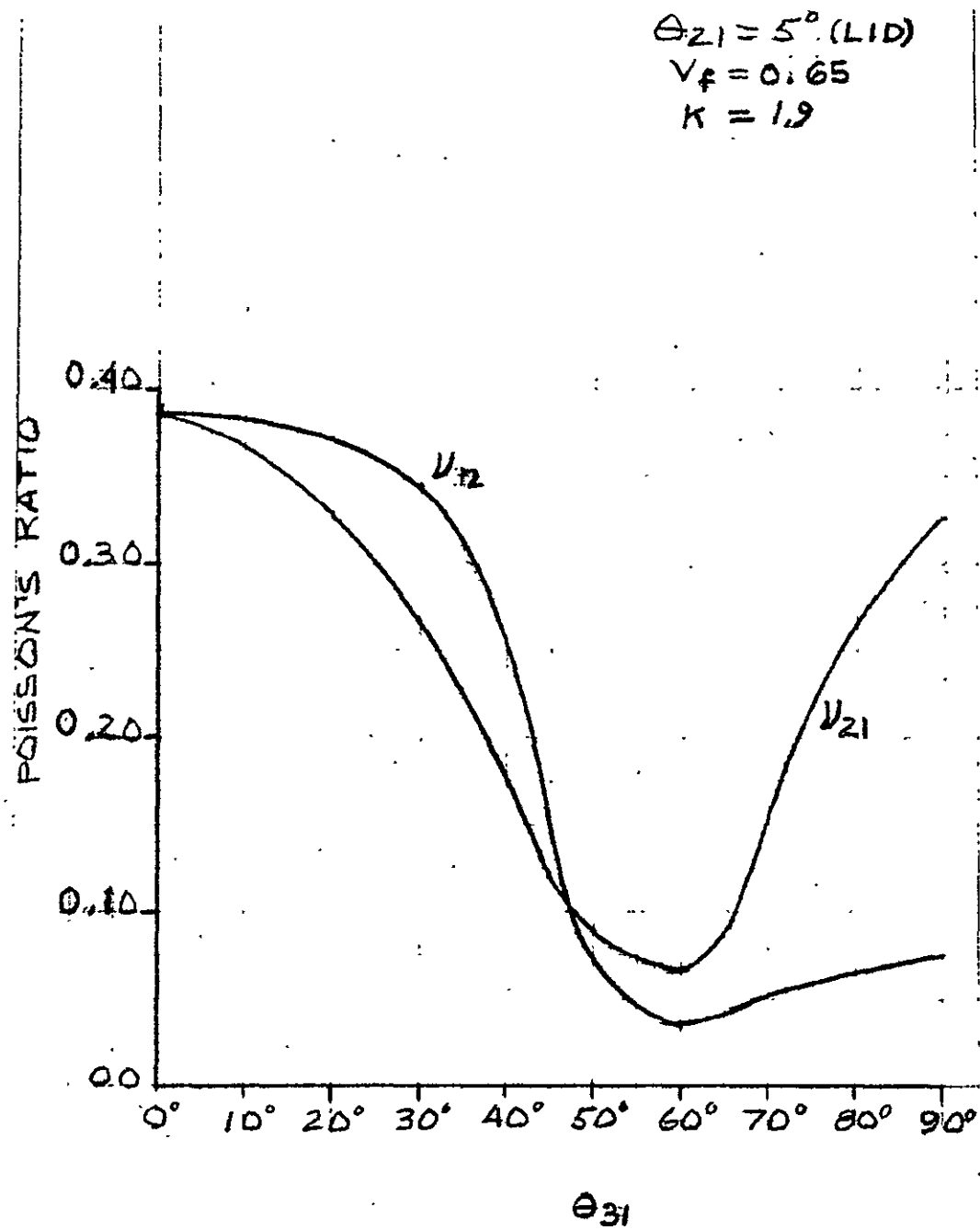


Figure 10-43. Poisson's Ratio for  
Morganite II Omniweave Composites

$\theta_{12} = 5^\circ$   
 $V_f = 0.65 \quad K = 1.9$   
 INPUTS INTO COMPUTER PROGRAM  
 $\alpha_b = 45 \times 10^{-6}$   
 $\alpha_f = 2 \times 10^{-6}$

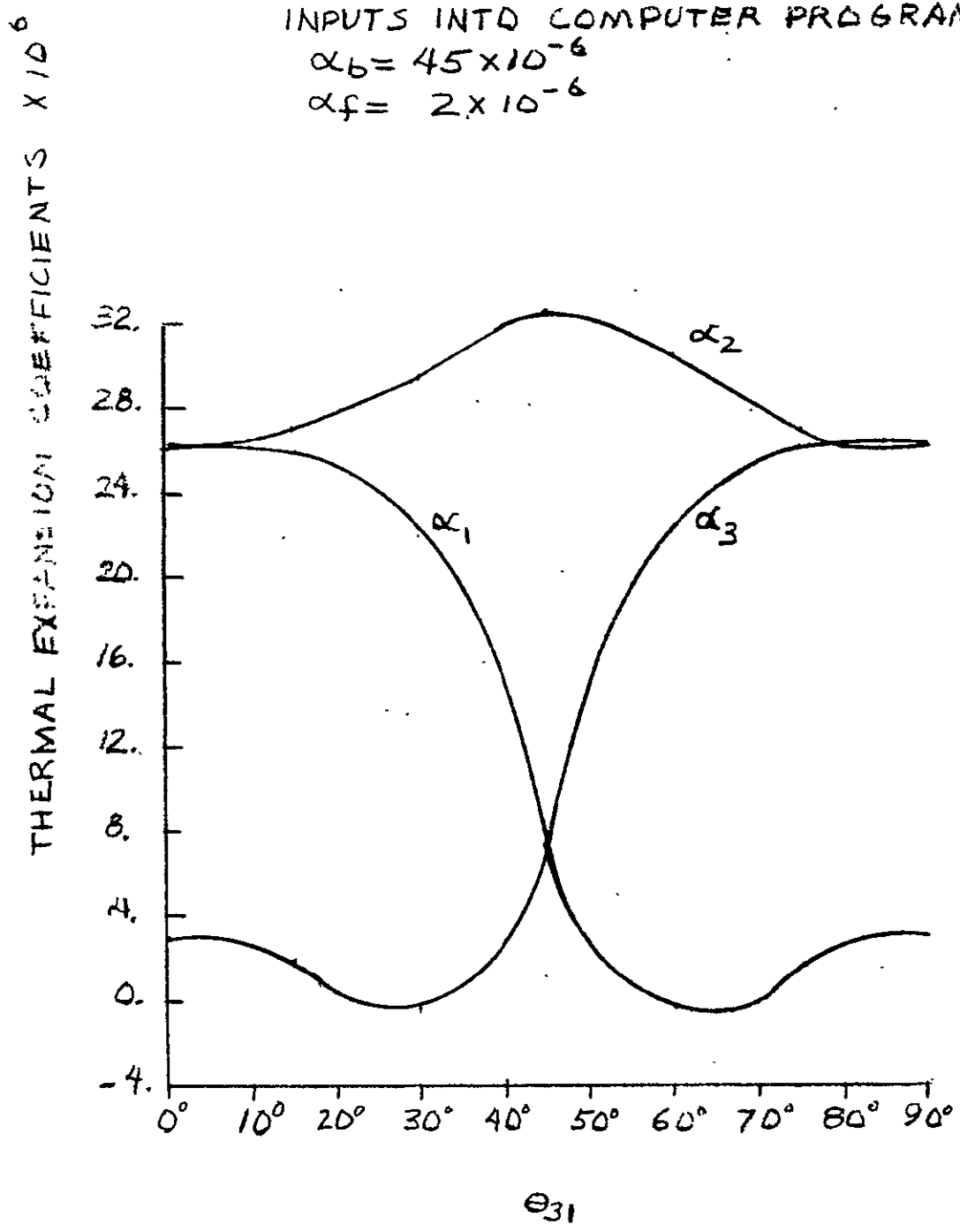


Figure 10-44. Coefficients of Thermal Expansion for Morganite II Omniweave Composites

$$\theta_{12} = 5^\circ$$

$$V_b = 0.45$$

$$K = 1.9$$

ASSUMED UNIDIRECTIONAL  
STRENGTH SET

$$F_{11} = 169,200$$

$$F_{22} = 9,000$$

$$F_{12} = 9,000$$

$$F_{21} = 9,000$$

$$F_{c1} = 169,200$$

$$F_{c2} = 36,000$$

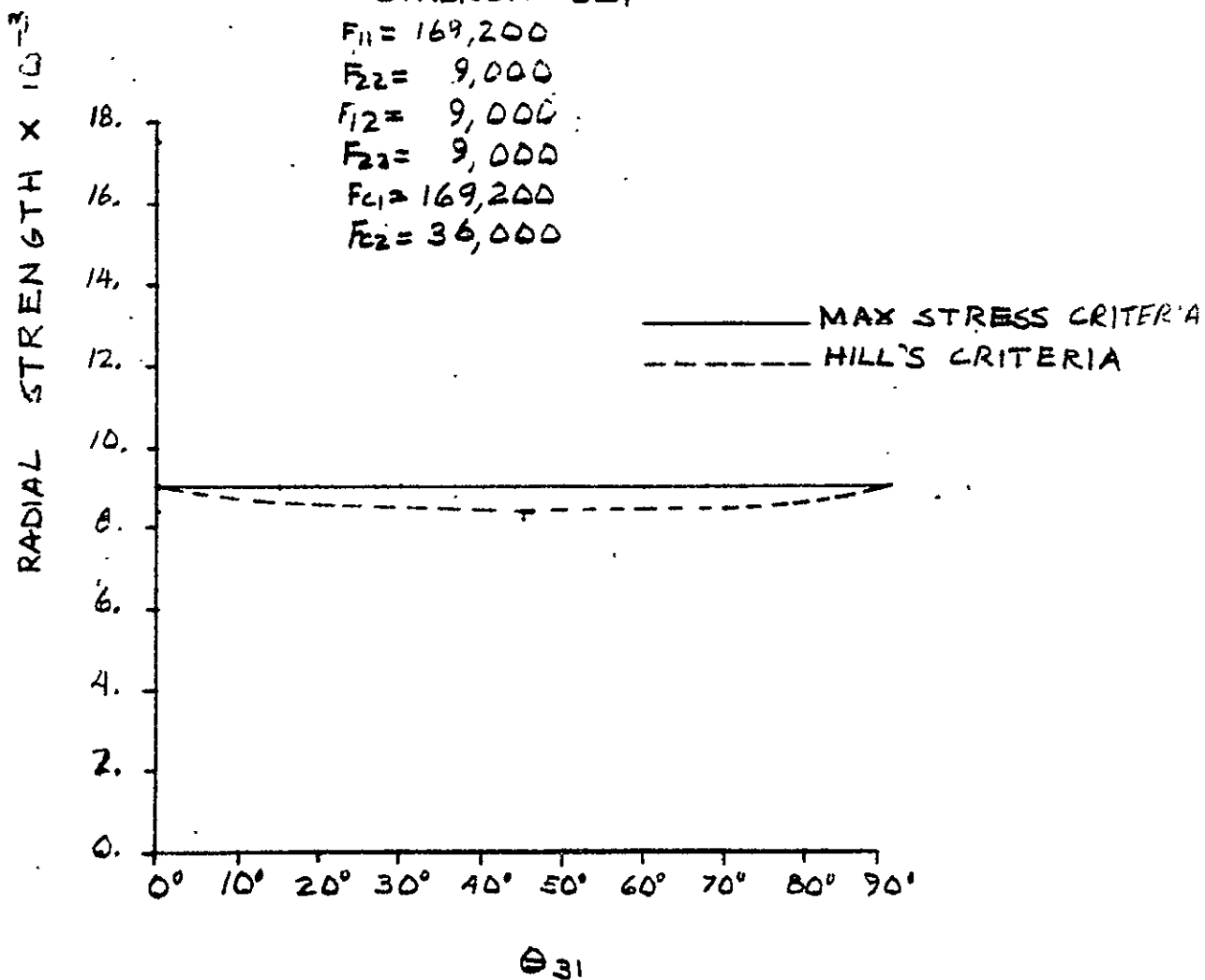


Figure 10-45. Radial Strength of  
Morganite II Omniweave Composites

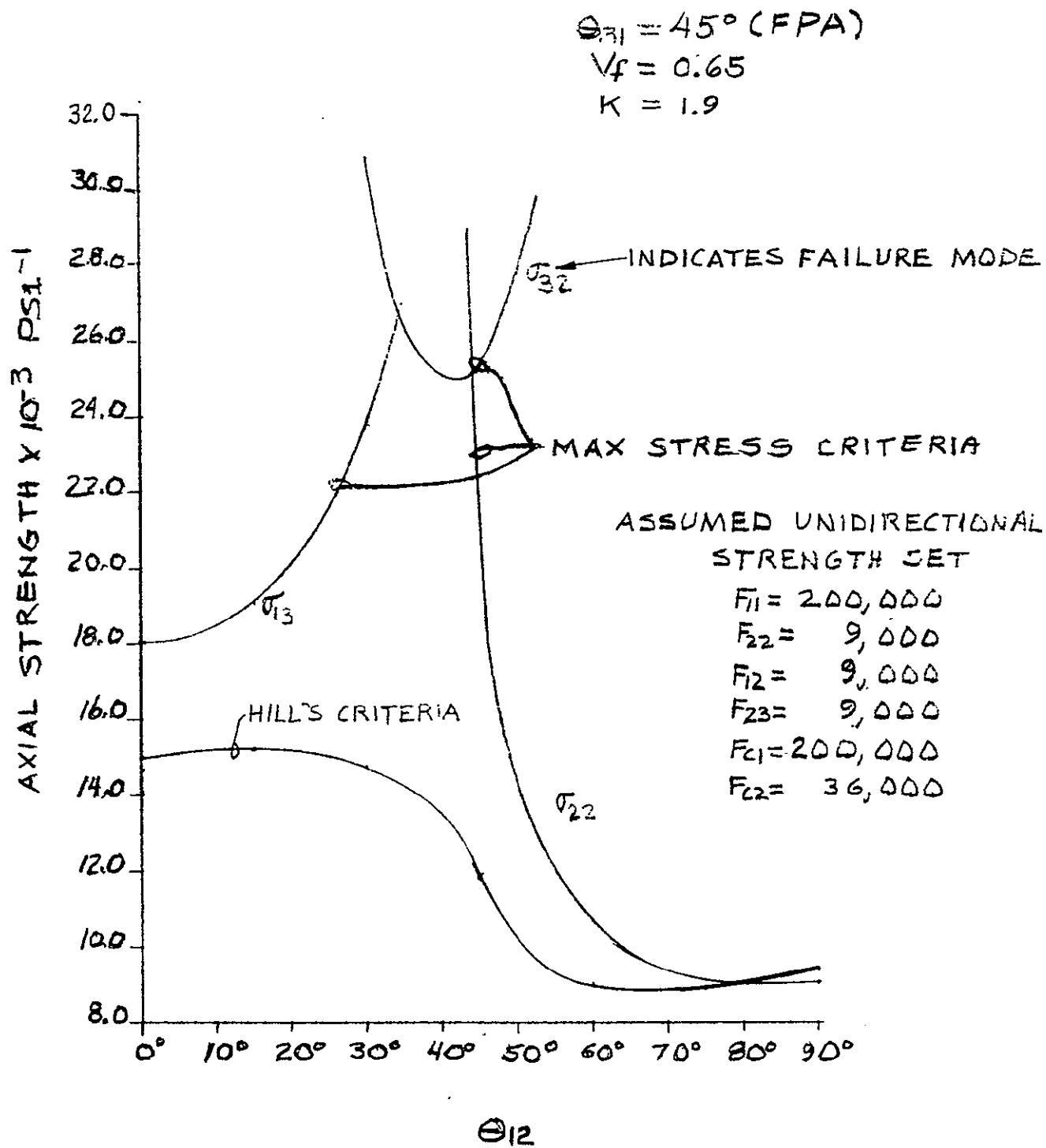


Figure 10-46. Axial Strength Predictions for Morganite II Omniweave Composites

$V_f = 0.65$   
 $\theta_{31} = 45^\circ \text{ (FPA)}$   
 $K = 1.9$

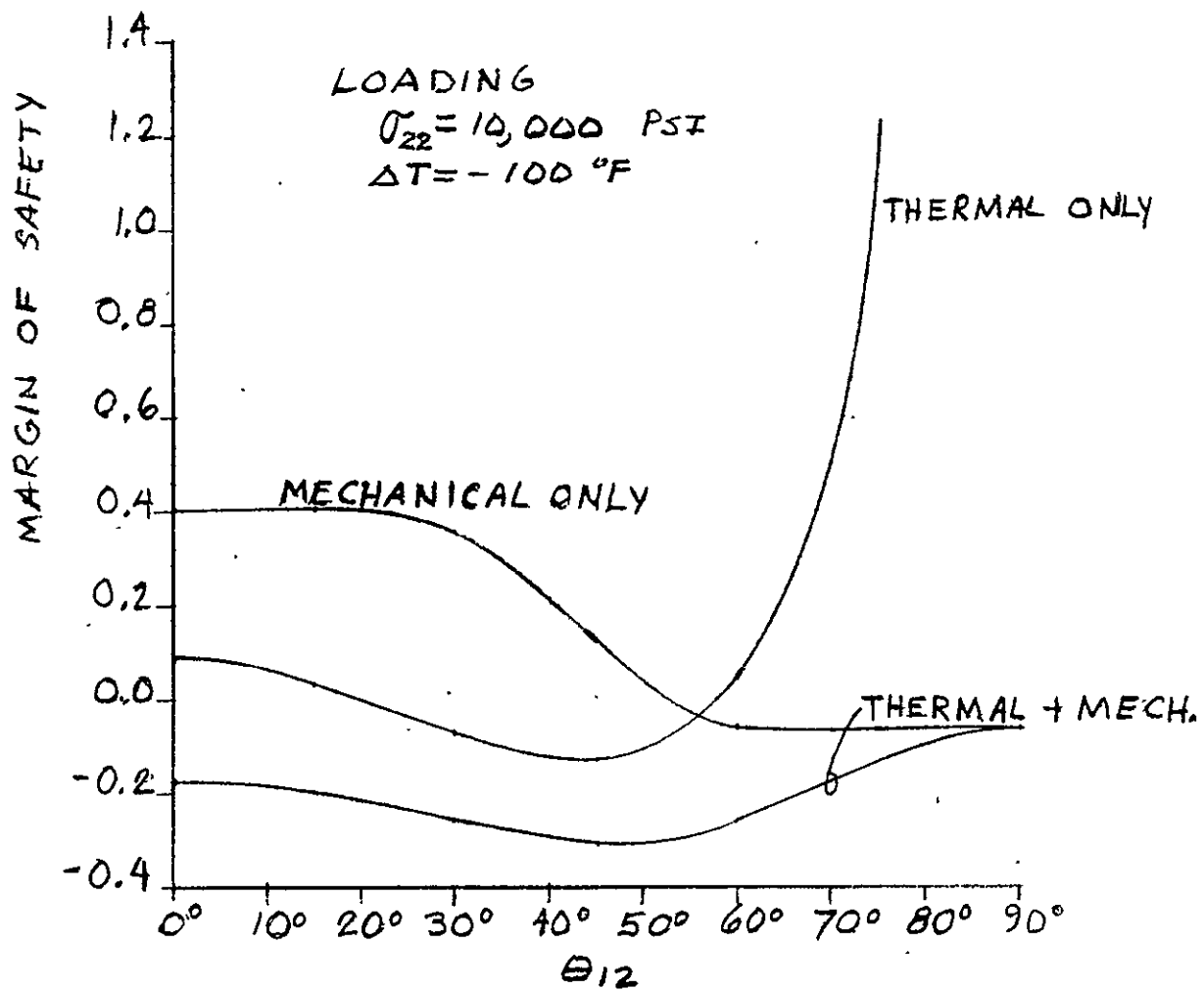


Figure 10-47. Hill's Margins of Safety for  
 Morganite II Omniweave Composites



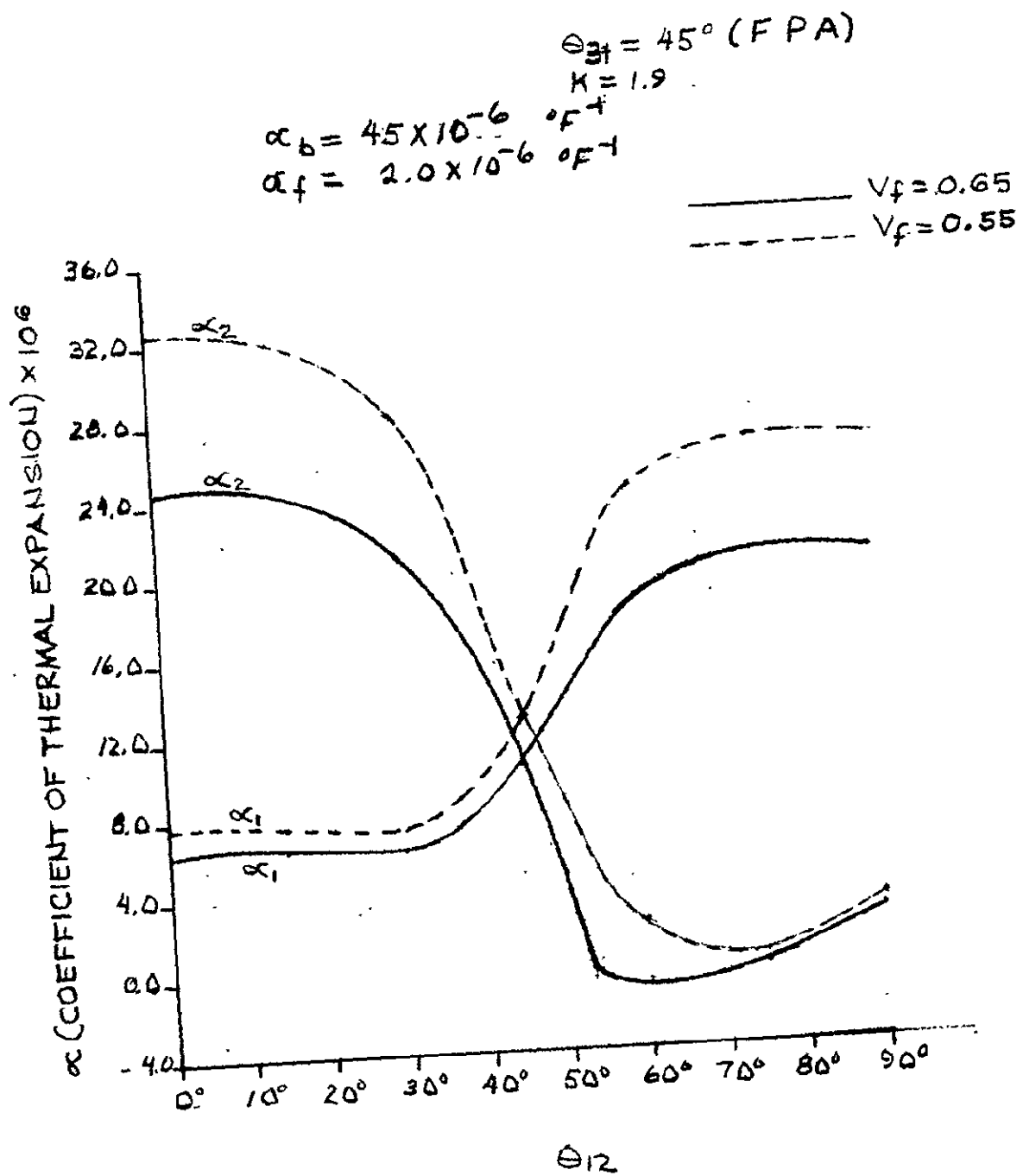


Figure 10-48. Coefficients of Thermal Expansion for Morganite II Omniweave Composites

$$\theta_{31} = 45^\circ$$

$$K = 1.9$$

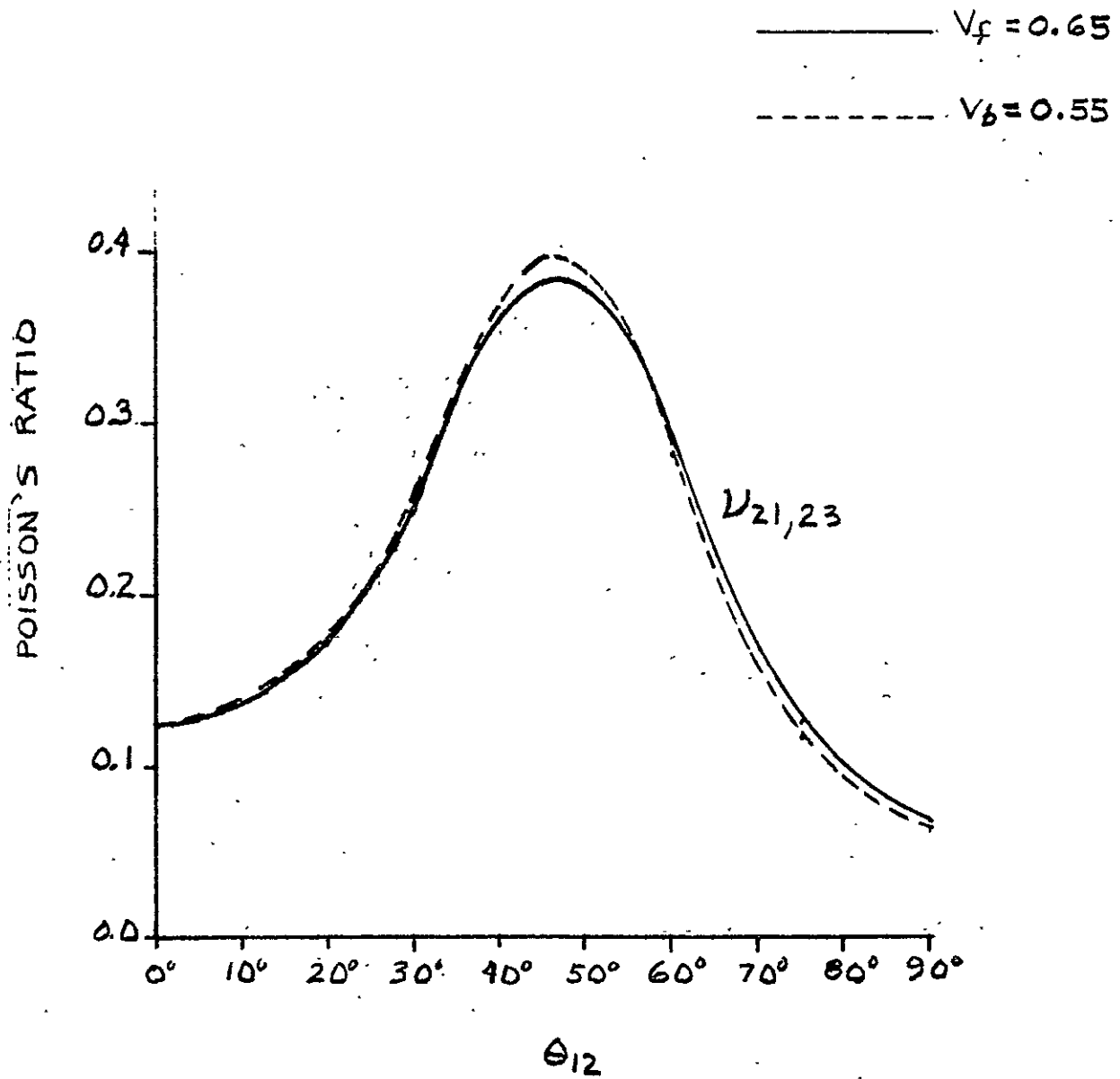


Figure 10-49. Poisson's Ratio of Morganite II Omniweave Composites

$$\theta_{31} = 45^\circ$$

$$K = 1.9$$

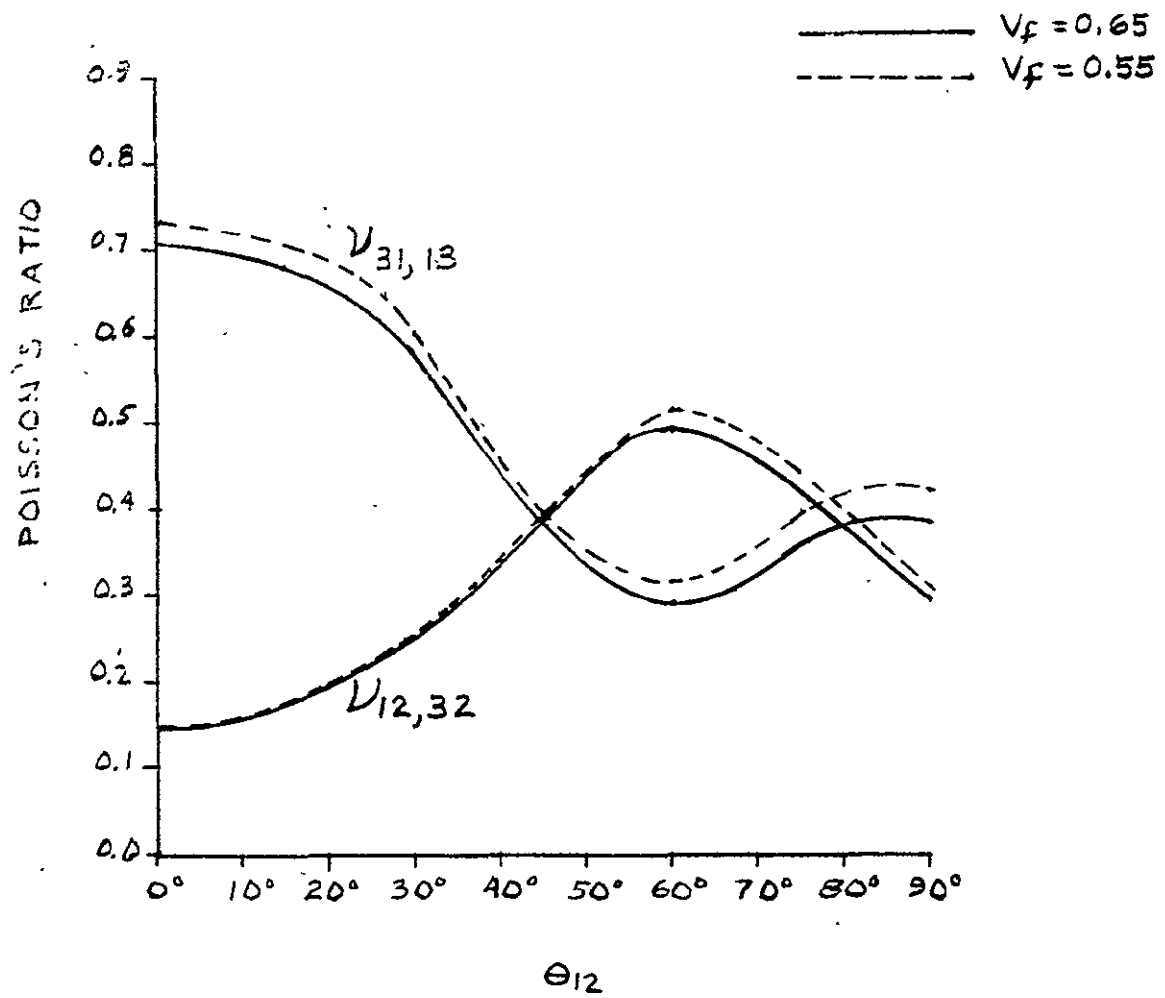


Figure 10-50. Poisson's Ratio of Morganite II Omniweave Composites

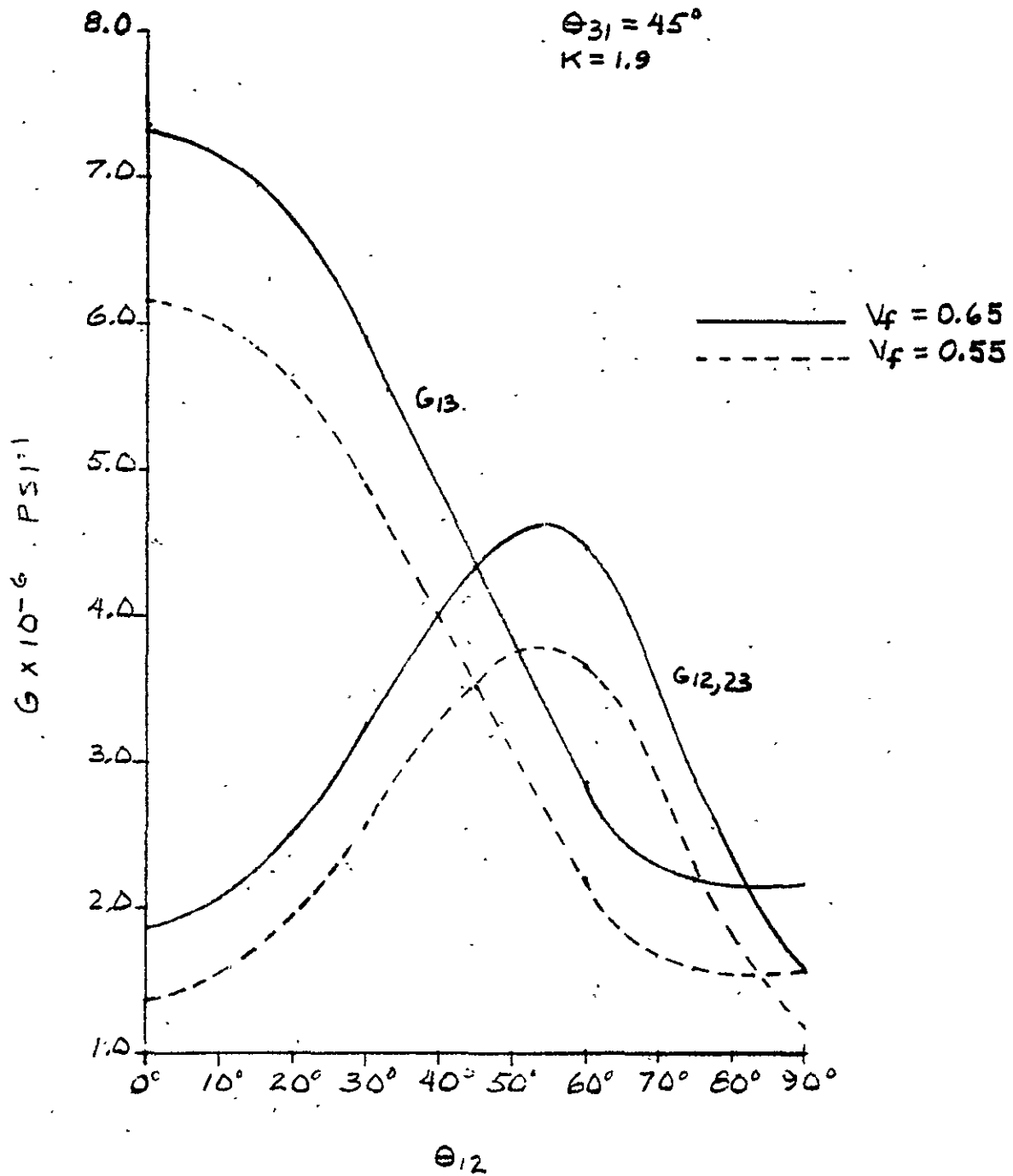


Figure 10-51. Shear Moduli Curves for Morganite II Omniweave Composites

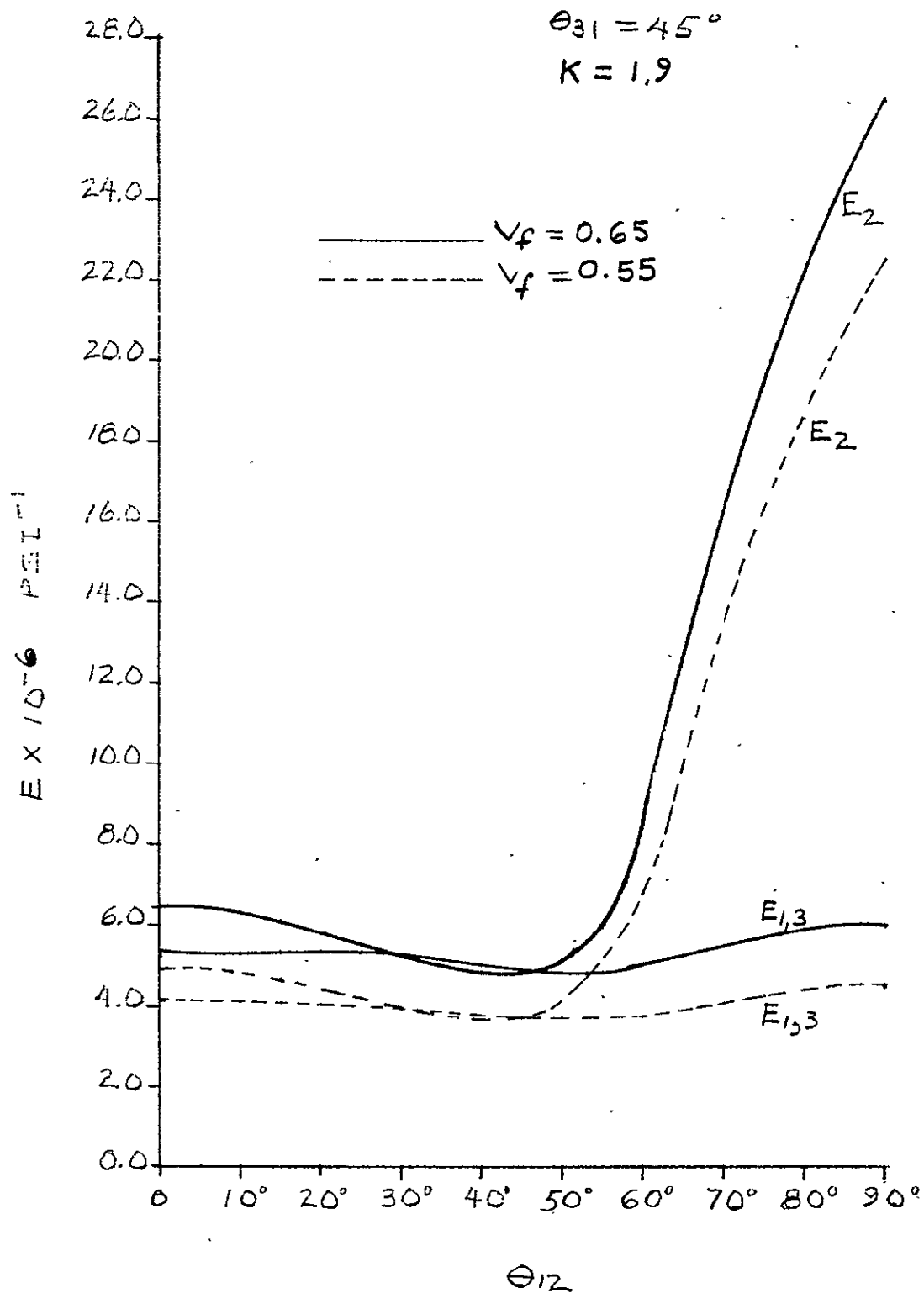


Figure 10-52. Elastic Moduli Curves for Morganite II Omniweave Composites

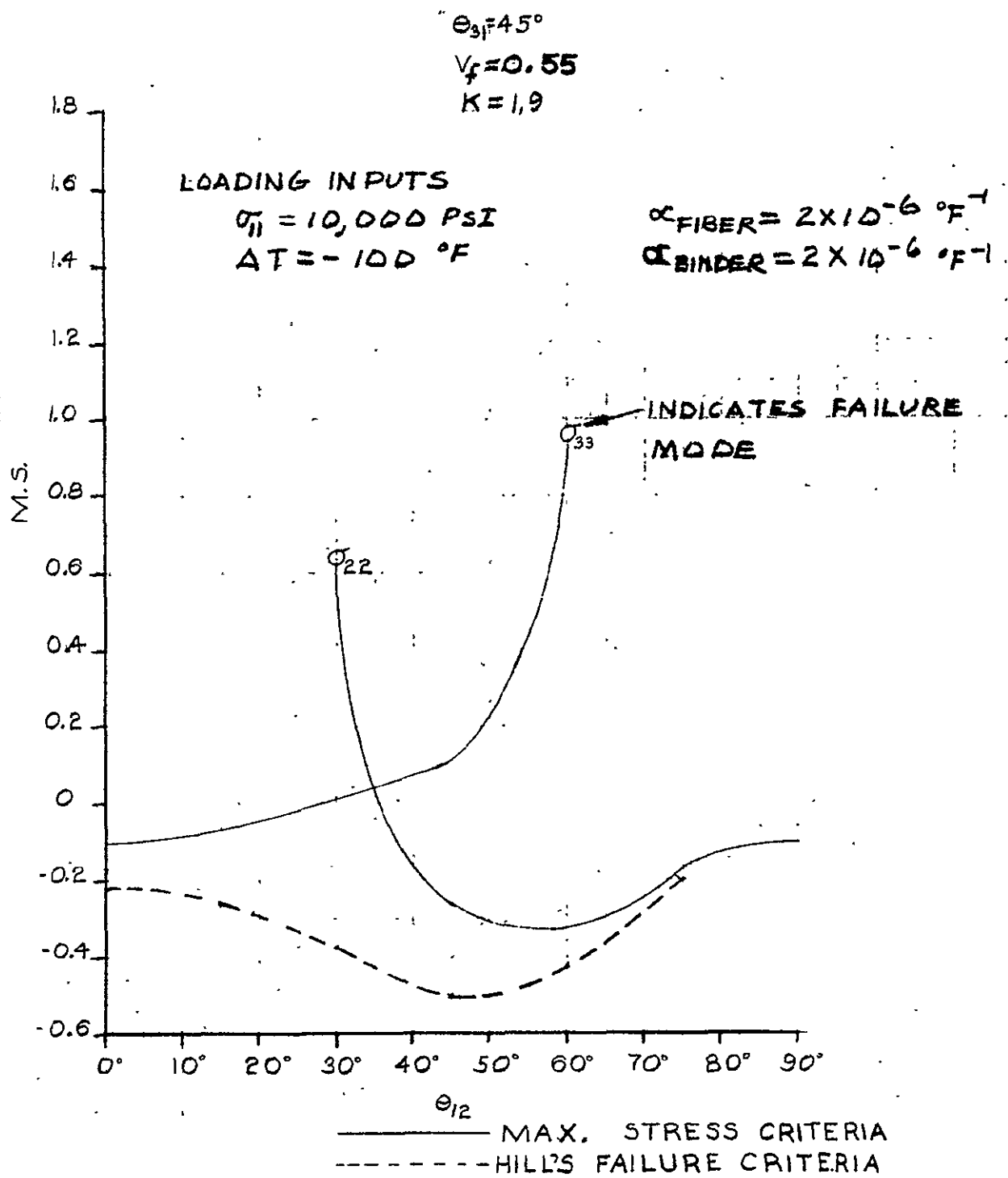


Figure 10-53. Margins of Safety (Thermal Plus Mechanical Loading) for Morganite II Omniweave Composites

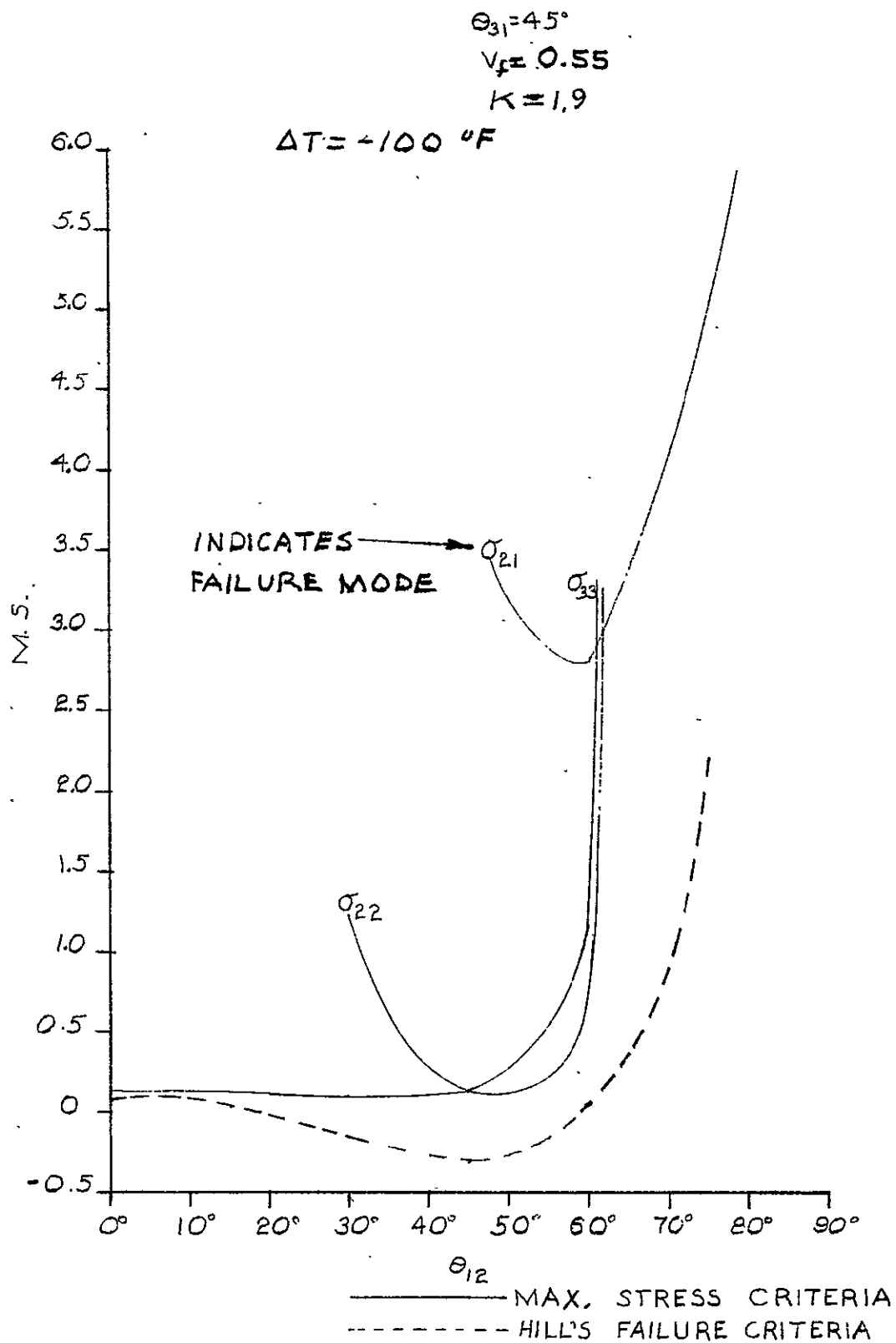


Figure 10-54. Margins of Safety (Thermal Load Only) for  
Morganite II Omniweave Composites

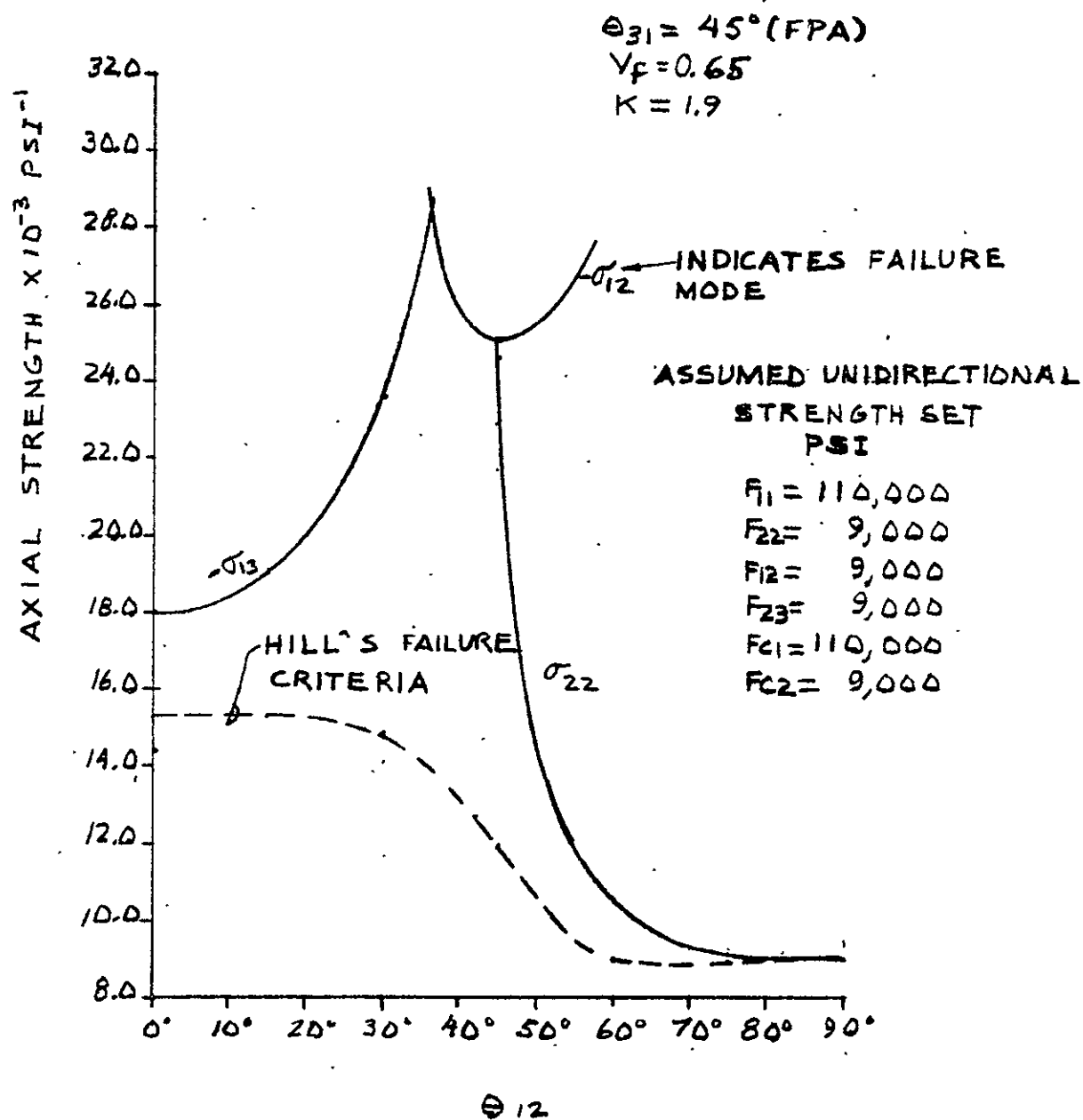


Figure 10-55. Axial Strength Curves for Thornel 50 Omniweave Composites using Max Stress Criteria



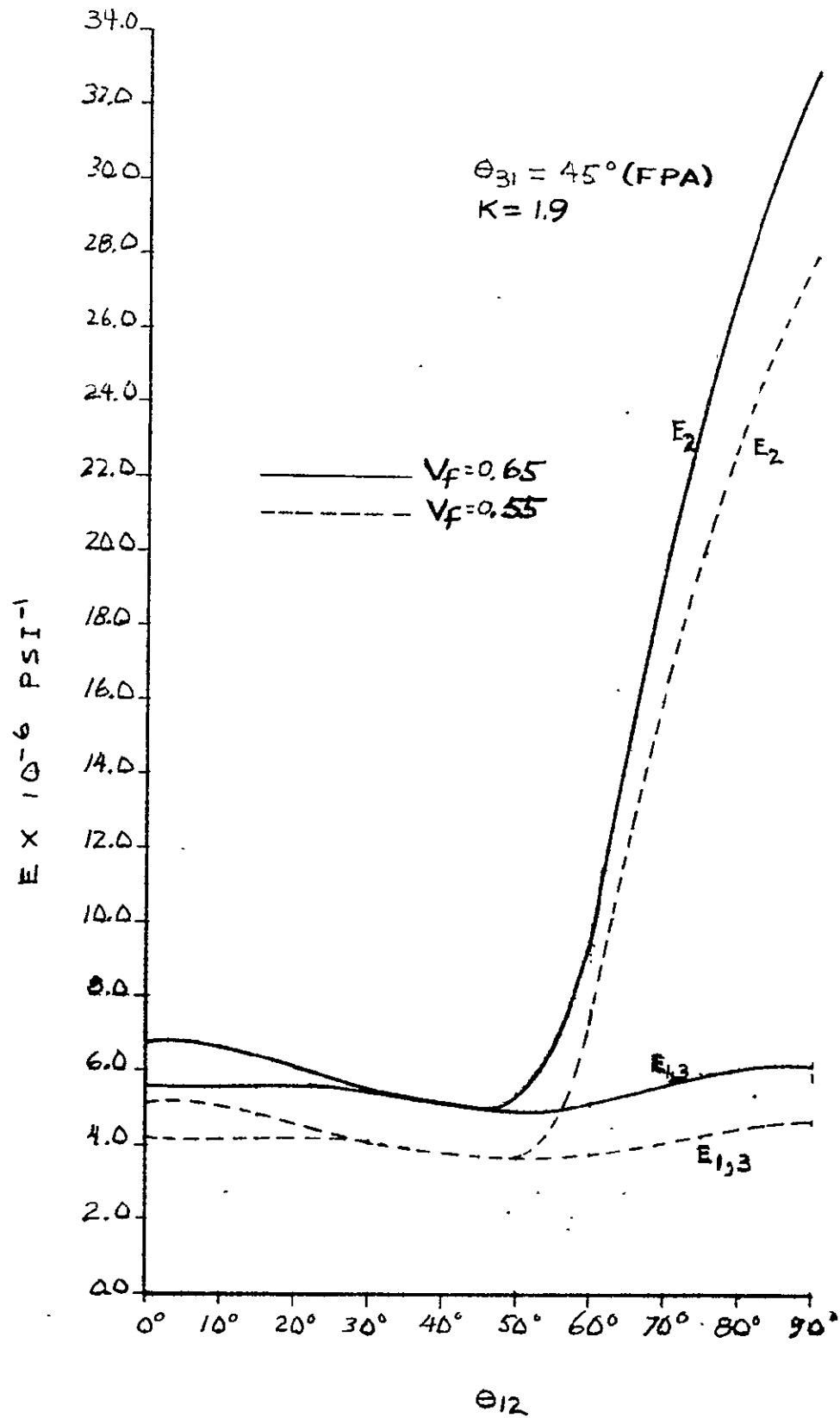


Figure 10-56. Elastic Moduli of Omniweave Composites

$$\theta_{31} = 45^\circ \text{ (FPA)}$$

$$V_f = 0.65$$

$$K = 1.9$$

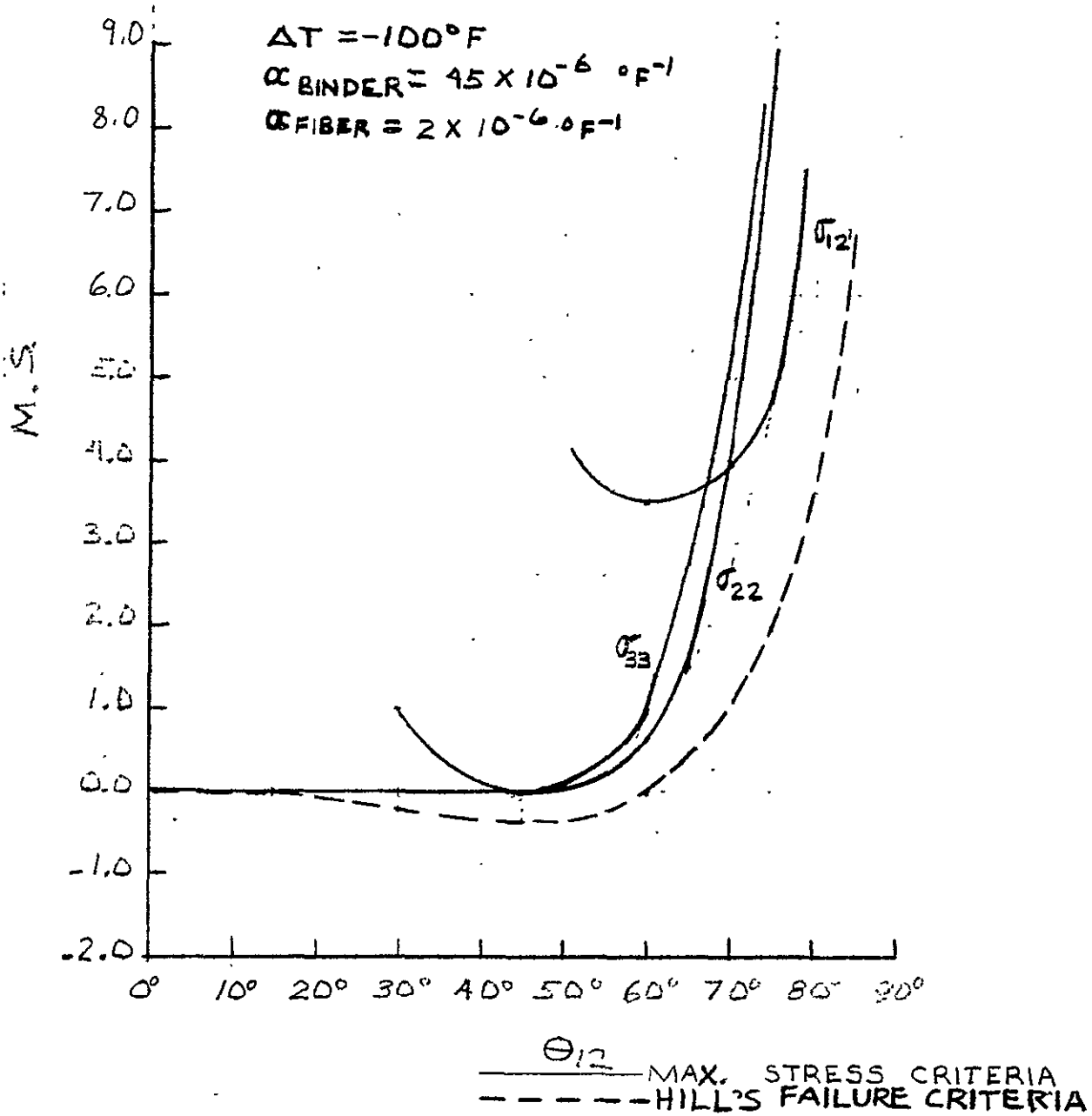


Figure 10-57. Margins of Safety (Thermal Loading Only) for Thornel 50 Omniweave Composites

$$\theta_{31} = 45^\circ \text{ (FPA)}$$

$$V_f = 0.65 \quad K = 1.9$$

LOADING

$$\sigma_{11} = 10,000 \text{ PSI}$$

$$\Delta T = -100^\circ \text{ F}$$

$$\alpha_{\text{FIBER}} = 2 \times 10^{-6} \text{ } ^\circ \text{ F}^{-1}$$

$$\alpha_{\text{BINDER}} = 45 \times 10^{-6} \text{ } ^\circ \text{ F}^{-1}$$

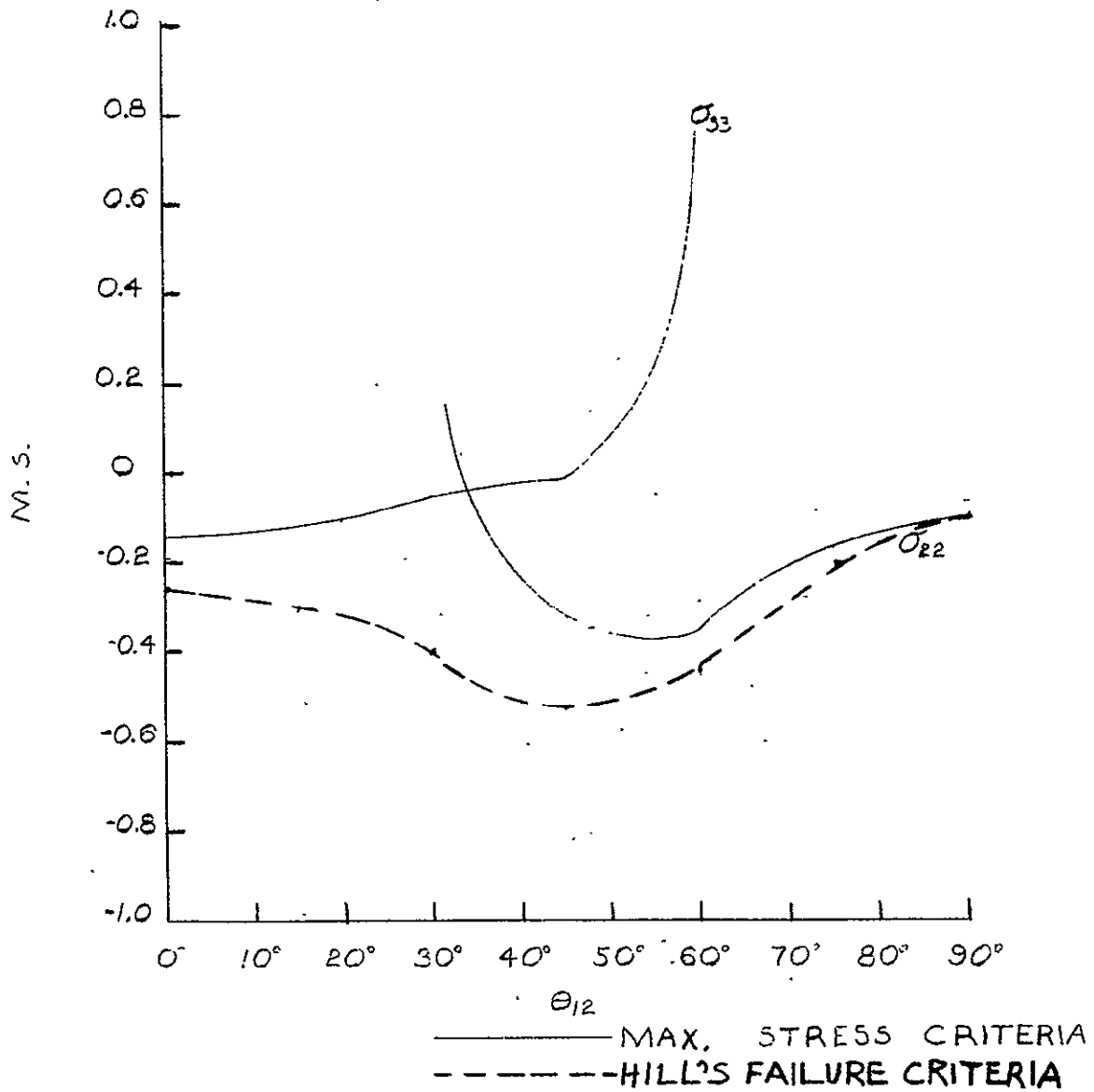


Figure 10-58. Margins of Safety (Thermal Plus Mechanical Loading) for ThorneI 50 Omniweave Composites

$$\theta_{31} = 45^\circ \text{ (FPA)}$$

$$K = 1.9$$

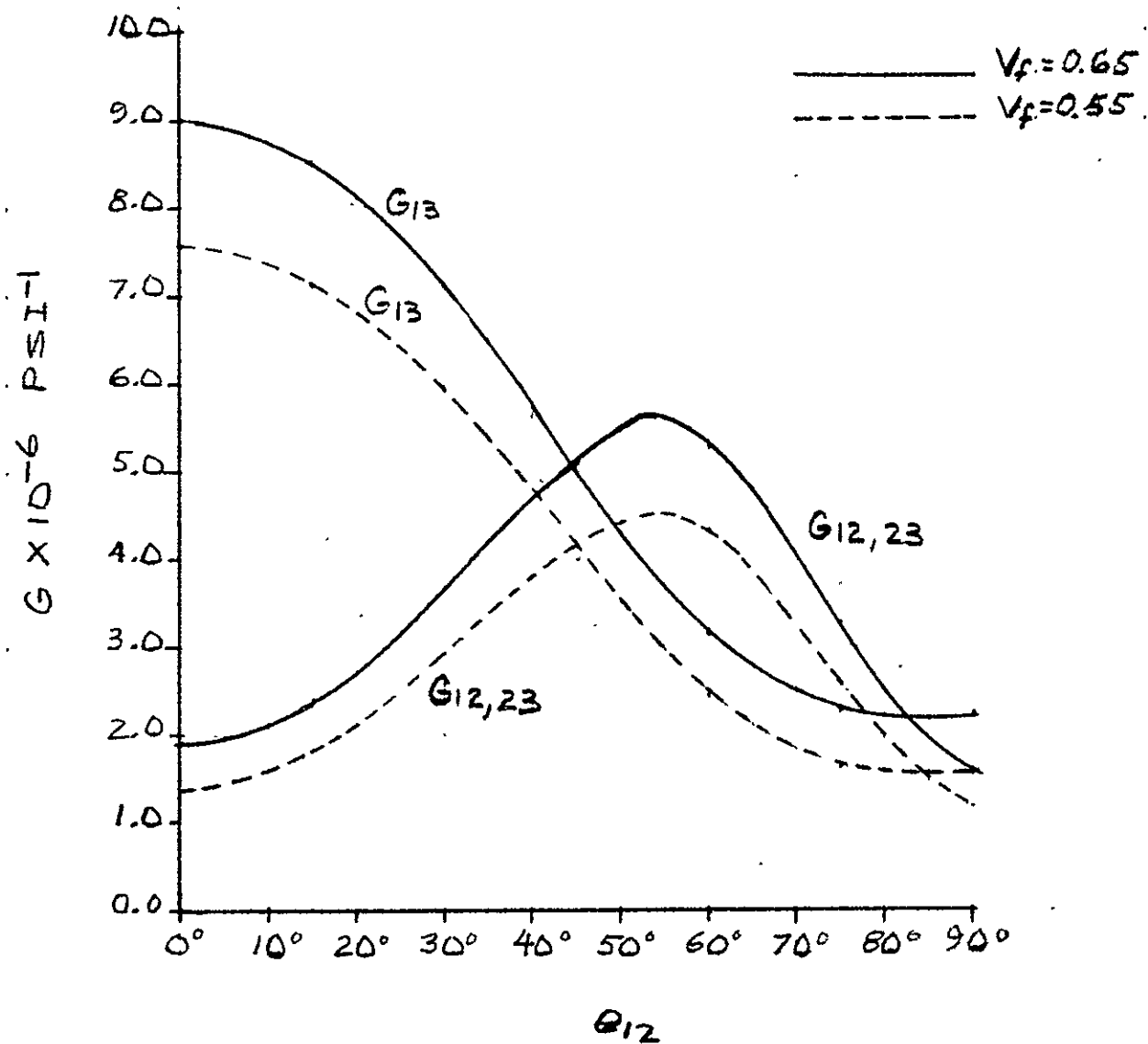


Figure 10-59. Shear Moduli Curves for Thornel 50 Omniweave Composites

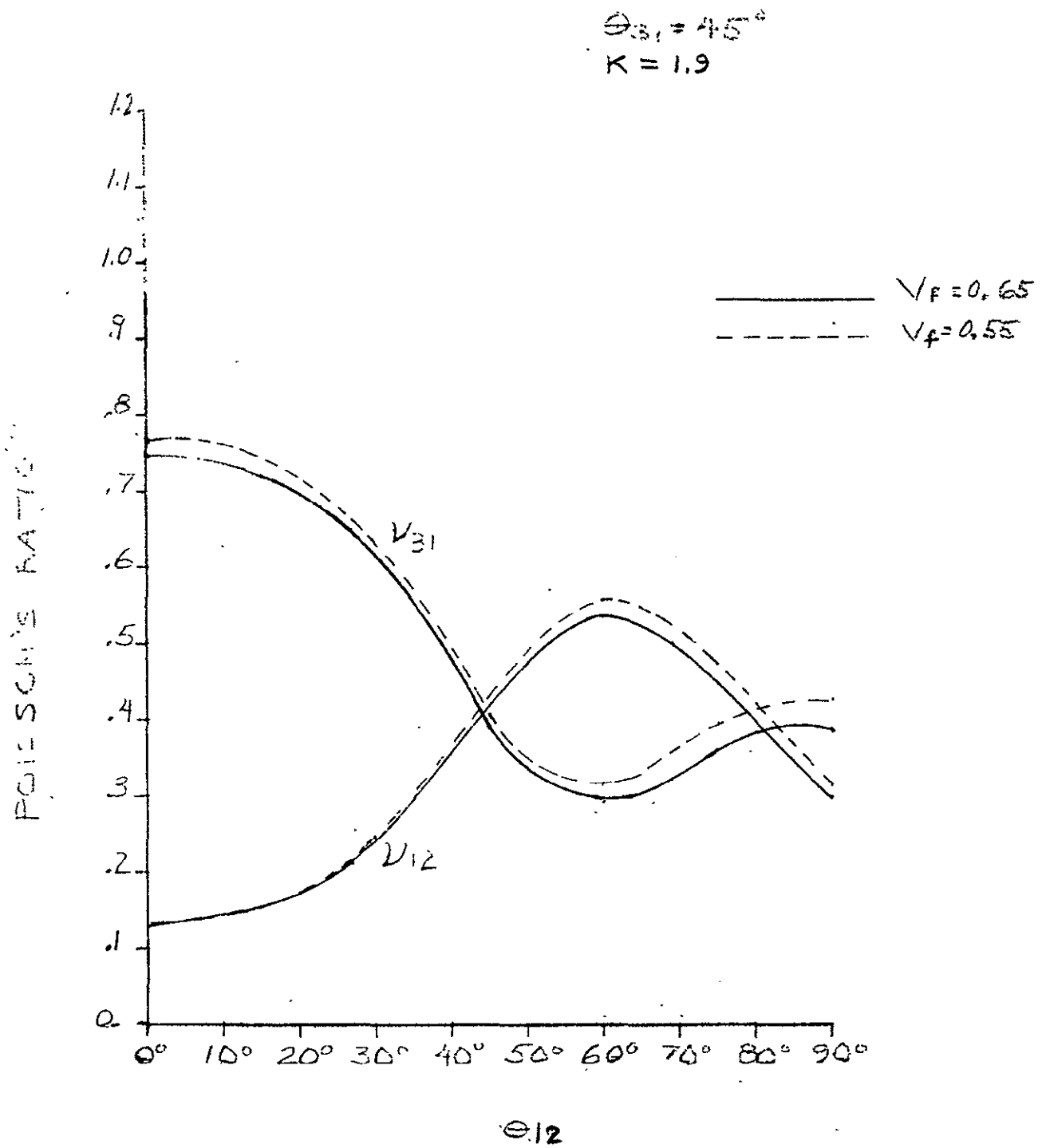


Figure 10-60. Poisson's Ratios for Thornel 50 Omniweave Composites

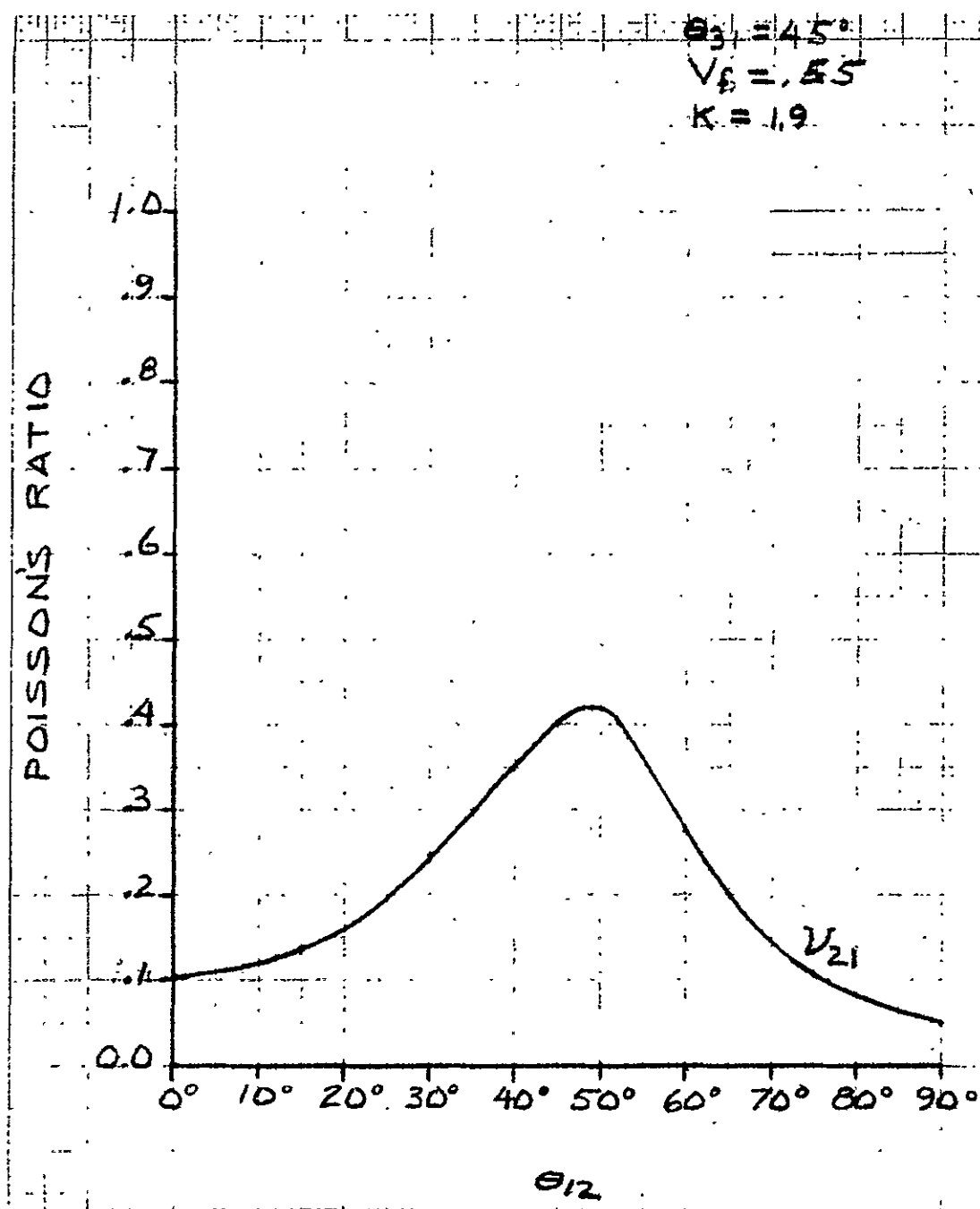


Figure 10-61. Poisson's Ratios for Thornel 50 Omniweave Composites

$$\theta_{31} = 45^\circ$$

$$V_b = .35$$

$$K = 1.9$$

$$\alpha_{\text{BINDER}} = 45 \times 10^{-6} \text{ } ^\circ\text{F}^{-1}$$

$$\alpha_{\text{FIBER}} = 2 \times 10^{-6} \text{ } ^\circ\text{F}^{-1}$$

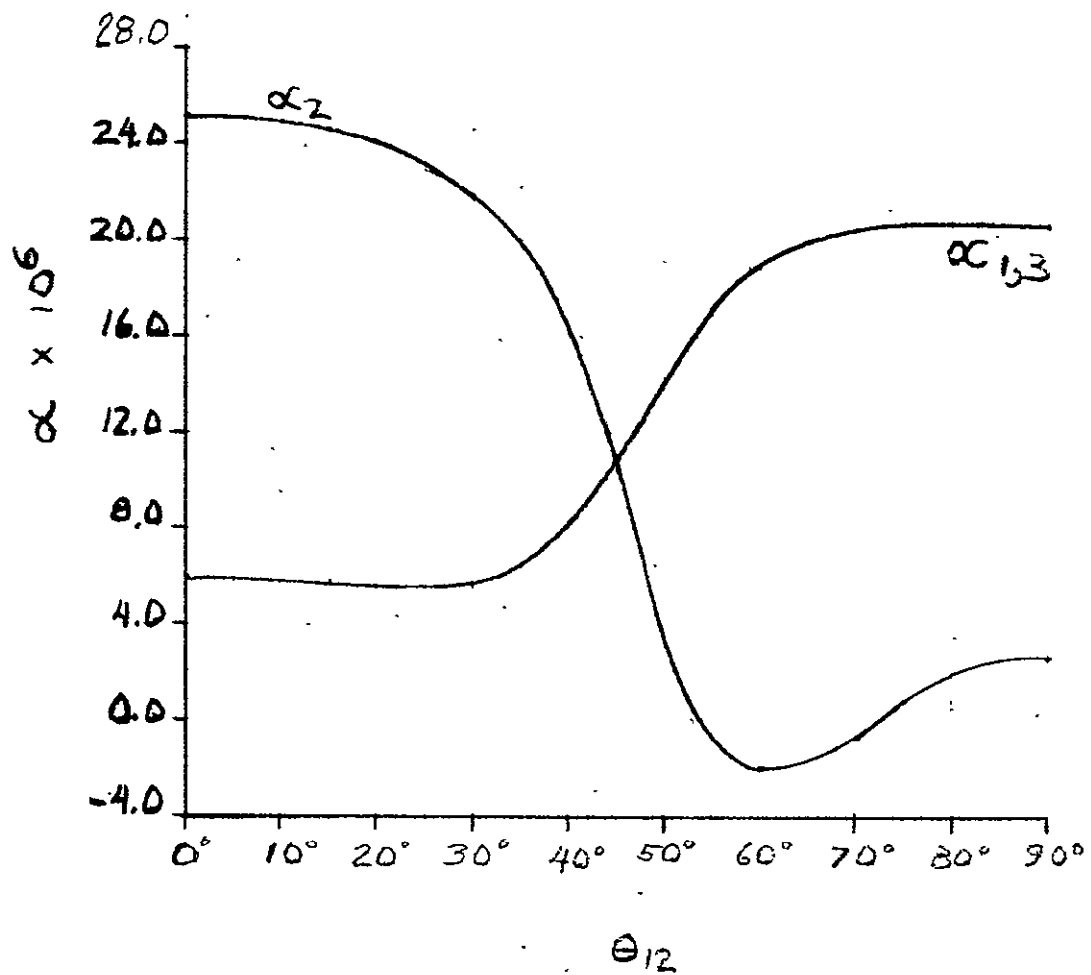


Figure 10-62. Thermal Expansion Curves for Thornel 50 Omniweave Composites

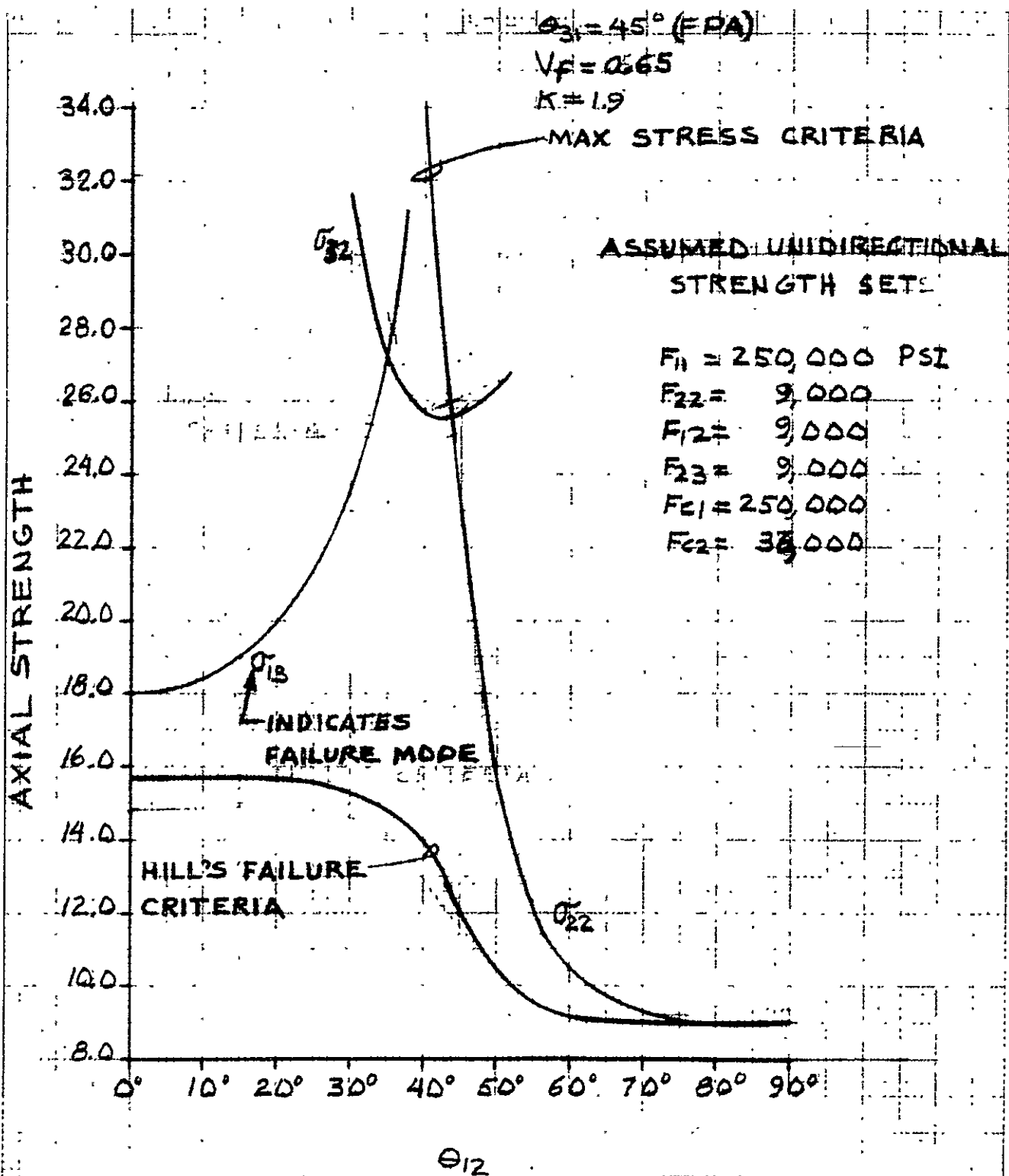


Figure 10-63. Axial Strength of Boron  
Omniweave Composites



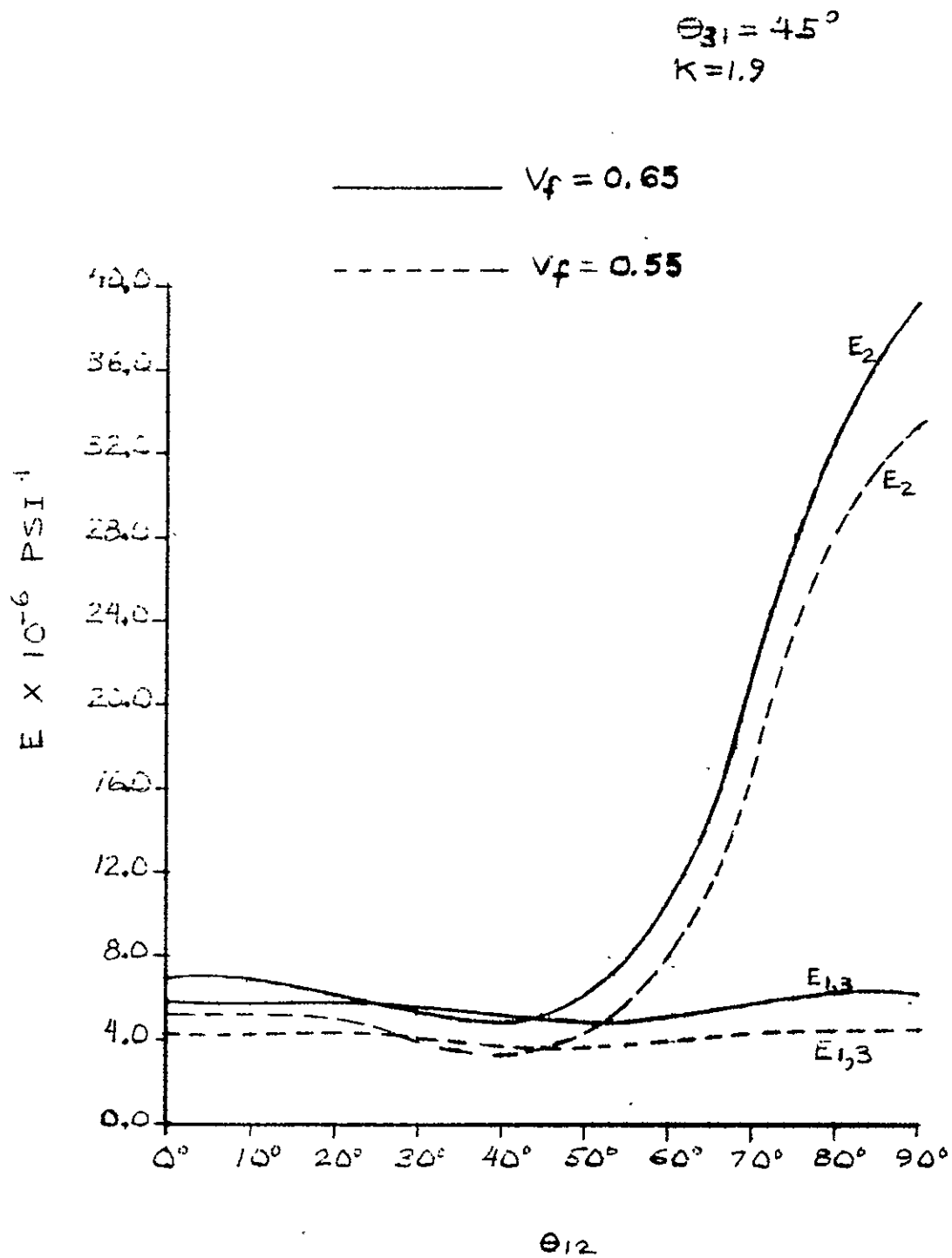


Figure 10-64. Elastic Moduli Boron  
Omniweave Composites

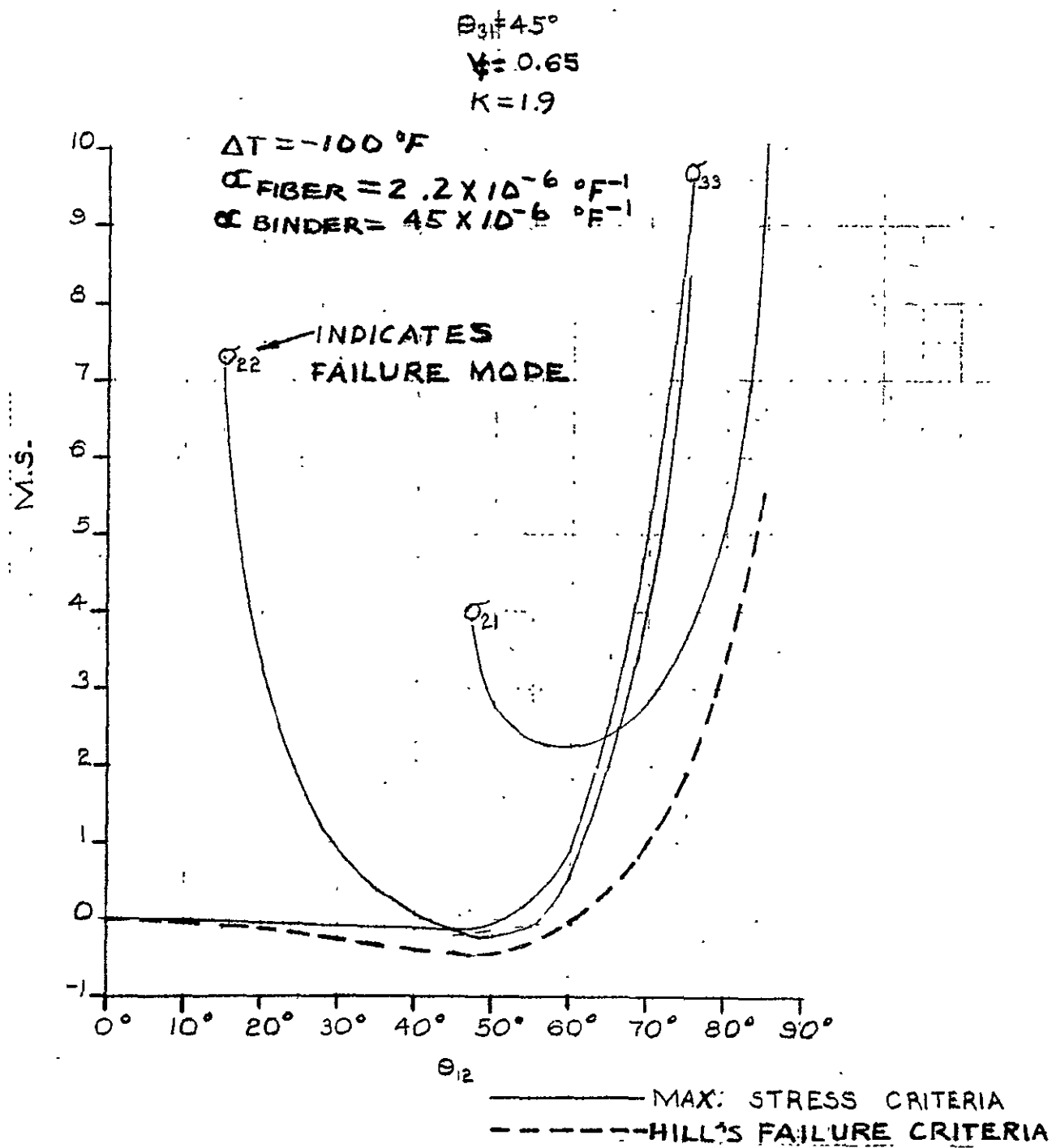


Figure 10-65. Margins of Safety (Thermal Loading Only) for Boron Omniweave Composites

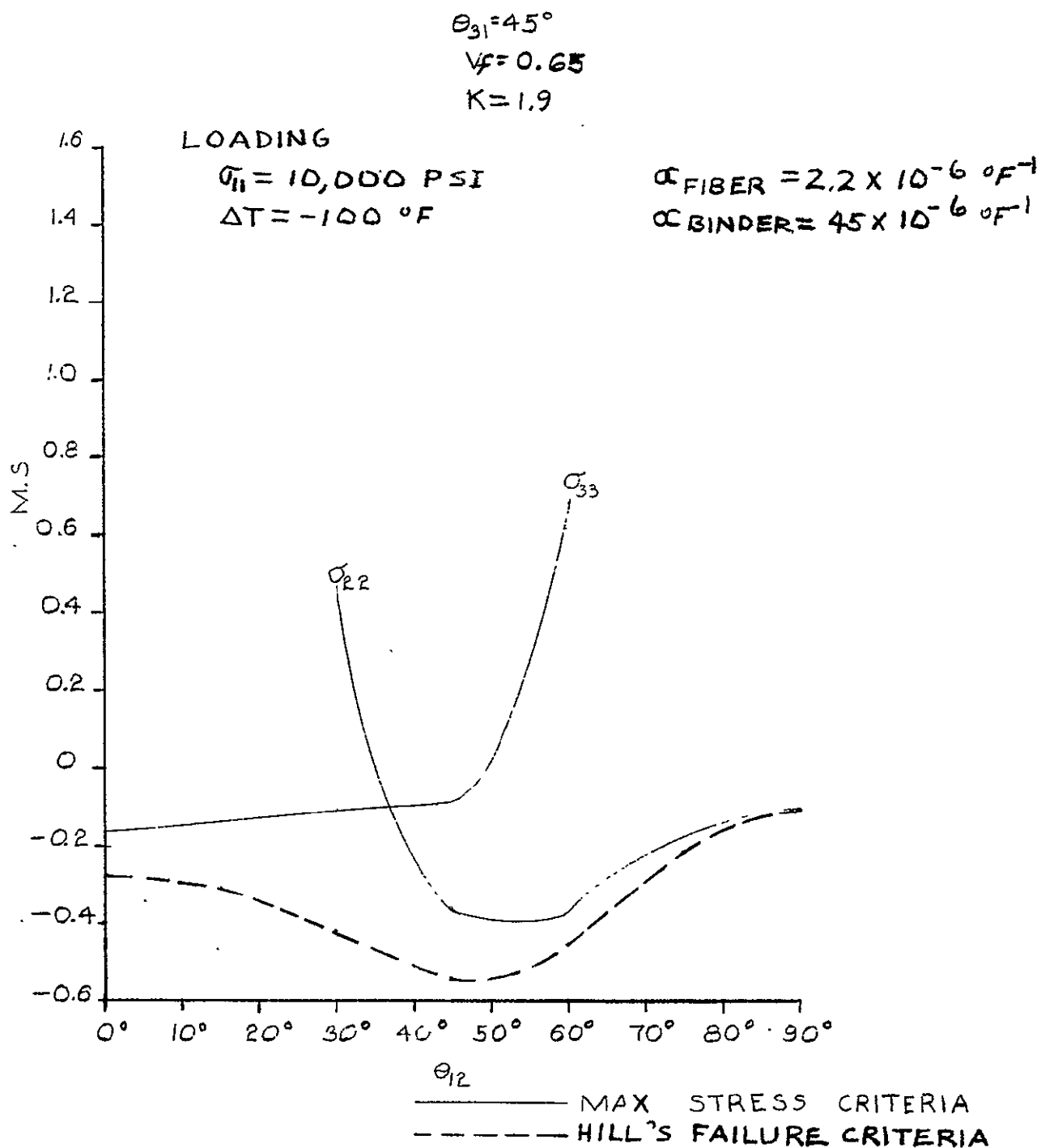


Figure 10-66. Margins of Safety (Thermal Plus Mechanical Loading) for Boron Omniweave Composites

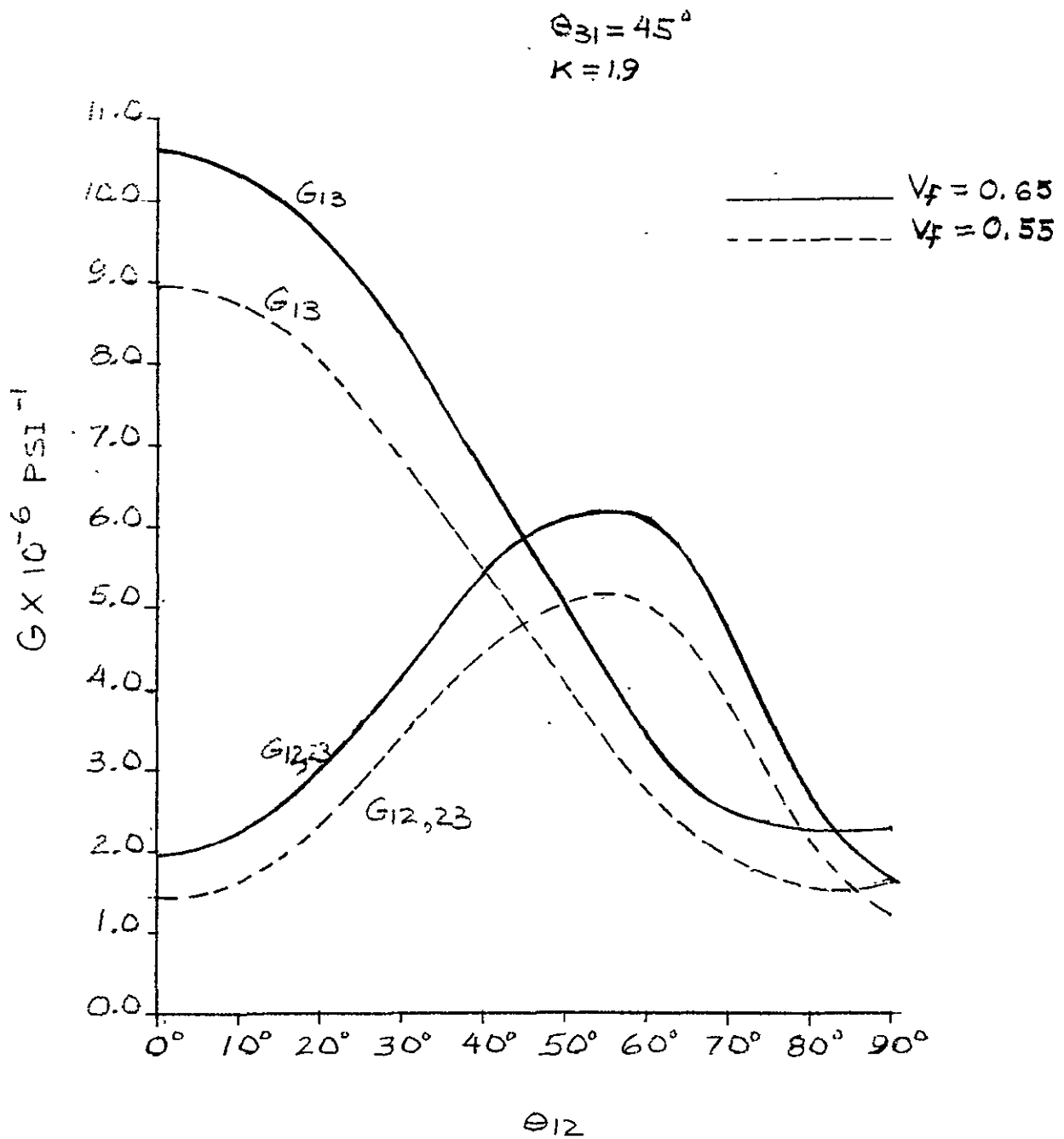


Figure 10-67. Shear Moduli Curves for Boron Omniweave Composites

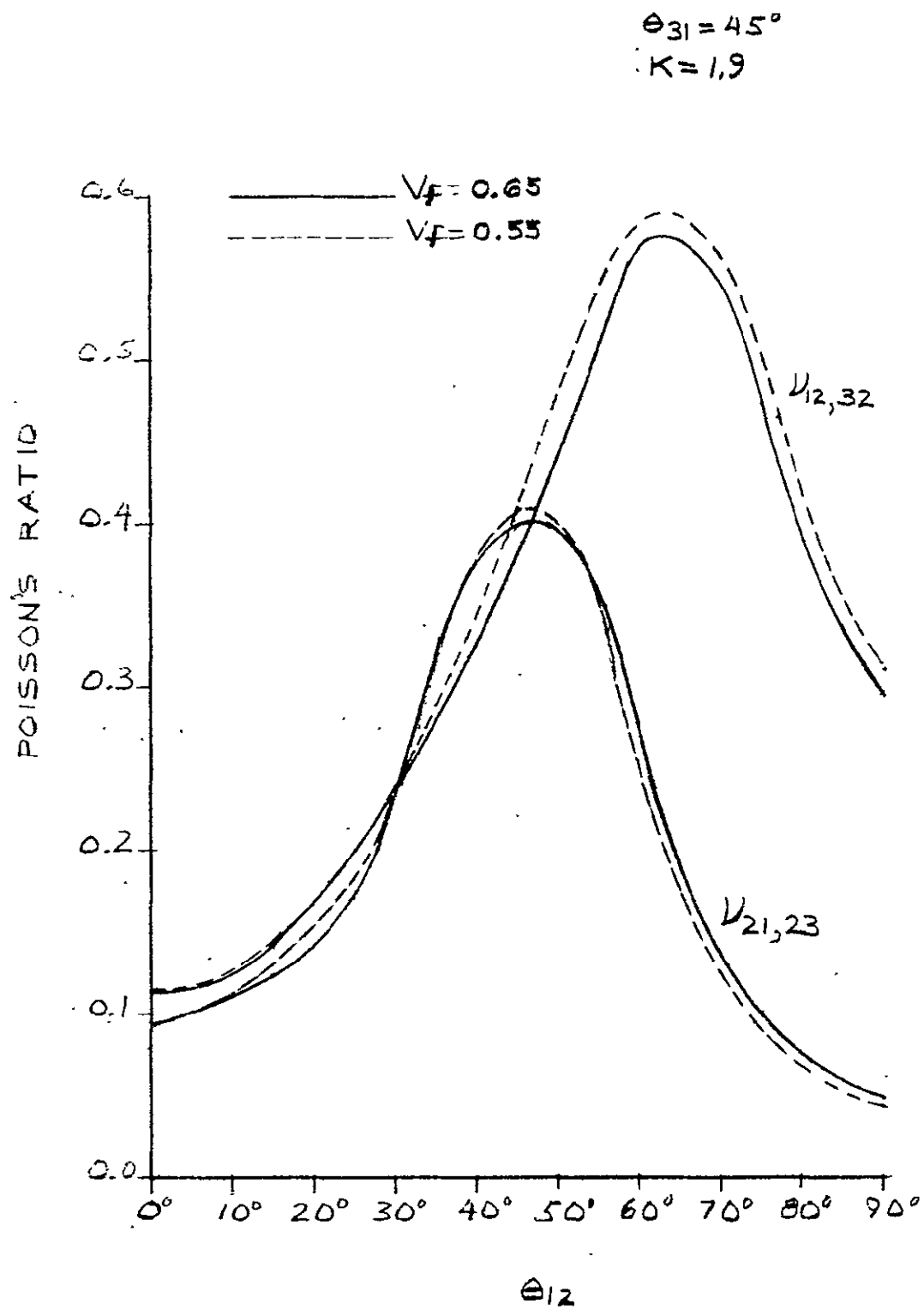


Figure 10-68. Poisson's Ratios of Boron Omniweave Composites

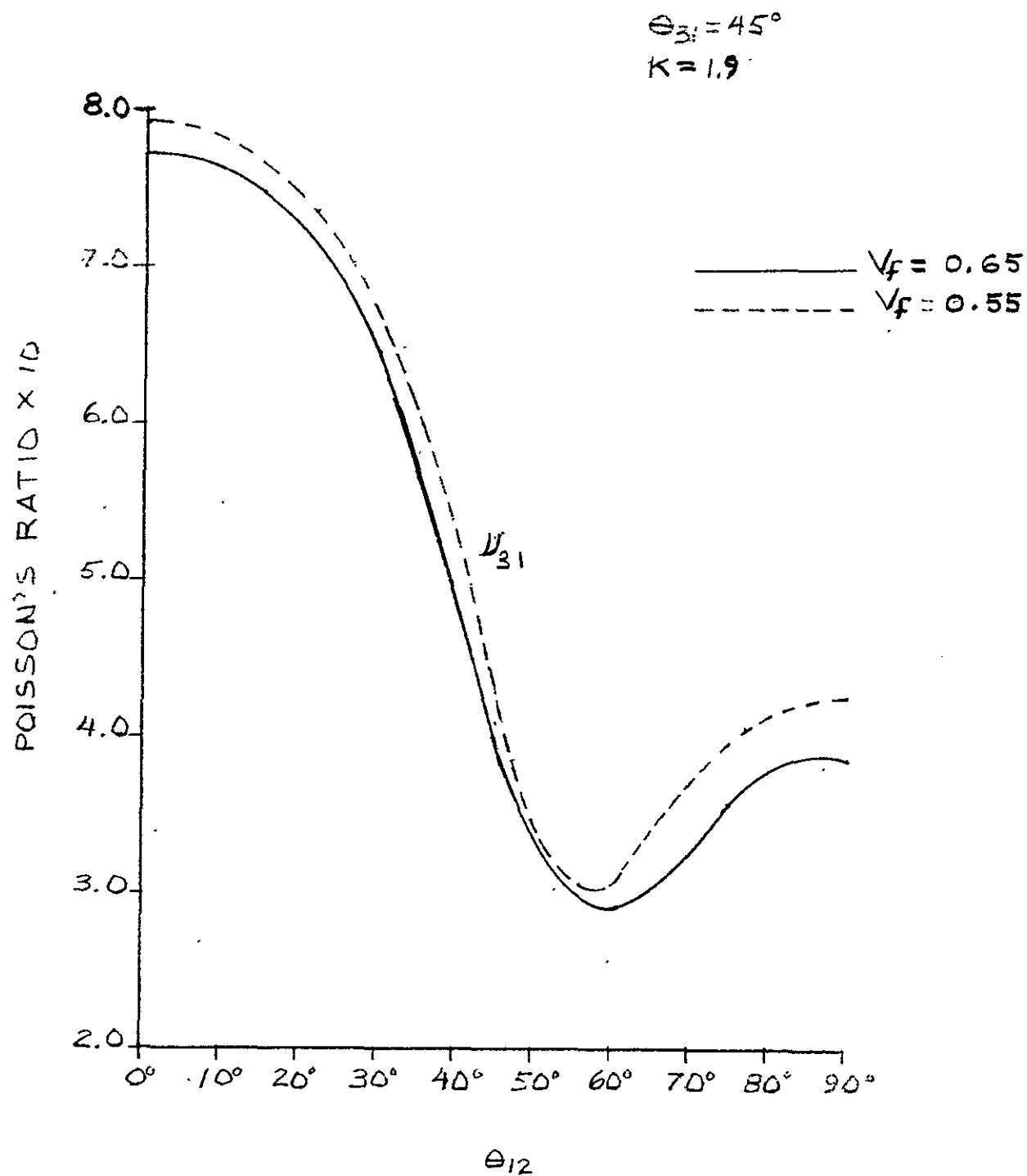


Figure 10-69. Poisson's Ratio Curves for Boron Omniweave Composites

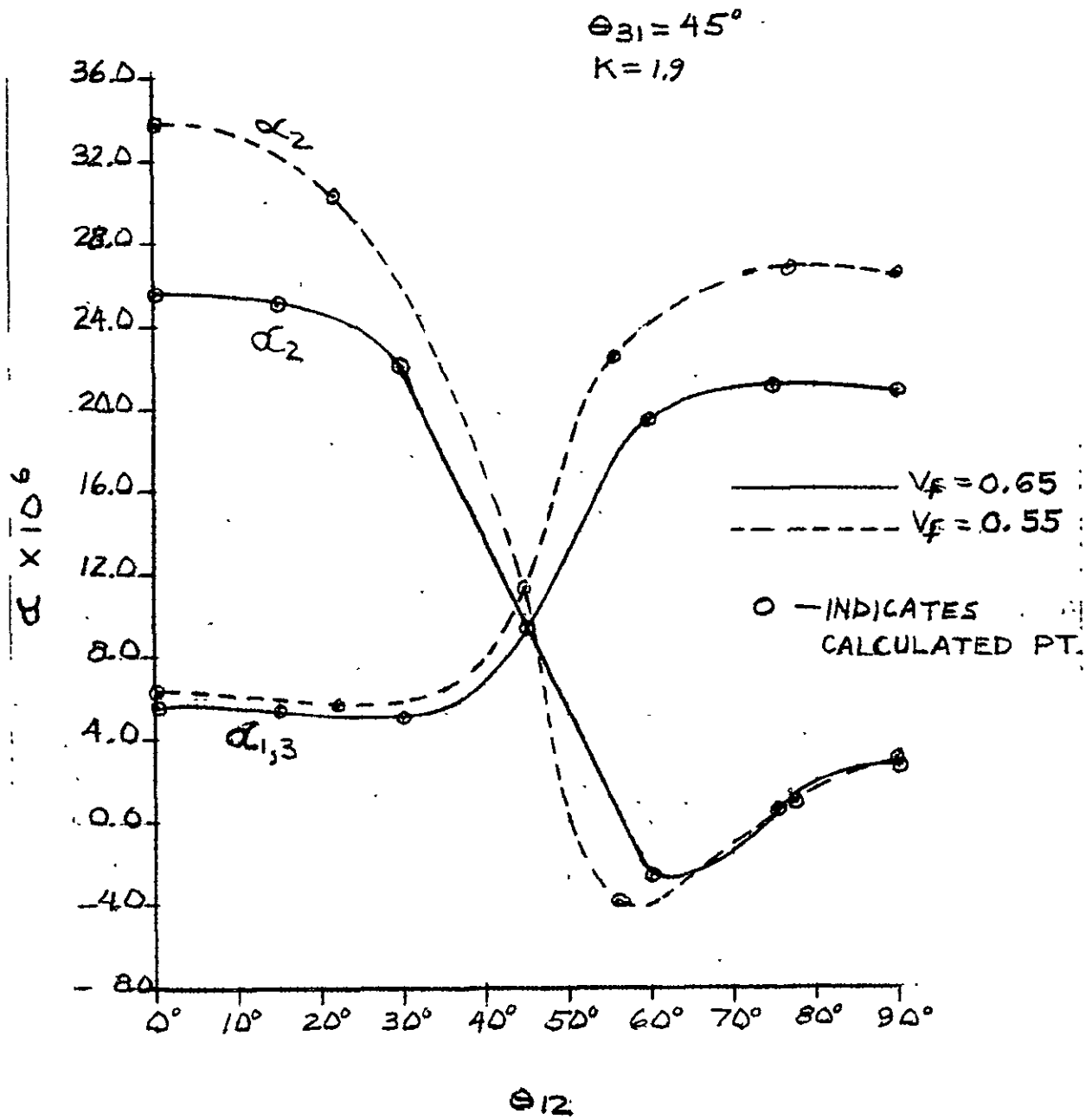


Figure 10-70. Coefficients of Thermal Expansion for Boron Omniweave Composites